



Fakultät Wissenschaftszentrum Weihenstephan für Ernährung, Landnutzung und Umwelt
Lehrstuhl für Biotechnologie der Nutztiere, Prof. Angelika Schnieke, Ph.D.

Genetic porcine models for *in vivo* genome editing and for xenotransplantation

Beate Rieblinger

Vollständiger Abdruck der von der Fakultät Wissenschaftszentrum Weihenstephan für Ernährung, Landnutzung und Umwelt der Technischen Universität München zur Erlangung des akademischen Grades eines

Doktors der Naturwissenschaften

genehmigten Dissertation.

Vorsitzende/-r: Prof. Dr. Martin Klingenspor

Prüfende/-r der Dissertation:

1. Prof. Angelika Schnieke, Ph.D.
2. apl. Prof. Dr. Reinhard Schwitzer
3. Prof. Dr. Wolfgang Wurst

Die Dissertation wurde am 04.07.2019 bei der Technischen Universität München eingereicht und durch die Fakultät Wissenschaftszentrum Weihenstephan für Ernährung, Landnutzung und Umwelt am 06.01.2020 angenommen.

Table of contents

Abstract	V
Zusammenfassung.....	VII
1 Introduction	9
1.1 Xenotransplantation.....	9
1.1.1 Pigs as organ donors	9
1.1.2 Immunological rejection as major hurdle for xenotransplantation.....	10
1.1.2.1 Antibody-mediated rejection processes	10
1.1.2.2 Cellular rejection processes.....	13
1.1.3 Strategies to prevent xenograft rejection.....	14
1.1.3.1 Elimination of porcine xenoreactive antigens.....	14
1.1.3.2 Complement regulation.....	16
1.1.3.3 Endothelium protection	17
1.1.3.4 Coagulation control.....	18
1.1.3.5 Immune cell regulation.....	20
1.2 Five-fold transgenic pigs for xenotransplantation	22
1.3 Genetic modification of livestock.....	23
1.3.1 Generation of genetically modified animals.....	23
1.3.1.1 Microinjection	23
1.3.1.2 Somatic cell nuclear transfer	24
1.3.2 Random transgene integration.....	25
1.3.3 Precise genetic modification	26
1.3.3.1 Gene targeting via homologous recombination.....	26
1.3.3.2 Genome editing by site-specific nucleases	27
1.3.3.3 Transgene insertion via site-specific recombinases	29
1.3.4 <i>In vivo</i> genome editing	30
1.4 Porcine <i>ROSA26</i> locus.....	30
1.5 Objectives	31
2 Materials and methods	32
2.1 Materials	32
2.1.1 Chemicals.....	32
2.1.2 Enzymes and enzyme buffers.....	34
2.1.3 Kits.....	34
2.1.4 Cells.....	35
2.1.4.1 Bacterial strains.....	35
2.1.4.2 Eukaryotic cells	35
2.1.5 Antibodies.....	36

2.1.6	Oligonucleotides.....	37
2.1.6.1	Primers and probes.....	37
2.1.6.2	gRNA oligonucleotides.....	39
2.1.7	Nucleic acid ladders	40
2.1.8	Molecular cloning vectors and DNA constructs.....	40
2.1.9	Tissue culture media, supplements and reagents.....	41
2.1.10	Bacterial culture media and supplements.....	42
2.1.11	Buffers and solutions.....	42
2.1.12	Laboratory equipment	44
2.1.13	Consumables.....	45
2.1.14	Software and online tools.....	46
2.2	Methods	47
2.2.1	Molecular biology	47
2.2.1.1	Isolation of mammalian genomic DNA	47
2.2.1.2	Isolation of plasmid DNA	48
2.2.1.3	Determination of DNA and RNA concentration	48
2.2.1.4	Polymerase chain reaction	48
2.2.1.5	Agarose gel electrophoresis	51
2.2.1.6	Proteinase K digest.....	51
2.2.1.7	Purification of DNA fragments and PCR products	52
2.2.1.8	DNA sequencing	52
2.2.1.9	Oligonucleotide annealing	52
2.2.1.10	Restriction digest	52
2.2.1.11	Dephosphorylation of cleaved DNA.....	53
2.2.1.12	Blunting	53
2.2.1.13	Ligation.....	53
2.2.1.14	Colony PCR	54
2.2.1.15	Droplet digital PCR	54
2.2.1.16	RNA isolation	55
2.2.1.17	cDNA synthesis.....	55
2.2.1.18	Quantitative real-time PCR.....	55
2.2.1.19	<i>In vitro</i> transcription.....	56
2.2.1.20	Poly(A) tailing	56
2.2.1.21	RNA purification	56
2.2.1.22	Protein isolation.....	56
2.2.1.23	Determination of protein concentration	57
2.2.1.24	Western blot.....	57

2.2.1.25	Immunohistochemistry	58
2.2.1.26	Generation of CRISPR/Cas9 components	59
2.2.1.27	Determination of indel efficiencies	60
2.2.2	Microbiological methods.....	61
2.2.2.1	Cultivation of bacterial cells	61
2.2.2.2	Transformation of bacterial cells.....	61
2.2.2.3	Preservation of bacterial cultures	61
2.2.3	Cell culture.....	62
2.2.3.1	Isolation of mammalian cells.....	62
2.2.3.2	Cultivation of mammalian cells	62
2.2.3.3	DNA transfection	63
2.2.3.4	RNA transfection	63
2.2.3.5	Selection of stable transfected cell clones	64
2.2.3.6	Isolation of cell clones.....	64
2.2.3.7	Cryopreservation.....	64
2.2.3.8	Enrichment of α Gal- negative cells via magnetic bead selection	64
2.2.3.9	Preparation of mammalian cells for somatic cell nuclear transfer	65
2.2.3.10	Flow cytometry	65
2.2.3.11	Caspase-Glo 3/7 Assay	65
3	Results	66
3.1	Transgene stacking at the porcine <i>ROSA26</i> locus.....	67
3.1.1	<i>ROSA26</i> retargeting and the generation of CD55, HO-1 expressing piglets....	68
3.1.2	Analysis of a <i>ROSA26</i> -CD55-HO-1 retargeted piglet.....	68
3.1.3	Generation of a third-round- <i>ROSA26</i> targeting vector	72
3.2	Bxb1 integrase-mediated transgene placement in five-fold transgenic cells	74
3.2.1	Generation of a seven-fold transgene vector	74
3.2.2	Introduction of an attP/MIN site into the CD46-flanking region	76
3.3	Pigs deficient in the major xenoreactive antigens.....	79
3.3.1	Evaluation of gRNA sequences against xenorelevant genes	79
3.3.1.1	Influence of gRNA sequence length on on- and off-target cleavage.....	79
3.3.1.2	Identification of efficient gRNA sequences.....	80
3.3.2	<i>CMAH</i> knockout cells and pigs	82
3.3.3	<i>GGTA1/CMAH</i> double-knockout pigs	84
3.3.3.1	<i>GGTA1/CMAH</i> double-knockout, five-fold transgenic pigs.....	84
3.3.3.2	Female <i>GGTA1/CMAH</i> double-knockout pigs	86
3.3.4	<i>GGTA1/CMAH/B4GALNT2/B2M</i> four-fold knockout pig	91
3.4	<i>ROSA26</i> -hSpCas9 pigs for <i>in vivo</i> genome editing	97

3.4.1	<i>ROSA26</i> targeting and the generation of hSpCas9 expressing pigs	97
3.4.2	Analysis of <i>ROSA26</i> -hSpCas9 pigs.....	98
4	Discussion.....	103
4.1	Transgene stacking at the <i>ROSA26</i> locus	103
4.2	Seven-fold transgene placement at the CD46 3' flanking region.....	105
4.2.1	Bxb1 integrase-mediated transgene placement.....	105
4.2.2	Composition of the seven-fold transgene array.....	107
4.3	The CRISPR/Cas9 system for gene editing in pigs	109
4.3.1	Strategies for high gene editing efficiencies	109
4.3.2	Strategies to minimise off-target cleavage	110
4.4	Pigs deficient in the major xenoreactive antigens.....	112
4.4.1	<i>CMAH</i> knockout pigs.....	112
4.4.2	<i>GGTA1/CMAH</i> double-knockout pigs	113
4.4.3	<i>GGTA1/CMAH/B4GALNT2/B2M</i> four-fold knockout pigs	113
4.5	<i>ROSA26</i> -hSpCas9 pigs for <i>in vivo</i> genome editing	115
5	Concluding remarks and outlook.....	118
6	Abbreviations	120
7	List of tables.....	123
8	List of figures.....	124
9	Literature	126
10	Supplementary	139
11	Acknowledgement.....	145
12	Curriculum vitae.....	148

Abstract

Xenodonor pigs require multiple genetic modifications to enable grafted cells and tissues to overcome rejection processes and provide clinical benefit for human recipients. The challenge has been to avoid segregation of the required xenoprotective transgenes during breeding, which simplifies the breeding regimen and reduces the number of experimental animals. Various strategies to assemble a transgene array at a single genomic locus were pursued in this work. The first was to assemble multiple independently-expressed transgenes at the porcine *ROSA26* locus by successive targeted transgene placement, termed “transgene stacking”. A HO-1 construct was placed at the porcine *ROSA26* locus and a CAG-driven human CD55 minigene subsequently inserted at this site. Transgenic founder animals were derived by somatic cell nuclear transfer, found to express very high expression levels from the two single-copy transgenes and cells derived had almost complete protection against human complement-mediated lysis.

The second approach was to place a multi-transgene vector at a site adjacent to an existing multi-transgene array previously generated at the Chair of Livestock Biotechnology. As targeted placement of a large construct via conventional targeting by homologous recombination is inefficient in somatic cells, a Bxb1-serine recombinase-mediated approach was chosen. An attP/Min site was placed within the 3' flanking region of a human CD46 transgene, which was present as a single copy within the array. A multi-transgene vector was prepared for future Bxb1-mediated recombination with the attP/MIN site. The vector carried seven independently expressed transgenes (hPD-L1, hHT, mutCIITA, hCD47, hHO-1, hTM and hEPCR) designed to further reduce or prevent cellular xenograft rejection and coagulation incompatibilities.

Besides addition of human transgenes, it is also necessary to remove xenoreactive antigens that can lead to antibody-mediated rejection processes. Within this project, the most important xenoreactive antigen-coding genes were inactivated by targeted single- and multiplexed gene editing using the CRISPR/Cas9 system. *CMAH* knockout, *GGTA1/CMAH* double-knockout and *GGTA1/CMAH/B4GALNT2/B2M* four-fold knockout pigs were produced, and functionality of the knockouts shown by absence of the respective xenoantigens. Kidney fibroblast cells derived from these pigs showed reduced levels of human IgG and IgM antibody binding after incubation with human serum, with the lowest levels observed for cells from the *GGTA1/CMAH/B4GALNT2/B2M* four-fold knockout pig.

The last part of this work describes the generation of a new resource for *in vivo* genome editing in pigs, a transgenic pig line with ubiquitous Cas9 expression. A humanised version of Cas9 from *streptococcus pyogenes* (hSpCas9) was placed at the porcine *ROSA26* locus and

transgenic founder animals derived by somatic cell nuclear transfer. The resulting transgenic pigs showed correct targeting, expression of hSpCas9 in all tissues examined and functionality.

Zusammenfassung

Xenodonor-Schweine benötigen mehrere genetische Veränderungen, um sicherzustellen, dass transplantierte Zellen und Gewebe Abstoßungsprozesse überwinden und den menschlichen Empfängern klinischen Nutzen bringen können. Die Herausforderung bestand darin, die Segregation der notwendigen xenoprotektiven Transgene während der Zucht zu vermeiden, was den Zuchtplan vereinfacht und die Anzahl an Versuchstieren reduziert. Verschiedene Strategien zur Assemblierung eines Transgen-Arrays an einem einzelnen genomischen Locus wurden in dieser Arbeit verfolgt. Die Erste bestand darin, mehrere unabhängig exprimierte Transgene am *ROSA26* Locus des Schweins durch aufeinanderfolgende gezielte Transgenplatzierung zusammenzufügen, bezeichnet als "Transgen-Stacking". Im porzinem *ROSA26* Locus wurde ein HO-1 Konstrukt positioniert und dort anschließend ein CAG-gesteuertes humanes CD55-Minigen inseriert. Transgene Gründertiere wurden durch somatischen Zellkerntransfer gewonnen, exprimierten sehr hohe Level der beiden Einzelkopie-Transgene und gewonnene Zellen hatten einen nahezu vollständigen Schutz vor menschlicher Komplement-vermittelter Lyse.

Der zweite Ansatz bestand darin, einen Multi-Transgen-Vektor an einem Ort zu platzieren, der an einen bestehenden Multi-Transgen-Array angrenzt, welcher zuvor am Lehrstuhl für Biotechnologie der Nutztiere erzeugt wurde. Da die gezielte Platzierung eines großen Konstrukts durch konventionelles Targeting mittels homologer Rekombination in somatischen Zellen ineffizient ist, wurde ein Bxb1-Serin Rekombinase vermittelter Ansatz gewählt. Eine attP/Min-Stelle wurde innerhalb der 3'-flankierenden Region eines menschlichen CD46-Transgens platziert, welches als Einzelkopie innerhalb des Arrays vorlag. Es wurde ein Multi-Transgen-Vektor für die zukünftige Bxb1-vermittelte Rekombination mit der attP/MIN Stelle erstellt. Der Vektor beinhaltet sieben unabhängig voneinander exprimierte Transgene (hPD-L1, hHT, mutCIITA, hCD47, hHO-1, hTM und hEPCR), welche die zelluläre Xenotransplantatabstoßung und Gerinnungsstörungen weiter reduzieren oder verhindern sollen.

Neben dem Hinzufügen humaner Transgene ist es auch notwendig, xenoreaktive Antigene zu entfernen, die zu antikörpervermittelten Abstoßungsprozessen führen können. Im Rahmen dieses Projekts wurden die wichtigsten xenoreaktiven antigenkodierenden Gene durch gezielte Einzel- und Multiplex-Geneditierungen mittels des CRISPR/Cas9-Systems inaktiviert. *CMAH* Knockout, *GGTA1/CMAH* Doppel-Knockout und *GGTA1/CMAH/B4GALNT2/B2M* Vierfach-Knockout Schweine wurden produziert und die Funktionalität der Knockouts durch Abwesenheit der jeweiligen Xenoantigene gezeigt. Nieren-Fibroblast Zellen dieser Schweine zeigten verringerte Werte an humaner IgG- und IgM-Antikörperbindung nach Inkubation mit

Humanserum, wobei die niedrigsten Werte für Zellen des *GGTA1/CMAH/B4GALNT2/B2M* Vierfach-Knockout-Schweins beobachtet wurden.

Der letzte Teil der Arbeit beschreibt die Generierung einer neuen Ressource für die *in vivo* Genom-Editierung in Schweinen, eine transgene Schweinelinie mit ubiquitärer Cas9-Expression. Eine humanisierte Version von Cas9 aus *Streptococcus pyogenes* (hSpCas9) wurde am *ROSA26* Locus des Schweins platziert und transgene Gründertiere durch Kerntransfer somatischer Zellen generiert. Die resultierenden transgenen Schweine zeigten korrektes Targeting, Expression von hSpCas9 in allen untersuchten Geweben und Funktionalität.

1 Introduction

1.1 Xenotransplantation

Organ transplantation is the only life-saving treatment for many patients suffering from end-stage organ failure. However, there is a critical shortage of human organs from deceased and living donors, and this is expected to become worse as the global population ages [1]. For example, in January 2019, 14129 patients were registered on the Eurotransplant waiting list, but only 7394 allotransplantations were carried out in 2018 [2]. One promising approach to alleviate the shortage is to use animals as donors.

Xenotransplantation (gr. *xènos* = foreigner) is the transplantation of organs, tissues and cells between different species. It offers several potential advantages over reliance on human sources - allotransplantation. Animal donors can be raised in essentially unlimited numbers, minimising the waiting time to receive a new organ; transplantation can be planned in advance, enabling pre-treatment of the donor and the recipient to enhance graft acceptance; transport and storage of explanted organs can be minimised; donor organs are not subjected to damaging effects as a consequence of brain death [3]; and chronic diseases and infections can be excluded beforehand [4].

1.1.1 Pigs as organ donors

Non-human primates would be the preferred organ source for transplantation into humans due to their evolutionary similarity. However, such species are either endangered, or too small to provide organs suitable for transplantation into adult humans. There are also concerns regarding cross-species transmission of pathogenic viruses [5-7]. As a consequence, pigs are widely regarded as the most promising donor species for xenotransplantation. Pigs share similar organ sizes with humans and many similarities in anatomy and physiology. They have favourable breeding characteristics, such as short gestation and large litter sizes, which enable large herds to be generated in a relatively short time. As pigs have long been raised as a food source, there are fewer ethical issues than with primates. Methods for genetic engineering pigs are now well established [8, 9]. Pigs also present a lower risk of zoonotic infection than non-human primates due to their greater phylogenetic distance [7, 10]. Pigs serving as potential organ donors can be selected to be free of infectious pathogens and be housed in specific pathogen free facilities.

However, the greater phylogenetic distance between pigs and humans raises several obstacles, such as immunological rejection.

1.1.2 Immunological rejection as major hurdle for xenotransplantation

Transplantation of porcine organs into human recipients leads to severe immunological rejection, which can be classified as antibody-mediated- and immune-cell-mediated rejection mechanisms.

1.1.2.1 Antibody-mediated rejection processes

Antibody-mediated rejection includes hyperacute rejection (HAR) and acute humoral xenograft rejection (AHXR). HAR is the most rapid rejection process, and leads to graft failure within minutes to hours after xenotransplantation. It is mediated by human anti- α Gal antibodies that bind to galactose- α 1,3-galactose (α Gal) epitopes on endothelial cells of vascularised grafts [11-13]. The α Gal epitope is abundantly expressed on glycolipids and glycoproteins of non-primates and new world monkeys but is absent in humans and old world monkeys due to a loss-of-function mutation estimated to have occurred 29-25 million years ago in the α 1,3-galactosyltransferase gene (*GGTA1*), responsible for α Gal synthesis [14]. Species that lack *GGTA1* activity are however exposed to α Gal expressed on the surface of intestinal bacteria. Consequently, humans and old world monkeys produce high levels of anti- α Gal antibodies which constitute 1% of circulating immunoglobulins [15, 16]. Binding of human anti- α Gal antibody to α Gal on the endothelium of a vascularised xenograft, activates the complement cascade which in turn activates the coagulation cascades, leading to destruction of the graft (Figure 1A). HAR is characterised histologically by massive intestinal haemorrhage, oedema, destruction of the vessel endothelium and thrombosis [13, 17, 18].

If HAR is overcome, a xenograft is then subjected to acute humoral xenograft rejection (AHXR), also termed acute vascular rejection (AVR). AHXR is initiated days to weeks after xenotransplantation [19] and is caused by binding of preformed and elicited antibodies to xenoreactive non-Gal antigens on the graft endothelium. Rejection mechanisms include antibody-dependent cell-mediated cytotoxicity (ADCC) where macrophages, natural killer (NK) cells and neutrophils induce phagocytosis and lysis. AHXR also involves activation of the complement- and coagulation cascades which in turn are associated with endothelium activation. These events contribute to apoptosis, thrombosis and oedema [17, 20-22] (Figure 1B).

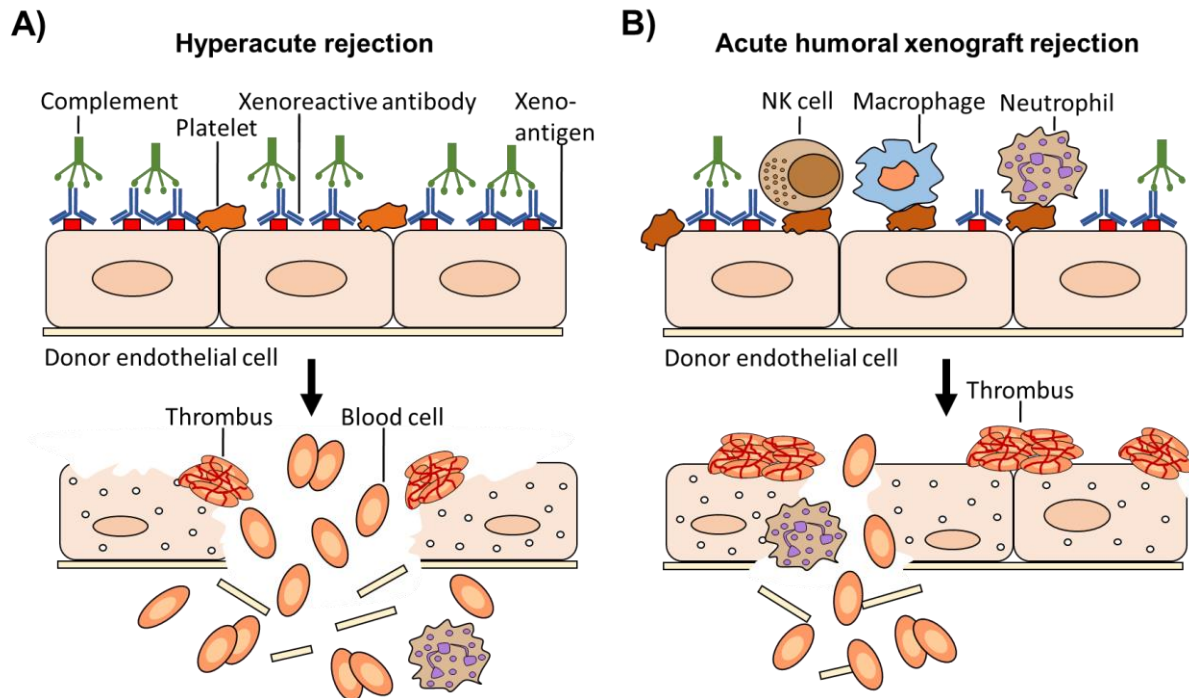


Figure 1: Antibody-mediated rejection processes. (A) Hyperacute rejection (HAR) is induced by binding of natural anti- α Gal antibodies to α Gal epitopes on the porcine graft and results in complement activation and endothelium disruption. (B) Acute humoral xenograft rejection (AHXR) is induced by binding of natural and elicited xenoreactive antibodies. This leads to complement activation, antibody-dependent cellular cytotoxicity (ADCC), endothelial-cell activation, thrombosis and edema. Illustration adapted from Yang and Sykes, 2007 [20].

An important xenoreactive antigens involved in AHXR is N-glycolylneuraminic acid (Neu5Gc), also known as Hanganutziu-Deicher (H-D) antigen (Figure 2) [23, 24]. This epitope is widely expressed on endothelial cells of all mammals except humans [25] and new-world monkeys [26] and is a potential target for human preformed and elicited anti-non-Gal antibodies [27-29]. Neu5Gc is synthesised from the substrate N-acetylneuraminic acid (Neu5Ac) by the enzyme cytidine monophosphate-N-acetylneuraminic acid hydroxylase (CMAH). Almost all mammals, including non-human primates and pigs, possess a functional *CMAH* gene and thus produce Neu5Gc. Humans lack *CMAH* activity due to a 92 bp inactivating deletion that occurred ~2 million years ago [30-33]. However, exogenous Neu5Gc can be taken up from Neu5Gc-rich foods, such as red meat and milk products, and metabolically incorporated leads to low levels on the surface of human epithelial and endothelial cells [34-36]. The human immune system recognises Neu5Gc as foreign and generates anti-Neu5Gc antibodies with broad and variable specificity [34, 37]. These antibodies induce activation of porcine endothelial cells upon challenge of porcine *GGTA1* knockout cells with human serum [38, 39]. In mice, sera from *CMAH*-knockout mice initiated complement-mediated lysis against Neu5Gc-positive cells *in vitro* and Neu5Gc-positive splenocytes were eliminated upon transplantation into syngeneic *CMAH*-knockout mice [27].

A further gene involved in AHXR is porcine β 1,4-N-acetylgalactosaminyl transferase (*B4GALNT2*) [40]. In humans, *B4GALNT2* catalyses the transfer of N-acetyl-D-galactosamine (GalNAc) to a sialic acid modified lactosamine and thereby produces Sda antigens. The Sda antigen itself is a trisaccharide located on different underlying sugar structures present on glycolipids and glycoproteins (Figure 2) [41]. As most human serum samples contain antibodies directed against the products of porcine *B4GALNT2* activity [42], it is currently thought that porcine *B4GALNT2* generates a pattern of Sda-bearing epitopes different to that in humans, and recognised as foreign [41, 43]. Baboons that received a porcine xenograft raised antibodies to glycans produced by porcine *B4GALNT2* [40, 44]. Additionally, expression of porcine *B4GALNT2* by HEK293 cells increases complement-mediated cytotoxicity after challenge with serum from xenograft-recipient baboons [44].

Exposure of porcine α Gal-, Neu5Gc- and Sda-deficient cells to serum from patients waiting for kidney transplants revealed that approximately one third of serum samples lacked binding antibodies, while two thirds displayed an antibody response [45]. As many patients have antibodies against HLA (Human Leucocyte Antigen) epitopes, Martens et al. hypothesised that SLA (Swine Leucocyte Antigen), the porcine homologue to HLA, acts as a xenoreactive antigen and that these patients have antibodies against these epitopes. This is supported by the finding that SLA class I knockout cells bind less human antibodies than do SLA class I wild type cells [45]. Hence SLA class I molecules constitute a further group of xenoreactive antigens.

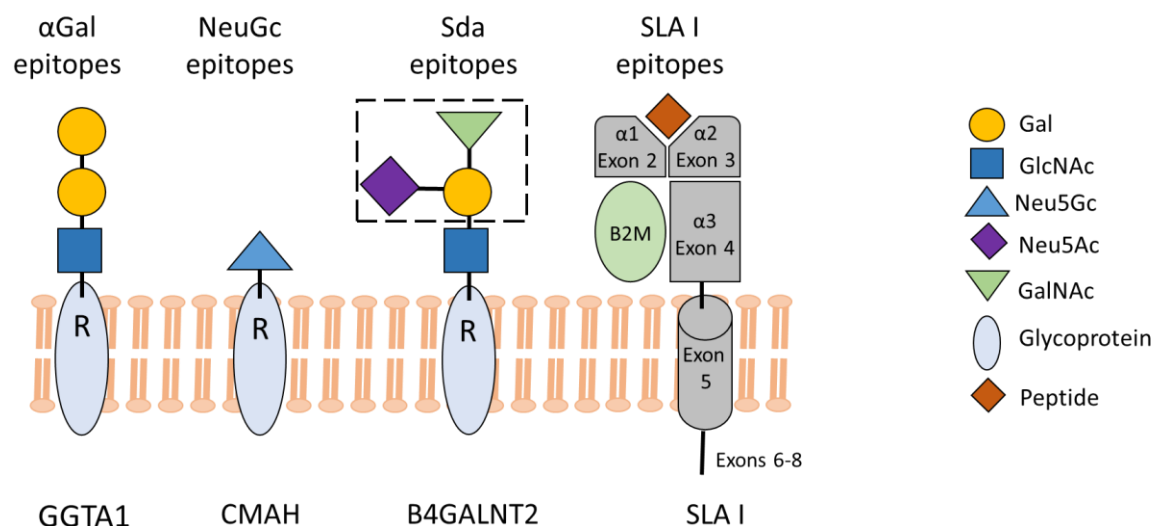


Figure 2: Structure of the major carbohydrate xenoreactive antigens α Gal, Neu5Gc and Sda, and the protein-based xenoreactive antigen SLA class I. Carbohydrate epitopes are found on glycoproteins and -lipids. Porcine SLA class I is a heterotrimeric complex that is composed of polymorphic SLA class I proteins, beta-2 microglobulin (B2M) and a short peptide.

1.1.2.2 Cellular rejection processes

Cellular rejection mechanisms are another obstacle to the function and survival of porcine xenografts in human recipients. In acute cellular xenograft rejection (ACXR) circulating mononuclear cells recognise the xenograft vascular endothelium and migrate into the xenogeneic tissue. This rejection process is thus characterised by cellular infiltrates of T- and B-lymphocytes, macrophages and natural killer (NK) cells and is associated with direct tissue damage. In contrast to humoral rejection processes, vascular thrombosis, interstitial haemorrhage, complement- and immunoglobulin deposition are very mild or absent in ACXR [21]. The activity of T cells, macrophages and NK cells is regulated through stimulatory and inhibitory receptor signalling. However, the inability of porcine molecules to mediate proper cell signalling leads to the activation of these immune cells [46] (Figure 3).

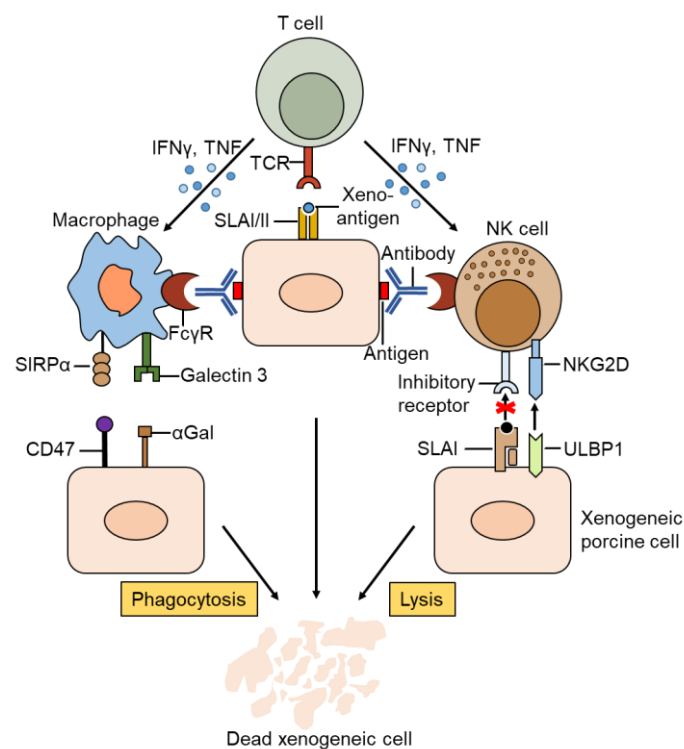


Figure 3: Cellular rejection mechanisms. NK cells, T cells and macrophages recognise xenogeneic porcine cells and are activated by improper signalling. Illustration adapted from Yang and Sykes, 2007 [20].

T cells are activated via direct or indirect pathways [47, 48], which both require interaction between the T cell receptor (TCR) and a complex of a donor-derived peptide and the main histocompatibility complex (MHC) on antigen presenting cells (APC). Complete T cell activation also requires a co-stimulatory signal between CD28 on T cells and the B7 ligands CD80 and CD86 on APCs [49]. Indirect activation occurs via interaction between recipient T cells and recipient APCs presenting a donor-derived peptide on the human leucocyte antigen complex. In contrast, direct activation is induced by binding of recipient T cells to donor APCs

presenting donor-derived peptides on the swine leucocyte antigen receptor [47, 50]. However, SLA class I and II molecules are not only expressed on APCs, but also on porcine vascular endothelial cells [51, 52], which are permanently present in the whole organ and mediate a long-term immunogenic potential by triggering direct activation of T cells. In addition, permanent expression of CD86 as well as induced expression of CD80 on porcine endothelial cells mediates co-stimulatory signals for direct T cell activation [53, 54].

Macrophages and NK cells also play important roles in cellular rejection of porcine xenografts. Beside activation via signals from the Fc γ receptor upon interaction with xenoreactive-antibody-targeted porcine cells [55], macrophages contribute to rapid clearance of transplanted xenogeneic cells via cytolytic and phagocytotic activity in an antibody- and complement-independent manner [56]. Macrophages are either activated by cytokines released from xenoreactive T cells, or by α Gal on porcine cells interacting with the activating receptor galectin-3 on macrophages [57, 58] (Figure 3).

Similar to macrophages, NK cells can be activated by cytokines released from xenoreactive T cells or by Fc γ receptor-mediated signals upon interaction of xenoreactive-antibody-targeted porcine cells with the Fc γ receptor on human NK cells [57, 59]. Direct activation also occurs by binding of UL 16 binding protein 1 (ULBP1) on donor cells to the activating receptor natural killer group 2D (NKG2D) on recipient NK cells [60] (Figure 3). Porcine ULBP1 is able to bind human NKG2D and thus activates human NK cells [61].

1.1.3 Strategies to prevent xenograft rejection

Effective inhibition of xenograft rejection requires a combination of various strategies. These include elimination of the major porcine xenoantigens responsible for HAR and AHXR. As both rejection mechanisms involve improper coagulation control and activation of the complement and the endothelium, overexpression of human complement- and coagulation regulators and endothelium protective genes offer means of xenoprotection. Cellular rejection processes can be inhibited via controlled immune cell regulation.

1.1.3.1 Elimination of porcine xenoreactive antigens

To date, α Gal, Neu5Gc and the porcine Sda epitopes are considered to be the major carbohydrate xenoantigens. SLA class I molecules also constitute xenoreactive antigens in HLA-sensitised patients [45].

Several strategies have been employed to remove α Gal epitopes and prevent HAR. These include immunoabsorption of α Gal epitopes [62] or overexpression of human 1,2-fucosyltransferase (H-transferase; HT) to compete GGTA1 for the enzyme substrate N-

acetyllactosamine [63, 64]. However the most effective means of removing α Gal epitopes is inactivation of the *GGTA1* gene. In 2002, two independent groups generated the first pigs with heterozygous *GGTA1* knockout using gene targeting and somatic cell nuclear transfer (SCNT) [65, 66]. One year later, the first homozygous *GGTA1* knockout pigs were derived, and showed a α Gal-negative phenotype [67]. Subsequent progress in genetic engineering has enabled the generation of several independent homozygous *GGTA1* knockout lines [68, 69]. Using organs from only *GGTA1* knockout animals for transplantation into baboons resulted in prevention of HAR and graft survival at a heterotopic position of up to 179 days for heart and 83 days for kidney [70, 71].

Inactivation of *GGTA1* in pigs largely prevents HAR and improves graft survival. It does however not affect AHXR, which is induced by elevated levels of antibodies against other porcine non-Gal epitopes [72]. Overcoming AHXR requires the elimination of further major carbohydrate xenoantigens, such as Neu5Gc and Sda. Neu5Gc epitopes can be removed by inactivating the synthesising gene *CMAH*. This was first demonstrated by Lutz et al. who used zinc finger nucleases (ZFN) to generate *GGTA1/CMAH* double-knockout pigs [73]. Xenoantigenicity can be reduced further by elimination of Sda epitopes by inactivating porcine *B4GALNT2*. *B4GALNT2* knockout pigs that additionally carried *GGTA1* and *CMAH* knockouts have been generated via CRISPR/Cas9 gene editing [42]. Cells from these triple-knockout pigs showed less human and non-human primate Immunoglobulin M (IgM) and Immunoglobulin G (IgG) antibody binding compared to *GGTA1* only, or *GGTA1/CMAH* double-knockout cells.

As mentioned previously, it is also advantageous to remove SLA class I molecules [45]. The porcine SLA class I receptor is a heterotrimeric complex presented at the cell surface composed of polymorphic SLA class I proteins, B2M and a short peptide [74, 75] (Figure 2). B2M is crucial for receptor assembly [76] and, because it is encoded by a single non-polymorphic gene, it has been identified as a suitable target to block surface SLA class I expression. The SLA class I genes can also be disrupted, but this is much more challenging because the several polymorphic SLA class I genes exist as multiple allelic variants [77]. However, the exon 4 region of each SLA gene is conserved and thus offers a possible target for gene inactivation. Exon 4 encodes the extracellular $\alpha 3$ domain, which is critical for assembly with B2M and transport to the cell surface [78, 79]. SLA class I deficient pigs have been generated by inactivation of either *B2M* [80] or multiple SLA class I alleles [81].

1.1.3.2 Complement regulation

Overexpression of human complement regulatory proteins (CRP) is a supplemental strategy to inhibit complement activation in antibody-mediated rejection, such as HAR and AHXR. The complement system is part of the innate immune system and can be activated via the classical, alternative, and the lectin pathways (Figure 4). Activation leads to the formation of the C3 and C5 convertases and ultimately the membrane attack complex (MAC) that initiates cell lysis by forming pores within the membrane [82]. Complement activation is tightly regulated by endogenous CRPs, such as CD46, CD55 and CD59. CD46 inhibits C3 convertase activation by acting as cofactor for C3b and C4b degradation [83]. CD55 inhibits both C3 and C5 convertases by accelerating their decay and preventing their assembly [84]. CD59 directly inhibits formation of the MAC by binding the C5b-C8 complex and disturbing the incorporation of C9 molecules which form the molecular pore [85]. Despite differing opinions regarding the species-specificity of CRPs [86, 87], there has been a strong focus on overexpression of human CD46, CD55 and CD59 in pigs to overcome uncontrolled complement activation after xenotransplantation. One prerequisite is that these human CRPs are expressed at reasonable levels. For CD55 it has been shown that at least five-fold the human endogenous CD55 level is required to efficiently inhibit complement activation [88]. Transgenic pigs that express the human complement regulators CD46, CD55 and CD59 alone [89-91] or in combination [92, 93] have been produced and shown to prolong graft survival and prevent HAR of porcine organs transplanted into baboons [89, 92, 94]. Furthermore, expression of CRPs in *GGTA1* knockout pigs improved graft survival compared to pigs carrying only a *GGTA1* knockout [95].

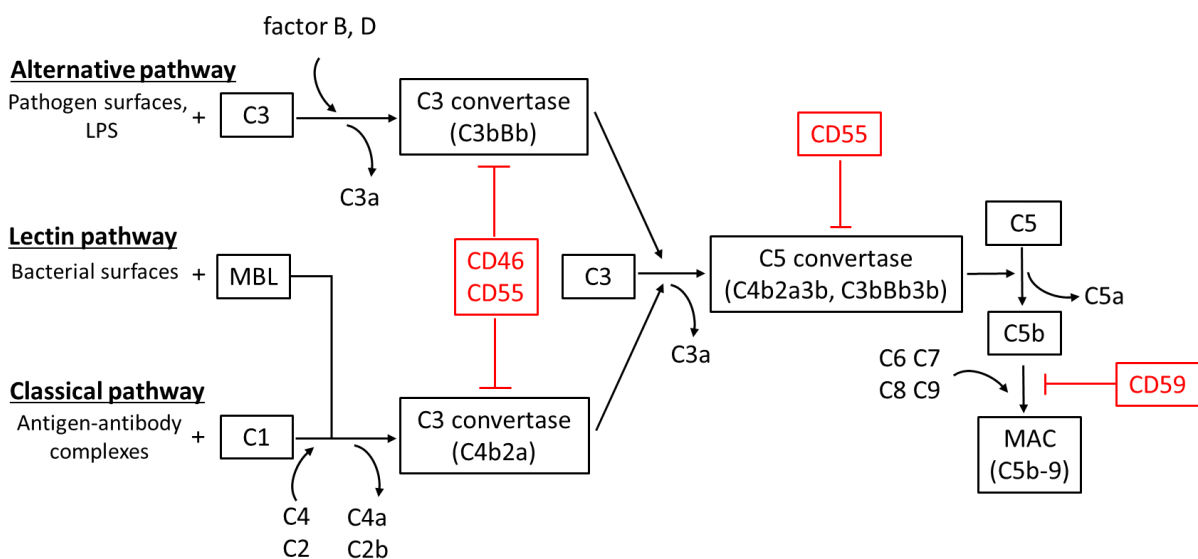


Figure 4: The complement cascade and its control by CD46, CD55 and CD59. Illustration adapted from Sarma et al. (2011) [82].

1.1.3.3 Endothelium protection

Additional protective transgenes with anti-inflammatory and anti-apoptotic properties are required to prevent the activation of the donor endothelium typical for AHXR.

An important molecule is human heme oxygenase 1 (HO-1), an inducible enzyme with anti-oxidative, anti-apoptotic and anti-inflammatory properties. HO-1 mediates degradation of heme into free iron, carbon monoxide (CO) and biliverdin (Figure 5). Free iron induces ferritin expression which protects cells from oxidative damage [96]. CO mediates anti-apoptotic and anti-inflammatory effects by activation of the p38 MAPK pathway [97, 98]. CO also induces vasodilation and inhibits platelet aggregation [99, 100]. Biliverdin is reduced to bilirubin which acts as a potent antioxidant and inhibits endothelial activation, complement activation and leukocyte infiltration [101, 102]. Fibroblasts from human HO-1 transgenic pigs are protected from H₂O₂ damage and tumor necrosis factor-alpha (TNF- α) and cycloheximide-mediated apoptosis is inhibited [103]. Petersen et al. further demonstrated significant protection of human HO-1 transgenic porcine aortic endothelial cells against TNF- α -mediated apoptosis and protection of human HO-1 transgenic kidneys against xenograft rejection during *ex vivo* perfusion with human blood [104].

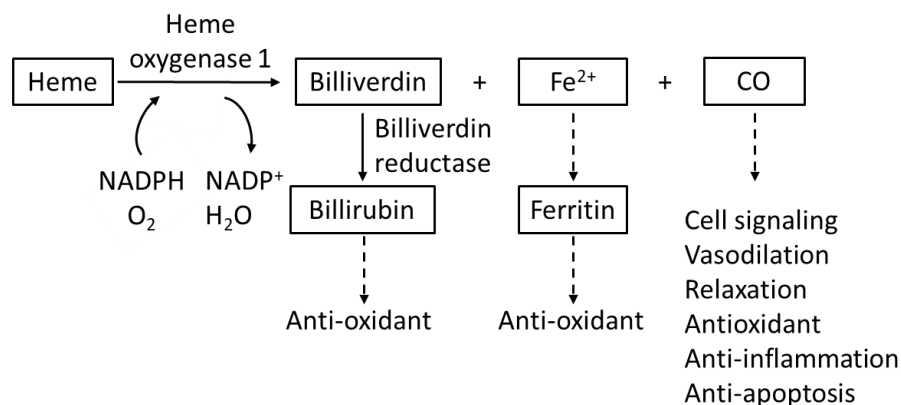


Figure 5: Biological functions of HO-1 mediating graft-protective properties. Illustration adopted from Babusikova et al. (2008) [105].

Another molecule with protective function against apoptotic and inflammatory stimuli is A20, also called tumour necrosis factor-alpha induced protein 3 (TNFAIP3). This cytoplasmatic zinc finger protein inhibits nuclear factor kappaB activation [106] and thereby prevents inflammatory responses mediated by pro-inflammatory cytokines such as TNF- α and Interleukin-1 β [107]. Porcine aortic endothelial cells (PAEC) from A20 transgenic pigs revealed significantly reduced TNF- α -mediated apoptosis compared to wild type PAECs and partial protection against CD59(Fas)L-mediated cell death. In addition, A20 transgenic pig hearts showed better myocardial function and a diminished leucocyte influx upon ischemia-reperfusion injury [108].

To date, there are two pig lines that express both endothelium-protective genes HO-1 and A20 in addition to other useful genetic modifications. Ahrens et al. generated a *GGTA1* knockout, HO-1- and A20 double-transgenic pig. Cells from this animal had reduced susceptibility to complement-mediated cell lysis, and *ex vivo* perfused kidneys showed prolonged organ survival [109]. Our group has also created a *GGTA1* knockout, CD46-, CD55-, CD59-, HO-1- and A20-transgenic pig line. PAEC cells from this pig showed reduced increase of caspase activity and diminished E-selectin expression compared to wild type on challenge with human TNF- α [68].

1.1.3.4 Coagulation control

Although HAR can be prevented using genetically modified pigs that lack α Gal expression and/or overexpress human complement regulators [70, 92, 95], graft loss due to improper coagulation control remains a major problem. Xenografts from *GGTA1*-knockout and/or human CRP transgenic pigs frequently revealed thrombotic microangiopathy characterised by progressive thrombocytopenia, increased clotting times, platelet-rich fibrin thrombi leading to intravascular coagulation, thrombosis and ultimately graft failure [70, 110-112]. There are two major reasons for coagulation disorders in xenografts. First, coagulation is a consequence of rejection, as also observed for AVR of allografts. Xenotransplantation of *GGTA1* knockout- or complement regulatory protein expressing pig organs into baboons revealed typical signs of AHXR, such as IgM, IgG and complement deposition as well as activated endothelial cells finally leading to coagulation disorders [111, 113]. Second, there are rejection-independent mechanisms that lead to improper coagulation control including molecular incompatibilities between porcine and human coagulation regulators.

A critical regulator of coagulation is the protein C/thrombomodulin pathway. Thrombomodulin is a transmembrane glycoprotein expressed on endothelial cells and encoded by the THBD gene [114]. By binding to thrombin, thrombomodulin inhibits the procoagulant activity of thrombin, blocking conversion of fibrinogen to fibrin. Thrombin now becomes an anticoagulant, increasing protein C activation more than 1000-fold [115, 116]. The activated protein C protease inactivates factor Va and VIIIa and thereby inhibits the enzymatic cascade responsible for clot formation [115, 117, 118] (Figure 6).

Thrombomodulin also has anti-inflammatory and complement-regulatory properties. The lectin-like domain directly inhibits complement activation via the classical and lectin pathways [119], provides protection from neutrophil-mediated tissue damage [120] and mediates degradation of the proinflammatory molecule high mobility group box 1 protein (HMGB1) [121]. Moreover, thrombomodulin is capable of inactivating the anaphylatoxic complement peptides C3a and C5a via activation of thrombin-activatable fibrinolysis inhibitor (TAFI) [122] (Figure 6).

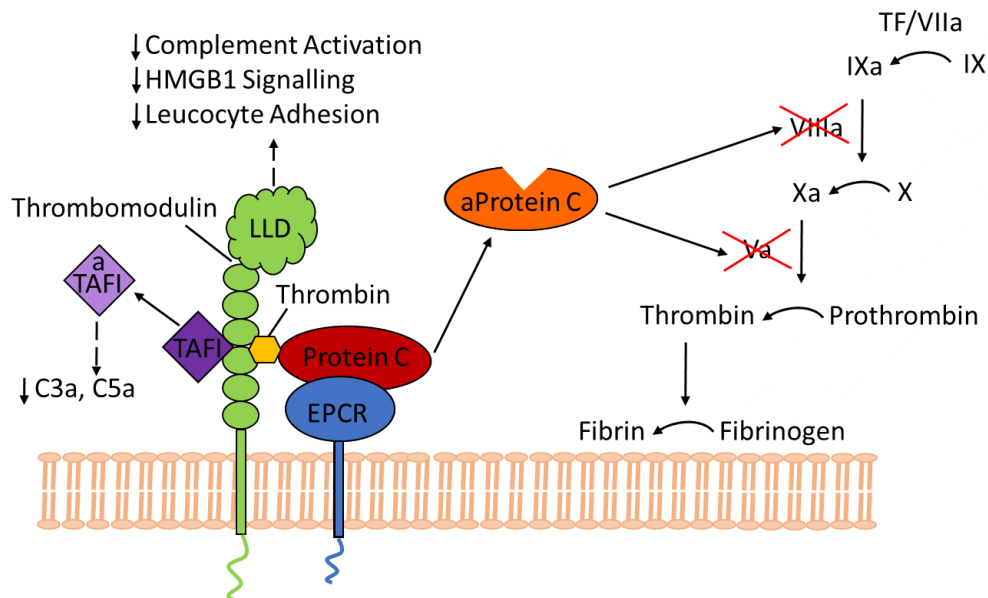


Figure 6: Functions of thrombomodulin. Thrombomodulin has anti-coagulant, anti-inflammatory and complement-regulatory properties. Protein C is activated (aProtein C) by the thrombin-thrombomodulin complex and suppresses coagulation by cleaving factors V/Va and VIII/VIIIa. Thrombin activatable fibrinolysis inhibitor (TAFI) is activated by thrombomodulin (aTAFI) and diminishes inflammation. Thrombomodulin's lectin-like domain (LLD) has direct anti-inflammatory and complement-regulatory properties. HMGB1 indicates high mobility group box-1. Illustration adapted from Foley et al. (2016) [123].

Despite the ability of porcine thrombomodulin to bind human protein C, it is a poor cofactor for the activation of human protein C [124], which leads to impaired coagulation control in xenografts. Pigs transgenic for human thrombomodulin revealed increased activated protein C production in an *in vitro* coactivity assay, but no disturbance of the porcine coagulation system [125]. Furthermore, endothelial cells from *GGTA1* knockout, human CD46 and human thrombomodulin transgenic pigs showed significantly increased clotting time in a coagulation assay with human whole blood [126]. *GGTA1* knockout plus human CD46 and human thrombomodulin transgenic pig hearts survived up to 945 days in a heterotopic location in baboons [127], and recently 195 days survival was reported in an orthotopic life-supporting baboon model [128].

Another important molecule in the protein C/thrombomodulin pathway is the transmembrane protein endothelial protein C receptor (EPCR), encoded by the *PROCR* gene. EPCR binds protein C and presents it to the thrombomodulin/thrombin complex, thereby enhancing protein C activation up to 20-fold *in vivo* [129-131]. As mentioned above, activated protein C is then able to inactivate factor Va and VIIIa and thus inhibit clot formation. EPCR also has cytoprotective and anti-inflammatory properties. [132-134]. Overexpression of human EPCR in porcine cells might be beneficial, as endogenous EPCR is mainly expressed on the endothelium of larger vessels. EPCR expression is poor or completely absent on small vessels,

such as capillaries, which are subject to microvascular thrombosis [135]. Transgenic expression of human EPCR in mice is associated with abundant transgene expression levels also on the microvasculature [136, 137]. Moreover it has beneficial effects on coagulation control and graft survival. In a heterotopic mouse-to-rat xenograft model hearts from human EPCR transgenic mice exhibited less haemorrhage and oedema as well as improved organ survival [137]. *Ex vivo* perfusion of pig lungs with human blood showed significantly prolonged survival for the EPCR, CD46 transgenic, *GGTA1* knockout combination [138].

1.1.3.5 Immune cell regulation

Control of the T cell response as well as macrophage- and NK cell activity are central to inhibiting cellular rejection.

The recipient's T cell response to a xenograft can be controlled by various means, such as preventing the interaction between MHC molecules and the T cell receptor, inhibiting costimulatory signals, or enhancing inhibitory signals (Figure 7). Interaction between porcine APCs and human T cells can be modulated by downregulation or elimination of the porcine SLA class I and II molecules on APCs. As outlined in section 1.1.3.1, the porcine SLA class I receptor is a heterotrimeric complex composed of polymorphic SLA class I molecules, B2M and a porcine peptide. Removal of this complex should lead to a lack of activated CD8⁺ T cells. SLA class I deficient pigs have been generated by inactivation of *B2M* [80], or SLA class I genes [81] and these pigs had reduced levels of CD8⁺ T cells [81]. Moreover, skin grafts of *B2M* knockout pigs exhibited prolonged survival on xenogeneic wounds compared to wild type skin grafts [80].

Porcine SLA class II expression can be modulated by class II transactivator (CIITA), the master regulator of MHC class II expression [139]. A dominant-negative variant of the CIITA gene (mutCIITA, CIITA-DN) leads to a lack of MHC class II expression in patients with severe immunodeficiency [140]. Expression of a human mutCIITA construct under the control of a ubiquitous CMV enhancer/chicken β -actin/rabbit globin (CAG) promoter and an endothelial specific Tie2-enhancer in pigs was associated with significantly reduced SLA class II expression on porcine APCs and complete suppression on porcine endothelial cells. In addition, a reduced human CD4⁺ T cell response to mutCIITA transgenic porcine endothelial cells was observed [141].

Besides direct interaction between APCs and T cells, T cell activation also requires a co-stimulatory signal. Inhibition of this signal can be used to block T cell activation (Figure 7). A potent co-stimulation inhibitor is the cytotoxic T lymphocyte-associated antigen 4 (CTLA4). This molecule inhibits the co-stimulatory interaction between CD28 on T cells and CD80/CD86 on APCs via binding to CD80 and CD86 with 100-fold higher affinity than the competing CD28

[142, 143]. Pharmaceutical treatment with CTLA4-Ig extended xenograft survival in mice [144]. Porcine CTLA4-Ig transgenic pigs have been generated, with porcine CTLA4 fused to the constant regions of human IgG1 [145]. These pigs showed ubiquitous CTLA4-Ig expression, and were severely immuno-compromised [145]. More restricted expression can avoid such deleterious effects. Pancreatic- β -cell specific expression of LEA29Y, a high affinity variant of CTLA4-Ig [146], provided complete protection of porcine β -cells against rejection in a humanised mouse model with no health problems [147].

An alternative means of inhibiting T cell activation is to enhance the inhibitory signals (Figure 7). The programmed cell death-1(PD-1)/PD- ligand 1 (PD-L1) signal pathway is crucial for suppressive immunoregulation and the maintenance of self-tolerance [148, 149]. PD-L1 molecules expressed on APCs bind to the PD-1 receptor on activated lymphocytes and mediate inhibitory signals that suppress proliferation of self-reactive T cells [150]. PD-L1 expression plays an important role in both allo- and xenotransplantation. Allografted islet cells from PD-L1 deficient mice had decreased survival [151]. Porcine cells that overexpress human PD-L1 diminished human immune responses *in vitro* [152, 153]. Cells from human PD-L1 transgenic pigs have recently been shown to have reduced capacity to stimulate proliferation of human CD4⁺ T cells, and to be partially protected from cell-mediated lysis by human cytotoxic effector cells [154].

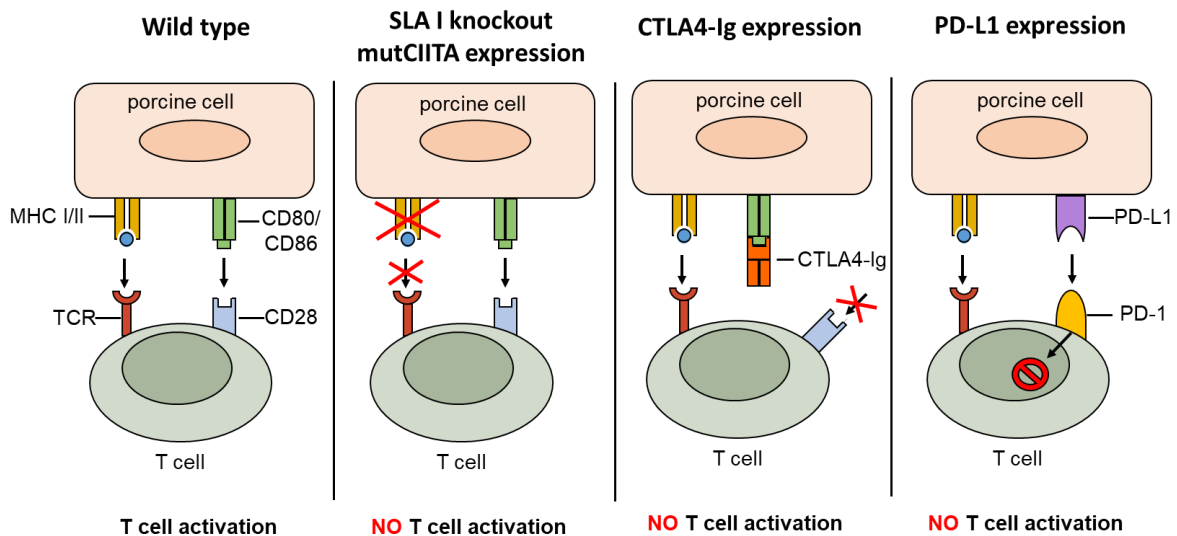


Figure 7: Strategies to prevent T cell activation. T cell activation can be diminished by preventing the interaction between MHC molecules and the T cell receptor (SLA class I knockout or mutCIITA overexpression), by inhibiting costimulatory signals (CTLA1-Ig overexpression), or by enhancing inhibitory signals (PD-L1 overexpression).

Inhibitory signals can also suppress the activation of macrophages and NK cells. The signal regulatory protein α (SIRP α) is an inhibitory receptor on macrophages that recognises the ubiquitously expressed surface molecule CD47. The SIRP α -CD47 interaction mediates inhibitory signals and prevents autologous phagocytosis by macrophages [155-157]. However,

porcine CD47 is not able to induce inhibitory SIRP α signalling in human macrophages due to inter-species incompatibility [46]. Effective blockade of macrophage activation thus requires overexpression of human CD47 in the porcine graft. *In vitro* experiments have revealed that human CD47 transfected pig cells lead to reduced phagocytosis by human macrophages [46].

Autologous NK cell activation is inhibited by binding of HLA-E to the inhibitory receptor NKG2A on NK cells [158]. However, porcine SLA I is not able to interact with the inhibitory receptor NKG2A on human NK cells, resulting in failure of the inhibitory signal and thus NK cell activation [159]. Overexpression of the human counterpart offers a possibility to inhibit macrophage activation. HLA-E/human B2M transgenic pigs have been generated and lymphoblasts as well as endothelial cells derived from these animals showed protection against human NK cell-mediated cytotoxicity [160].

1.2 Five-fold transgenic pigs for xenotransplantation

Various single- and multiple transgenic pigs have been generated for xenotransplantation [93, 161, 162]. A very promising pig line, which carries an array of five transgenes at a single locus, was previously generated at the Chair of Livestock Biotechnology (Figure 8A) [68]. This was generated by cotransfection of DNA vectors (Figure 8C) carrying genomic constructs of human CD46, CD59, CD55, and additional cDNA constructs of HO-1 and A20, screening cell clones for expression *in vitro*, and subsequent nuclear transfer. Analysis of the resultant pigs revealed transgene cointegration at a single site at chromosome 6q22 (Figure 8B). It was shown that this locus supports high levels of transgene expression, and these protect against immune responses *in vitro* and *ex vivo* [68]. Furthermore, the transgene array has proven to be stable over at least four generations and no negative health effects have been observed in heterozygous animals. This transgene array thus provides a good foundation onto which further transgenes can be added. Analysis of the array has shown that the CD46 transgene is present as a single copy. This transgene contains a 54 kb 3' flanking region that provides a promising site to place further transgenes. Such an approach would maintain the co-localisation of all transgenes at a single site and avoid segregation. This five-fold transgenic line is also a promising basis for the inactivation of the major xenoreactive antigens mentioned earlier.

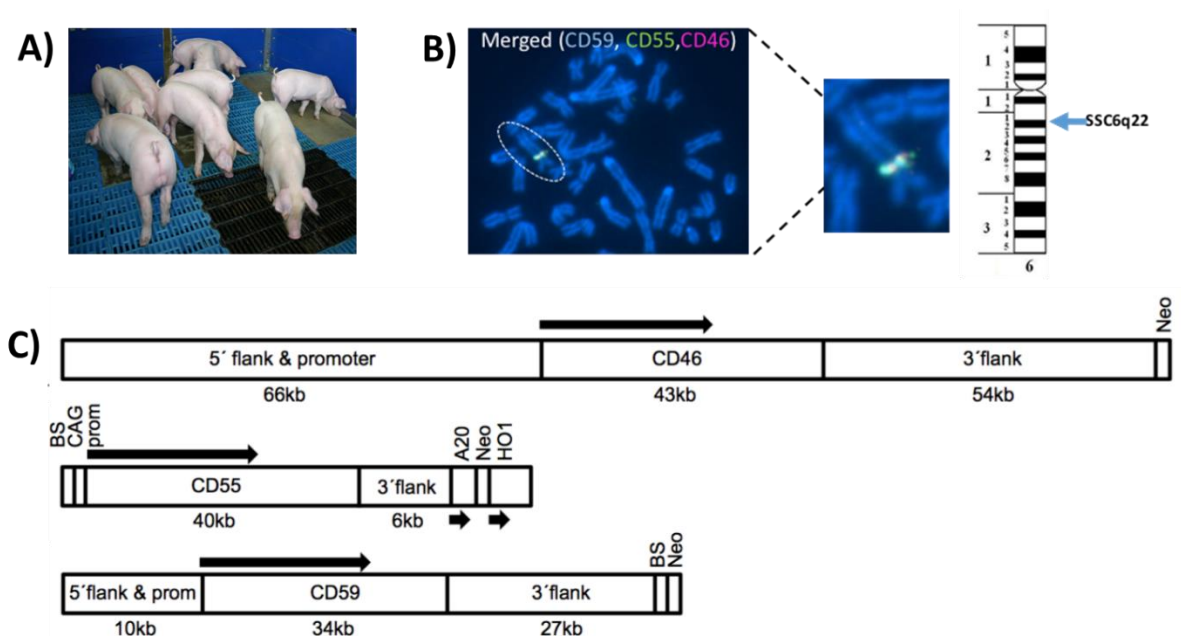


Figure 8: Five-fold transgenic pig line generated at the Chair of Livestock Biotechnology. (A) A herd of five-fold transgenic pigs expressing the human complement regulators CD46, CD55 and CD59 and the cDNA constructs HO-1 and A20. (B) Metaphase chromosome spreads and Q-banding of porcine kidney fibroblasts from a five-fold transgenic pig mapping the integration site of all cotransfected constructs to chromosome 6q22. (C) Constructs used to generate the five-fold transgenic pig line. Figures B and C adapted from Fischer et al. (2016) [68].

1.3 Genetic modification of livestock

1.3.1 Generation of genetically modified animals

1.3.1.1 Microinjection

The generation of genetically modified animals became a reality with the development of pronuclear microinjection. The first animals generated using this technique were mice [163], but this approach was soon extended to livestock species including pigs [164]. Pronuclear microinjection involves injection of exogenous DNA, such as a transgene expression construct, into the pronucleus of a fertilised oocyte which is then transferred into a surrogate mother (Figure 9). A proportion of the resultant animals carry the exogenous DNA stably integrated into the genome. This method is straightforward, but has several drawbacks. DNA microinjection is very inefficient in terms of the proportion of transgenic animals obtained, typically less than 3% for mice and only 1% in livestock species [164-166]. Besides potentially detrimental effects of transgene integration at random locations, further described in section 1.3.2, multiple independent integrations and mosaicism arising from delayed transgene integration hamper the analysis of transgenic animals and reduce the proportion of offspring with desired levels of transgene expression. Species that have opaque, high-lipid oocytes, such as pigs, also present particular problems in visualising the pronuclei. [167].

1.3.1.2 Somatic cell nuclear transfer

The availability of embryonic stem (ES) cells capable of undergoing genetic modification in culture and then colonising the germ line of chimeric mice has facilitated the efficient production of a huge range of genetically modified mice [168]. The lack of fully functional ES cells for livestock species motivated the development of somatic cell nuclear transfer (SCNT) as an alternative approach to generate genetically modified animals; to overcome the inefficiency of transgene microinjection and to enable more sophisticated modifications, notably gene targeting. SCNT involves placement of a genetically modified somatic cell into the perivitelline space of an enucleated MII oocyte. After fusion and embryo activation, embryos are transferred into a surrogate mother (Figure 9).

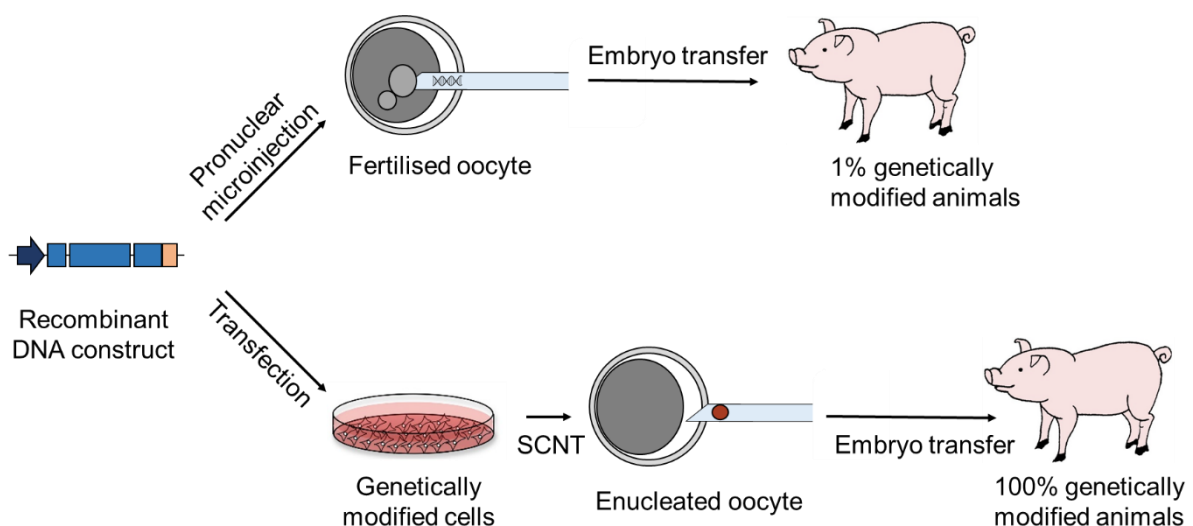


Figure 9: Generation of genetically modified animals by means of pronuclear microinjection and somatic cell nuclear transfer.

The first successful nuclear transfer experiments were carried out in sheep. The earliest experiments were based on the transfer of individual early embryonic blastomeres into enucleated MII oocytes [169]. This approach was however of limited usefulness for the generation of genetically modified animals due to the limited supply of donor blastomeres and their very short time in culture. Subsequently, SCNT-derived sheep were generated using cultured embryonic-, fetal- and adult donor cells [170, 171]. This provided the opportunity to introduce genetic modifications into the donor cells prior to SCNT. The first transgenic sheep generated via this procedure expressed coagulation factor IX from a random position [172] and soon after the first gene-targeted livestock animal was generated [173]. This approach was successfully extended to many other livestock species. With regard to pigs, three different groups almost simultaneously reported the successful cloning of pigs using somatic cells [8,

174, 175]. Lai et al. generated the first gene knockout pig, in which *GGTA1* was inactivated via homologous recombination [66]. This opened the possibility of xenotransplantation from genetically modified pigs.

SCNT provides several advantages over microinjection. Perhaps the most important is the ability to introduce precise sequence addition, deletion, or replacement via homologous recombination or more recently via gene editing. [176]. SCNT was also an advance for random transgene addition because, unlike DNA microinjection, 100% of the resulting animals carry the transgene. Culture of cells destined for nuclear transfer enables detailed analysis of the particular genetic modification in individual cell clones, and in some circumstances about transgene expression and functionality, with the most suitable cell clones used for SCNT. The sex of the resultant animals can also be predetermined by using male or female donor cells.

Nevertheless, there are some disadvantages associated with this method: SCNT is difficult, time-intensive and the efficiency, measured as development to term/ adulthood as a proportion of oocytes used, is very low (1-2%) [177, 178]. Moreover, cloned piglets have a high mortality- and morbidity rate, probably due to inadequate epigenetic reprogramming [177, 178].

1.3.2 Random transgene integration

Various strategies can be used to introduce single and multiple transgenes into the porcine genome. As especially xenotransplantation requires the addition of multiple transgenes, this section focuses on the integration of multiple transgenes by means of random integration. Perhaps the simplest approach is cotransfection of individual transgene constructs, which often cointegrate at a random location. This does however have some drawbacks. Transgene expression levels and expression patterns can vary considerably between different integration sites as a consequence of adjacent host regulatory sequences, such as enhancer, silencer or other promoter elements, and also the hetero- or euchromatin structure of the region [179, 180]. Random transgene integration also risks altering or damaging the function of endogenous genes, possibly leading to a deleterious phenotype. Also, cotransfected transgenes do not necessarily cointegrate, in which case they will segregate during breeding, reducing the proportion of multi-transgenic offspring.

To avoid transgene segregation, transgenes can be combined within a single vector. This approach has often used cDNA or minigene constructs expressed by a single promoter, to avoid the difficulties of manipulating large DNA fragments and to coordinate the expression of different transgenes. Transgene coding regions can be linked by 2A self-cleaving peptide systems [181-184], or by an internal ribosome entry sites (IRES) [185]. Both systems however have disadvantages. Expression of the downstream gene is often reduced using IRES [186,

187], and to a lesser extent with 2A systems [181, 182, 187]. There are also reports that 2A peptide cleavage can be incomplete [182], with possible cytotoxic effects.

Previous work at the Chair of Livestock Biotechnology adopted an approach termed 'combineering'. As outlined more detailed in section 1.2, this was based on independent transgene constructs grouped in large bacterial artificial chromosome (BAC) and phage artificial chromosome vectors which cointegrated a previously unknown site within the porcine genome (6q22) that supports abundant and ubiquitous expression [68]. Whether this integration affected any endogenous genes remains to be seen, but multiple generations of heterozygous animals have so far shown no deleterious effects.

1.3.3 Precise genetic modification

The alternative to random transgene integration is precise transgene placement at a predetermined site. There are several means to achieve this, including gene targeting by homologous recombination [173] and site-specific recombination [188]. Targeted transgene placement has several advantages over random integration. Integration sites can be chosen that avoid disruption of endogenous genes and possible effects on health and development. A suitable site will also be free of the influence of local regulatory elements that may affect transgene expression, and would ideally support abundant and ubiquitous expression. However, gene targeting by homologous recombination is a rare event compared to random integration in somatic cells, making targeting efficiencies low for many loci [189] and targeted transgene placement technically challenging.

1.3.3.1 Gene targeting via homologous recombination

Homologous recombination is naturally a DNA repair mechanism that is activated by the presence of a double-strand break (DSB) and uses a homologous DNA sequences to precisely repair the break. In nature this is normally the homologous sister chromatid, but providing an exogenous homologous DNA fragment allows experimental gene targeting. A typical classical gene targeting vector consists of the transgene or mutation of interest and some form of selection cassette, all flanked by two homologous 'arms' corresponding to the target locus. Gene targeting has successfully been carried out in various cell types from several livestock species and used in combination with nuclear transfer to produce gene targeted animals [65, 173].

However, gene targeting by homologous recombination is a very rare event in primary mammalian cells with total targeting efficiencies of only one correctly targeted cell clone out 10^6 - 10^7 cells [189, 190]. Various approaches have been shown to enhance homologous recombination frequencies, such as linearisation of the targeting vector and maximising the

length of the homology arms [191, 192]. 'Promotor trap' selection using a promoterless neomycin construct can significantly enrich the proportion of correctly targeted clones by reducing the proportion of antibiotic-resistant random integrants [193, 194]. However, the most effective way of increasing the frequency of homology-directed repair (HDR) is to introduce a DSB at the target region [195, 196].

1.3.3.2 Genome editing by site-specific nucleases

In recent years a series of artificial site-specific nucleases have been developed to enable gene manipulation by introduction of a double-strand break at a predetermined genomic location, an approach termed gene or genome editing. These include Zinc Finger Nucleases (ZFN), Transcription Activator-like Effector Nucleases (TALEN) and the Clustered Regulatory Interspaced Short Palindromic Repeats (CRISPR) nucleases. Introduction of a DSB within the genome of a eukaryotic cell can activate two distinct repair mechanisms (Figure 10). Most frequently, non-homologous end joining (NHEJ) is initiated which rejoins both DNA ends without any repair-template. This is an error-prone mechanism and end-rejoining often introduces small insertions and deletions (indels) that can affect gene function, e.g. by shifting the translational reading frame. This pathway is thus a useful way of generating a loss-of-function mutation in a particular gene. The second mechanism, HDR, requires a template with homologous arms flanking the double-strand break site. An exogenous DNA fragment can thus be used to introduce precise insertions, point mutations or deletions. However, HDR is less frequent than NHEJ [197].

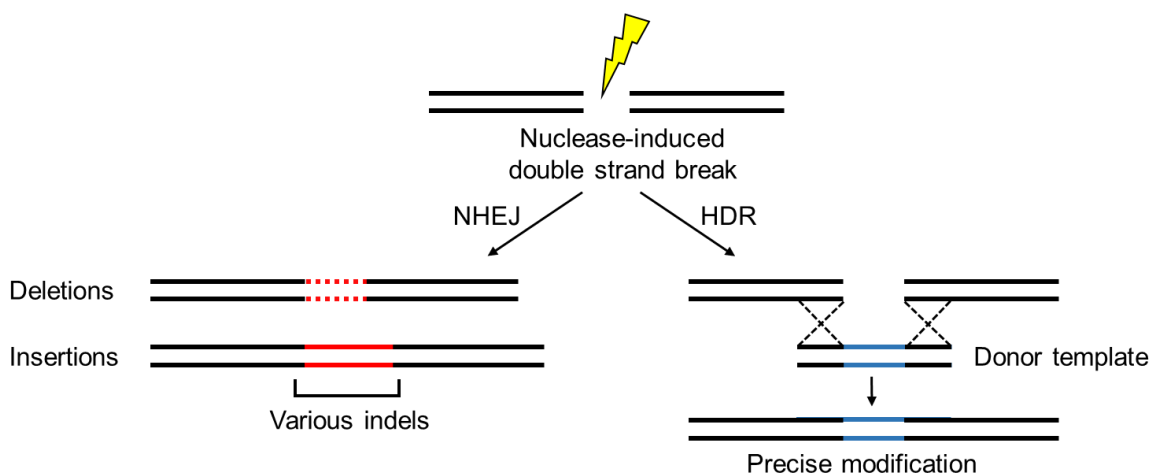


Figure 10 Double-strand break repair mechanisms in eukaryotic cells. Non-homologous end joining (NHEJ) as an error-prone mechanism introduces various indels, whereas homology directed repair (HDR) uses a donor template for double-strand repair. Illustration adapted from Sander et al (2014) [198].

Early methods of gene editing include protein-based systems, such as ZFN and TALENs, which are artificial proteins consisting of a pair of engineered DNA binding domains each fused to a non-specific FokI nuclease monomer. Binding of the ZFN/TALEN pair to their target motifs leads to dimerisation and activation of the FokI domains and cleavage at the target site [199, 200]. However, the generation of functional highly specific ZFN and TALENs is a time- and cost intensive undertaking. Gene editing using an RNA-guided endonuclease is far simpler and is now the method of choice for most applications.

The CRISPR/CRISPR-associated (Cas) systems were first discovered in bacteria and archaea where they provide sequence-specific adaptive protection against foreign DNA, such as plasmids and viruses [201, 202]. The *Streptococcus pyogenes* type II CRISPR system has provided the most widely used genome editing tool. A complex consisting of CRISPR-RNA (crRNA) and trans-activating crRNA (tracrRNA) guides Cas9 nuclease to the target site where the enzyme introduces a site-specific DSB [203] (Figure 11). Site-specific cleavage is determined by a 20 bp sequence (gRNA) at the 5' end of the crRNA which is complementary to the target site. In addition, site-specific cleavage requires a short protospacer adjacent motif (PAM) directly downstream of the target site which consists of a NGG-motif [203]. Thus, any genomic sequence of the form 5'-X₂₀NGG-3' can be targeted using the CRISPR/Cas9 system, where X₂₀ corresponds to the gRNA sequence and N is any base. Fusion of the crRNA 3' terminus to the tracrRNA 5' terminus results in a single chimeric RNA molecule, termed single guide RNA (sgRNA), which is sufficient to direct a site-specific double-strand break by Cas9 [203]. This two-component system provides a simple and versatile RNA-directed gene editing tool that was rapidly adopted in a multitude of species, including yeast, fruit fly, zebrafish, mouse, pig and human [42, 204-208]. Importantly, the CRISPR/Cas9 system also enables multiplex genome editing, targeting several genes simultaneously [42, 207].

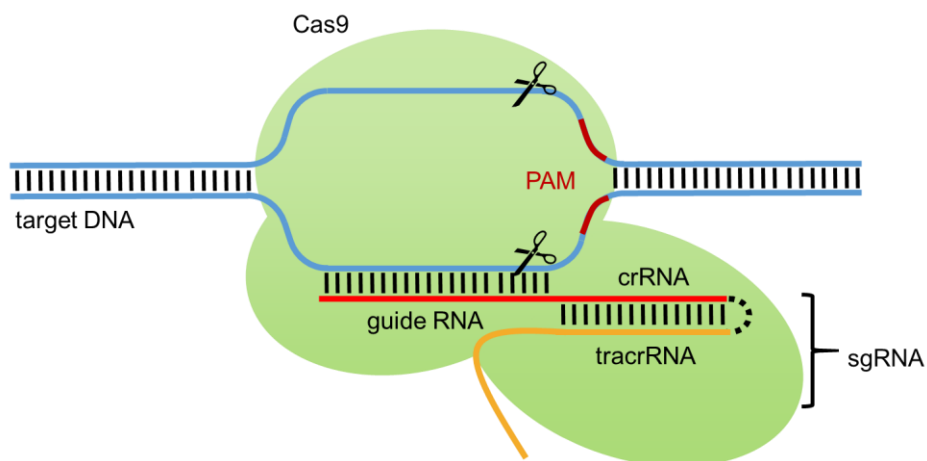


Figure 11: The CRISPR/Cas9 system as potent tool for genome editing. Illustration adopted from Redman et al. (2016) [209].

1.3.3.3 Transgene insertion via site-specific recombinases

Site-specific recombinases offer another means of placing a transgene cassette at a predetermined site. These enzymes catalyse recombination at specific sites and cause insertions, deletions or inversions [210]. Site-specific recombinases can be classified into two evolutionary and mechanistically distinct types: tyrosine- and serine- recombinases [211, 212]. While tyrosine recombinases, such as Cre and Flp, are well suited for efficient deletion of DNA fragments flanked by two directly repeated recombination sites, these are inefficient for transgene placement as the excision reaction is strongly favoured [213]. Serine recombinases, such as ϕ C31- or Bxb1 integrases, provide a better tool for targeted transgene insertion [214]. Serine recombinases act unidirectionally and mediate recombination between a phage attachment site (attP) and a bacterial attachment site (attB) [215, 216]. These sites are two distinct short DNA sequences originally located on phage- and bacterial genomes. Serine recombinase-mediated recombination between attP and attB promotes integration of transgenes [217, 218] within the former attP site and leads to the generation of hybrid attL and attR sites, each consisting of a half attP and attB site (Figure 12). As the newly generated sites are not able to form a stable synaptic complex promoting recombination, the reaction is irreversible [219, 220].

Mulholland et al. developed a strategy for efficient and rapid site-specific transgene placement using the Bxb1 integrase [214]. This approach comprises CRISPR/Cas9-assisted integration of an attP site, also termed multifunctional integrase (MIN) tag, within a predetermined site of the host genome. In a second step, Bxb1 mediates recombination between the genomic MIN/attP site and an attB site on a vector used for transfection which additionally harbours a transgene of interest (Figure 12). This recombination process is associated with highly efficient transgene integration within the MIN/attP site. Studies conducted in various mammalian cells revealed efficiencies of 92% in chinese hamster ovary cells [221], 67% in murine embryonal stem cells [214] and more than 80% in human cells [222].

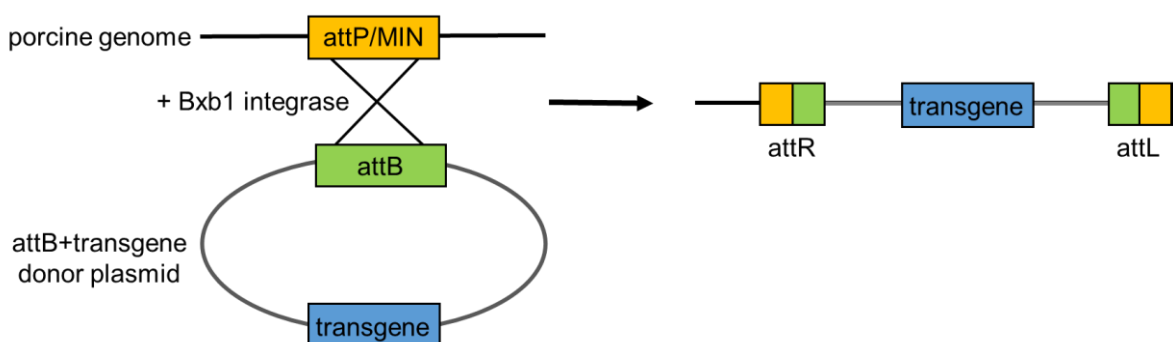


Figure 12: Schematic outline of Bxb1 serine recombinase- mediated transgene placement in the porcine genome. Illustration adapted from Fish et al. (2007) [223].

1.3.4 *In vivo* genome editing

Despite the power and versatility of the CRISPR/Cas9 system, the generation of gene-edited pigs remains challenging due to the continued reliance on somatic cell nuclear transfer [224]. To circumvent this bottleneck, attempts have been made to carry out genome editing in *in vivo*. Direct *in vivo* genome editing was first carried out in mice by adeno-associated virus- (AAV) or lentivirus-mediated delivery of an expression vector containing both Cas9 and sgRNAs and revealed successful gene editing in a variety of different tissues, such as lung, liver and heart [225-227]. However, these experiments achieved relatively low rates of gene editing as the combination of the commonly used *Streptococcus pyogenes* Cas9 variant (SpCas9) together with a CMV- or EF1 α -promoter and other regulatory sequences exceeded the packaging limit of both lentiviruses and AAVs. Transgene vectors exceeding the packaging capacity of AAVs (~5.2 kb) are truncated during the packaging process which leads to low transgene expression upon transduction [228]. Lentiviral delivery requires high virus titres to mediate reasonable transgene expression, however these decrease with increasing size of the transgene vector to be packaged [229]. A more efficient approach was provided by the development of an intein-mediated split-Cas9 system, where the N- and C-terminal halves of SpCas9 are each fused to a corresponding intein sequence and the constructs distributed on two separate vectors [230]. This bypasses the packaging limit of AAVs, but requires co-delivery and -expression of both fusion-constructs to reconstitute a functional SpCas9 protein within a single cell [230]. Such experiments also incur a safety risk and have to be carried out under S2 conditions. Where the animal target DNA sequence is closely related to that in humans, accidental exposure to Cas9 and sgRNAs could cause somatic mutations in those cells affected.

Animals that express the hSpCas9 component could provide a suitable platform for efficient and safe CRISPR/Cas9-mediated *in vivo* genome editing. Only the sgRNA component needs to be delivered into these animals via lentiviruses or AAVs, and these would be harmless on accidental exposure. Mice have been generated that express a CAG-driven hSpCas9 transgene either ubiquitously, or in a tissue-specific manner from the *Rosa26* locus [231]. These mice were fertile, revealed no signs of morphological abnormalities and could be bred to homozygosity. Moreover, both *in vivo* and *ex vivo* genome editing was achieved in a variety of different cells and tissues from these mice by AAV-, lentivirus-, or particle-mediated delivery of the sgRNAs [231].

1.4 Porcine *ROSA26* locus

The *Rosa26* locus was first identified in mice. In 1991, Friedrich and Soriano used a β -geo promoter trap construct for random retroviral gene trapping in mouse ES cells and generated the ROSA β geo26 (Reverse Orientated Splice Acceptor β geo clone 26) mouse strain [232].

This strain revealed ubiquitous transgene expression without any adverse effects on development and physiology [233]. Analysis of the integration region showed that the trapped gene, termed *Rosa26*, contains three non-coding transcripts (NR_027008.1, NR_027009.1 and NR_027010.1) with unknown function. The *Rosa26* locus supports abundant expression of transgenes placed within it and is now widely used for targeted transgene placement in mice [234, 235].

The human and rat orthologues of *ROSA26* were subsequently identified and revealed similar useful properties as the murine counterpart [236, 237]. Due to a high degree of conservation between the individual species, the porcine *ROSA26* locus was identified in previous work conducted at the Chair of Livestock Biotechnology [238]. Porcine *ROSA26* is located on chromosome 13 and reveals a similar genomic organisation as the human and murine loci. Porcine *ROSA26* shares a bidirectional promoter with its downstream neighbour *SETD3* and overlaps in a tail-to-tail (3' → 3') fashion with the upstream gene *THUMPD3*. The gene itself has four exons and expresses at least two non-coding transcripts comprising two and four exons. Targeting of *ROSA26* in pigs revealed ubiquitous reporter gene expression in all tissues analysed without any adverse effects regarding development and physiology [238].

1.5 Objectives

The overall aim of this work was to improve genetic models, especially for xenotransplantation and *in vivo* genome editing, by means of targeted transgene placement and by targeted inactivation of endogenous porcine genes.

As clinically effective xenodonor pig will require multiple genetic modifications, it is important to group transgenes at a single site to avoid transgene segregation during breeding and obtain a high proportion of multi-transgenic pigs. The remit of the project was to explore various means of assembling a multi-transgene array at a single genomic locus. These included successive assembly of a transgene battery via “transgene stacking”, or simultaneous placement of a multiple-transgene vector. The porcine *ROSA26* locus and a site adjacent to the transgene-array at locus 6q22 available at the Chair of Livestock Biotechnology were the integration sites of choice. A further aim was to develop efficient means of inactivating endogenous xenoreactive porcine genes. The idea was to use the CRISPR/Cas9 system for targeted single- and multiplexed gene editing, thereby removing the major xenoreactive antigens.

An additional objective was to develop a tool for *in vivo* porcine genome editing by generating a pig line with ubiquitous Cas9 expression at reasonable expression levels. The approach to be taken was based on targeted placement of a humanised version of Cas9 from *streptococcus pyogenes* (hSpCas9) at the porcine *ROSA26* locus.

2 Materials and methods

2.1 Materials

2.1.1 Chemicals

Table 1: Chemicals

Name	Source
Acetic acid (C ₂ H ₄ O ₂)	AppliChem, Darmstadt, GER
Advanced protein assay reagent	Cytoskeleton, Denver, CO, USA
Agarose	Sigma-Aldrich, Steinheim, GER
Ammonium acetate (C ₂ H ₇ NO ₂)	Riedel-de Haen, Seelze, GER
Ammonium chloride (NH ₄ Cl)	Sigma-Aldrich, Steinheim, GER
Ammonium persulphate ((NH ₄) ₂ S ₂ O ₈)	Carl Roth, Karlsruhe, GER
Biocoll, density 1.077 g/ml	Biochrom, Berlin GER
Boric acid (H ₃ BO ₃)	AppliChem, Darmstadt, GER
Bromophenol blue	Sigma-Aldrich, Steinheim, GER
BSA (fraction V)	Biomol, Hamburg, GER
Calcium chloride dihydrate (CaCl ₂ x 2 H ₂ O)	Sigma-Aldrich, Steinheim, GER
Cycloheximide	Sigma-Aldrich, Steinheim, GER
DAB enhanced liquid substrate system	Sigma-Aldrich, Steinheim, GER
Deoxynucleotide (dNTP) solution mix	New England Biolabs, Frankfurt, GER
DEPC-treated water (H ₂ O)	Thermo Fisher Scientific, Waltham, MA, USA
Droplet generator oil for probes	Bio-Rad Laboratories, Munich, GER
DTT (C ₄ H ₁₀ O ₂ S ₂)	Omnilab-Laborzentrum, Bremen, GER
Dynabeads biotin binder	Thermo Fisher Scientific, Waltham, MA, USA
EDTA	AppliChem, Darmstadt, GER
Ethanol (EtOH) absolute	Fisher Scientific, Loughborough, GBR
Ethanol (EtOH) denatured	CLN GmbH, Niederhummel, GER
Formaldehyde solution 37% (CH ₂ O)	AppliChem, Darmstadt, GER
Gel loading dye, purple (6x)	New England Biolabs, Frankfurt, GER
Glycerol anhydrous (C ₃ H ₈ O ₃)	AppliChem, Darmstadt, GER
Glycine (C ₂ H ₅ NO ₂)	Carl Roth, Karlsruhe, GER
HEPES	Sigma-Aldrich, Steinheim, GER
human TNF- α	PeptoTech, Hamburg, GER
Hydrochloric acid 37% (HCl)	Sigma-Aldrich, Steinheim, GER
Hydrogen peroxide (H ₂ O ₂)	Carl Roth, Karlsruhe, GER
IPTG	Bioline, Luckenwalde, GER
Isolectin B4 (<i>Bandeiraea simplicifolia</i>), (biotin conjugate)	Enzo Life Sciences, Farmingdale, NY, USA
Magnesium chloride hexahydrate (MgCl ₂ x 6 H ₂ O)	Carl Roth, Karlsruhe, GER
Methanol (CH ₃ OH)	Sigma-Aldrich, Steinheim, GER

Milk powder, blocking grade	Carl Roth, Karlsruhe, GER
Neu5Gc assay blocking solution (40x)	Biolegend, San Diego, CA, USA
Normal goat serum	PAA Laboratories, Pasching, AUT
peqGREEN dye	VWR International, Ismaning, GER
Phenol:chloroform:isoamylalcohol (25:24:1)	AppliChem, Darmstadt, GER
Pierce ECL Plus western blotting substrate	Thermo Fisher Scientific, Waltham, MA, USA
Ponceau S	Sigma-Aldrich, Steinheim, GER
Porcine serum	PAA Laboratories, Pasching, AUT
Potassium bicarbonate (KHCO ₃)	Sigma-Aldrich, Steinheim, GER
Potassium chloride (KCl)	Carl Roth, Karlsruhe, GER
Propan-2-ol (C ₃ H ₈ O)	Fisher Scientific, Loughborough, GBR
Proteinase inhibitor cocktail (PIC), cOmplete tablets, Mini EASY pack	Roche Diagnostics, Mannheim, GER
Roti-Histokitt	Carl Roth, Karlsruhe, GER
Rotiphorese gel 40 (29:1)	Carl Roth, Karlsruhe, GER
SDS	Omnilab-Laborzentrum, Bremen, GER
Silicon grease	Obermeier, Bad Berleburg, GER
Sodium acetate (C ₂ H ₃ NaO ₂)	AppliChem, Darmstadt, GER
Sodium azide (NaN ₃)	Merck, Darmstadt, GER
Sodium bicarbonate (NaHCO ₃)	Sigma-Aldrich, Steinheim, GER
Sodium chloride (NaCl)	AppliChem, Darmstadt, GER
Sodium dihydrogen phosphate monohydrate (NaH ₂ PO ₄ ·H ₂ O)	Merck, Darmstadt, GER
Sodium hydroxide (NaOH)	Sigma-Aldrich, Steinheim, GER
Sodium lactate 60% (C ₃ H ₅ NaO ₃)	Sigma-Aldrich, Steinheim, GER
Sucrose (C ₁₂ H ₂₂ O ₁₁)	Carl Roth, Karlsruhe, GER
TEMED (C ₆ H ₁₆ N ₂)	Carl Roth, Karlsruhe, GER
Tris, ultrapure (C ₄ H ₁₁ NO ₃)	AppliChem, Darmstadt, GER
Tris-HCl (C ₄ H ₁₁ NO ₃ ·HCl)	Sigma-Aldrich, Steinheim, GER
Tri-sodium citrate dihydrate (C ₆ H ₅ NaO ₇ ·2 H ₂ O)	AppliChem, Darmstadt, GER
Triton X100	Omnilab-Laborzentrum, Bremen, GER
Trypan blue solution	
Tween 20	Sigma-Aldrich, Steinheim, GER
X-Gal	Bioline, Luckenwalde, GER
X-ray developer T32	Calbe Chemie GmbH, Calbe, GER
X-ray fixing solution Superfix 25	Tetenal Europe, Norderstedt, GER
Xylene, mixture of isomers for histology	AppliChem, Darmstadt, GER

2.1.2 Enzymes and enzyme buffers

Table 2: Enzymes and enzyme buffers

Name	Source
Antarctic phosphatase	New England Biolabs, Frankfurt, GER
Calf intestine phosphatase	New England Biolabs, Frankfurt, GER
ddPCR supermix for probes (no dUTP) 2x	Bio-Rad Laboratories, Hercules, CA, USA
DNA polymerase I, large (Klenow) fragment	New England Biolabs, Frankfurt, GER
Exonuclease I	New England Biolabs, Frankfurt, GER
GoTaq G2 DNA polymerase, 5x Green GoTaq reaction buffer	Promega, Mannheim, GER
PCR Extender polymerase mix, 10x tuning buffer	5 Prime, Hilden, GER
Proteinase K (20 mg/ml)	Sigma-Aldrich, Steinheim, GER
Q5 high-fidelity DNA polymerase, 5x Q5 reaction buffer, 5x Q5 high GC enhancer	New England Biolabs, Frankfurt, GER
Restriction endonucleases, Restriction buffers 1.1, 2.1, 3.1, CutSmart	New England Biolabs, Frankfurt, GER
RNAse A	Sigma-Aldrich, Steinheim, GER
SuperScript III/IV reverse transcriptase, Superscript III RT 5x first strand buffer/ 5x SSVI buffer	Invitrogen, Karlsruhe, GER
T4 DNA ligase T4 DNA ligase buffer (10x)	New England Biolabs, Frankfurt, GER
TaqMan Fast Universal PCR master mix	Life Technologies, Carlsbad, CA, USA
AccuStart Taq DNA polymerase HiFi 10x HiFi PCR buffer	QuantaBio, Beverly, MA, USA
2x FastGene Optima HotStart ready mix	NIPPON Genetics Europe, Düren, GER

2.1.3 Kits

Table 3: Kits

Name	Source
Caspase-Glo 3/7 assay system	Promega, Mannheim, GER
CytoBuster protein extraction reagent	Merck KGaA, Darmstadt, GER
GenElute mammalian genomic DNA miniprep kit	Sigma-Aldrich, Steinheim, GER
InnuSPEED tissue RNA kit	Analytic Jena, Jena, GER
MEGAclear kit	Ambion, Austin, TX, USA
MEGAshortscript T7 kit	Ambion, Austin, TX, USA
Mix2Seq kit	Eurofins, Ebersberg, GER
mMESSAGE mMACHINE T7 kit	Ambion, Austin, TX, USA

NucleoBond Xtra Maxi kit	Macherey-Nagel, Düren, GER
NucleoBond Xtra Midi kit	Macherey-Nagel, Düren, GER
PlateSeq DNA kit	Eurofins, Ebersberg, GER
Poly(A) tailing kit	Ambion, Austin, TX, USA
SurePrep RNA/DNA/protein purification kit	Fisher Scientific, Hampton, NH, USA
SurePrep true total RNA purification kit	Fisher Scientific, Hampton, NH, USA
T-PER tissue protein extraction reagent	Thermo Fisher Scientific, Waltham, MA, USA
Vectastain Elite ABC-HRP kit (peroxidase, standard)	Vector Laboratories, Burlingame, CA, USA
Wizard SV gel and PCR clean-up system	Promega, Mannheim, GER

2.1.4 Cells

2.1.4.1 Bacterial strains

Table 4: Bacterial strains

Name	Genotype	Source
E. coli ElectroMAX DH10B	<i>F⁻mcrA</i> $\Delta(mrr\text{-}hsdRMS\text{-}mcrBC)$ $\Phi80lacZ\Delta M15$ $\Delta lacX74$ <i>recA1</i> <i>endA1</i> <i>araD139</i> $\Delta(ara, leu)7697$ <i>galJ galK</i> λ <i>rpsL nupG</i>	Thermo Fisher Scientific, Waltham, MA, USA

2.1.4.2 Eukaryotic cells

Table 5: Eukaryotic cells

Cell type	Genotype	Source
Porcine fetal fibroblasts (251113_4)	Wild type	Chair of Livestock Biotechnology, TUM, Freising, GER
Porcine kidney fibroblasts (several preparations)	Wild type	Chair of Livestock Biotechnology, TUM, Freising, GER
Porcine kidney fibroblasts (1706)	CD46, CD55, CD59, A20, HO-1	Chair of Livestock Biotechnology, TUM, Freising, GER
Porcine kidney fibroblasts (74)	ROSA26-HO-1	Chair of Livestock Biotechnology, TUM, Freising, GER
Porcine kidney fibroblasts (814)	CD46, CD55, CD59, A20, HO-1, <i>GGTA1</i> ^{-/-} , <i>CMAH</i> ^{+/-} ,	Chair of Livestock Biotechnology, TUM, Freising, GER
Human bone-marrow derived mesenchymal stem cell line (SCP1)	hTERT-immortalised	Chirurgische Klinik und Polyklinik Innenstadt, LMU, München, GER

Swine testis cell line (ST)	wild type	Kindly provided by Prof. Jochen Seißler, Diabetes Center, LMU, München, GER
-----------------------------	-----------	---

2.1.5 Antibodies

Table 6: Antibodies

Name	Source	Applied dilution
Primary antibodies		
Biotin mouse anti-human CD55 clone IA10, #555692	BD Bioscience, Franklin Lakes, NJ, USA	1:25 (FACS)
Isolectin B4 (Bandeiraea simplicifolia),(FITC conjugate)	Enzo Life Sciences, Farmingdale, NY, USA	1:100 (FACS)
Monoclonal anti-GAPDH antibody produced in mouse; clone GAPDH-71.1	Sigma-Aldrich, St. Louis, MO, USA	1:3000 (WB)
PE anti-human CD46 antibody; clone TRA-2-10 (#352401)	BioLegend, San Diego, CA, USA	1:100 (FACS)
PE anti-human CD59 antibody; clone p282(H19) (#304707)	BioLegend, San Diego, CA, USA	1:100 (FACS)
Polyclonal guinea pig anti-insulin (A0564)	Dako, Carlinteria, CA, USA	1:400 (IF)
Purified anti-Neu5Gc antibody (Poly21469) chicken polyclonal IgY	BioLegend, San Diego, CA, USA	1:10000 (WB) 1:250 (FACS)
Purified mouse anti-human CD55 clone IA10, #555691	BD Bioscience, Franklin Lakes, NJ, USA	1:100 (IHC, IF)
Secondary antibodies		
Donkey anti-chicken IgY-FITC	Jackson ImmunoResearch, West Grove, PA, USA	1:100 (FACS)
Donkey anti-guinea pig IgG (H&L) Alexa Fluor 594 (706-585-148)	Dianova, Hamburg, GER	1:200 (IF)
Donkey anti-mouse IgG (H&L) Alexa Fluor 488 (A21202)	Thermo Fisher Scientific, Waltham, MA, USA	1:200 (IF)
Goat anti-chicken IgY-HRP (sc2428)	Santa Cruz Biotechnology, Dallas, TX, USA	1:5000 (WB)
Goat anti-mouse IgG-B, sc2039	Santa Cruz Biotechnology, Dallas, TX, USA	1:100 (IHC)
PE-streptavidin (#349023)	BD Bioscience, Franklin Lakes, NJ, USA	1:8 (FACS)
Rabbit anti-mouse IgG (H&L)(HRP) (ab6728)	Abcam, Cambridge, GBR	1:5000 (WB)

2.1.6 Oligonucleotides

2.1.6.1 Primers and probes

Table 7: Primers and probes. All oligonucleotides were purchased from MWG Eurofins, Ebersberg, GER.

Name	Sequence	
ROSA26 retargeting screening		
ROSA26_I1F2 BS_Rneu	5`-tatgggcgggattctttgc-3` 5`-cgggtgtccatcactgtcct-3`	3.0 kb
CD55_qPCR7F ROSA26_I3R2	5`-tcccaccaacagttcagaaacct-3` 5`-caggtggaagctaccctagcc-3`	9.3 kb
ROSA26_I1F2 ROSA26_I1R3	5`-tatgggcgggattctttgc-3` 5`-gtttgcacaggaaaccaag-3`	3.1 kb
CD46-MIN targeting screening		
CD46_5HA_F1 Hygro_R	5`-accctctgcacctcactg-3` 5`-aaaccatcgcgcgactatt-3`	3.0 kb
CD46_5HA_F1 MIN-site_R1	5`-accctctgcacctcactg-3` 5`-ccgtacaccactgagaccgc-3`	4.7 kb
MIN-site_F1 CD46_3HA_R1	5`-cgcggtctcagtgggtgacg-3` 5`-tcccctgccccactgtgtt-3`	5.6 kb
CD46_5HA_F1 CD46_3HA_R1	5`-accctctgcacctcactg-3` 5`-tcccctgccccactgtgtt-3`	Targeted: 10.3 kb Wild type: 7.8 kb
ROSA2-hSpCas9 targeting screening		
ROSA26_I1F2 Neo_KF	5`-tatgggcgggattctttgc-3` 5`-agcccctgatgctcttcgtc-3`	3.1 kb
Cas9_3`LRF1 ROSA26_I3R2	5`-gcagatcagcgagttctcca-3` 5`-caggtggaagctaccctagcc-3`	5.6 kb
ROSA26_I1F2 ROSA26_I1R3	5`-tatgggcgggattctttgc-3` 5`-gtttgcacaggaaaccaag-3`	3.1 kb
Copy number determination		
ddHO-1_F1 ddHO-1_R1 ddHO-1-FAM_probe	5`-acatctatgtggcctggag-3` 5`-gcttcacatagcgctgcat-3` 5` FAM-gacctggccttctggtacgg-BHQ 3`	183 bp
ddCD55_F ddCD55_R ddCD55-FAM_probe	5`-aattcctggcgagaaggact-3` 5`-cacaacagtaccgactggaa-3` 5` FAM-taggtagctgaggtgcca-BHQ 3`	163 bp
ddGAPDH_F ddGAPDH_R ddGAPDH-HEX_probe	5`-ctcaacgaccacttcgtaa-3` 5`-ccctgtgctgtagccaaat-3` 5` HEX-tgtgatcaagtctggtgcc-BHQ 3`	181 bp
ddHygro_F3 ddHygro_R3 ddHygro-FAM_probe	5`-cagcttcgatgtaggagggc-3` 5`-tcttgcaacgtgacaccctg-3` 5`-FAM-gcgccgatggttctacaaa-BHQ-3`	195 bp
ddCas9_F1 ddCas9_R1 ddCas9 F1/R1-FAM	5`-agttcatcaagccatcctg-3` 5`-tctttcccgggtgtccttc-3` 5`-FAM-gcacgccattctgcggcggc-BHQ-3`	198 bp
RT-PCRs		
CD55_E1F1	5`-ctgctgctggtgctgtgtg-3`	169 bp

CD55_2cR	5'-agtccttctcgccaggaat-3'	
hHO_Ex1F1 HMOX_3cR	5'-gatggagcgtccgcaacc-3' 5'-cttcacatagcgtgcatggc-3'	349 bp
F.GAPDH_S.scrofa R.GAPDH_S.scrofa	5'-ttccacggcacagtcaaggc-3' 5'-gcaggtcaggtccacaac-3'	576 bp
CIITA_ScrR1 CIITAmut_F1	5'-catggggcagagtggagatg-3' 5'-tgctggctccaaagaagaa-3'	298 bp
CD47_E4F1 CD47_R2	5'-ccattctttctgcccagggtg-3' 5'-cagccaaccacagcgagga-3'	188 bp
EPCR_RTF1 EPCR_RTR1	5'-aaggcccagacaccaacacc-3' 5'-ccgcagttcataccgagtg-3'	362 bp
hPDL_E2-E3F1 hPDL_E4R1	5'-ggcatttgctgaacgcattt-3' 5'-tggattggtggtggtggtc-3'	516 bp
hTM_F hTM_R	5'-tacgggagacaacaacacca-3' 5'-aaccgctgcccaggatgtag-3'	977 bp
HT_ScrF2 HT_ScrR3	5'-ccaacgcctcctctctctgt-3' 5'-ggatctgttcccggagatgg-3'	354 bp
ROSA26_E1F1 ddNeo_R1	5'-cgcctagagaagaggctgtgc-3' 5'-ctctgatgcccgctgttcc-3'	407 bp
Cas9_3' LRF1 ROSA26_BGHR1	5'-gcagatcagcgagttctcca-3' 5'-gggaggggcaacaacagat-3'	415 bp
q-RT-PCR		
CD55_qPCRF2 CD55_qPCRR2 hCD55_probe	5'-gggcagtcaatggtcagatat-3' 5'-acggcactcatattccacaac-3' 5'-FAM-agggatgcagaatttagccttgttg- BHQ-3'	142 bp
HO_qPCRF2 HO_qPCRR2 HO-1_probe	5'-gccctggaggaggagattga-3' 5'-tggctggtgtgtaggggatg-3' 5'-FAM-gacctggccttctgttacgg-BHQ-3'	154 bp
ddHPRT_F1 ddHPRT_R1 ddHPRT_probe	5'-cttgctcgagatgtgatgaa-3' 5'-agatcatctccaccaattactttt-3' 5'-FAM-ttcttctgacctgctgga-BHQ-3'	221 bp
Generation of sgRNA mRNA		
T7_for Trac_rev	5'-gtacaaaatacgtgacgtagaaag-3' 5'-aaaaaaagcaccgactcgggtgc-3'	251 bp
Screening of gRNA target sites		
pB2M_E1T1_F pB2M_E1T1_R	5'-ccaccagtccaaccttggcc-3' 5'-ccagagttagcggccggagt-3'	377 bp
CMAH_E10T1_F CMAH_E10T1_R	5'-tgccgtaaacaagaggggatt-3' 5'-ttgtctgctgggtgggattc-3'	357 bp
GGTA1_E8T4_F GGTA1_E8T4_R	5'-tcccagaggttacattacccca-3' 5'-gcacatcctggcccacatcc-3'	269 bp
GGTA1_E8T3_F GGTA1_E8T3_R	5'-aagaccatcggggagcacat-3' 5'-ggcttcatcatgccactcg-3'	346 bp
GGTA1_E7T6_F GGTA1_E7T6_R	5'-gccagtcaccacaagccatg-3' 5'-tggccctgtgacaccattct-3'	362 bp
B4G_E3T3_F B4G_E3T3_R	5'-gaacctgctggccctaaaaa-3' 5'-agctccgctccatctcagg-3'	247 bp

2.1.6.2 gRNA oligonucleotides

Table 8: gRNA oligonucleotides. Oligonucleotides were obtained from MWG Eurofins, Ebersberg, GER.

gRNA target site	Oligonucleotide name	Sequence
B2M_E1T1	PX_B2M_E1T1_F PX_B2M_E1T1_R	5`-caccgtagcgatggctcccctcg-3` 5`-aaaccgaggggagccatcgctac-3`
B4GALNT2_E3T1	PX_B4GALNT2_E3T1_F PX_B4GALNT2_E3T1_R	5`-caccgtgacgccttcgggcatc-3` 5`-aaacgatgccgaaggcgtcac-3`
B4GALNT2_E3T2	PX_B4GALNT2_E3T2_F PX_B4GALNT2_E3T2_R	5`-caccgagctttctgtatgccga-3` 5`-aaactcgggcatcaggaagctc-3`
B4GALNT2_E3T3	PX_B4GALNT2_E3T3_F PX_B4GALNT2_E3T3_R	5`-caccgaggaaagctataacttg-3` 5`-aaaccaagttagctttcctc-3`
CMAH_E10T1 (20 bp+GG)	CMAH_E10T1(GG+20bp)F CMAH_E10T1(GG+20bp)R	5`-cacctaataatacgactcactataggggaagaa actcctgaactaca-3` 5`-aaactgtagttcaggagtttctcccctatagtgag tcgtattatta-3`
CMAH_E10T1 (18 bp)	CMAH_E10T1(18bp)_F CMAH_E10T1(18bp)_R	5`-cacctaataatacgactcactatagagaaactcc tgaactaca-3` 5`-aaactgtagttcaggagtttctctatagttagtgcg attatta-3`
CMAH_E10T1 (20 bp)	CMAH_E10T1(20bp)_F CMAH_E10T1(20bp)_R	5`-cacctaataatacgactcactataggaagaaac tctgaactaca-3` 5`-aaactgtagttcaggagtttctctatagttagtc gtattatta-3`
CMAH_E10T1	PX_CMAH_E10T1_F PX_CMAH_E10T1_R	5`-caccgagaaactcctgaactaca-3` 5`-aaactgtagttcaggagtttctc-3`
CMAH_E6T3	CMAH_E6T3_F CMAH_E6T3_R	5`-cacctaataatacgactcactataggtcctgcttt gcgagga-3` 5`-aaactcctcgcgaaaagcaggacctatagt agtcgtattatta-3`
GGTA1_E6T7	GGTA1_E6T7_F GGTA1_E6T7_R	5`-cacctaataatacgactcactataggagcttccg ctagtggac-3` 5`-aaacgtccactagcggaagctcctatagttagt cgattatta-3`
GGTA1_E7T5	GGTA1_E7T5_F GGTA1_E7T5_R	5`-cacctaataatacgactcactatagcaaacaga aaattaccgt-3` 5`-aaacacggtaattttctggttctatagttagtcgta ttatta-3`
GGTA1_E7T6	GGTA1_E7T6_F GGTA1_E7T6_R	5`-cacctaataatacgactcactataggtcgtgacc ataaccaga-3` 5`-aaactcgttatggtcagcagcctatagttagtcg tattatta-3`
GGTA1_E7T6	PX_GGTA1_E7T6_F PX_GGTA1_E7T6_R	5`-caccgctgaccataaccaga-3` 5`-aaactcgttatggtcagcagc-3`
GGTA1_E8T2	GGTA1_E8T2_F GGTA1_E8T2_R	5`-cacctaataatacgactcactatagtactgctgg gattatcatat-3` 5`-aaacatatgataatcccagcagcactatagttag tcgtattatta-3`
GGTA1_E8T3	PX_GGTA1_E8T3_F PX_GGTA1_E8T3_R	5`-caccgacgagttcacctacgag-3` 5`-aaacctgtaggtgaactcgtc-3`

GGTA1_E8T4	GGTA1_E8T4_F GGTA1_E8T4_R	5`-cacctaataatacgcactcactatagatggggat gatatctcc-3` 5`-aaacggagatatcatccaccatctatagtgagtc gtattatta-3`
------------	------------------------------	--

2.1.7 Nucleic acid ladders

Table 9: Nucleic acid ladders

Name	Source
1 kb DNA ladder	New England Biolabs, Frankfurt, GER
100 bp DNA ladder	New England Biolabs, Frankfurt, GER
2-log DNA ladder (0.1-10.0 kb)	New England Biolabs, Frankfurt, GER
Colour prestained protein standard, broad range (11-245 kDa)	New England Biolabs, Frankfurt, GER
Ribo Ruler high range RNA ladder + 2x RNA loading dye	Thermo Scientific, Waltham, MA, USA

2.1.8 Molecular cloning vectors and DNA constructs

Table 10: Molecular cloning vectors and DNA constructs

Name	Source
CD46-MIN targeting vector	Dr. Konrad Fischer, Chair of Livestock Biotechnology, TUM, Freising, GER
hTMmod2	Kindly provided by Dr. Nikolai Klymiuk, Chair of Molecular Animal Breeding and Biotechnology, LMU, Oberschleißheim, GER
pBACe3.6	BACPAC Resources, Oakland, CA, USA
pBS-U6-chimaeric RNA (Jinek)	Kindly provided by Dr. Oskar Ortiz Sanchez, IGD, Helmholtz Zentrum München, Oberschleißheim, GER
pCAG-Cas9-bpA	Kindly provided by Dr. Oskar Ortiz Sanchez, IGD, Helmholtz Zentrum München, Oberschleißheim, GER
pcDNA3.1-hygro(+)-CAG-CD55-mini	Dr. Konrad Fischer, Chair of Livestock Biotechnology, TUM, Freising, GER
pcDNA3.1-hygro-CCL2-PD-L1	Dr. Konrad Fischer, Chair of Livestock Biotechnology, TUM, Freising, GER
pcDNA3.1-hygro-CD47	Dr. Konrad Fischer, Chair of Livestock Biotechnology, TUM, Freising, GER
pcDNA3.1-hygro-mutCIITA	Dr. Konrad Fischer, Chair of Livestock Biotechnology, TUM, Freising, GER
pSL1180 rev-U6-trac (plasmid #756)	Daniela Huber, Chair of Livestock Biotechnology, TUM, Freising, GER

pSL1180-EPCR	Dr. Konrad Fischer, Chair of Livestock Biotechnology, TUM, Freising, GER
pSL1180-HT-HO1	Dr. Konrad Fischer, Chair of Livestock Biotechnology, TUM, Freising, GER
pX330-CD46-T2	Dr. Konrad Fischer, Chair of Livestock Biotechnology, TUM, Freising, GER
pX330-U6-Chimeric_BB-CBh-hSpCas9_MCS (plasmid #705)	Daniela Huber, Chair of Livestock Biotechnology, TUM, Freising, GER
pX330-U6-Chimeric_BB-CBh-hSpCas9 (Addgene plasmid #42230)	Addgene, Cambridge, MA, USA
pX330-U6-Chimeric_BB-CBh-hSpCas9-T2A-puro_MCS (plasmid #841)	Daniela Huber, Chair of Livestock Biotechnology, TUM, Freising, GER
ROSA26-CD55 retargeting vector #36	Dr. Konrad Fischer, Chair of Livestock Biotechnology, TUM, Freising, GER
ROSA26-HO-1 TV	Dr. Konrad Fischer, Chair of Livestock Biotechnology, TUM, Freising, GER
ROSA26-PDX-Cre TV	Chair of Livestock Biotechnology, TUM, Freising, GER

2.1.9 Tissue culture media, supplements and reagents

Table 11: Tissue culture media, supplements and reagents

Name	Source
Accutase	Sigma-Aldrich, St. Louis, MO, USA
Ala-Gln, 200 mM	Sigma-Aldrich, St. Louis, MO, USA
Amphotericin B	Sigma-Aldrich, St. Louis, MO, USA
Blasticidin S	InvivoGen, San Diego, CA, USA
Cell culture water	Sigma-Aldrich, St. Louis, MO, USA
Collagenase type IA (C2674)	Sigma-Aldrich, St. Louis, MO, USA
DMEM- high glucose	Sigma-Aldrich, St. Louis, MO, USA
DMSO	Sigma-Aldrich, St. Louis, MO, USA
FBS Superior	Biochrom GmbH, Berlin, GER
G418 sulphate	Genaxxon Bioscience, Ulm, GER
Hypoosmolar buffer	Eppendorf, Hamburg, GER
Lipofectamine 2000	Thermo Fisher Scientific, Waltham, MA, USA
MEM non-essential amino acid solution, 100x	Sigma-Aldrich, St. Louis, MO, USA
OptiMEM	Gibco by Life Technologies, Paisley, GBR
Penicillin/Streptomycin	Sigma-Aldrich, St. Louis, MO, USA
Phosphate-buffered saline (PBS)	Sigma-Aldrich, St. Louis, MO, USA
Puromycin	InvivoGen, San Diego, CA, USA
Sodium pyruvate solution, 100 mM	Sigma-Aldrich, St. Louis, MO, USA
Trypan blue stain	Gibco by Life Technologies, Paisley, GBR

2.1.10 Bacterial culture media and supplements

Table 12: Bacterial culture media and supplements

Name	Source
Ampicillin (C ₁₆ H ₁₉ N ₃ O ₄ S)	Carl Roth, Karlsruhe, GER
Chloramphenicol (C ₁₁ H ₁₂ Cl ₂ N ₂ O ₅)	Sigma-Aldrich, Steinheim, GER
LB agar, Miller (Luria-Bertani)	Difco BD, Sparks, MD, USA
Luria Broth, Base, Miller	Difco BD, Sparks, MD, USA

2.1.11 Buffers and solutions

Table 13: Buffers and solutions

Type	Component	Quantity
APS 10%	(NH ₄) ₂ S ₂ O ₈ H ₂ O	1g Add to 10 ml
Blocking buffer for immunohistochemistry	1x TBST Normal goat serum	5 ml 250 µl
Blocking buffer for western blot (5% Milk powder)	Milk powder 1x TBST	5 g 100 ml
Blocking buffer for western blot (Neu5Gc-free)	Neu5Gc Assay blocking solution (40x) 1x TBST	250 µl 10 ml
Erythrocyte lysis buffer	NH ₄ Cl KHCO ₃ EDTA H ₂ O	8.3 g 1.1 g 100 mg Add to 1 l
FACS wash buffer	BSA NaN ₃ PBS	500 mg 100 mg Add to 100 ml
Lämmli buffer 4x	0.5 M Tris-HCl, pH 6.8 10% SDS C ₁₂ H ₂₂ O ₁₁ DTT 1 M Saturated bromophenol blue H ₂ O	5 ml 4 ml 4 g 260 µl 110 µl Add to 10 ml
DNA miniprep solution I	C ₁₂ H ₂₂ O ₁₁ EDTA Tris H ₂ O	1.7 g 2.9 g 3.0 g Add to 1 l
DNA miniprep solution II	NaOH SDS H ₂ O	8.0 g 10.0 g Add to 1 l
DNA miniprep solution III	C ₂ H ₃ NaO ₂ H ₂ O	246.1 g Add to 1 l
Ponceau S solution	Ponceau S C ₂ H ₄ O ₂	1 g 2 ml

	H ₂ O	Add to 200 ml
Electrophoresis running buffer 10x	Tris C ₂ H ₅ NO ₂ SDS H ₂ O	30 g 144 g 10 g Add to 1 l
SDS 10%	SDS H ₂ O	10 g Add to 100 ml
Semi-dry blotting buffer	Tris C ₂ H ₅ NO ₂ CH ₃ OH SDS H ₂ O	3.0 g 14.4 g 200 ml 1.0 g Add to 1 l
Sodium citrate buffer, 10 mM	C ₆ H ₅ NaO ₇ · 2 H ₂ O H ₂ O	2.9 g Add to 1 l Adjust pH to 6.0
TAE, 50x	Tris 0.5 M EDTA C ₂ H ₄ O ₂ H ₂ O	242 g 100 ml 57.1 ml Add to 1 l
TBE, 10x	Tris H ₃ BO ₃ EDTA dH ₂ O	545 g 275 g 39.2 g Add to 5 l
TBS, 10x	Tris NaCl H ₂ O	24.2 g 80 g Add to 1 l
TBST, 1x	10x TBS Tween 20 H ₂ O	100 ml 1 ml Add to 1 l
TE buffer	Tris-HCl EDTA H ₂ O	158 mg 29 mg Add to 100 ml
TL-HEPES + Ca ²⁺	NaCl KCl CaCl ₂ · 2 H ₂ O NaH ₂ PO ₄ · 2 H ₂ O MgCl ₂ · 6 H ₂ O NaHCO ₃ HEPES C ₃ H ₅ NaO ₃ (60%) H ₂ O	3.3 g 119 mg 147 mg 28 mg 51 mg 84 mg 1.2 g 1.1 g Add to 500 ml
	Adjust pH to 7.3; sterile filter; freeze down 50 ml aliquots	
	TL-HEPES + Ca ²⁺ Stock C ₃ H ₃ NaO ₃ solution, 100 mM C ₁₂ H ₂₂ O ₁₁ BSA	50 ml 125 µl 55 mg 200 mg
	Sterile filter; store at 4°C; use within 2 weeks	
Tris-HCl 0.5 M; pH 6.8	Tris H ₂ O HCl H ₂ O	15.1 g 125 ml Adjust pH to 6.8 Add to 250 ml

Tris-HCl 1 M; pH 8.8	Tris H ₂ O HCl H ₂ O	39.4 g 125 ml Adjust pH to 8.8 Add to 250 ml
TTE buffer	Tris Triton X 100 EDTA H ₂ O	242 mg 1 ml 584 mg Add to 100 ml

2.1.12 Laboratory equipment

Table 14: Laboratory equipment

Name	Source
7500 fast real-time PCR cycler	Life Technologies, Carlsbad, CA, USA
Automated cell counter "Countess"	Invitrogen, Carlsbad, CA, USA
Blue light table	Serva, Heidelberg, GER
Centrifuges "Sigma 3-16", "Sigma 1-15", "Sigma 1-15K", "Sigma 4K15"	Sigma, Osterode, GER
CO ₂ incubator "Forma Steri-Cycle 371"	Thermo Fisher Scientific, Waltham, MA, USA
Cryo 1°C freezing container "Mr. Frosty"	Thermo Fisher Scientific, Waltham, MA, USA
Digital microscope "M8"	PreciPoint, Freising, GER
Droplet generator "QX200"	Bio-Rad Laboratories, Hercules, CA, USA
Droplet reader "QX200"	Bio-Rad Laboratories, Hercules, CA, USA
Dry block heater/cooler "PCH-2"	Grant instruments, Royston, GBR
Electrophoresis system (buffer chamber, gel trays, combs)	Peqlab Biotechnologie, Erlangen, GER
Electroporator "Multiporator"	Eppendorf, Hamburg, GER
ELISA reader "Multiscan Ex"	Thermo Fisher Scientific, Waltham, MA, USA
Flow cytometer "FACSCalibur"	BD Bioscience, Franklin Lakes, NJ, USA
Freezer -20°C "GS 2481"	Liebherr, Bulle, SUI
Freezer -80°C "Forma 900 Series"	Thermo Fisher Scientific, Waltham, MA, USA
Fridge "TSE1283"	Beko, Neu-Isenburg, GER
Gel documentation imaging system "Quantum ST5"	Vilber Lourmat, Eberhardzell, GER
Glasware	Marienfeld GmbH, Landa, GER
Ice maker	Manitowoc Ice, Manitowoc, WI, USA
Incubator "BD115"	Binder, Tuttlingen, GER
Magnet "Dynamag-15"	Life Technologies, Carlsbad, CA, USA
Magnetic stirrer "AREC_X", "AGE"	VELP Scientific, Usmate, ITA
Microscope "Axiovert 40CLF", "Axiovert 200 M", "Primo Star"	Carl Zeiss, Jena, GER
Microwave "MW17M70G-AU"	MDA Haushaltswaren, Barsbüttel, GER
Mini centrifuge "perfect spin mini"	Peqlab Biotechnologie, Erlangen, GER
Orbital shaker	Thermo Fisher Scientific, Waltham, MA, USA

PCR cycler "peqStar 2x"	Peqlab Biotechnologie, Erlangen, GER
PCR cycler "DNA Engine DYAD, PTC 0220"	BioRad Laboratories, Munich, GER
PCR plate sealer "PX1"	Bio-Rad Laboratories, Hercules, CA, USA
Pipettes "Pipetman" (0.2-2 µl; 2-20 µl; 20-200 µl; 200-1000 µl)	Gilson, Middleton, WI, USA
Pipettes "accu jet pro"	Brand, Wertheim, GER
Plate centrifuge "MPS 100"	Labnet International, Edison, NY, USA
Power supply "EPS 301"	Amersham Bioscience, Little Chalfont, UK
Power supply "peqPOWER"	Peqlab Biotechnologie, Erlangen, GER
Radiographic cassette, 24x30cm	Rego X-Ray GmbH, Augsburg, GER
Rocker shaker "Unitwist 3-D"	Uniequip, Munich, GER
Rotary microtome "Microm HM355"	Microm International, Walldorf, GER
Safety cabinet "HERAsafe HS 12"	Kendro Laboratory Products, Hanau, GER
Slide staining system "M920 StainTray"	Simport, Beloeil, CAN
Slide warmer	Barnstead, Melrose Park, IL, USA
SpeedMill Plus	Analytic Jena, Jena, GER
Thermal printer "P95"	Mitsubishi Electric, Kyoto, JPN
Trans-Blot SD semi-dry transfer cell	Biorad Laboratories, Munich, GER
Vortex mixer "Vortex Genie 2", "Vortexer 2x3"	VELP Scientific, Usmate, ITA
Water bath "WNB22"	Memmert, Schwabach, GER
Western blot "Mini PROTEAN tetra handcast system"	Biorad Laboratories, Munich, GER

2.1.13 Consumables

Table 15: Consumables

Name	Source
Cellstar tubes (15 ml and 50 ml)	Greiner Bio-One, Frickenhausen, GER
Cloning rings	Brand, Wertheim, GER
Cover slips (24x 60 mm)	Menzel, Braunschweig, GER
Cryo vials	Corning Incorporated, Corning, NY, USA
DG8 cartridge for QX200 droplet generator	Bio-Rad Laboratories, Hercules, CA, USA
DG8 gasket	Bio-Rad Laboratories, Hercules, CA, USA
Electroporation cuvette (2 mm)	Peqlab Biotechnologie, Erlangen, GER
Electroporation cuvette (4 mm)	Bio-Rad Laboratories, Hercules, CA, USA
Elisa plate "Costar EIA/RIA plate 96 well"	Corning Incorporated, Corning, NY, USA
FACS 96-well plate	Sarstedt, Nürnberg, GER
Filter paper (extra thick blot paper)	Biorad Laboratories, Munich, GER
Filter pipette tips „Fisherbrand Sure One“	Fisher Scientific, Hampton, NH, USA
Glass pasteur pipettes	Brand, Wertheim, GER
MicroAmp fast optical 96-Well reaction plates	Life Technologies, Carlsbad, CA, USA

Microscope slide “Menzel Gläser Superfrost Plus”	Thermo Fisher Scientific, Waltham, MA; USA
PCR tubes 0.2 ml 8-Strip PCR tubes	Starlab, Hamburg, GER
Petri dishes	Greiner Bio-One, Frickenhausen, GER
Phase lock gel	
pierceable foil heat seal	Bio-Rad Laboratories, Hercules, CA, USA
Pipette tips	Brand, Wertheim, GER
Plastic pipettes “Costar Stipette” (1-50 ml)	Corning Incorporated, Corning, NY, USA
PVDF membrane “Roti-PVDF; 0.45 µm)	Carl Roth, Karlsruhe, GER
Reaction tubes (1.5 ml and 2 ml)	Zefa Laborservice, Harthausen, GER
Reaction tubes (5 ml)	Starlab, Hamburg, GER
Scalpel	Braun, Melsungen, GER
Sterile filter 0.22 µm	Berrytec, Grünwald, GER
Syringes	BD Bioscience, Le Pont De Claix, FRA
Tissue culture flasks (T25, T75, T150)	Corning Incorporated, Corning, NY, USA
Tissue culture plates (10 cm, 15 cm, 6-, 12-, 24, 98-well)	Corning Inc., Corning, NY; USA
Tubes (14 ml)	Corning Incorporated, Corning, NY, USA
twin.tec PCR Plate 96	Eppendorf, Hamburg, GER
X-Ray film “Cronex 5”	Agfa Healthcare, Mortsel, BEL

2.1.14 Software and online tools

Table 16: Software and online tools

Name	Source
Crispr design tool (http://crispr.mit.edu/)	Zhang Lab, MIT, Cambridge, MA, USA
ddPCR software “QuantaSoft Software”	Bio-Rad Laboratories, Hercules, CA, USA
Digital microscope software “Touch Microscope V.2015-05-03”	PreciPoint, Freising, GER
Digital microscope software “Virtual Microscope V.2015-05-03”	PreciPoint, Freising, GER
ELISA reader software “Ascent Software, Version 2.6”	Thermo Fisher Scientific, Waltham, MA, USA
Flow cytometry software “FlowJo”	FlowJo LLC, Ashland, OR, USA
Chromatogram viewer software “Finch TV”	Geospiza Inc., Seattle, WA, USA
Gel documentation software “Quantum ST5 v16.15”	Vilber Lourmat, Eberhandzell, GER
Genome database “Ensembl”: (https://www.ensembl.org/index.html)	EMBL-EBI, Hinxton, GBR
Microscope software “Axio Vision”	Carl Zeiss, Göttingen, GER

Primer design tool "Primer3" http://primer3.ut.ee/	Whitehead Institute for Biomedical Research, Cambridge, MA, USA
qPCR software "7500 fast real time PCR system"	Applied Biosystems, Carlsbad, CA, USA
Reverse Complement (https://www.bioinformatics.org/sms/rev_comp.html)	Paul Stothard, University of Alberta, Edmonton, CAN
Sequence alignment tool "Clustal Omega" (https://www.ebi.ac.uk/Tools/msa/clustalo/)	EMBL-EBI, Hinxton, GBR
TIDE: Tracking of Indels by DEcomposition (https://tide.deskgen.com/)	Desktop Genetics, London, GBR
Vector design software "Everyvector" (http://www.everyvector.com/)	everyVECTOR Software Inc., Cambridge, MA, USA

2.2 Methods

2.2.1 Molecular biology

2.2.1.1 Isolation of mammalian genomic DNA

Genomic DNA from eukaryotic cells was isolated using QuickExtract DNA extraction solution. Cells were detached and a third 12-well to a half 6-well used for DNA isolation. Cells were transferred to a tube, centrifuged at 300 x g for 5 min and the supernatant aspirated. The cell pellet was resuspended in 30 µl QuickExtract DNA extraction solution and heated to 68°C for 15 min, followed by 98°C for 8 min.

If purer genomic DNA was required, DNA was isolated using the SurePrep RNA/DNA/protein purification kit. Cells were detached and up to 10⁶ cells used for DNA isolation according to the manufacturers' protocol.

For genomic DNA isolation from mammalian tissues, the GenElute mammalian genomic DNA miniprep kit was used according to the manufacturers' protocol.

If both DNA and RNA from mammalian tissues were required, the innuSPEED tissue RNA kit was used in combination with the SpeedMill Plus homogenisator as described in 2.2.1.16, with the following modification: Instead of discarding the Spin filter D with the bound DNA, 50 µl water was applied, 1 min incubated and DNA eluted by centrifugation at 6000 x g for 1 min.

2.2.1.2 Isolation of plasmid DNA

Different methods were used for isolating plasmid DNA from *E.coli* cultures, depending on the quantity and purity of DNA required. Small amounts of impure DNA were isolated by the miniprep protocol. A midi- or maxiprep was performed if larger amounts of pure DNA for cloning and transfection purposes were required.

For minipreps, 2 ml overnight culture was centrifuged for 1 min at 14,000 rpm, the supernatant discarded and the cell pellet resuspended in 100 µl miniprep solution I. Alkaline lysis was performed by addition of 200 µl miniprep solution II, gently mixing and incubation at room temperature for 3 min. 150 µl miniprep solution III was added to the lysate, the solutions mixed by inverting the tube several times and incubated on ice for 30 min. Cell debris and DNA were separated by centrifugation at 14,000 rpm for 5 min. The supernatant, containing the plasmid DNA, was transferred into a new tube and precipitated by addition of 1 ml 95% ethanol. After pelleting for 15 min at 4°C and 14,000 rpm, the supernatant was discarded and the pellet washed with 1 ml 80% ethanol. The mixture was centrifuged for 10 min at 4°C and 14,000 rpm and the procedure repeated with 1 ml 95% ethanol. Finally, the pellet was air-dried and resuspended in 50 µl H₂O supplemented with RNase.

A midiprep was performed to isolate plasmid DNA using the NucleoBond Xtra Midi kit. 100 ml overnight culture was used and the high-copy NucleoBond Xtra Midi protocol followed according to the manufacturers' recommendation.

A maxiprep was carried out to isolate BAC-vector DNA using the NucleoBond Xtra Maxi kit. 500 ml overnight culture was used and the low-copy NucleoBond Xtra Midi protocol followed according to the manufacturers' recommendation.

2.2.1.3 Determination of DNA and RNA concentration

DNA and RNA concentrations were determined using NanoDrop light spectrophotometer according to the manufacturers' protocol.

2.2.1.4 Polymerase chain reaction

Polymerase chain reaction (PCR) was performed to amplify desired DNA fragments from plasmid, genomic or cDNA templates. Various polymerases were used depending on the template DNA and length of the desired fragment. Shorter fragments from plasmid, genomic and cDNA templates were amplified using GoTaq G2 polymerase or FastGene Optima HotStart ready mix. If proofreading was necessary, these were amplified using Q5 high fidelity polymerase. For genomic templates and long-range PCR, either PCR extender system or

AccuStart Taq DNA polymerase HiFi were used. Table 17-Table 21 show PCR reaction composition and cycling conditions for the different polymerases used.

Table 17: GoTaq G2 polymerase PCR reaction composition and cycling conditions

GoTaq G2 polymerase					
Reaction composition		Cycling conditions			
Component	Final concentration	Step	Temperature	Time	No of cycles
DNA	< 250 ng	Initial denaturation	95°C	2 min	1
5x green GoTaq reaction buffer	1x	Denaturation	95°C	30 s	35-40
dNTPs	200 µM each	Annealing	58-62°C	45 s	
Forward primer	0.2 µM	Elongation	72°C	1 min/kb	
Reverse primer	0.2 µM	Final elongation	72°C	5 min	1
GoTaq G2 DNA polymerase	0.03 U/µl	Storage	8°C	Indefinite	
H ₂ O	Add to 25 µl				

Table 18: FastGene Optima HotStart Ready Mix reaction composition and cycling conditions

FastGene Optima HotStart ready mix					
Reaction composition		Cycling conditions			
Component	Final concentration	Step	Temperature	Time	No of cycles
DNA	50 ng	Initial denaturation	95°C	3 min	1
2x FastGene Optima HotStart ready mix	1x	Denaturation	95°C	15 s	35-40
Forward primer	0.5 µM	Annealing	58-62°C	15 s	
Reverse primer	0.5 µM	Elongation	72°C	1 min/kb	
H ₂ O	Add to 25 µl	Final elongation	72°C	5 min	1
		Storage	8°C	Indefinite	

Table 19: Q5 high-fidelity DNA polymerase PCR reaction composition and cycling conditions

Q5 high-fidelity DNA polymerase					
Reaction composition		Cycling conditions			
Component	Final concentration	Step	Temperature	Time	No of cycles
DNA	< 1000 ng	Initial denaturation	98°C	30 s	1
5x Q5 reaction buffer	1x	Denaturation	98°	10 s	35
5x Q5 high GC enhancer (opt.)	1x	Annealing	58-62°C	30 s	
dNTPs	200 µM each	Elongation	72°C	30 s/kb	
Forward primer	0.5 µM	Final elongation	72°C	2 min	1
Reverse primer	0.5 µM	Storage	8°C	indefinite	1
Q5 high-fidelity DNA polymerase	0.02 U/µl				
H ₂ O	Add to 25 µl				

Table 20: PCR extender system reaction composition and cycling conditions

PCR extender system					
Reaction composition		Cycling conditions			
Component	Final concentration	Step	Temperature	Time	No of cycles
DNA	100 ng	Initial denaturation	93°C	3 min	1
10x tuning buffer	1x	Denaturation	93°C	30 s	10
dNTPs	500 µM each	Annealing	60-64°C	1 min	
Forward primer	0.4 µM	Elongation	68°C	1 min/kb	
Reverse primer	0.4 µM	Denaturation	93°C	30 s	30
PCR extender polymerase mix	0.04 U/µl	Annealing	60-64°C	1 min	
H ₂ O	Add to 50 µl	Elongation	68°C	1 min/kb + 20 s/cycle	
		Final elongation	68°C	5 min	1
		Storage	8°C	Indefinite	1

Table 21: AccuStart Taq DNA polymerase HiFi PCR reaction composition and cycling conditions

AccuStart Taq DNA polymerase HiFi					
Reaction composition		Cycling conditions			
Component	Final concentration	Step	Temperature	Time	No of cycles
DNA	100 ng	Initial denaturation	94°C	1 min	1
10x HiFi buffer	1x	Denaturation	94°C	20 s	35-40
MgSO ₄	2 mM	Annealing	58-62°C	30 s	
dNTPs	200 µM each	Elongation	68°C	1 min/kb	
Forward primer	0.2 µM	Final elongation	68°C	5 min	1
Reverse primer	0.2 µM	Storage	8°C	Indefinite	
AccuStart Taq DNA polymerase HiFi	0.02 U/µl				
H ₂ O	Add to 50 µl				

2.2.1.5 Agarose gel electrophoresis

Agarose gel electrophoresis was performed to separate DNA fragments or determine their size. 1x TAE buffer was used for preparative and 1x TBE buffer for analytical gels. Gels were prepared containing 0.8-2% agarose and 4 µl PeqGREEN dye per 100 ml. Samples were mixed with 6x gel loading dye, or used directly if the PCR reaction buffer included loading dye. Samples were loaded and 80-120 V applied until the fragments were separated sufficiently. DNA fragments were analysed under UV light at 366 nm using a Quantum ST5 gel documentation imaging system.

The size of RNA fragments was determined by agarose gel electrophoresis as described above with following modifications: A 0.8% TBE gel was prepared containing 6 µl PeqGREEN dye and 800 µl formaldehyde per 100 ml agarose gel. RNA samples were mixed with 2x RNA loading dye, incubated at 70°C for 10 min, followed by 4°C for 5 min and immediately loaded onto the gel.

2.2.1.6 Proteinase K digest

Proteinase K digest was performed to inactivate nucleases that might degrade DNA or RNA during purification. Proteinase K and SDS were added to the DNA to final concentrations of 0.5% SDS and 1 µg/µl Proteinase K and the mix was incubated at 50°C for 30 min.

2.2.1.7 Purification of DNA fragments and PCR products

PCR products and DNA fragments isolated from agarose gels were purified using the Wizard SV gel and PCR clean-up system according to the manufacturers` protocol.

PCR products for sequencing were enzymatically purified to remove residual primers and dNTPs that could interfere with the sequencing reaction. The PCR reaction was incubated with 0.4 µl antarctic phosphatase and 0.2 µl exonuclease I for 30 min at 37°C, followed by 80°C for 15 min.

DNA to be used as template for *in vitro* transcription was purified by phenol-chloroform extraction to remove residual RNases and other impurities. DNA was mixed with an equal volume of phenol-chloroform-isoamyl alcohol and vortexed. The mixture was transferred to a phase lock gel, incubated for 10 min and centrifuged for 10 min at 14,000 rpm. The upper aqueous phase, containing the DNA, was transferred to a new reaction tube under a sterile laminal flow cabinet. 1/10 volume of 5 M ammonium acetate and two volumes of 100% ethanol were added, mixed thoroughly and incubated at -20°C for 2 h. The DNA was pelleted by centrifugation at 14,000 x g for 5 min at 4°C and the supernatant aspirated. The pellet was dried and resuspended in 20 µl nuclease-free water.

2.2.1.8 DNA sequencing

DNA sequencing was carried out by MWG Eurofins Operon (Ebersberg, GER). Sample and primers were prepared according to the Mix2Seq kit guidelines.

2.2.1.9 Oligonucleotide annealing

Both complementary single-stranded oligonucleotides were diluted in 100 µl TE buffer to a final concentration of 10 ng/µl each. For double-strand hybridisation, the solution was heated to 100°C for 5 min and cooled slowly to room temperature.

2.2.1.10 Restriction digest

For cloning as well as transfection of linearised plasmids, preparative restriction digests were performed using 10-20 µg DNA. To confirm correct plasmid length, an analytical restriction digest was performed using 1-2 µg DNA. The reaction was set up according to Table 22 and incubated at the enzyme`s reaction optimum for 1-3 h.

Table 22: DNA restriction digest

Component	Final concentration
DNA	Analytical digest: 1-2 µg Preparative digest: 10-20 µg
10x NEB buffer	5 µl
Enzyme	3 U/µg DNA
H ₂ O	Add to 50 µl

2.2.1.11 Dephosphorylation of cleaved DNA

To avoid religation, 5' phosphates were removed from the vector backbone using calf intestinal alkaline phosphatase. A restriction digest was performed as described in 2.2.1.10, then 2 µl enzyme added to the reaction and incubated for 30 min at 37°C.

2.2.1.12 Blunting

Blunting was used to ligate DNA fragments with incompatible sticky ends using DNA polymerase I, large (Klenow) fragment to remove 3' and fill up 5' overhangs. A preparative restriction digest was performed as described in 2.2.1.10. Subsequently, dNTPs to a final concentration of 60 µM and DNA polymerase I, large (Klenow) fragment (1 U/µg) were added and incubated at 25°C for 15 min. The reaction was stopped by addition of EDTA to a final concentration of 10 mM and heating for 20 min at 75°C.

2.2.1.13 Ligation

DNA vector backbones and insert DNA fragments were ligated using T4 DNA ligase. Reactions were set up according to Table 23 and incubated for 2 h at room temperature, followed by 4°C overnight.

Table 23: Ligation reaction

Component	Final concentration
Vector DNA	100 ng
Insert DNA	Molar ratio of 1:3-1:10 (vector:insert)
T4 DNA ligase buffer (10x)	1x
T4 DNA ligase (400 U/µl)	27 U/µl
H ₂ O	Add to 30 µl

2.2.1.14 Colony PCR

Colony PCR was conducted to identify *E.coli* colonies carrying the correct plasmid constructs. Primers were designed to amplify a fragment consisting of the vector backbone and the insert. Single cell colonies were selected, streaked on an agar plate and resuspended in 30 µl TTE buffer. Bacteria were lysed by heating the TTE buffer-bacteria mixture to 95°C for 5 min. Subsequently, 2 µl of the mixture was used as DNA template for PCR according to Table 17.

2.2.1.15 Droplet digital PCR

Transgene copy numbers were determined using droplet digital PCR (ddPCR). Genomic DNA was digested with HindIII, as described in 2.2.1.10, and heat inactivated at 65°C for 20 min. TaqMan PCR reaction was set up according to Table 24. Glyceraldehyde-3-Phosphate Dehydrogenase (*GAPDH*) was chosen as a reference gene. 20 µl TaqMan PCR reaction and 70 µl droplet generator oil were pipetted into the corresponding wells of a cartridge for droplet generation and droplets generated using a QX200 droplet generator. Droplets were transferred to a 96-well plate and the plate sealed with a pierceable foil heat seal. PCR was performed as described in Table 24 using a heated lid set to 105°C and setting the sample volume to 40 µl. The proportion of PCR-positive and PCR-negative droplets was determined using the QX200 droplet reader and data analysed using QuantaSoft software.

Table 24: ddPCR reaction composition and cycling conditions

Reaction composition		Cycling conditions				
Component	Final concentration	Step	Temperature	Time	Ramp rate	No of Cycles
DNA (HindIII digested)	40-100 ng	Enzyme activation	95°C	10 min	2°C/s	1x
2x ddPCR supermix for probes (no UTP)	1x	Denaturation	94°C	30 s		40x
20x target primers/probe (FAM)	900 nM primer 250 nM probe	Annealing/extension	60°C	1 min		1x
20x reference primer/probe (HEX)	900 nM primer 250 nM probe	Enzyme inactivation	98°C	10 min		
H ₂ O	Add to 23 µl	Hold	4°C	Indefinite		

2.2.1.16 RNA isolation

RNA from eukaryotic cells was isolated using the SurePrep RNA/DNA/protein purification kit. Cells were detached using accutase solution and up to 10^6 cells used for RNA isolation according to the manufacturers' protocol.

For RNA isolation from porcine tissues, the SpeedMill Plus homogenisator was used in combination with the innuSPEED tissue RNA Kit. 35 mg tissue was homogenised for 30 s, followed by 30 s cooling time. For samples of tough tissue, homogenisation was repeated once. RNA was extracted from the homogenised lysate using the innuSPEED tissue RNA kit according to the manufacturers' protocol.

2.2.1.17 cDNA synthesis

CDNA was generated using Superscript III or IV reverse transcriptase according to the manufacturers' protocol.

2.2.1.18 Quantitative real-time PCR

Quantitative real-time PCR (q-RT-PCR) was performed using the TaqMan Fast Universal PCR master mix and 5'FAM/3'BHQ labelled probes. A master mix was prepared according to Table 25 and each sample measured in triplicate. PCR was carried out in a 7500 fast real-time PCR cycler with PCR conditions used as shown in Table 25.

Table 25: q-RT-PCR reaction composition and cycling conditions

Reaction composition		Cycling conditions			
Component	Final concentration	Step	Temperature	Time	No of cycles
cDNA	130 ng	Initial denaturation	95°C	30 s	1
TaqMan fast universal PCR master mix (2x)	1x	Denaturation	95°C	3 s	45
Forward primer	1 μ M	Annealing/elongation	60°C	30 s	
Reverse primer	1 μ M				
H ₂ O	Add to 10 μ l				

The housekeeping gene Hypoxanthine-guanine phosphoribosyltransferase (*HPRT*) was used for data normalisation and the human MSC cell line SCP1 chosen as a reference for gene expression level. Expression levels were calculated according to equation 1-3.

$$\Delta c_t = c_t (\text{target gene}) - c_t (\text{housekeeping gene}) \quad (\text{Equation 1})$$

$$\Delta\Delta c_t = \Delta c_t (\text{clone}) - \Delta c_t (\text{SCP1}) \quad (\text{Equation 2})$$

$$\text{n-fold expression} = 2^{-\Delta\Delta c_t} \quad (\text{Equation 3})$$

2.2.1.19 *In vitro* transcription

In vitro transcription of DNA templates coding for sgRNAs was carried out using the MEGAshortscript T7 kit. *In vitro* transcription of DNA templates encoding RNA transcripts of 0.3-5 kb length was performed using the mMACHINE T7 kit. Transcription reactions were set up under a sterile laminar flow cabinet following the manufacturers` instruction with following modifications: Using the MEGAshortscript T7 kit, 3-5 µg template DNA was used and the reaction was incubated for 4 hours. For the mMACHINE T7 kit, 5-6 µg template DNA was used, 0.5 µl GTP added to the transcription reaction and incubation time was extended to 4 h.

2.2.1.20 Poly(A) tailing

A poly(A) tail was added to RNA transcripts generated by the mMACHINE T7 kit using the poly(A) tailing kit according to the manufacturers` instructions.

2.2.1.21 RNA purification

In vitro transcribed and poly(A) tailed RNA was purified using the MEGAclear kit according to the manufacturers` instructions.

2.2.1.22 Protein isolation

Proteins from blood cells were isolated using the CytoBuster protein extraction reagent. 5 ml blood was incubated with 25 ml erythrocyte lysis buffer for 15 min on ice. Leucocytes were pelleted for 10 min at 400 x g and 4°C, the supernatant aspirated and the procedure repeated with 10 ml erythrocyte lysis buffer. The remaining cell pellet was resuspended in 800 µl CytoBuster Protein Extraction Reagent containing 1/7 volume of Proteinase Inhibitor Cocktail. The mixture was incubated for 5 min at room temperature, followed by 30 min at -80°C and centrifuged for 5 min at 16,000 x g, 4°C. Aliquots of the protein extract containing supernatant were stored at -80°C.

Proteins from porcine tissues were isolated using the T-PER tissue protein extraction reagent. 40 mg tissue was mixed with 500 µl T-PER tissue protein extraction reagent containing 1/7 volume of proteinase inhibitor cocktail. The mixture was homogenised for 30 s using the SpeedMill Plus homogenisator, followed by 30 s cooling. For tough tissue, homogenisation

was repeated once. The sample was then centrifuged at 10,000 x g for 5 min at 4°C to pellet cell- and tissue debris. Aliquots of the protein extract containing supernatant were stored at -80°C.

2.2.1.23 Determination of protein concentration

Protein concentrations were determined using advanced protein assay reagent. 5 µl protein extract was mixed with 995 µl 1x advanced protein assay reagent and incubated for 5 min at room temperature. Each sample was distributed into three wells of a 96-well plate (300 µl each) and absorption at 595 nm measured in triplicate. Protein concentration was calculated according to equation 4.

$$\text{Protein concentration} = \frac{(\text{OD}_{\text{sample (595 nm)}} - \text{OD}_{\text{blank (595 nm)}})}{5 \mu\text{l}} \times 37.5 \mu\text{g} \quad (\text{Equation 4})$$

2.2.1.24 Western blot

Western blotting was performed to separate and detect specific proteins. A polyacrylamide gel was prepared composed of a 5% stacking gel on top of a 12% separation gel. Separation and stacking gels were prepared according to Table 26 and subsequently polymerised within a casting module. Protein samples were denatured by mixing with 4x Laemmli buffer and incubating for 5 min at 95°C. The gel was loaded with 10 to 40 µg denatured protein per lane and electrophoresis carried out at 100 V for 40 min followed by 200 V for 50 min. A PVDF membrane and two filter papers were prepared, the membrane activated in 100% methanol for 1 min and all components equilibrated in semi-dry blotting buffer. The semi-dry blotting chamber was assembled according to the manufacturers' instructions, air bubbles removed and proteins blotted onto the PVDF membrane for 50 min at 12.5 V per gel. Ponceau S staining was carried out to confirm successful transfer and the membrane was washed with 1x TBST three times for 1 min followed by three times for 10 min. Blocking was performed for 1.5 h at room temperature with 1x TBST containing either 5% milk powder or 1% NeuGc blocking solution. The membrane was incubated overnight at 4°C in primary antibody diluted in blocking solution according to the manufacturers' recommendation. The membrane was then washed three times with 1x TBST for 1 min followed by three times for 10 min. Secondary antibody diluted in blocking solution was added and incubated for 1 h at room temperature. Washing steps were conducted as before, and the membrane covered with Pierce ECL Plus western blotting substrate according to the manufacturers' protocol. The chemiluminescent signal produced by the reaction with horseradish peroxidase was detected by exposing the membrane to X-ray film for between 10 s to 10 min, and the film developed and fixed.

Table 26: Separation- and stacking gel composition

12% Separation gel		5% Stacking gel	
Component	Volume	Component	Volume
40% polyacrylamide (29:1)	1.8 ml	40% polyacrylamide (29:1)	250 μ l
1 M Tris-Cl pH 8.8	2.3 ml	0.5 M Tris-Cl pH 6.8	500 μ l
10% APS	60 μ l	10% APS	20 μ l
10% SDS	60 μ l	10% SDS	20 μ l
TEMED	2.4 μ l	TEMED	2 μ l
H ₂ O	1.8 ml	H ₂ O	1.2 ml

2.2.1.25 Immunohistochemistry

Tissue pieces were fixed with 4% formaldehyde for 24 h and stored in 80% ethanol until embedding in paraffin. 4 μ m thick tissue sections were prepared and dried at room temperature for at least 24 h. For deparaffinisation, dry tissue sections were incubated at 60°C for 10 min and washed in xylene three times for 5 min. Tissue sections were rehydrated by washing in 100% ethanol, 95% ethanol and H₂O each twice for 5 min. For antigen unmasking, slides were heated and maintained in 10 mM sodium citrate buffer (pH 6.0) for 10 minutes at sub-boiling temperature. Slides were allowed to cool in the buffer for 30 min and then three times washed with H₂O. To block endogenous peroxidases, tissue sections were incubated in 3% H₂O₂ for 10 min and washed twice with H₂O and once with TBST for 5 min each. Non-specific signals were blocked by incubating tissue sections in blocking buffer for 1 h at room temperature. Tissue sections were labelled overnight at 4°C with primary antibody diluted in blocking buffer and subsequently washed with TBST for 5 min each. Sections were incubated with secondary antibody diluted in TBST, for 2 h at room temperature and subsequently rinsed three times in TBST for 5 min each. After staining with Vectastain ABC reagent for 30 min, slides were washed with TBST three times for 5 min. Staining was visualised using DAB enhanced liquid substrate system. Tissue sections were then washed twice with H₂O for 5 min and dehydrated by incubation in 95% ethanol, 100% ethanol and xylene twice each for 20 s. Finally, slides were mounted with Roti-Histokitt and capped with cover slips. Imaging was performed using an M8 digital microscope and the corresponding software.

2.2.1.26 Generation of CRISPR/Cas9 components

Guides were identified using the CRISPR design tool provided by Zhang Lab, MIT, Cambridge, MA, USA. Guides with minimal likelihood of off-target binding were chosen and oligonucleotides designed that result in a double-stranded DNA fragment upon hybridisation.

When CRISPR/Cas9 components were to be introduced into cells as RNA, oligonucleotides were designed to contain overhangs compatible to the BbsI-digested Pbs-U6-chimaeric vector, a T7 promoter sequence for *in vitro* transcription and a target guide sequence. Both forward and reverse oligonucleotides were annealed and cloned into a BbsI-digested Pbs-U6-chimaeric vector (Figure 13A). Religants were eliminated by a BbsI redigest, positive clones confirmed by sequencing and plasmid DNA isolated via midiprep. For *in vitro* transcription of the sgRNA encoded by the construct generated, the sgRNA encoding sequence was amplified by Q5 high-fidelity DNA polymerase using the primers T7_for and Trac_rev. The PCR reaction was gel-purified to remove the plasmid template and a 4-fold consecutive nested PCR performed using the same primers. Each PCR reaction was enzymatically purified, proteinase K digested and then purified by phenol-chloroform extraction. 3-5 µg purified DNA was used as template for *in vitro* transcription by the MEGAshortscript T7 kit. *In vitro* transcribed RNA was purified using the MEGAclean kit and sgRNA aliquots stored at -80°C.

Cas9 mRNA was *in vitro* transcribed using the plasmid pCAG-Cas9-bpA as template. The plasmid was linearised with MluI, proteinase K digested and subsequently purified by phenol-chloroform extraction. *In vitro* transcription was performed using the mMACHINE T7 kit, subsequently polyA-tailed by the poly(A) tailing kit and purified with the MEGAclean kit.

When CRISPR/Cas9 components were to be delivered as DNA, oligonucleotides were designed to contain overhangs compatible to the BbsI-digested pX330-U6-Chimeric_BB-CBh-hSpCas9 vector, a single G to initiate U6 promoter transcription and a target guide sequence. Both forward and reverse oligonucleotides were annealed and cloned into a BbsI-digested pX330-U6-Chimeric_BB-CBh-hSpCas9 vector (Figure 13B). Alternatively, oligonucleotides were cloned into modified versions of pX330-U6-Chimeric_BB-CBh-hSpCas9 carrying an additional multiple cloning site (MCS) (Plasmid #705) or an MCS plus a puromycin resistance cassette linked to hSpCas9 via T2A (Plasmid #841). Religants were eliminated by BbsI redigestion, positive clones confirmed by sequencing and plasmid DNA isolated by midiprep. The vector generated, containing both sgRNA and hSpCas9 coding sequences, was used directly for DNA transfection.

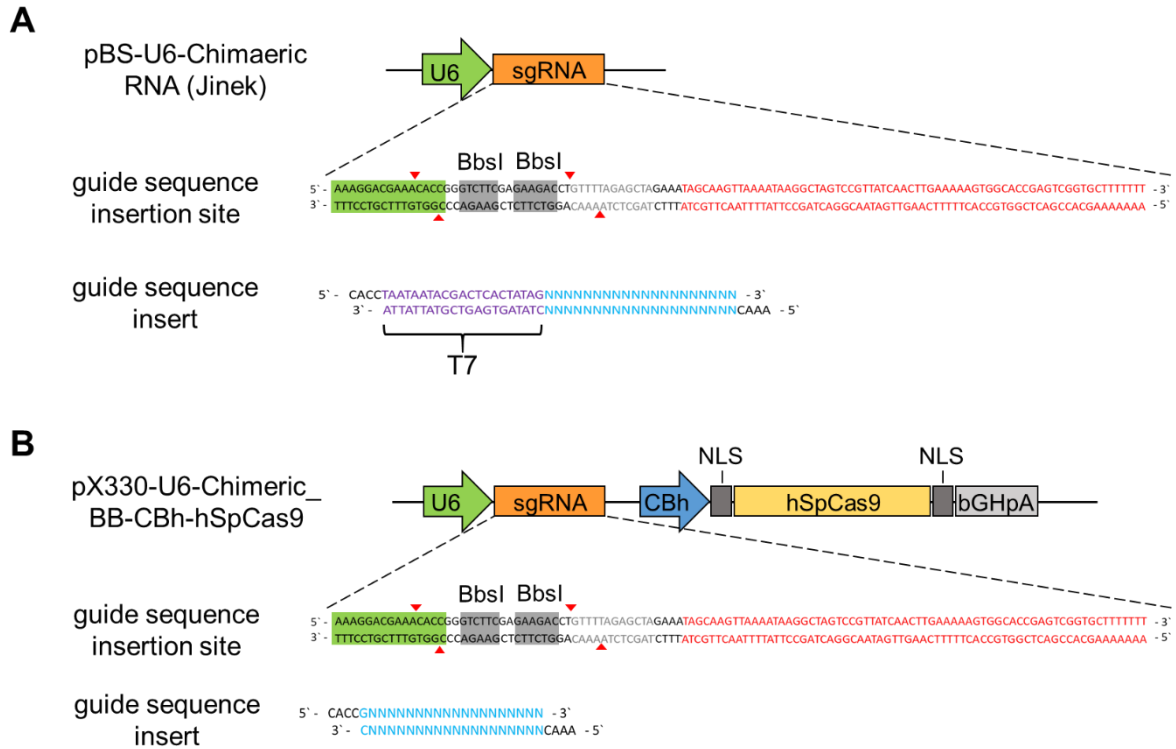


Figure 13: Cloning of target guide sequence into CRISPR/Cas9 vectors. (A) Generation of pBS-U6-Chimaeric RNA (Jinek) + target sequence. Both forward and reverse oligonucleotides were annealed and cloned into a BbsI-digested pBS-U6-Chimaeric RNA (Jinek) vector. Oligonucleotides contained 5' overhangs compatible to the BbsI restriction site (black), a T7 promoter sequence (purple) and a target guide sequence (turquoise). (B) Generation of pX330-U6-Chimeric_BB-CBh-hSpCas9 + target sequence. Both forward and reverse oligonucleotides were annealed and cloned into a BbsI-digested pX330-U6-Chimeric_BB-CBh-hSpCas9 vector. Oligonucleotides contained 5' overhangs compatible to the BbsI restriction site (black), a U6 promoter transcription start site (G) and a target guide sequence (turquoise). Red triangles: BbsI restriction sites, green boxed sequence: part of U6 promoter, grey boxed sequence: BbsI recognition site, grey sequence: crRNA, red sequence: tracrRNA. Adapted from Addgene [239].

2.2.1.27 Determination of indel efficiencies

To identify and quantify indels in cell clones or pools transfected with CRISPR/Cas9 plasmids, PCR was performed across the target site and the amplified products sequenced. For individual cell clones, sequences were analysed manually and both monoallelic and biallelic indel efficiencies calculated according to equations 5.1 and 5.2.

$$\text{monoallelic indel efficiency [\%]} = \frac{\text{number of monoallelic mutated clones}}{\text{number of total clones}} \times 100 \quad (\text{Equation 5.1})$$

$$\text{biallelic indel efficiency [\%]} = \frac{\text{number of biallelic mutated clones}}{\text{number of total clones}} \times 100 \quad (\text{Equation 5.2})$$

For cell pools, sequences were analysed using the online tool TIDE (Tracking of Indels by Decomposition). TIDE is used to determine the spectrum and frequency of targeted mutations produced within a cell pool by genome editing tools such as CRISPR/Cas9 [240]. The gRNA sequence, the test sample chromatogram and a wild type chromatogram as a control were uploaded as .abi1 files and the parameters for analysis adjusted. The algorithm reconstructed the spectrum of indels and reported the identity of the indels detected, their frequencies and the total mutation efficiency. For quality control, a statistical R^2 value between zero and one was shown as a goodness-of-fit measure. For reliable results the R^2 value should be at least >0.9 , which indicates that at least 90% of variance could be explained by the model and less than 10% by noise or large deletions. [240]

2.2.2 Microbiological methods

2.2.2.1 Cultivation of bacterial cells

E.coli bacteria were cultivated overnight at 37°C as either colonies on agar plates, or suspended in LB medium in an orbital shaker at 220 rpm, supplemented with either 100 µg/ml ampicillin or 12.5 µg/ml chloramphenicol depending on the plasmid drug resistance gene. Different volumes of overnight cultures were prepared: For minipreps, 5 ml LB medium containing the appropriate antibiotics was inoculated with a bacteria colony picked from an agar plate. For midi- and maxipreps, 100 µl bacteria culture from a glycerol stock was added to 100 ml (midiprep) or 500 ml (maxiprep) LB medium containing the appropriate antibiotics.

2.2.2.2 Transformation of bacterial cells

Plasmids were introduced into bacterial cells by electroporation. 50 µl electro-competent DH10B *E.coli* was thawed on ice, mixed with 3 µl ligation reaction and transferred to an electroporation cuvette with 2 mm electrode distance. Cells were electroporated at 2500 V for 5 ms and incubated in LB medium without antibiotics at 37°C for 30 min. Subsequently, bacteria were plated on LB plates containing antibiotics and incubated overnight at 37°C.

2.2.2.3 Preservation of bacterial cultures

Bacterial cultures carrying plasmids of interest were stored for long periods as glycerol stocks, prepared by mixing 1 ml overnight culture with 0.5 ml 99% glycerol and stored at -80°C.

2.2.3 Cell culture

2.2.3.1 Isolation of mammalian cells

Porcine kidney fibroblasts (PKF) were isolated from German Landrace pig kidneys obtained either from the TUM experimental facility Thalhausen, or from a slaughterhouse. Porcine ear fibroblasts (PEF) were isolated from porcine ear tissue. A 1 cm³ piece of kidney tissue free of any skin, large blood vessels and fat or a piece of ear tissue was washed twice in 80% EtOH and PBS. The tissue was minced mechanically and washed with PBS until the supernatant remained clear. Tissue pieces were further dissociated by incubation with 10 ml collagenase type IA (10 mg/ml) in an Erlenmeyer flask with a rotating magnetic stir bar for 30 min at 37°C. Medium was added and cells centrifuged for 5 min at 300 x g. The cell pellet was resuspended in fresh medium and distributed into three T-150 flasks. During the first week of cultivation, medium containing penicillin, streptomycin and amphotericin B was used and exchanged daily. Subsequently, cells were grown in antibiotic-free medium.

Peripheral blood mononucleated cells (PBMC) were isolated from fresh whole blood samples. 25 ml whole blood was diluted with the same volume of PBS (without Ca²⁺ and Mg²⁺) and 10 ml biocoll (density 1.077 g/ml) added to a 50 ml falcon tube. The biocoll layer was carefully overlaid with the diluted blood and the mixture centrifuged at slow acceleration- and deceleration for 30 min at 400 x g. PBMCs, visible as a white ring on top of the biocoll layer, were transferred into a new 50 ml tube, cells washed with PBS and centrifuged at 300 x g for 5 min. If necessary, the cell pellet was resuspended in 10 ml erythrocyte lysis buffer and subsequently rewashed with PBS. Cells were resuspended in an appropriate volume of medium and used directly for further experiments.

2.2.3.2 Cultivation of mammalian cells

PKF, PEF and porcine fetal fibroblast (PFF) cells were cultured with Dulbecco's Modified Eagle Medium (DMEM), supplemented with 2 mM Ala-Gln, 1x MEM non-essential amino acid solution, 1 mM sodium pyruvate solution and 10% fetal bovine serum at 37°C, 5% CO₂ in a humidified CO₂ incubator. Tissue culture work was performed in a sterile class II laminar flow hood. Medium was exchanged every third day and cells were passaged at 80-90% confluence. To passage cells, medium was aspirated, cells washed with PBS and incubated with accutase at 37°C until they detached from the tissue culture vessel wall. The accutase reaction was inactivated by addition of medium and cells were transferred to an appropriate tissue culture vessel.

2.2.3.3 DNA transfection

Eukaryotic cells were transfected with DNA by either electroporation or lipofection. For electroporation, cells were detached from the cell culture vessel, 1×10^6 cells centrifuged at $300 \times g$ for 5 min, and the cell pellet resuspended in 400 μ l hypoosmolar buffer. 4-6 μ g linearised targeting vector DNA was added, the mixture pipetted into a 4 mm electroporation cuvette, 5 min incubated at room temperature and an electroporation pulse of 1200 V applied for 85 μ s. After 5 min incubation at room temperature, 1 ml medium was added and the suspension distributed into three 10 cm dishes. The next day, cells were washed with PBS and the culture medium exchanged.

For lipofection, cells were seeded at a density of 30-50%. The next day, medium was aspirated, cells washed with PBS and cultured in 4 ml (per 10 cm dish) or 1 ml (per 6-well) Opti-MEM. A DNA mix and a transfection reagent mix were prepared and each incubated at room temperature for 5 min. For transfection of a 10 cm dish, 5 μ g DNA was mixed with OptiMEM to a final volume of 300 μ l and 6 μ l Lipofectamine 2000 transfection reagent was combined with 294 μ l OptiMEM. For transfection of a 6-well, up to 1 μ g DNA was mixed with OptiMEM to a final volume of 50 μ l and 1 μ l Lipofectamine 2000 transfection reagent was combined with 49 μ l OptiMEM. The transfection reagent mix was then added dropwise to the DNA mix and incubated for 20 - 25 min at room temperature. The mixture was dropped directly onto the cells and cultivated in the incubator for 5 h. Then, 8 ml (per 10 cm dish) or 1 ml (per 6-well) PKF medium was added, cells cultured overnight and the medium exchanged on the next day.

2.2.3.4 RNA transfection

RNA transfections were carried out using Stemfect RNA transfection kit. Cells were seeded in a 12-well tissue culture plate at a density of 80-90% and cultured overnight. The next day, medium was aspirated and 1 ml fresh culture medium added 1-2 h prior to transfection. Stemfect RNA transfection reagent and Stemfect transfection buffer were equilibrated to room temperature and mRNA thawed on ice. 2 μ l Stemfect transfection reagent was diluted with 25 μ l Stemfect transfection buffer and a mRNA mix prepared by combining 25 μ l Stemfect transfection buffer with 400 ng Cas9 mRNA and 200 ng sgRNA each. The diluted Stemfect transfection reagent was added to the RNA mix and incubated for 25 min at room temperature. The RNA-transfection reagent mix was added to the cells dropwise, evenly distributed and incubated at 37°C, 5% CO₂. The medium was exchanged after 24 h.

2.2.3.5 Selection of stable transfected cell clones

Selection of cell clones with stable transgene integration was started 48 h after transfection, using the appropriate antibiotics at a concentration determined in a 'killing curve' trial for the cell type used. Selection medium was exchanged at least every second day and, if necessary, dead cells were removed by an additional washing step with PBS. Selection was stopped once clones with no or negligible background were apparent.

2.2.3.6 Isolation of cell clones

Well separated cell colonies were marked and the plate washed with PBS. Cloning rings were dipped into sterile silicon grease and placed over each marked colony. Accutase solution was added into each cloning ring, plates incubated at 37°C until cells had detached properly and the accutase reaction then stopped by addition of medium. Suspended cells were transferred into a well of a 12- or 6-well cell culture plate, an appropriate volume of medium added and cell clones cultured further at 37°C, 5% CO₂.

2.2.3.7 Cryopreservation

For freezing, cells were detached and spun down for 5 min at 300 x g. The cell pellet was resuspended in 1.5 ml cryomedium containing 10% DMSO, 20% DMEM and 70% fetal bovine serum (FBS), transferred to a cryovial and immediately frozen at -80°C. For long term storage, cryovials were stored in the gas phase of liquid nitrogen tanks.

Frozen cryovials were thawed by transfer to a 37°C water bath and incubated until the cryomedium was almost completely thawed. 10 ml medium was added and centrifuged at 300 x g for 5 min. The diluted cryomedium was aspirated and the cell pellet resuspended in fresh culture medium. Cells were transferred to an appropriate culture vessel and cultivated at 37°C, 5% CO₂.

2.2.3.8 Enrichment of αGal- negative cells via magnetic bead selection

PKF cells were transfected with either a DNA expression vector or mRNA encoding Cas9 and sgRNAs designed to inactivate the porcine *GGTA1* gene, as described in 2.2.3.3 and 2.2.3.4. Cells were expanded and 1x 10⁶ cells used to enrich αGal-negative cells via magnetic bead selection. Cells were detached, washed with PBS, centrifuged and the supernatant aspirated. The cell pellet was resuspended in 50 µl isolectin B4, (biotin conjugate; 0.5 mg/ml) and incubated on ice for 15 min. Cells were then washed twice with PBS, centrifuged at 300 x g for 5 min and the supernatant aspirated. 200 µl streptavidin-coated magnetic beads (Dynabeads biotin binder) were purified by diluting in 3 ml PBS and applying a magnetic field for 1 min. The

supernatant was aspirated, the procedure repeated twice and the purified beads resuspended in 200 µl TL-HEPES + Ca²⁺ buffer. 200 µl purified beads were added to the cells and incubated on ice for 30 min. PBS was then added, a magnetic field applied for 1 min and the supernatant transferred to a new tube. A magnetic field was again applied for 1 min, the supernatant transferred to a new tube and centrifuged at 300 x for 5 min. The pellet, containing the αGal-negative cells, was resuspended in culture medium and seeded into a new tissue culture vessel.

2.2.3.9 Preparation of mammalian cells for somatic cell nuclear transfer

Cell clones to be used for SCNT were thawed as described in 2.2.3.7 and cultivated in standard PKF medium. Two days before SCNT, cell cycle synchronisation was induced by culture in low serum (starvation) medium. The standard cultivation medium was removed, cells were washed twice with PBS and medium replaced with standard medium containing only 0.5% FBS.

2.2.3.10 Flow cytometry

Flow cytometry was conducted using either PKF cells or porcine PBMCs. 0.2-0.5x 10⁶ cells were transferred to a well of a 96-well plate, centrifuged, the supernatant aspirated and cells resuspended in the remaining medium. Blocking of non-specific signals was carried out using 10 µl porcine serum. For *CMAH* and *GGTA1* knockout cells, no blocking was performed to avoid antigen transmission. Primary antibody was added and incubated on ice for 20 min in the dark. Cells were washed with FACS wash buffer, centrifuged, the supernatant aspirated and cells resuspended in the remaining wash buffer. Secondary antibody was added and incubated on ice for 20 min in the dark. Again, cells were washed with wash buffer, centrifuged and the supernatant aspirated. Cells were resuspended in 300 µl wash buffer and used for flow cytometry measurements. Data were acquired using a FACSCalibur flow cytometer and analysed using FlowJo software. Dead cells were excluded from the analysis.

2.2.3.11 Caspase-Glo 3/7 Assay

PKF cells were incubated with 20 ng/ml human TNF-α and 10 µg/ml cycloheximide for 24 h. Cells were detached and caspase 3/7 activity measured using the Caspase-Glo 3/7 assay according to the manufacturer's protocol.

3 Results

Pigs require multiple genetic modifications before they can be used to provide functional organs and tissues for human recipients. These include the addition of xenoprotective transgenes to overcome rejection by the host immune response and also to compensate for inter-species protein incompatibilities. Effective xenodonor pigs should also lack major cell surface antigens known to elicit an immune response in humans. This is best achieved by inactivating the endogenous porcine genes responsible.

Sections 3.1 and 3.2 describe two different approaches for the production of pigs with multiple xenoprotective transgenes. Section 3.1 focuses on step-by-step assembly of multiple transgenes at the porcine *ROSA26* locus by sequential transgene addition. As the capacity of the porcine *ROSA26* locus still remains unknown and as sequential transgene addition is very time consuming, an alternative approach is addressed in section 3.2 using integrase-mediated transgene placement. This approach comprises the addition of an attP/MIN site at a predetermined position within the porcine genome followed by integrase-mediated placement of an entire transgene battery which was prepared within this project.

Section 3.3 focuses on inactivation of endogenous porcine genes associated with xenograft rejection via the CRISPR/Cas9 system. To determine the most efficient gRNAs with minimal off-target effects, gRNAs designed to inactivate various xenorelevant genes were tested in section 3.3.1 and the influence of the length of the gRNA sequence on on- and off-target cleavage efficiency determined. The best gRNA sequences were then used to generate single-double- and four-fold knockout pigs which lack the major surface antigens eliciting an immune response in humans. At the outset of the work, the aim was to generate only *CMAH* knockout animals (Section 3.3.2). Upcoming methods, such as enrichment of *GGTA1* knockout cells and suitable selection methods, facilitated the generation of gene-edited animals and allowed first the generation of *GGTA1/CMAH* double-knockout animals (section 3.3.3) and then the generation of a four-fold knockout animal deficient in the major xenoreactive antigens α Gal, Neu5Gc and Sda and SLA class I epitopes (section 3.3.4).

Section 3.4 addresses the use of the CRISPR/Cas9 system for tissue-specific *in vivo* genome editing and describes the generation of Cas9 expressing pigs by placement of Cas9 at the porcine *ROSA26* locus.

3.1 Transgene stacking at the porcine *ROSA26* locus

To simplify breeding of xenodonor animals and thus ensure an adequate supply of organs and tissues for transplantation, xenoprotective transgenes are best grouped at a single locus. This section describes a means of assembling multiple independently-expressed transgenes at a single site by successive targeted transgene placement. The porcine *ROSA26* locus is a promising site for this approach because, it can be targeted efficiently and provides a safe haven for abundant transgene expression [238]. The aim of this project was to investigate the feasibility of sequential targeted transgene addition, 'transgene stacking', as a controlled method of assembling a set of xenoprotective transgenes grouped within the *ROSA26* locus. Replacement of the antibiotic marker at each stage avoids the accumulation of unwanted antibiotic resistance genes, and Cre-mediated deletion of floxed resistance genes provides the opportunity to generate final donor animals free of resistance markers (Figure 14).

Dr. Konrad Fischer (Chair of Livestock Biotechnology, TUM, Freising) had previously placed a SV40-driven human HO-1 cDNA construct within porcine *ROSA26* and a transgenic animal was derived [241]. The focus of my project was retargeting of this locus to place further transgenes adjacent to HO-1, commencing with a CAG promoter-driven human CD55 minigene (Figure 14). Much of the data described here have already been published [242].

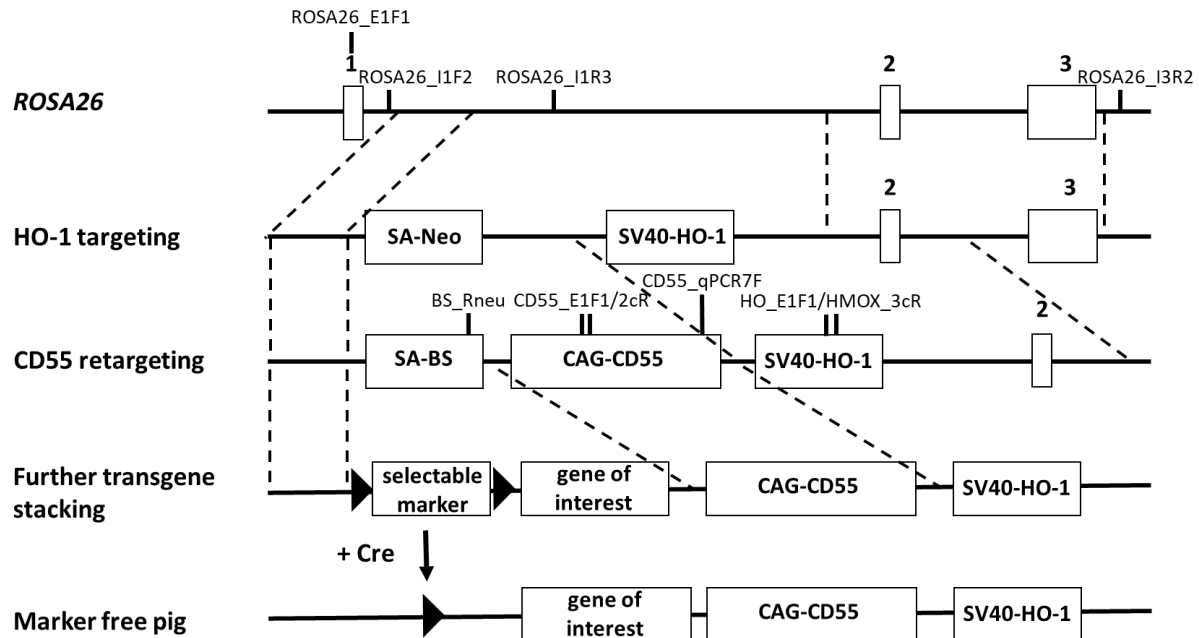


Figure 14: Transgene stacking at the porcine *ROSA26* locus. Top, structure of porcine *ROSA26*. Second row, placement of a SV40 driven HO-1 cassette. Middle, retargeting to place a CAG-driven CD55 construct adjacent to HO-1 and replace the previously introduced resistance cassette. Fourth row, repeated retargeting to stack further transgenes. Bottom, Cre-mediated removal of the loxP flanked marker cassette to generate a pig free of drug resistance genes. Primers used to identify correct retargeting and check for transgene expression are indicated. Exons are indicated by numbered boxes, regions of homology by dotted lines and loxP sites by rectangles. SA = Splice acceptor.

3.1.1 ROSA26 retargeting and the generation of CD55, HO-1 expressing piglets

To stack a human CD55 minigene upstream of HO-1 at *ROSA26*, a previously generated ROSA26-CD55-retargeting vector (see 2.1.8) was used. This promoter-trap vector consisted of: a 2.2 kb 5' homologous arm; a 1.2 kb fragment composed of splice acceptor, Kozak sequence and a promoterless blasticidin S resistance gene; a 3.7 kb CAG-driven human CD55 minigene; and a 5.2 kb 3' homologous arm (Figure 15). The CD55 minigene consisted of genomic CD55 sequence from exon one to two ligated to cDNA encoding the membrane-bound form of CD55 at a HindIII-site within exon two.

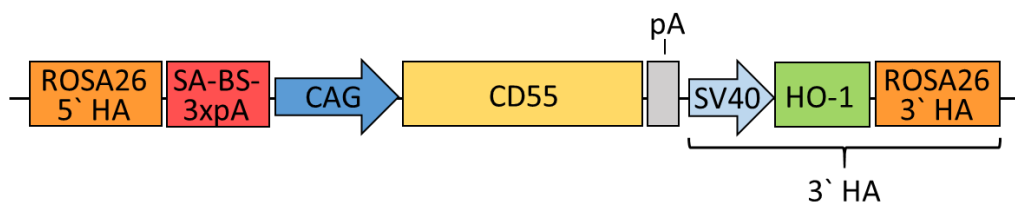


Figure 15: Structure of the ROSA26-CD55-retargeting vector. HA= Homology arm; SA= Splice acceptor; pA= BGH polyadenylation signal. Figure not to scale.

PKF cells from ROSA26-HO-1 pig #74 were transfected, cell clones isolated and further expanded. Genomic DNA was isolated and correctly targeted cell clones identified by long-range PCR across the 5' and 3' junctions. To identify mono- or biallelic targeting, the wild type *ROSA26* allele was amplified. 11% of all blasticidin S-resistant clones revealed correct, monoallelic targeting. At the RNA level, expression of both transgenes and correct splicing from *ROSA26* exon one and splice acceptor-kozak-blasticidin S was shown by reverse transcriptase PCR (RT-PCR). Positive cell clones were used for somatic cell nuclear transfer and two liveborn piglets obtained, these however were very weak and survived for only one and three days. Nuclear transfer was performed by the group of Prof. Eckhard Wolf (Chair for Molecular Animal Breeding and Biotechnology, LMU, Oberschleißheim), unless stated otherwise.

3.1.2 Analysis of a ROSA26-CD55-HO-1 retargeted piglet

Sample collection was only possible from ROSA26-CD55-HO-1 pig #559, so this animal provided the basis for further analysis. DNA was isolated from ear clip tissue, organ samples were collected and PKF cells derived for functional analysis. Correct retargeting was confirmed by long-range PCR across the 5' and 3' junctions of the retargeted allele and monoallelic targeting was shown by PCR across the non-targeted *ROSA26* allele (Figure 16A).

To detect possible random integration events, the copy number of human CD55 and HO-1 transgenes was determined by ddPCR). This revealed a hHO-1 copy number of 0.95 (± 0.07)

and a hCD55 copy number of 0.98 (± 0.05) (Figure 16B). In combination with the targeting PCR result, these data excluded the possibility of random integration.

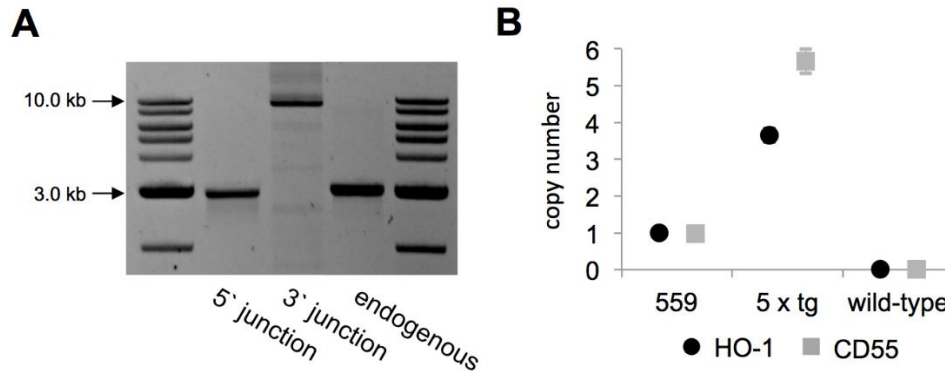


Figure 16: Targeting PCR and copy number of ROSA26-CD55-HO-1 pig #559. (A) Targeting PCR of ROSA26-CD55-HO-1 pig #559. Correct retargeting revealed 3.0 kb 5' junction and 9.3 kb 3' junction PCR products. Monoallelic targeting was evidenced by detection of a 3.1 kb endogenous PCR product from the wild type allele. (B) Copy number of human HO-1 and CD55 transgenes in ROSA26-CD55-HO-1 pig #559. DNA from a five-fold transgenic animal (5x tg) was used as positive control expressing three to four copies of HO-1 and five to six copies of CD55. Wild type DNA served as negative control.

RT-PCR analysis revealed strong HO-1 and CD55 mRNA expression in all organs analysed (Figure 17A). Quantification by q-RT-PCR (Figure 17B) revealed marked overexpression of CD55 relative to the human mesenchymal stem cell line SCP1, with the highest levels detected in muscle, lung and heart (up to 394-fold). HO-1 was expressed at similar levels to SCP1 in heart and liver and overexpressed in lung and muscle (up to 23-fold).

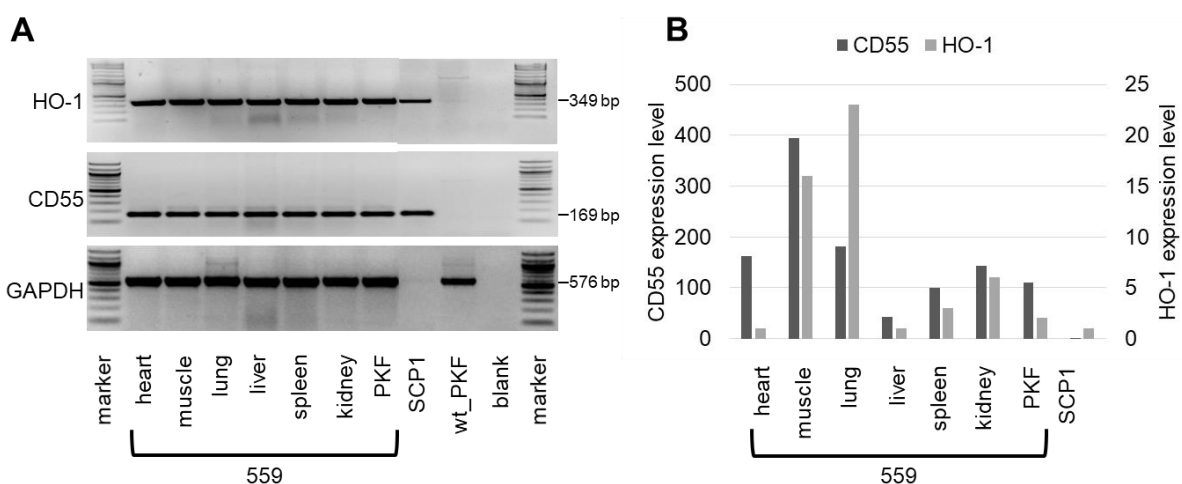


Figure 17: mRNA expression analyses of ROSA26-CD55-HO-1 pig #559. (A) RT-PCR analyses of ROSA26-CD55-HO-1 pig #559 organs and cultured cells. CD55 expression revealed a 169 bp amplicon, HO-1 expression a 349 bp PCR-fragment and pGAPDH expression a 576 bp amplicon. GAPDH primers were specific for porcine *GAPDH* and did not bind to human *GAPDH* (SCP1). Human MSC line SCP1 and wild type PKFs were used as controls. (B) q-RT-PCR analyses of ROSA26-CD55-HO-1 pig #559 organs and cultured cells. Expression values are shown relative to human MSC line SCP1 (expression = 1).

Immunohistochemical analysis revealed high CD55 protein expression in all tissues examined. In contrast to mRNA data, the strongest expression was detected in heart, spleen and pancreas, while liver and muscle showed weaker signals (Figure 18A). Consistent with mRNA data, CD55 expression was weaker in the liver but blood vessel walls within the liver showed strong staining. High expression in blood vessels was also observed in heart, lung and kidney. This is an important finding because the vasculature of grafted organs makes primary contact with the recipient's blood. Besides whole organs, pancreatic islets are an important goal for xenotransplantation. It was thus encouraging to find high CD55 expression in both exocrine pancreas and islet beta cells detected by immunofluorescence analyses carried out by Dr. Marion Schuster (Diabetes Center, LMU), (Figure 18B).

Flow cytometry analysis of PKF cells derived from piglet ROSA26-CD55-HO-1 #559 confirmed abundant CD55 expression (Figure 18C). For comparison, expression of this single copy transgene was even higher than expression from five to six copies of a genomic CD55 construct from a five-fold transgenic pig (Figure 16B, Figure 18C). As reported by Fischer et al. [68], this five-fold transgenic pig itself displayed high CD55 levels.

Specific detection of human HO-1 by immunohistochemistry or flow cytometry was not possible because all available antibodies cross-react with porcine HO-1. [104, 109]

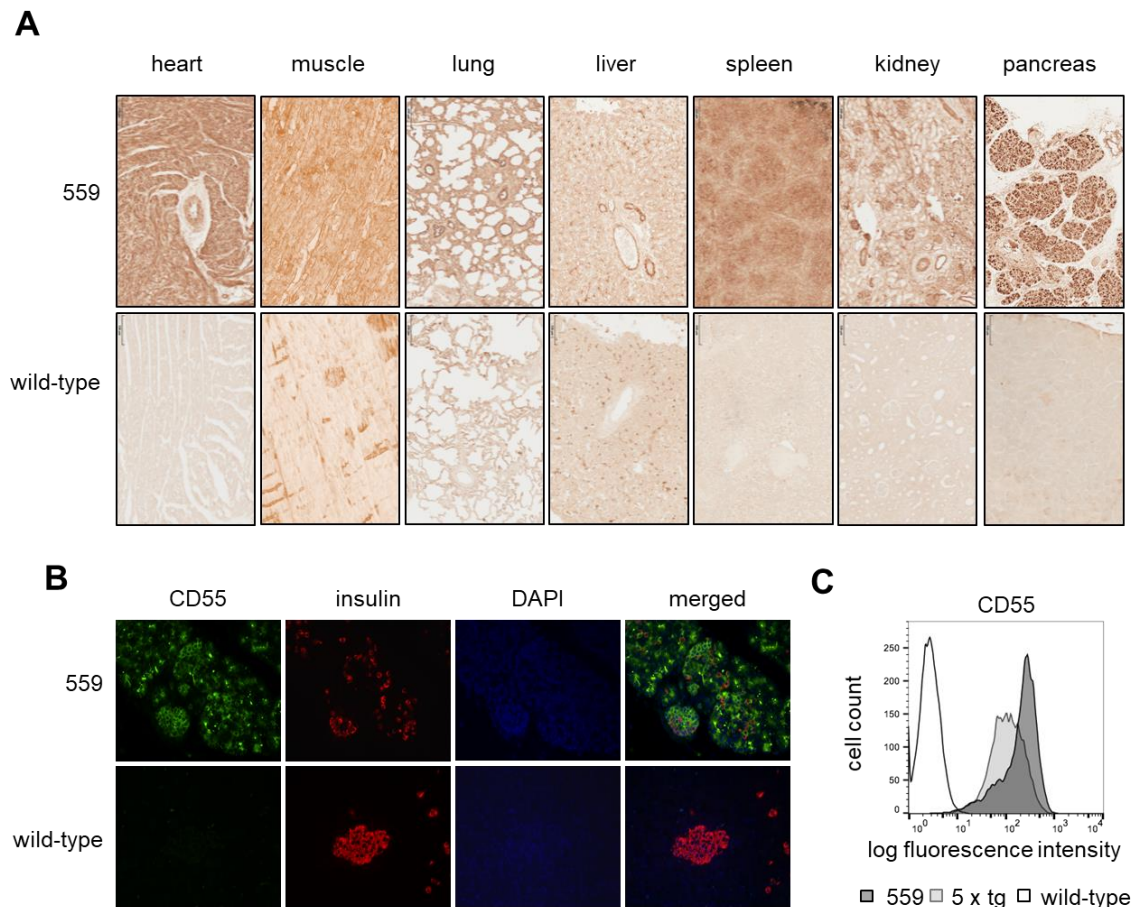


Figure 18: CD55 protein detection in tissues and cells of ROSA26-CD55-HO-1 pig #559. (A) Immunohistochemical detection of human CD55 in tissues of ROSA26-CD55-HO-1 pig #559. Brown staining indicates human CD55 expression. (B) Immunofluorescence staining of CD55 and insulin in pancreas of pig #559. Green fluorescence indicates human CD55 expression, red fluorescence porcine insulin expression. (C) Flow cytometry analysis of CD55 expression in PKF cells from pig #559 and PKF cells from a five-fold transgenic pig (5x tg) carrying five to six copies of a genomic CD55 transgene. In each case wild type pig samples are shown as controls.

Xenograft rejection is typically accompanied by inflammatory mechanisms leading to cytokine-mediated apoptosis of the xenogenic tissue or organ via caspase activation. HO-1 provides protection from apoptosis via inhibition of caspase 3/7 activity [103]. Protection of CD55 and HO-1 double-transgenic cells against caspase 3/7 induced apoptosis was tested by induction of apoptosis using TNF- α and cycloheximide. PKF cells from ROSA26-CD55-HO-1 pig #559 showed a two-fold increase of caspase 3/7 activity, whereas PKF cells from different wild type pigs showed between seven-to 14-fold increase compared to non-treated cells (Figure 19A).

Complement-mediated cell lysis is the first attack mounted by a recipient against a xenograft. The resistance of CD55 and HO-1 double-transgenic cells against human complement-mediated cell lysis was tested by incubation with human complement-preserved serum. HO-1 single transgenic PKF cells from ROSA26-HO-1 pig #74 showed reduced lysis compared to wild type. CD55, HO-1 double-transgenic PKF cells from ROSA26-CD55-HO-1 pig #559 were almost completely protected against lysis and thus comparable to PKF cells from a five-fold transgenic animal that expresses high levels of all three complement regulators CD46, CD55, CD59, as well as A20 and HO-1 (Figure 19B). The human complement-mediated cell lysis assay was carried out by Wiebke Baars (Transplantationslabor, MHH, Hannover).

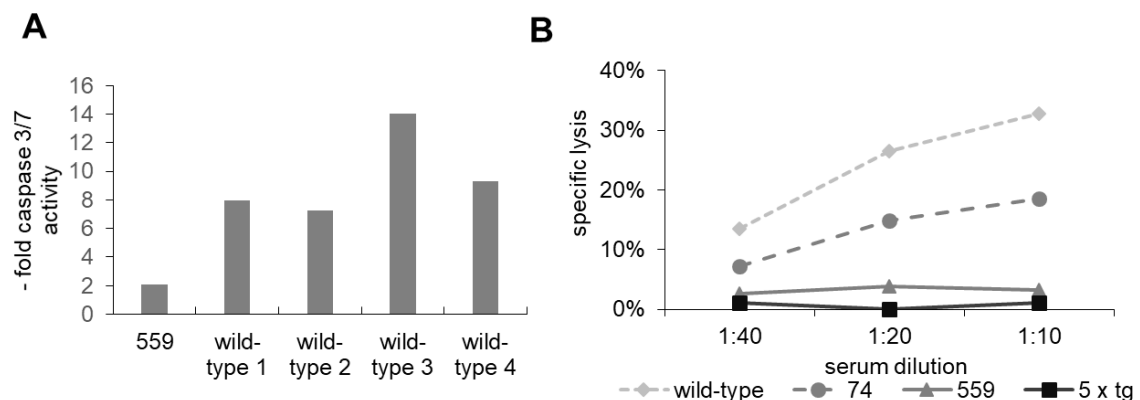


Figure 19: Protection of PKF cells from ROSA26-CD55-HO-1 pig #559. (A) Protection of PKF cells from ROSA26-CD55-HO-1 pig #559 against TNF- α and cycloheximide induced apoptosis. Cells from ROSA26-CD55-HO-1 pig #559 and four different wild type pigs were incubated with TNF- α and cycloheximide and caspase 3/7 activity measured. (B) Protection of transgenic PKF cells against human complement-mediated cell lysis. ^{51}Cr labelled cells from wild type, HO-1 single transgenic (ROSA26-HO-1 #74), CD55, HO-1 double-transgenic (ROSA26-CD55-HO-1 #559) and five-fold transgenic (5x tg) pigs were incubated with human complement preserved serum. All samples were measured in triplicate in two independent experiments.

3.1.3 Generation of a third-round-*ROSA26* targeting vector

Second round targeting of the porcine *ROSA26* locus was successful, with high targeting efficiencies and overexpression of both single-copy transgenes. Transgene stacking might thus be a suitable approach to assemble a set of xenoprotective transgenes at this locus.

To place a third transgene at the *ROSA26* locus, an 18.8 kb *ROSA26*-THBD targeting vector was generated. Construction of this vector is shown in Supplementary figure 2 and the outline structure in Figure 20A. The promoter-trap vector was designed to place a human thrombomodulin (THBD) gene under the control of a porcine THBD promoter at a site 5' of the CAG-CD55 and SV40-HO-1 transgenes (Figure 20B). It consisted of: a 2.2 kb 5' homologous arm; a 1.6 kb fragment composed of splice acceptor, kozak sequence and a promoterless neomycin resistance gene; a 1.7 kb single exon THBD gene driven by a 7.0 kb porcine THBD promoter; and a 3.8 kb 3' homologous arm.

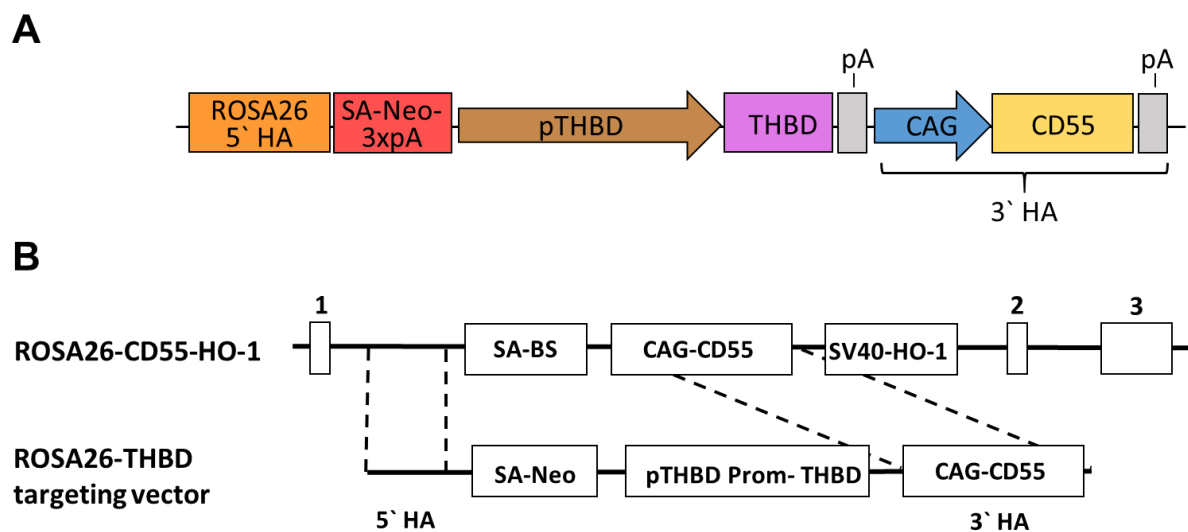


Figure 20: Third-round-targeting of the *ROSA26*-CD55-HO-1 locus. (A) Schematic structure of the *ROSA26*-THBD targeting vector. HA= Homology arm; SA= Splice acceptor; 3xPA= Triple- polyadenylation site; pA= BGH- polyadenylation site. (B) Third-round-targeting of the *ROSA26*-CD55-HO-1 locus to insert a human thrombomodulin gene (THBD) under the control of a porcine THBD promoter and exchange the blastocyst S resistance cassette with a neomycin resistance cassette. Figure not to scale.

The targeting vector could be used for a third-round-targeting approach at the *ROSA26*-CD55-HO1 locus as outlined in Figure 20B. This allows placement of a human THBD gene under the control of a porcine THBD promoter at a site 5' of the CAG-CD55 and SV40-HO-1 transgenes and simultaneously allows exchange of the blastocyst S- with a neomycin resistance cassette. However, after construction of this vector it was decided not to follow this transgene stacking approach, as transgene stacking relies on serial nuclear transfer. At that time, the group was encountering significant problems with nuclear transfer and those piglets obtained were weak

and thus not considered suitable for cell isolation and subsequent re-cloning. Nevertheless, this finding does not negate the concept of successive transgene stacking, but rather underlines its dependence on successful nuclear transfer, which remains an inefficient and imperfectly understood procedure. An alternative, more direct approach involving fewer nuclear transfer steps was therefore investigated within the next section.

3.2 Bxb1 integrase-mediated transgene placement in five-fold transgenic cells

As outlined in the introduction more in detail, a five-fold transgenic pig line with all transgenes located at a single site (chromosome 6q22) was previously generated at the Chair of Livestock Biotechnology [68]. Analysis of the transgene array has shown that the CD46 transgene is present as a single copy within this array and contains a 54 kb 3' flanking region providing a promising site to place further transgenes. Such an approach would maintain the colocalization of all transgenes at a single site and avoid segregation.

To avoid heavy reliance on serial nuclear transfer, the strategy taken was to group a set of independently-expressed transgenes on a single vector and then place it in one step within the CD46 3' flanking region in the existing array. Because targeted integration of a 40 kb construct by homologous recombination would probably be difficult, it was decided to use Bxb1 integrase-mediated transgene placement approach. This required the integration of an attP/MIN (multifunctional integrase) site within the CD46 3' flanking region by conventional gene targeting which is shown in section 3.2.2. In a second step, a transgene construct constructed in section 3.2.1 could then be placed at the attP/MIN site by site-specific Bxb1 integrase-mediated integration. The addition of an attP/MIN site in the existing array has the significant advantage that it allows parallel introduction of vectors carrying different sets of xenoprotective transgenes to generate a range of possible genotype that can be assessed to identify the most effective combination for a xenodonor pig.

3.2.1 Generation of a seven-fold transgene vector

The existing five-fold transgene array was demonstrated to provide efficient protection against complement activation and apoptosis [68]. To provide robust protection against rejection and ensure survival of the graft, further transgenes have to be added. This section describes the selection of a set of seven transgenes to provide efficient protection against different aspects of xenograft rejection and the generation of a seven-fold transgene vector.

Porcine carbohydrate xenoantigens are the main stimulus for human antibody-mediated rejection and must thus be eliminated from the donor pig. However, inactivating the enzyme responsible for their synthesis, such as alpha-1,3-galactosyltransferase, carries the risk that the substrate might then be exposed and used by other enzymes to generate another potentially immunogenic glycosylation pattern. Human H-transferase (HT) was thus selected for inclusion in the transgene array as it uses the same substrate used for α Gal synthesis to generate a well-tolerated human blood group O antigen instead of a potential new xenoantigen.

Coagulation disorders that arise as a consequence of incompatibility between the human and porcine coagulation regulators are an important contributor to xenograft failure. It was thus

decided to include the human coagulation regulators thrombomodulin (THBD) and endothelial protein C receptor (EPCR) in the set of selected transgenes to provide compatibility with the human coagulation system and thus improve the anti-coagulative properties of the xenograft.

A newly configured human HO-1 transgene was chosen for the set of new transgenes, because expression of the existing HO-1 transgene is very weak, and HO-1 has beneficial anti-apoptotic and anti-inflammatory properties. The new HO-1 construct is driven by the synthetic CAG promoter rather than the SV40 promoter, which can be prone to silencing.

Long term xenograft survival requires inhibition of cellular rejection mechanisms. To inhibit T cell activation via two distinct mechanisms, a dominant negative human CIITA-mutant (mutCIITA) and a human PD-L1 gene were included in the selected transgenes. PD-L1 inhibits T cell activation by enhancing inhibitory signals and mutCIITA by downregulation of MHC class II molecules on antigen presenting cells. Macrophage activation is usually regulated by inhibitory signals via binding of the ubiquitously expressed CD47 to SIRP α on macrophages. Porcine CD47 is incompatible with human SIRP α , so a human CD47 transgene was chosen to provide inhibitory signals and thus protect against macrophage activation.

To simultaneously place these xenoprotective transgenes within the CD46 3' flanking region, they have first to be assembled into a single vector. The single-transgene vectors (see 2.1.8) were already available at the Chair and were combined on a BAC-construct. Construction of the final vector pBACe3.6-PD-L1-HT-mutCIITA-CD47-HO1-THBD-EPCR, referred to as '7x transgene vector', is shown in Supplementary figure 1. Juliane Palluk (Master's student) participated in cloning of the last steps of this construct.

The outline structure of the 7x transgene vector is shown in Figure 21. The 40.6 kb vector comprises: a 6.4 kb BAC backbone and the seven transgenes, each driven by a separate promoter and followed by a 0.2 kb bovine growth hormone polyadenylation signal (BGHpA). The 0.9 kb human PD-L1-cDNA sequence is driven by a 0.5 kb CCL2-promoter. The human mutCIITA construct contains a 1.6 kb Tie2 enhancer, a 1.8 kb CAG-promoter and a 4.0 kb mutCIITA coding sequence. The mutCIITA coding sequence itself lacks the coding sequence for the N-terminal transactivator domain and comprises cDNA encoding amino acids 1-6, 151-1131, a nuclear localisation signal (NLS) and a 1.0 kb 3' untranslated region (UTR) fragment. The human THBD construct consists of a 7.0 kb porcine THBD-promoter and a 1.7 single exon human THBD sequence. The human HT- (1.1 kb), CD47- (1.0 kb), HO-1- (0.9 kb) and EPCR (0.7 kb) cDNA sequences were each driven by a 1.7 kb CAG promoter.

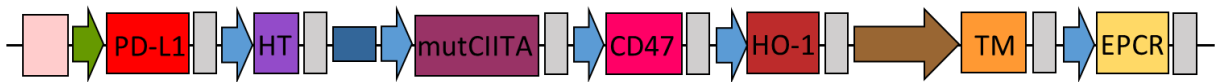


Figure 21: Structure of the final 7x transgene vector. Blue coloured arrows represent the CAG promoter, brown coloured arrows the porcine THBD promoter and green coloured arrows the CCL2 promoter. Grey coloured boxes represent the BGH polyadenylation signals, dark blue coloured boxes the Tie2 enhancer and pink boxes the pBACe3.6 backbone. Figure not to scale.

PKFs (isolate 250515) were transfected with the final 7x transgene vector. Figure 22 shows RT-PCR detection of expression of all seven transgenes within a cell pool (J. Palluk).

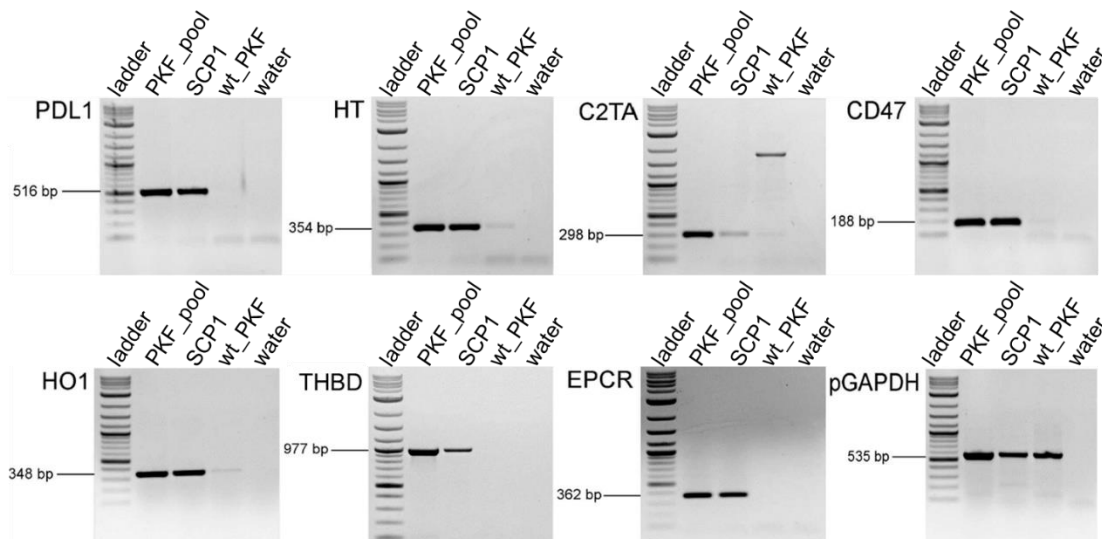


Figure 22: RT-PCR analysis of a 7x transgene vector transfected PKF cell pool. Human MSC line SCP1 and wild type PKFs were used as controls.

3.2.2 Introduction of an attP/MIN site into the CD46-flanking region

This section describes the placement of an attP/MIN site within the unique CD46 3' flanking region within the 6q22 transgene array by homologous recombination (Figure 23).

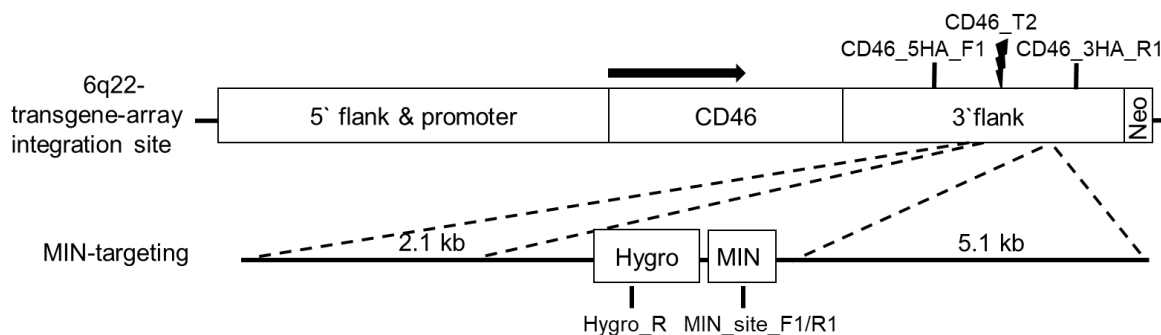


Figure 23: Targeting approach to integrate a MIN site within the CD46 3' flanking region. Top, structure of the human CD46 construct at position 6q22 in the porcine genome. Bottom, placement of an attP/MIN site within the 3' flanking region of CD46. Primers used to identify correct targeting are indicated by black bars and regions of homology by dotted lines. Figure not to scale.

A previously generated CD46-MIN targeting vector (see 2.1.8) was used to introduce an attP/MIN site within the 3' flanking region approximately 36 kb downstream of the human CD46 coding region. This vector consisted of: a 2.1 kb 5' homologous arm; a 2.1 kb fragment composed of SV40-promoter, hygromycin resistance gene and a triple-polyadenylation signal; a 47 bp attP/MIN site; and a 5.1 kb 3' homologous arm (Figure 24). To enhance homologous recombination efficiency, the targeting vector was used in combination with the CRISPR/Cas9 plasmid pX330-CD46-T2 (see 2.1.8) that has a guide RNA directed against a sequence in the 3' flanking region of CD46 flanked by both homologous arms of the targeting vector. Targeting was performed by Julia Zuber (Master's student).

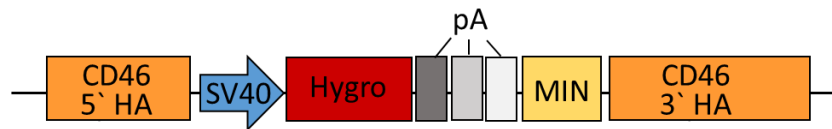


Figure 24: Structure of the CD46-MIN targeting vector. HA= Homology arm, pA= Polyadenylation site. Figure not to scale.

PKF cells from five-fold transgenic, *GGTA1*^{-/-}, *CMAH*^{+/-} pig #814 were cotransfected with the linearised CD46-MIN targeting vector and the CRISPR/Cas9 plasmid pX330-CD46-T2. Genomic DNA from individual cell clones was isolated and correctly targeted clones identified by long-range PCR across the 5' junction. The primer combination CD46 5HA F1 and Hygro R amplified a 3.0 kb fragment and 9 out of 80 (11%) hygromycin-resistant clones revealed correct, monoallelic targeting (Figure 25A). Correct targeting was further confirmed by an extended 5' junction PCR (4.7 kb) and by a 5.6 kb 3' junction PCR. In addition, the entire targeted region was amplified and revealed an approximately 2.1 kb integration. Figure 25B shows correct targeting for clone #1.5.

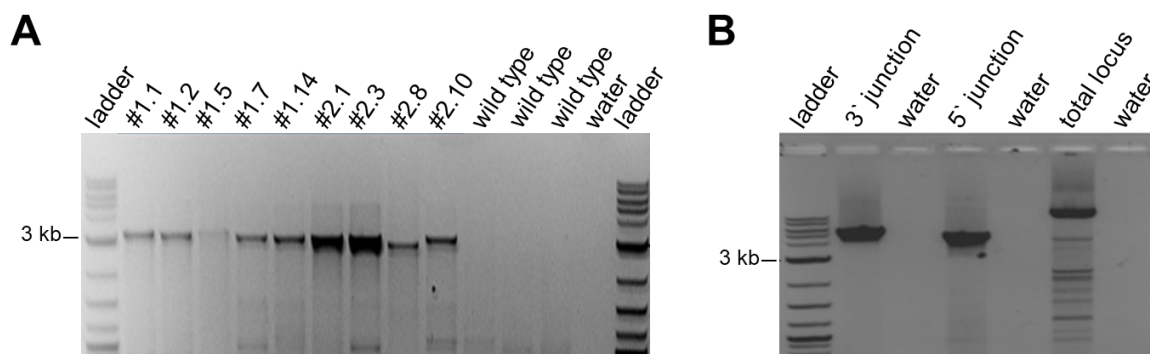


Figure 25: PCR-analyses of correctly targeted CD46-MIN clones. (A) 5' junction PCRs of correctly targeted CD46-MIN clones. Correct targeting revealed a 3.0 kb 5' junction PCR product. Wild type DNA served as negative control. (B) Targeting PCRs of CD46-MIN clone #1.5. Correct targeting revealed a 4.7 kb 5' junction and a 5.6 kb 3' junction PCR product. Amplification of the entire locus revealed a 10.3 kb PCR product and thus a 2.5 kb insertion.

To exclude additional, random integration of the targeting vector, hygromycin copy number was determined by ddPCR (J. Zuber). Five clones (#1.1, #1.2, #1.5, #1.14 and #2.3) had a single copy of hygromycin, the others had two (#1.7, #2.1, #2.8) or more (#2.10) copies (Figure 26).

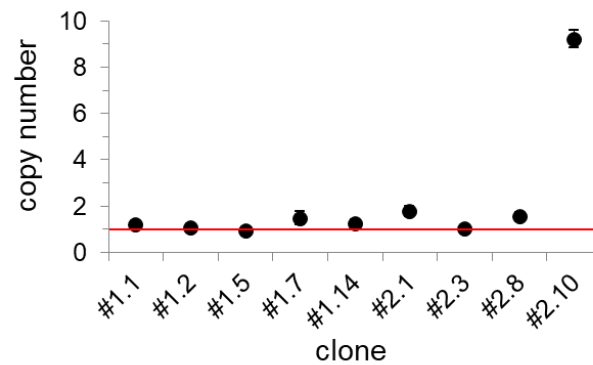


Figure 26: Hygromycin copy number of correctly targeted cell clones. Red line: copy number = 1.0

Cell clones with correct targeting and shown to carry just a single transgene copy are currently being used for somatic cell nuclear transfer. As soon as piglets are available, these will be used for cell isolation to carry out Bxb1-mediated transgene integration.

3.3 Pigs deficient in the major xenoreactive antigens

As mentioned earlier, several endogenous porcine genes must be inactivated to remove xenoreactive antigens to reduce rejection by human recipients. The most important genes in this context are *GGTA1*, *CMAH* and *B4GALNT2*, which synthesise xenogeneic glycosylation patterns. In addition, the SLA class I complex is a xenogeneic structure recognised by the recipients' immune system. This section describes the generation of cells and pigs deficient in at least one of the major xenoreactive antigens achieved by the CRISPR/Cas9 system.

3.3.1 Evaluation of gRNA sequences against xenorelevant genes

The CRISPR/Cas9 system enables efficient gene inactivation and can be used to simultaneously target several genes. Identification of gRNAs with a high on-target cleavage efficiency is key to success, especially where multiple genes are to be targeted. At the same time, low off-target cleavage efficiency is required to avoid accidental inactivation of any other gene. The influence of the length of the gRNA sequence on on- and off-target cleavage efficiency was determined within this section. Moreover, the most efficient gRNAs designed to inactivate various xenorelevant genes were identified.

3.3.1.1 Influence of gRNA sequence length on on- and off-target cleavage

It has been reported that the length of gRNAs influences the efficiency of both on- and off-target cleavage [243, 244]. To investigate this and to compare various gRNA sequence lengths, several sgRNAs were generated to inactivate the porcine *CMAH* gene. Each sgRNA contained a gRNA directed against a sequence in exon 10 of porcine *CMAH*, comprising either 20 bp plus two guanines at the 5' end, 20 bp- or 18 bp.

PKF 1706 cells were transfected with Cas9 mRNA and a sgRNA with modified gRNA length, cell clones were isolated and genomic DNA isolated. In total, 298 cell clones were analysed to determine on-target cleavage by PCR across the gRNA target site and subsequent sequencing. Furthermore, off-target analyses at the six most probable off-target sites were carried out in 17 clones that revealed on-target cleavage. The results are summarised in Table 27. Similar results regarding on-target cleavage efficiency were obtained using an 18- or 20 bp gRNA (8-10% biallelic- and 17-24% monoallelic indels). In contrast, the addition of two guanines (GG) to the 5' end of a 20 bp gRNA decreased on-target cleavage efficiency to only 10% of clones with monoallelic indels. No off-target cleavage was observed in any of the analysed clones irrespective of gRNA sequence length. Due to these results and the decreased off-target cleavage reported in the literature, sgRNAs that contained an 18 bp gRNA sequence were mainly used in the experiments below.

Table 27: Influence of the gRNA sequence length on on- and off-target cleavage efficiency.

gRNA length	gRNA sequence (CMAH_E10T1)	On-target cleavage efficiency		Off-target cleavage
		Biallelic	Monoallelic	
gg + 20 bp	gggaagaaactcctgaactaca	0%	10%	Not observed
20 bp	gaagaaactcctgaactaca	8%	24%	Not observed
18 bp	agaaactcctgaactaca	10%	17%	Not observed

3.3.1.2 Identification of efficient gRNA sequences

To identify gRNA sequences with high on-target cleavage efficiencies, various gRNAs were tested designed to inactivate the xenorelevant genes *B2M*, *B4GALNT2*, *CMAH* and *GGTA1*.

GRNA sequences were chosen to target various exons or different positions within an exon of the genes mentioned above. All gRNAs were tested in porcine primary cells (PKF or PFF) or in a swine testis (ST) cell line. Where possible, puromycin selection or enrichment of α Gal-negative cells via a magnetic bead selection (see 2.2.3.8) was applied and then single cell clones or cell pools analysed to determine on-target cleavage efficiencies. The results are shown in Table 28.

In summary, three gRNAs targeting exon three of *B4GALNT2* were analysed and the best results were obtained with gRNA B4GALNT2_E3T3, which revealed 10% gene editing efficiency without selection and 85% with puromycin selection. Three gRNA sequences were tested directed against various exons of the porcine *CMAH* gene and the highest indel efficiency was obtained in exon ten using the gRNA CMAH_E10T1 (17% monoallelic and 10% biallelic edited clones without any selection applied). Six gRNA sequences were tested targeting three different exons of the porcine *GGTA1* gene. For all gRNAs used, 0.2-11% of cells revealed biallelic indels at the respective gRNA target site without any selection applied. After enrichment of α Gal-negative cells, 100% of remaining cells were α Gal-negative and revealed biallelic indels at the target site. Only a single gRNA was tested targeting the porcine *B2M* gene in exon one. Interestingly, this gRNA was found to be inefficient without any selection applied (only 3% monoallelic clones). However, cotransfection with a gRNA directed against *GGTA1*, which is located on the same chromosome as *B2M*, and subsequent puromycin selection and enrichment of α Gal-negative cells, markedly increased gene editing efficiency (97% total efficiency).

Table 28: GRNA efficiencies for four xenorelevant genes. Where cell pools were analysed, a total indel efficiency is given. Where single cell clones were analysed, indel efficiency is further separated into monoallelic and biallelic. Indirect selection means that a gRNA was cotransfected with a gRNA directed against the porcine *GGTA1* gene and *GGTA1* knockout cells subsequently enriched. The gRNAs shown in bold were used to generate the knockout pigs described in the following sections of this thesis.

Name	gRNA target site	gRNA target sequence	Selection	Indel efficiency
B2M_E1T1	B2M exon 1	tagcgatggctcccctcg	no	3% monoallelic 0% biallelic
			puromycin resistance; indirect	97% total
B4GALNT2_E3T1	<i>B4GALNT2</i> exon 3	gtgacgccttcgggcatc	no	5% total
B4GALNT2_E3T2	<i>B4GALNT2</i> exon 3	agctttcctgatgccga	no	3% total
B4GALNT2_E3T3	B4GALNT2 exon 3	aggaaagctataactgg	no	10% total
			puromycin resistance	85% total
CMAH_E10T1	CMAH exon 10	agaaactcctgaactaca	no	17% monoallelic 10% biallelic
CMAH_E3T2	<i>CMAH</i> exon 3	acatgttcttacatgccttc	no	0% monoallelic 0% biallelic
CMAH_E6T1	<i>CMAH</i> exon 6	gtcctgctttgvcgagga	no	9% monoallelic 0% biallelic
GGTA1_E6T7	<i>GGTA1</i> exon 6	gagcttccgctagtggac	no	0.2% biallelic
			<i>GGTA1</i> ^{-/-} cell enrichment	100% biallelic
GGTA1_E7T5	<i>GGTA1</i> exon 7	caaacagaaaattaccgt	no	0.2% biallelic
			<i>GGTA1</i> ^{-/-} cell enrichment	100% biallelic
GGTA1_E7T6	GGTA1 exon 7	gtcgtgaccataaccaga	no	11% biallelic
			GGTA1 ^{-/-} cell enrichment	100% biallelic
GGTA1_E8T2	<i>GGTA1</i> exon 8	tactgctgggattatcatat	no	14% monoallelic 6% biallelic
GGTA1_E8T3	GGTA1 exon 8	gacgagttcacctacgag	no	2% biallelic
			GGTA1 ^{-/-} cell enrichment	100% biallelic
GGTA1_E8T4	GGTA1 exon 8	atggtgatgatatctcc	no	8% biallelic
			GGTA1 ^{-/-} cell enrichment	100% biallelic

3.3.2 *CMAH* knockout cells and pigs

The porcine *CMAH* enzyme synthesises one of the major xenoreactive antigens, Neu5Gc. Humans lack Neu5Gc expression and produce antibodies against this epitope and hence develop an immune response upon contact with xenogeneic cells or tissues. To avoid xenograft rejection, removal of these xenoreactive epitopes from porcine cells is required. The strategy taken was to inactivate the *CMAH* gene in pigs carrying the five-fold transgenic array at 6q22 mentioned above, and also to generate a female *CMAH* knockout line as suitable breeding partner to maintain Neu5Gc deficiency in the offspring. Wild type rather than five-fold transgenic female cells were chosen to avoid generating offspring homozygous for the 6q22 transgene array, which would express very high and possibly deleterious levels of complement regulators.

To inactivate the *CMAH* gene via the CRISPR/Cas9 system, a sgRNA (*CMAH_E10T1*) was chosen (see 3.3.1.2). Female wild type pFFs (251113_4) and male five-fold transgenic PKFs (1706) were transfected with the sgRNA and Cas9 mRNA, and genomic DNA from cell clones isolated. Gene-edited cell clones were then identified by PCR across the gRNA target site and subsequent sequencing.

For the female pFF cells, 16/124 clones (=13%) revealed monoallelic and 11/124 clones (=9%) biallelic gene editing at the gRNA target site. Clone #164 carried a biallelic single bp insertion 3 bp 5' of the PAM motive leading to an early stop codon. This clone was used for SCNT and a liveborn female piglet (#463) obtained. Unfortunately, this animal died due to a bacterial infection at an age of two weeks. PKF cells were isolated for further modification.

For the male five-fold transgenic cells, 22/129 clones (=17%) revealed monoallelic and 13/129 clones (=10%) biallelic gene editing at the gRNA target site. Cell clone #59 showed two gene-edited alleles carrying a single base insertion 3 bp 5' of the PAM motive and an 11 bp deletion. This clone revealed no off-target cleavage at the six most probable off-target-sites and was thus used for SCNT, which in this case was performed by the group of Prof. Heiner Niemann (Friedrich Löffler Institut, Mariensee). Two pregnancies were established, of which one was artificially terminated at day 27. Three foetuses were explanted, PFFs isolated (570/1-3) (carried out by Dr. Björn Petersen, Friedrich Löffler Institut, Mariensee) and used for further experiments. The other pregnancy resulted in one liveborn pig #890 (Figure 27). Unfortunately, this boar died shortly before sexual maturity for unknown reasons.



Figure 27: Picture of the five-fold transgenic, *CMAH* knockout boar #890 at an age of 3.5 months.

The generated pigs #463 and #890 as well as the three fetuses were analysed further. For genotypic analysis, DNA was isolated from ear clip tissue or from foetal cells, PCR across the *CMAH* E10T1 gRNA target site was performed using the primers *CMAH_E10T1_F/R* and the PCR products sequenced. The female pig #463, the male five-fold transgenic pig #890 and all three five-fold transgenic fetuses (#570/1-3), displayed biallelic indels at the gRNA target site (Figure 28). In accordance with the cell clone used for SCNT, pig #463 carried a biallelic single bp insertion 3 bases 5' of the PAM motive. Pig #890 and the three fetuses revealed a single bp insertion and an 11 bp deletion on the second allele.

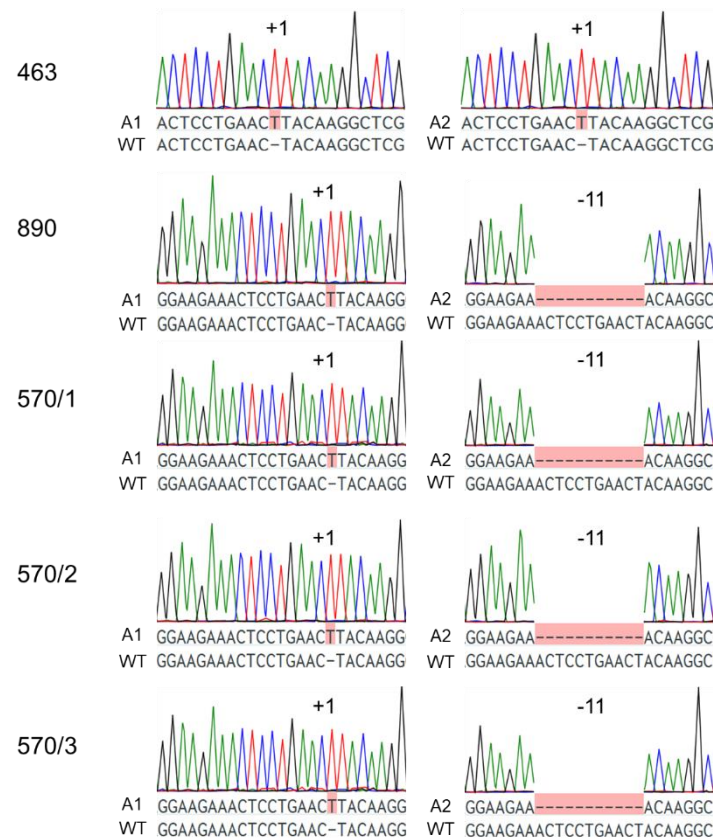


Figure 28: Genotypic analysis of *CMAH* knockout pigs. #463= female *CMAH* knockout pig, #890= male five-fold transgenic *CMAH* knockout pig, and 570/1-570/3= five-fold transgenic, *CMAH* knockout fetuses. A1= sequence for allele one, A2= sequence for allele two, WT= wild type sequence.

Western blot analyses were performed to determine whether the introduced indels had inactivated the CMAH enzyme. As CMAH is responsible for the conversion of Neu5Ac to Neu5Gc, inactivation of this enzyme results in absence of Neu5Gc epitopes. Neu5Gc epitopes are present on a huge variety of glycosylated proteins. Proteins isolated from a kidney of pig #463 and from blood of pig #890 showed complete absence of Neu5Gc epitopes and thus functional knockout of the *CMAH* gene, whereas proteins isolated from a wild type pig revealed Neu5Gc epitopes on a variety of proteins (Figure 29).

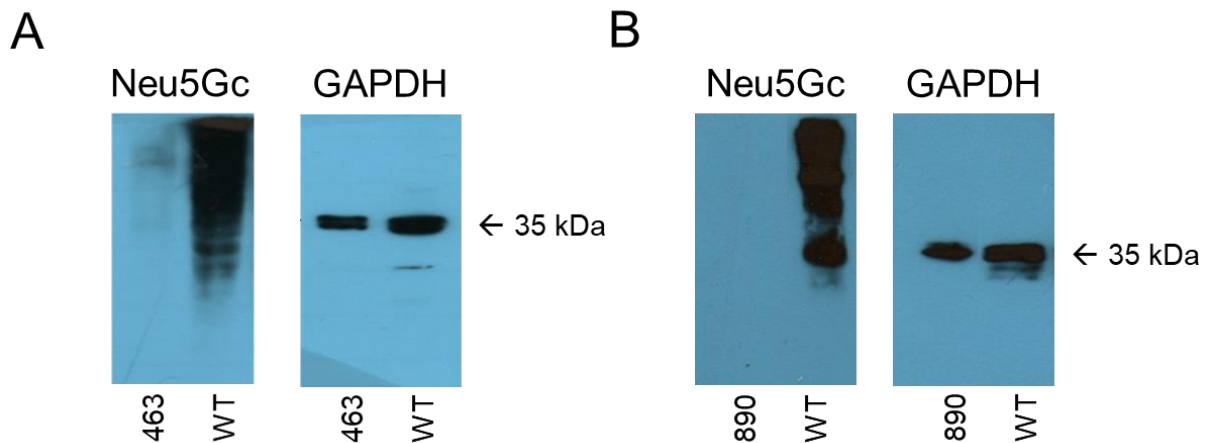


Figure 29: Neu5Gc and GAPDH western blot analyses of pig #463 and #890. Due to a functional *CMAH* knockout, Neu5Gc is absent on proteins isolated (A) from kidney tissue of pig #463 and (B) from blood cells of pig #890. Proteins isolated from a kidney of a wild type pig (=WT) served as positive control. GAPDH was used as loading control and revealed signals at the expected molecular weight of 35 kDa for both wild type- and *CMAH* knockout samples.

3.3.3 *GGTA1/CMAH* double-knockout pigs

α Gal is another major xenoantigen on porcine cells and is synthesised by the porcine *GGTA1* enzyme. Similar to Neu5Gc, humans lack α Gal due to mutations in the gene that encodes the enzyme responsible for its synthesis and produce antibodies against the α Gal epitope. Consequently, these xenogeneic structures must be removed from organ donor pigs to avoid xenograft rejection. This chapter describes the generation of α Gal- and Neu5Gc-double-deficient pigs via inactivation of the *GGTA1* and *CMAH* genes. This was achieved in a male, five-fold transgenic pig line and in female wild type- and *CMAH* knockout lines.

3.3.3.1 *GGTA1/CMAH* double-knockout, five-fold transgenic pigs

The porcine *GGTA1* gene was inactivated via the CRISPR/Cas9 system in *CMAH* knockout, five-fold transgenic PFF cells generated in section 3.3.2. A sgRNA (*GGTA1_E8T4*) was chosen (see 3.3.1.1) directed against a sequence in porcine *GGTA1* exon eight. Male *CMAH* knockout, five-fold transgenic PFF cells (#570/3) were transfected with the sgRNA and Cas9

mRNA, α Gal-negative cells enriched and genomic DNA from cell clones isolated. PCR across the gRNA target site GGTA1 E8T4 was performed and 100% biallelic edited clones identified by sequencing. Clone #24 revealed two edited alleles carrying an 11 bp deletion and an 18 bp insertion at the GGTA1_E8T4 target site. This clone was used for SCNT and resulted in two liveborn *GGTA1/CMAH* double-knockout, five-fold transgenic piglets (#544 and #545).

The *GGTA1/CMAH* double-knockout, five-fold transgenic piglets #544, #545 were further characterised. For genotyping, PCR across the GGTA1_E8T4 gRNA target site was performed with the primers GGTA1_E8T4_F/R and the amplified fragments sequenced. This revealed biallelic indels at the GGTA1_E8T4 gRNA target site. Consistent with the cell clone used for SCNT, two edited alleles were detected carrying an 11 bp deletion and an 18 bp insertion at the gRNA target site. In addition, genotypic analysis confirmed the presence of the previously introduced indels at the CMAH_E10T1-gRNA target site. One allele carried a single bp insertion and the second one an 11 bp deletion (Figure 30).

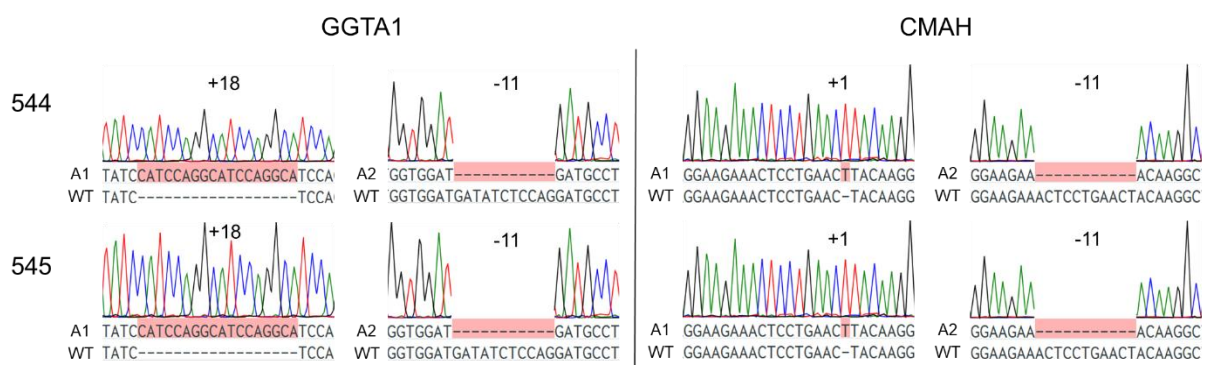


Figure 30: Genotypic analysis of the double-knockout, 5xtg pigs #544 and #545. A1= sequence for allele one, A2= sequence for allele two, WT= wild type sequence.

Piglet #544 unfortunately died six days after birth for unknown reasons. PKF cells were isolated and used for flow cytometry analysis, which was carried out by Anna Buermann (Transplantationslabor, MHH, Hannover). This analysis showed the absence of α Gal and Neu5Gc, consistent with *GGTA1* and *CMAH* knockouts. In addition, expression of the three complement regulators CD46, CD55 and CD59 was verified (Figure 31).

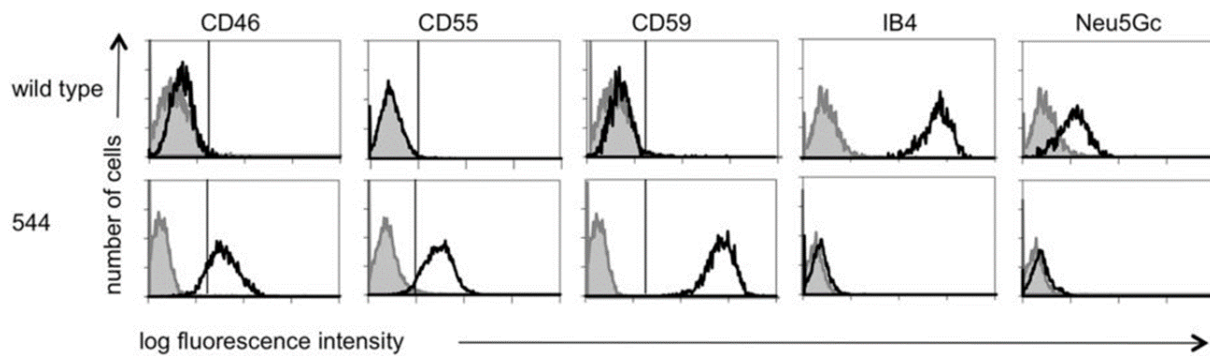


Figure 31: Flow cytometry analyses of PKFs from piglet #544 revealed loss of α -Gal and Neu5Gc epitopes as well as human CD46, CD55 and CD59 expression. α Gal was detected by binding of isolectin B4 (IB4). Grey histograms represent secondary antibody staining only.

3.3.3.2 Female *GGTA1/CMAH* double-knockout pigs

In addition to the male *GGTA1/CMAH* double-knockout, five-fold transgenic line presented above, female *GGTA1/CMAH* double-knockout animals were to be generated as breeding partners. Thus, both lines could be crossed in a time-saving manner without loss of homozygosity of the disrupted genes and without any disadvantageous inbred effects.

Two strategies were applied. One approach comprised a serial inactivation of both genes, whereas the other strategy aimed a simultaneous disruption (Figure 32).

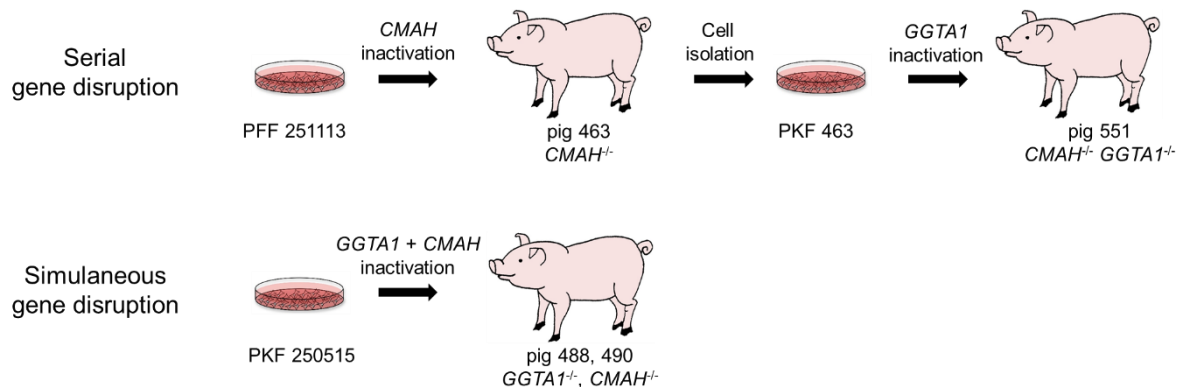


Figure 32: Workflow for the generation of female *GGTA1/CMAH* double-knockout pigs.

For serial inactivation, PKF cells from the *CMAH* knockout animal #463 (generated in section 3.3.2) were used to inactivate the porcine *GGTA1* gene via the CRISPR/Cas9 system. A sgRNA (*GGTA1_E7T6*) directed against a sequence in porcine *GGTA1* exon seven was chosen and together with Cas9 mRNA transfected into PKFs #463. α Gal-negative cells were enriched, the resulting cell pool used directly for SCNT and a liveborn female double-knockout piglet (#551) obtained (Figure 33). This animal was slaughtered at an age of 20 months as several attempts to establish a pregnancy were not successful. Examination revealed an underdeveloped uterus which was the likely cause of infertility.



Figure 33: Picture of sow #551 at an age of 20 months.

To avoid serial nuclear transfer which is a limiting factor in the generation of gene-edited animals due its inefficiency, simultaneous disruption of both *GGTA1* and *CMAH* was carried out in parallel. For this, a double-knockout vector pX330-U6-Chimeric_BB-CBh-hSpCas9-CMAH-GGTA1, referred to as #705-CMAH-GGTA1, was generated (Supplementary figure 3 and Figure 34). The 9.2 kb vector is composed of a CBh-driven hSpCas9 construct and sgRNA sequences carrying gRNAs directed against their target sequences in *GGTA1* exon eight (gRNA GGTA1_E8T3) and *CMAH* exon 10 (gRNA CMAH_E10T1). The CBh-driven hSpCas9 construct consists of a 0.8 kb CBh promoter, followed by a SV40 NLS, a 4.0 kb hSpCas9 gene, a nucleoplasmin NLS and a 0.2 kb BGHpA. SgRNA sequences are driven by a 0.2 kb U6 promoter and are composed of an 18 bp gRNA sequence and a sgRNA scaffold sequence

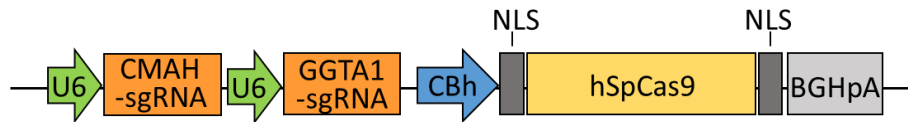


Figure 34: Structure of the double-knockout plasmid #705-CMAH-GGTA1. #705 refers to pX330-U6-Chimeric_BB-CBh-hSpCas9. Figure not to scale.

Female PKF (250515) cells were transfected with this vector, α Gal-negative cells enriched and genomic DNA from individual cell clones isolated. PCR across the gRNA target sites was performed using the primers CMAH_E10T1_F/R and GGTA1_E8T3_F/R. 18% of the analysed clones revealed biallelic indels at both gRNA target sites in *CMAH* exon ten and *GGTA1* exon eight. Cell clones carrying frameshift mutations were used for somatic cell nuclear transfer and two healthy, liveborn piglets obtained (#488 and #490) (Figure 35).



Figure 35: Pictures of sows #488 and #490 at an age of 25 months.

These two pigs (#488, #490) and pig #551 were analysed at the genotypic and phenotypic levels. For genotype analysis, DNA was isolated from ear clip tissue and PCR performed across the respective gRNA target sites. All three pigs displayed biallelic indels at the gRNA target sites within the *GGTA1*- and *CMAH* genes. Pigs #488 and #490 revealed a biallelic single bp insertion at the *GGTA1*_E8T3-gRNA target site in *GGTA1* exon 8. For *CMAH*, two edited alleles were identified, containing either a single bp insertion or a 14 bp deletion at the *CMAH*_E10T1-gRNA target site. For pig #551, two edited *GGTA1* alleles were detected. The first allele contained a 13 bp deletion combined with a single bp insertion at the *GGTA1*_E7T6-gRNA target site, whereas the second one revealed a 4 bp deletion. Regarding *CMAH*, a biallelic single bp insertion was detected at the *CMAH*_E10T1-gRNA target site (Figure 36).

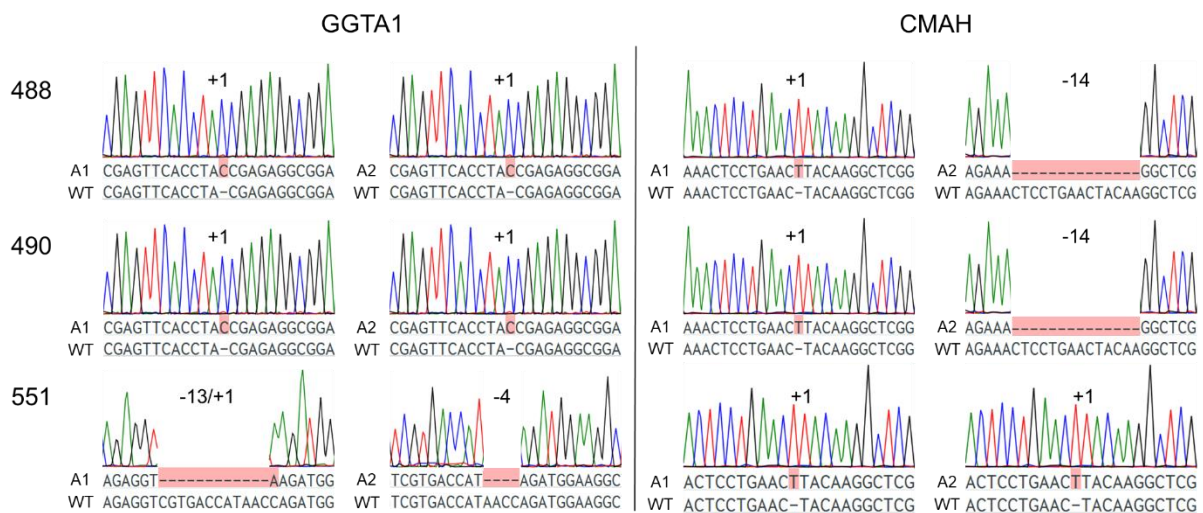


Figure 36: Genotypic analyses of the double-knockout pigs #488, #490 and #551. A1= Allele one, A2=Allele two and WT= wild type.

Pigs #488 and #490 were generated from a cell clone in which the *GGTA1/CMAH* double-knockout was mediated by transfection of a DNA vector. As shown in Figure 34, this vector contained a sequence coding for hSpCas9. To verify that the DNA vector did not integrate randomly within the porcine genome and enable constitutive expression of hSpCas9, a PCR across the C-terminal end of hSpCas9 was performed using the primers Cas9_3`LRF1 and

ROSA26_BGHR1. Amplification of a 415 bp amplicon was absent in genomic DNA from pigs #488, #490 and #551 and revealed no random vector integration (Figure 37).

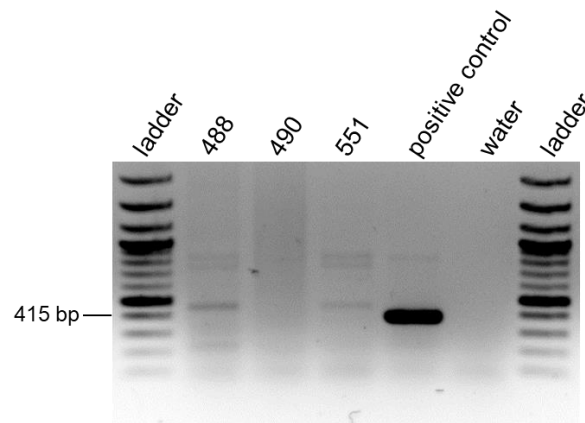


Figure 37: Absence of double-knockout vector integration within the genome of the female *GGTA1/CMAH* double-knockout pigs shown by PCR. DNA from ROSA26-hSpCas9 pig #42 was used as positive control.

As before, to determine whether the introduced indels had inactivated the *GGTA1* and *CMAH* enzymes, flow cytometry measurements were carried out using PBMCs from the *GGTA1/CMAH* double-knockout pigs #488, #490 and #551 and from wild type controls (Figure 38). This revealed the absence of α Gal and Neu5Gc, indicating functional inactivation of *GGTA1* and *CMAH*, whereas both epitopes were detected in wild type controls. Western blot analysis was also performed for pig #488 and #490 confirming the absence of Neu5Gc (Figure 39).

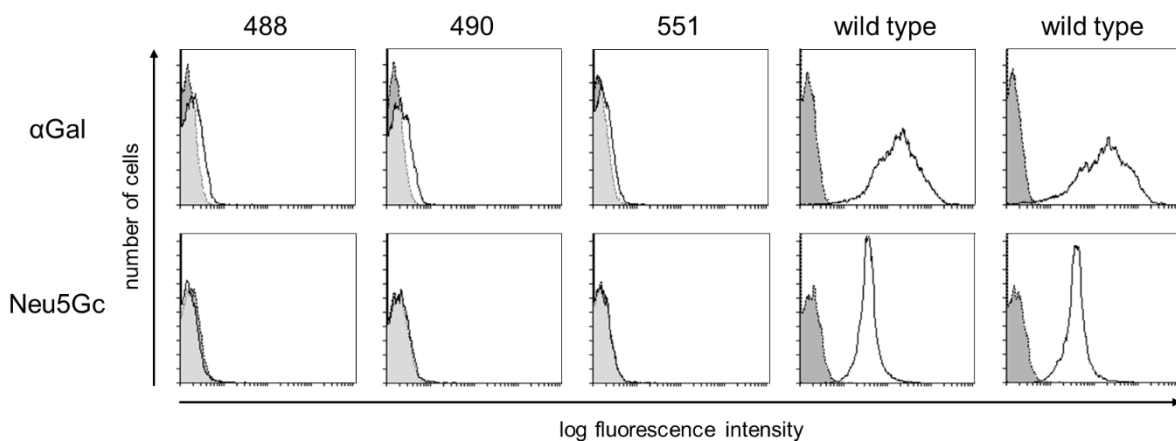


Figure 38: Flow cytometry analyses of PBMCs from pigs #488, #490 and #551. α Gal- and Neu5Gc epitopes were measured on gated lymphocytes. Lack of IB4 binding confirmed absence of α Gal and thus functional *GGTA1* knockout, lack of anti-Neu5Gc binding confirmed absence of Neu5Gc and thus functional *CMAH* knockout. Grey histograms represent secondary antibody staining only. PBMCs from wild type animals were used as controls.

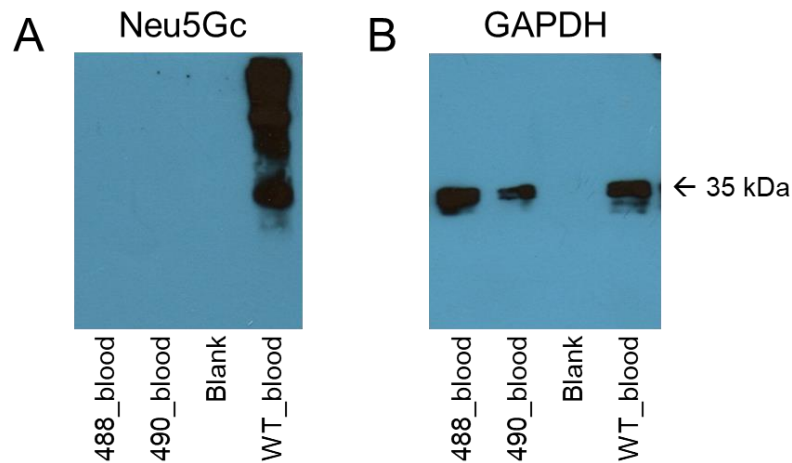


Figure 39: Neu5Gc and GAPDH western blot analyses of blood from pigs #488 and #490. (A) Western blot confirmed functional *CMAH* knockout by the absence of Neu5Gc in proteins isolated from blood cells of the *GGTA1/CMAH* double-knockout pigs #488 and #490. Proteins isolated from blood cells of a wild type (WT) pig served as positive control. (B) GAPDH was used as loading control and revealed signals at the expected molecular weight of 35 kDa for both wild type (WT) and *CMAH* knockout samples.

An indirect ELISA assay (Figure 40) detected preformed anti- α Gal- and anti-Neu5Gc antibodies in the sera of the *GGTA1/CMAH* double-knockout pigs #488, #490 and #551. In contrast, no preformed anti- α Gal- and anti-Neu5Gc antibodies were present in the sera of wild type pigs. Interestingly, anti- α Gal- and anti-Neu5Gc antibody titres both varied between individual double-knockout animals which is also the case with humans. ELISA assays were carried out by Dr. Robert Ramm (MHH, Hannover).

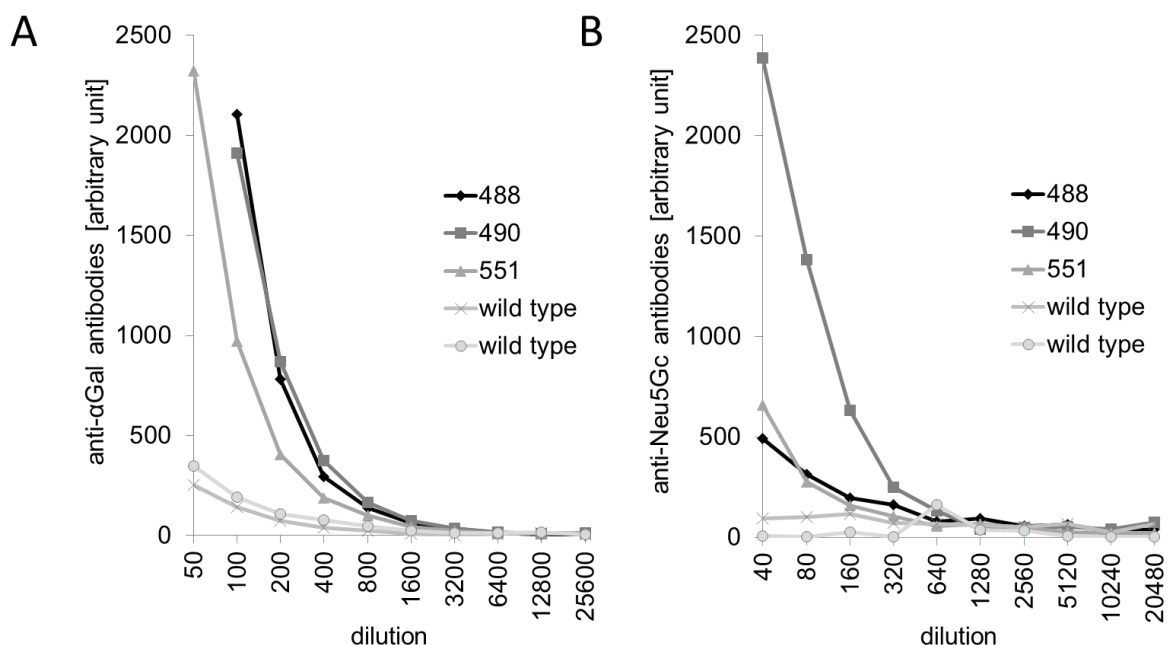


Figure 40: Preformed anti- α Gal antibodies (A) and anti-Neu5Gc antibodies (B) in sera of the *GGTA1/CMAH* double-knockout animals #488, #490 and #551.

The *GGTA1/CMAH* double-knockout sows #488 and #490 served as founder animals to establish a *GGTA1/CMAH* double-knockout, five-fold transgenic herd. Both *GGTA1/CMAH* double-knockout sows were bred with a *GGTA1* knockout, five-fold transgenic boar and gave birth to biallelic *GGTA1*/monoallelic *CMAH* knockout, five-fold transgenic piglets as well as biallelic *GGTA1*/monoallelic *CMAH* knockout piglets. By cross-breeding of the F1 generation, a large F2 generation herd has been obtained including seven *GGTA1/CMAH* double-knockout, five-fold transgenic pigs (Figure 41).

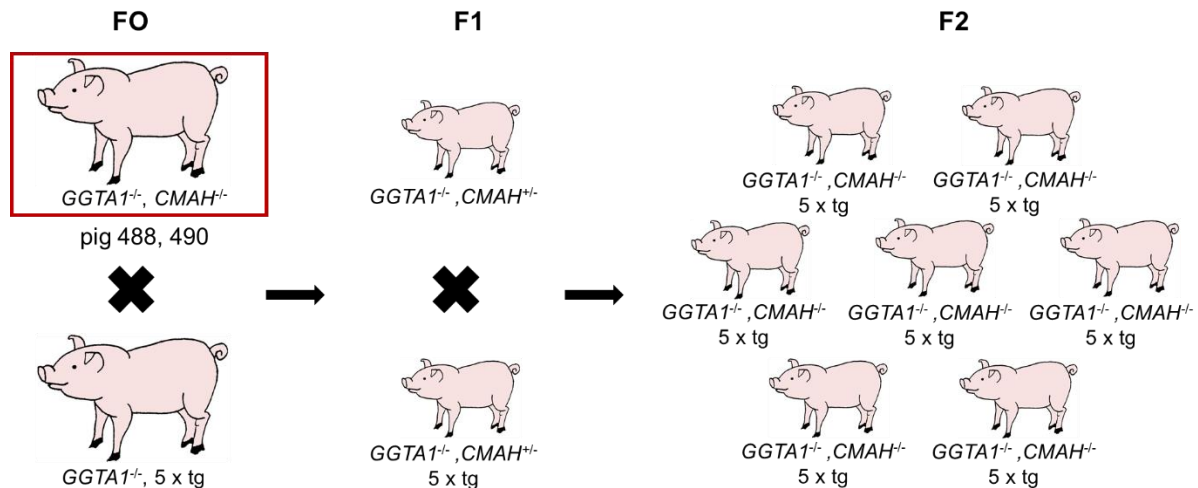


Figure 41: Breeding of *GGTA1/CMAH* double-knockout pigs # 488 and #490 with a *GGTA1* knockout, five-fold transgenic boar to establish a *GGTA1/CMAH* double-knockout, five-fold transgenic herd.

3.3.4 *GGTA1/CMAH/B4GALNT2/B2M* four-fold knockout pig

In addition to α Gal and Neu5Gc, an induced antibody response of xenograft recipient baboons to glycans produced by porcine *B4GALNT2* [44] and reduced human antibody binding to SLA class I knockout cells [45] indicate that a sugar epitope produced by *B4GALNT2* as well as surface molecules of the porcine SLA class I complex constitute important xenoreactive antigens and must therefore be removed. This section describes the inactivation of *GGTA1*, *CMAH*, *B4GALNT2* and *B2M*, which is crucial for surface presentation of SLA class I [80], to generate four-fold knockout porcine cells and then a pig. Much of the data described here have been handed in for publication (Viable pigs after simultaneous inactivation of porcine MHC class I and three xenoreactive antigen genes *GGTA1*, *CMAH* and *B4GALNT2*; Xenotransplantation; Fischer*, Rieblinger* et al.; *= equal contribution). The paper has meanwhile been accepted with minor revisions.

To increase the probability of hSpCas9 as well as all four sgRNAs being simultaneously taken up into a single porcine cell, a four-fold knockout vector #841-B4GALNT2-CMAH-GGTA1-B2M, referred to as #841-4xKO vector, was generated (Supplementary figure 4 and Figure 42). The vector has a size of 13.2 kb and is composed of: a CBh-driven hSpCas9 construct

linked to a puromycin resistance gene via a T2A signal; and sgRNA sequences directed against sequences in *B4GALNT2* exon three (*B4GALNT2_E3T3*), *CMAH* exon ten (*CMAH_E10T1*), *GGTA1* exon seven (*GGTA1_E7T6*) and *B2M* exon one (*B2M_E1T1*). The CBh-driven hSpCas9-T2A-puro construct consists of a 0.8 kb CBh promoter, followed by a SV40 NLS, a 4.0 kb hSpCas9 gene and a nucleoplasmin NLS linked to a 0.6 kb puromycin resistance cassette with a 0.2 kb BGHpA via a T2A signal. SgRNAs are each composed of an 18 bp gRNA- and a sgRNA-scaffold sequence and driven by a 0.2 kb U6 promoter.

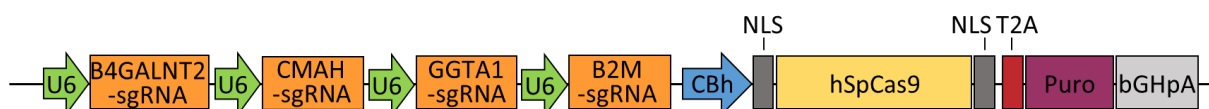


Figure 42: Structure of the four-fold knockout vector #841-4xKO. #841 refers to the vector pX330-U6-Chimeric_BB-CBh-hSpCas9-T2A-puro_MCS. Figure not to scale

Female PKF cells (120516) were transfected, puromycin-resistant cell clones selected and α Gal-negative cells enriched. DNA-fragments across the gRNA target sites *GGTA1_E7T6*, *CMAH_E10T1*, *B4GALNT2_E3T3* and *B2M_E1T1* were amplified by PCR. Subsequent TIDE analyses revealed high on-target cleavage efficiencies within the cell pool ranging from 36% for *B4GALNT2* to approximately 97% for *GGTA1* and *B2M* (Table 29).

Table 29: TIDE analyses of a multiple-knockout cell pool.

Gene	gRNA target site	Total on-target cleavage efficiency [%]	Coefficient of determination (R^2)
<i>GGTA1</i>	<i>GGTA1_E7T6</i>	97.5	0.97
<i>CMAH</i>	<i>CMAH_E10T1</i>	67.4	0.99
<i>B4GALNT2</i>	<i>B4GALNT2_E3T3</i>	36.3	0.98
<i>B2M</i>	<i>B2M_E1T1</i>	96.8	0.97

In addition, single cell clones were isolated and analysed for on-target cleavage at the gRNA target sites for all four genes. Full results are shown in Supplementary table 1. In summary, 12/14 clones (86%) showed at least monoallelic indels at the gRNA target sites in each of the four genes and 8/14 cell clones (= 57%) were characterised as biallelic four-fold knockout clones. Selected cell clones were used for SCNT and a healthy and normally developed piglet (#90) was obtained from clone #18 (Figure 43). Unfortunately, this piglet suffered from an infection at age six weeks and had to be sacrificed. Histological examination revealed an enlarged spleen.



Figure 43: Picture of the four-fold knockout piglet #90 at day 24.

Genotyping and cell isolation were carried out in cooperation with Dr. Konrad Fischer. DNA was isolated from ear clip tissue and porcine ear fibroblast cells derived (PEF) for functional analysis. Figure 44 shows the results of the genotypic analysis of pig #90. PCR and subsequent sequencing across the gRNA target site of *GGTA1* exon seven identified a biallelic 11 bp deletion causing a frameshift in the translational reading frame. At the gRNA target site of *CMAH* exon ten one allele revealed a single bp insertion leading to a frameshift and an early stop codon. The second allele carried a 3 bp deletion eliminating a single amino acid. For *B4GALNT2* exon three two alleles were identified, the first carried a 5 bp deletion and the second a 367 bp insertion at the gRNA target site, both leading to a shifted reading frame. Genotypic analysis of *B2M* exon one revealed three mutated alleles carrying either a 5 bp deletion combined with a 3 bp insertion, a 53 bp deletion or a 279 bp insertion.

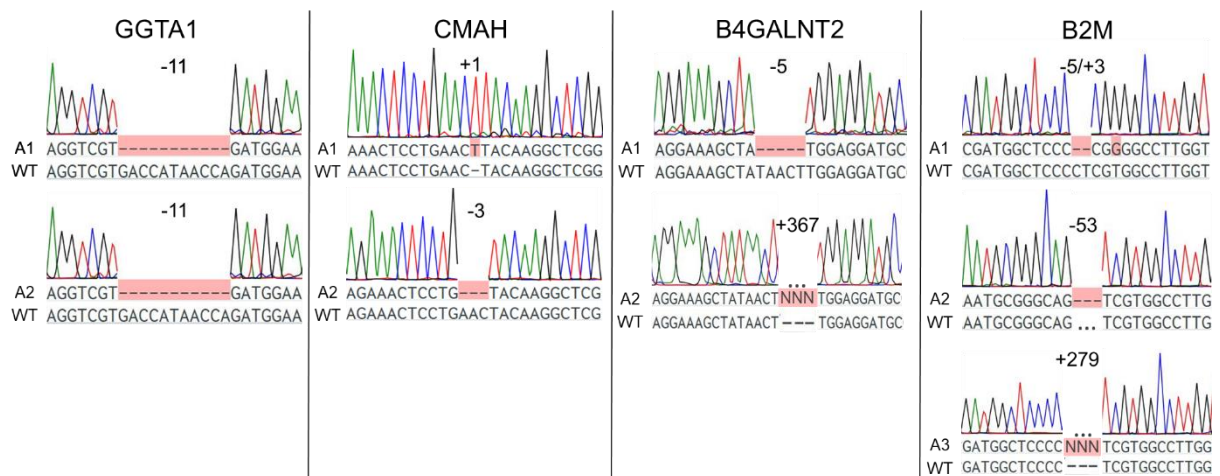


Figure 44: Genotypic analysis of the four-fold knockout pig #90. A1= Allele one, A2=Allele two and A3=Allele three, WT= wild type.

To determine whether the introduced indels had inactivated the respective genes, flow cytometry measurements were carried out using PEF cells from the four-fold knockout pig #90 (Figure 45). Flow cytometry analyses revealed absence of α Gal, SDa and B2M epitopes and thus functional inactivation of *GGTA1*, *B4GALNT2* and *B2M*, while wild type controls

expressed these epitopes. The effect of *B2M* inactivation was further tested by detection of surface SLA-I epitopes. SLA-I epitopes were absent in PEF cells of the four-fold knockout animal #90. Flow cytometry measurements were carried out by Rabea Hein (MHH, Hannover).

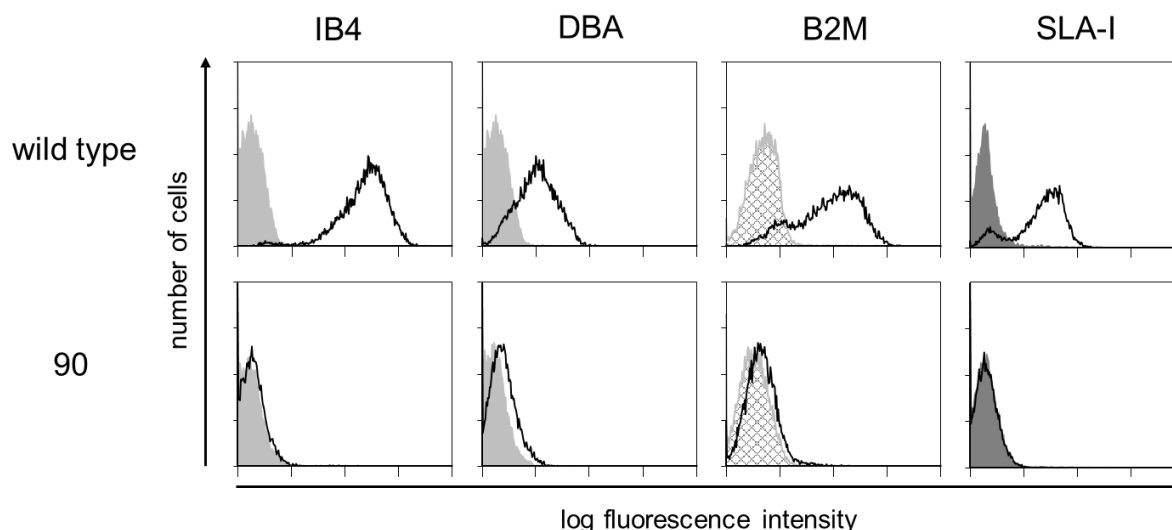


Figure 45: Flow cytometry analyses of PEFs from the four-fold knockout pig #90. Flow cytometry measurements revealed absence of α Gal, Sda and B2M molecules indicating functional inactivation of the corresponding genes. α Gal was detected by binding of isolectin B4 (IB4) and Sda by binding of DBA. Light grey histograms represent unstained controls, dark grey histograms represent secondary antibody staining only and squared histograms represent isotype controls. Fibroblasts from a wild type animals were used as positive control.

Functional inactivation of *CMAH* could not be tested by flow cytometry analysis because Neu5Gc epitopes are transferred to cells cultivated in medium containing fetal calf serum. To circumvent this problem, western blot analysis was performed using proteins isolated from tissue samples. Proteins from various organs of the four-fold knockout pig #90 revealed complete absence of Neu5Gc epitopes and thus functional *CMAH* knockout, whereas proteins isolated from various organs of a wild type pig revealed Neu5Gc epitopes on a variety of proteins (Figure 46).

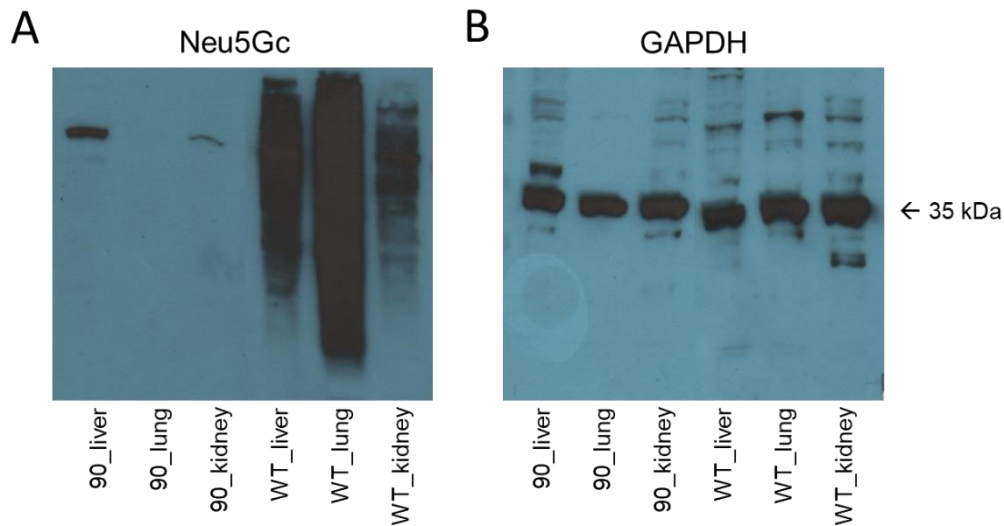


Figure 46: Neu5Gc and GAPDH western blot analyses of various organs from pig #90. (A) Due to a functional *CMAH* knockout, Neu5Gc is absent on proteins isolated from liver, lung and kidney tissue of the four-fold knockout pig #90. Proteins isolated from liver, lung and kidney of a wild type pig (=WT) served as positive control. (B) GAPDH was used as loading control and revealed signals at the expected molecular weight of 35 kDa for both wild type- and *CMAH* knockout samples.

To assess the effects of single- and multiple knockouts on human IgM and IgG antibody binding, PKF cells from *CMAH* knockout pig #463 (section 3.3.2), *GGTA1/CMAH* double-knockout pig #488 (section 3.3.3), *GGTA1/CMAH/B4GALNT2/B2M* four-fold knockout pig #90 and a wild type control were each cultured on microfluidic channels. Perfusion with normal human serum showed significantly reduced levels of IgG and IgM antibody binding to *CMAH* and *GGTA1/CMAH* knockout cells compared to wild type controls and a further reduction for *GGTA1/CMAH/B4GALNT2/B2M* four-fold knockout cells (Figure 47). These experiments were carried out by Riccardo Sfriso (University of Bern, Switzerland).

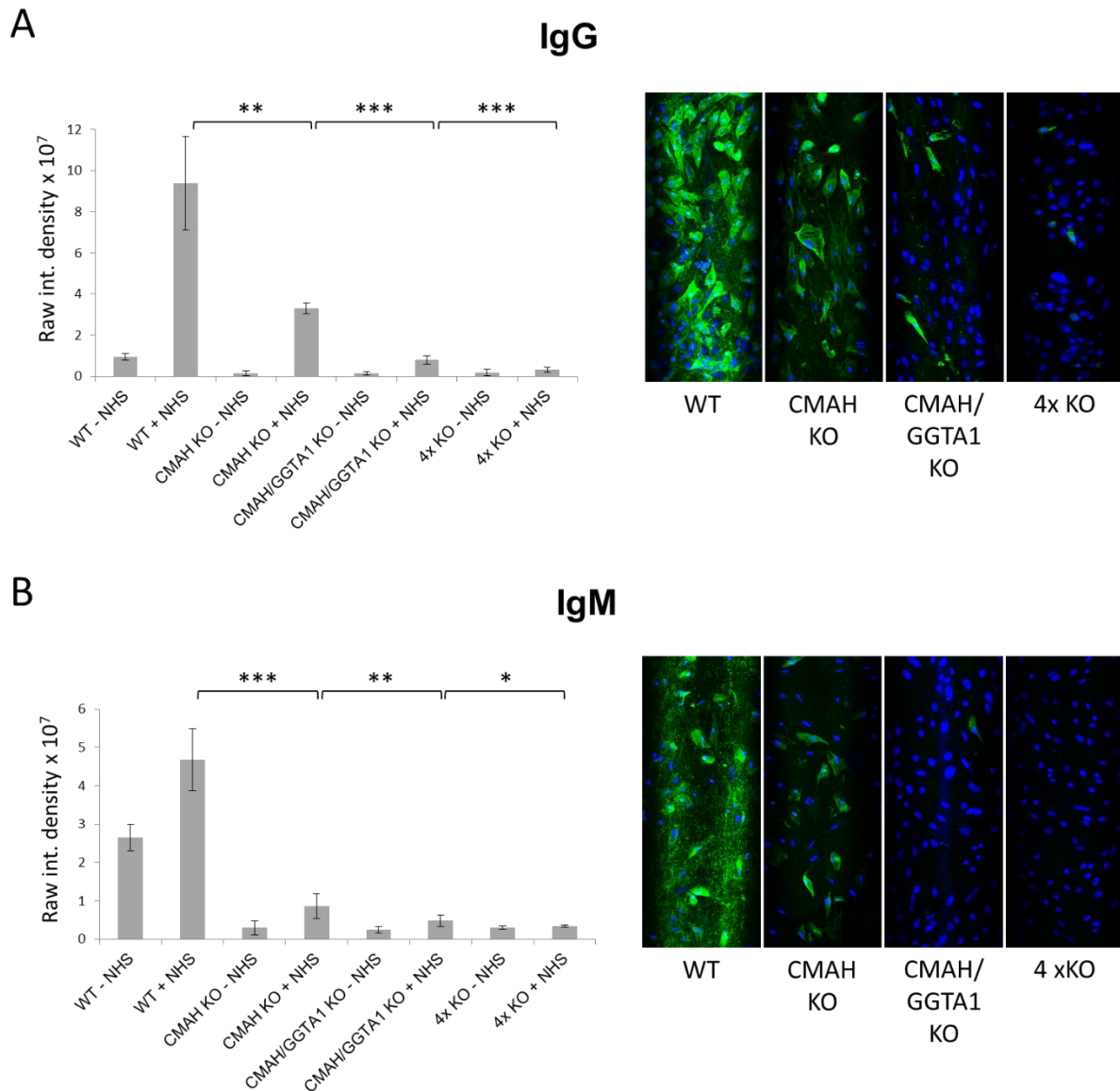


Figure 47: IgG and IgM antibody binding to single-, double- and four-fold knockout cells after incubation with human serum. Wild type (WT) cells served as control. (A) Binding of human IgG antibodies. (B) Binding of human IgM antibodies. NHS: Normal human serum, 4x KO: *GGTA1/CMAH/B4GALNT2/B2M* knockout cells

In summary, a four-fold knockout pig deficient in Neu5Gc, α Gal, Sda and B2M molecules was successfully generated and revealed functional inactivation of the genes responsible for the synthesis of the respective epitopes. As the four-fold knockout pig unfortunately died, re-cloning of the animal and subsequent housing under clean conditions is required to minimise infection risk. However, as inactivation of *B2M* is discussed to disturb iron homeostasis in mice [245], current work focuses on inactivating the classical *SLA class I* genes rather than *B2M*. *GGTA1/CMAH/B4GALNT2/SLA class I* knockout pigs have already been produced and are currently characterised.

3.4 ROSA26-hSpCas9 pigs for *in vivo* genome editing

The aim of this part of the project was to generate Cas9 expressing pigs to provide a platform for tissue-specific knockouts by genome editing *in vivo*. This was a parallel project useful for future xeno- applications and many other projects in the group, such as cancer- and cardiovascular disease modelling. Delivery of all necessary CRISPR/Cas9 components into tissues and organs of a live animal is problematic because the commonly used Cas9 variant (human codon optimised *Streptococcus pyogenes* Cas9 nuclease; hSpCas9) exceeds the packaging capacity of AAVs or lentiviruses. One means of overcoming this difficulty and facilitating *in vivo* genome editing in pigs is to generate a transgenic pig line that ubiquitously expresses hSpCas9. SgRNAs could then be injected directly into the tissue of interest and mediate a tissue-specific knockout of a particular gene. This section thus describes placement of a hSpCas9 transgene at the porcine *ROSA26* locus (Figure 48).

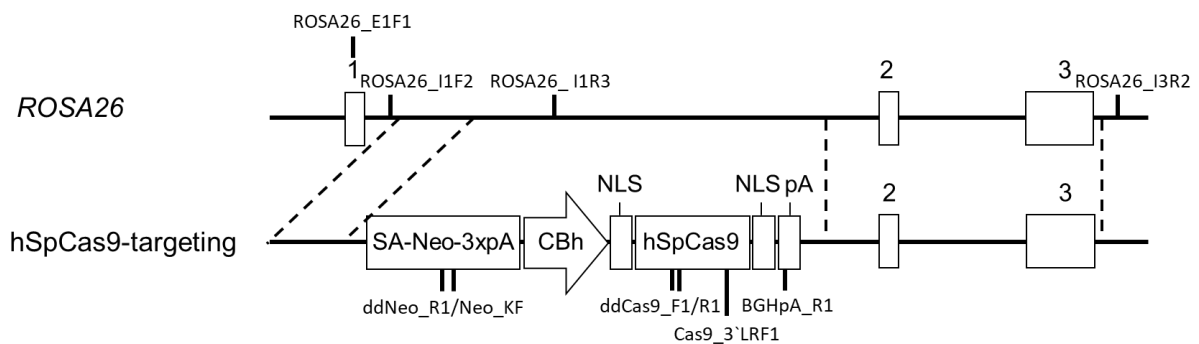


Figure 48: Targeting of porcine *ROSA26* to introduce hSpCas9. Top, structure of porcine *ROSA26*. Bottom, placement of a CBh-driven hSpCas9 cassette at the porcine *ROSA26* locus. Primers used to identify correct targeting and check for transgene expression are indicated. Exons are indicated by numbered boxes and regions of homology by dotted lines. SA = Splice acceptor, NLS= Nuclear localisation signal, pA= BGHpA signal. Figure not to scale.

3.4.1 *ROSA26* targeting and the generation of hSpCas9 expressing pigs

The generation of a vector to introduce a human codon-optimised SpCas9 gene at the porcine *ROSA26* locus is shown schematically in Supplementary figure 5, and the outline structure in Figure 49. The *ROSA26*-hSpCas9 promoter-trap vector consisted of: a 2.2 kb 5' homologous arm; followed by a 1.6 kb fragment composed of splice acceptor, kozak sequence, a promoterless neomycin resistance gene and triple-polyA signal; a 5.3 kb hSpCas9 expression cassette; and a 4.7 kb 3' homologous arm. The hSpCas9 cassette contained a 0.8 kb CBh promoter, followed by a SV40 NLS, a 4.0 kb hSpCas9 gene, a nucleoplasmic NLS and a 0.2 kb BGHpA.

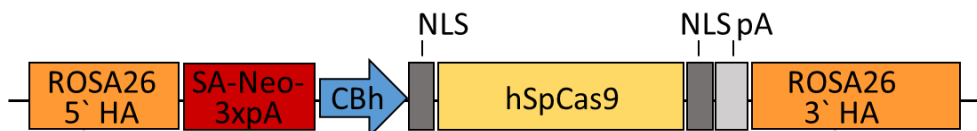


Figure 49: Structure of the ROSA26-hSpCas9 targeting vector. HA= Homology arm; SA= Splice acceptor; 3xpA= Triple polyadenylation site; pA= BGH polyadenylation site. Figure not to scale.

Female PKF cells (250515) were transfected, cell clones isolated and expanded. Genomic DNA was isolated and correctly targeted cell clones identified by long-range PCR across the 5' and 3' junctions. Monoallelic targeting was identified by PCR across the wild type *ROSA26* allele. 5% of all G418-resistant clones revealed correct, monoallelic targeting. Correct targeting was further confirmed by sequencing of the 5' and 3' junction PCRs. Transgene copy number was determined via ddPCR and 67% of the clones revealed a single copy of *hSpCas9*.

Correctly targeted clones with a single copy of *hSpCas9* were used for somatic cell nuclear transfer and two liveborn piglets obtained (ROSA26-hSpCas9 #41 and #42; Figure 50).



Figure 50: Picture of the ROSA26-hSpCas9 piglets #41 and #42. Left: ROSA26-hSpCas9 pig #41 at day 2. Right: ROSA26-hSpCas9 pig #42 at age 5 months.

3.4.2 Analysis of ROSA26-hSpCas9 pigs

ROSA26-Cas9 pigs #41 and #42 were further analysed. DNA was isolated from ear clip tissue and PEF cells derived for functional analysis. Correct targeting was confirmed by long-range PCR across the 5' and 3' junctions of the targeted allele and monoallelic targeting by PCR across the non-targeted *ROSA26* allele (Figure 51A). RT-PCR was carried out to analyse mRNA expression. This showed correct splicing between *ROSA26* exon one and the neomycin cassette, and expression of the *hSpCas9* transgene (Figure 51B).

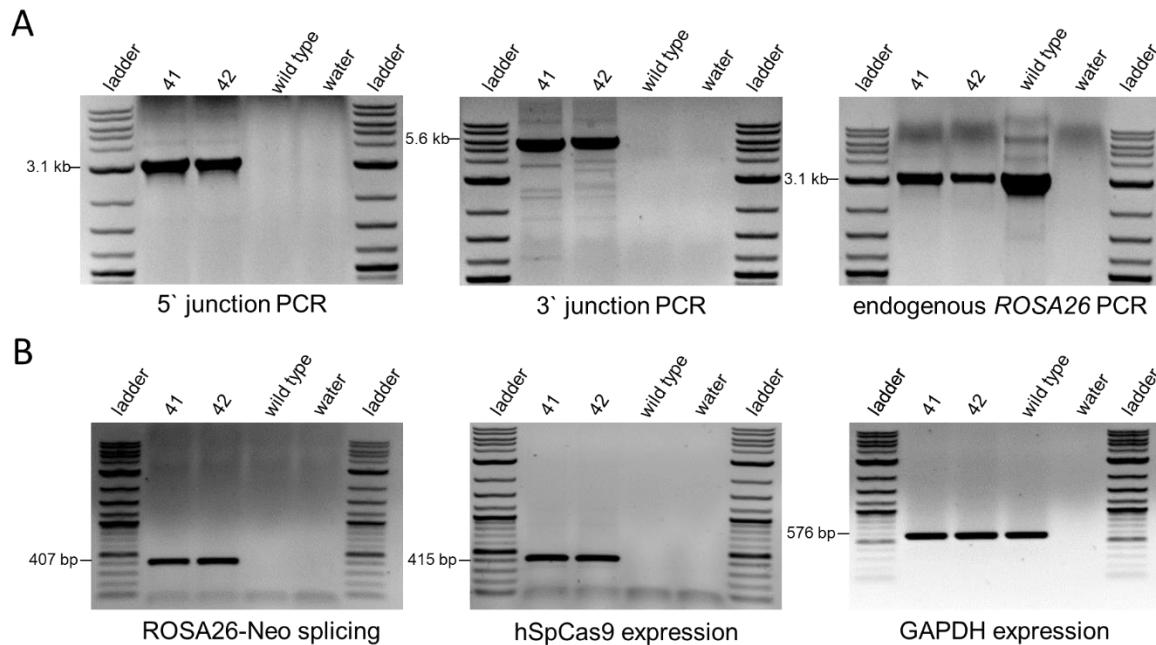


Figure 51: Targeting PCRs and hSpCas9 expression analysis of pigs #41 and #42. (A) Targeting PCRs. Correct targeting revealed a 3.1 kb 5' junction and a 5.6 kb 3' junction PCR product, monoallelic targeting was shown by a 3.1 kb endogenous PCR product. Wild type DNA was used as control. (B) RT-PCR analyses of PEF cells from ROSA26-hSpCas9 pigs #41 and #42. Correct splicing between *ROSA26* exon one and neomycin was shown by a 407 bp amplicon, hSpCas9 expression by a 415 bp fragment and pGAPDH expression by a 576 bp amplicon. Wild type cDNA was used as control.

To detect random integration events, transgene copy number was determined by ddPCR. ROSA26-hSpCas9 pig #41 revealed a hSpCas9 copy number of 1.05 (+0.08, -0.07) and ROSA26-hSpCas9 pig #42 a hSpCas9 copy number of 0.96 (+0.07, -0.14) (Figure 52). In combination with the specific targeting PCRs, these data exclude random integration.

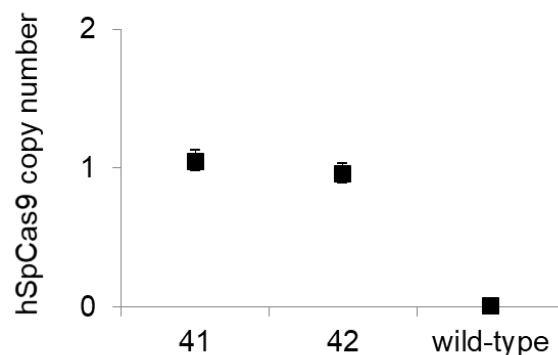


Figure 52: Copy number of hSpCas9 in ROSA26-hSpCas9 pigs #41 and #42. Wild type DNA served as negative control.

To test Cas9 function, the vector pX330-U6-Chimeric_BB-CBh-hSpCas9-T2A-puro_MCS (referred to as plasmid #841) was modified to contain a sgRNA directed against a sequence

in *B2M* and to remove the hSpCas9 coding sequence. Thus, cleavage of genomic DNA at the B2M_E1T1-gRNA target site only occurs if the hSpCas9 transgene is functional and mediates a site-specific double-strand break. Generation of the vector #841-B2M(-)Cas9 is shown in Supplementary figure 6 and the outline structure in Figure 53A.

PEF cells of ROSA26-hSpCas9 pigs #41 and #42 were transiently transfected with #841-B2M(-)Cas9, genomic DNA was prepared from cell pools, PCR amplification performed across the B2M_E1T1-gRNA target site and amplified fragments sequenced. The frequency of targeted indels across the B2M_E1T1-gRNA target site was identified by TIDE analysis, which revealed 19.9% total cleavage efficiency for ROSA26-hSpCas9 pig #41 and 8.4% for ROSA26-hSpCas9 pig #42 (Figure 53B). This indicates that the hSpCas9 construct placed at the porcine ROSA26 locus is capable of introducing indels upon delivery of sgRNAs.

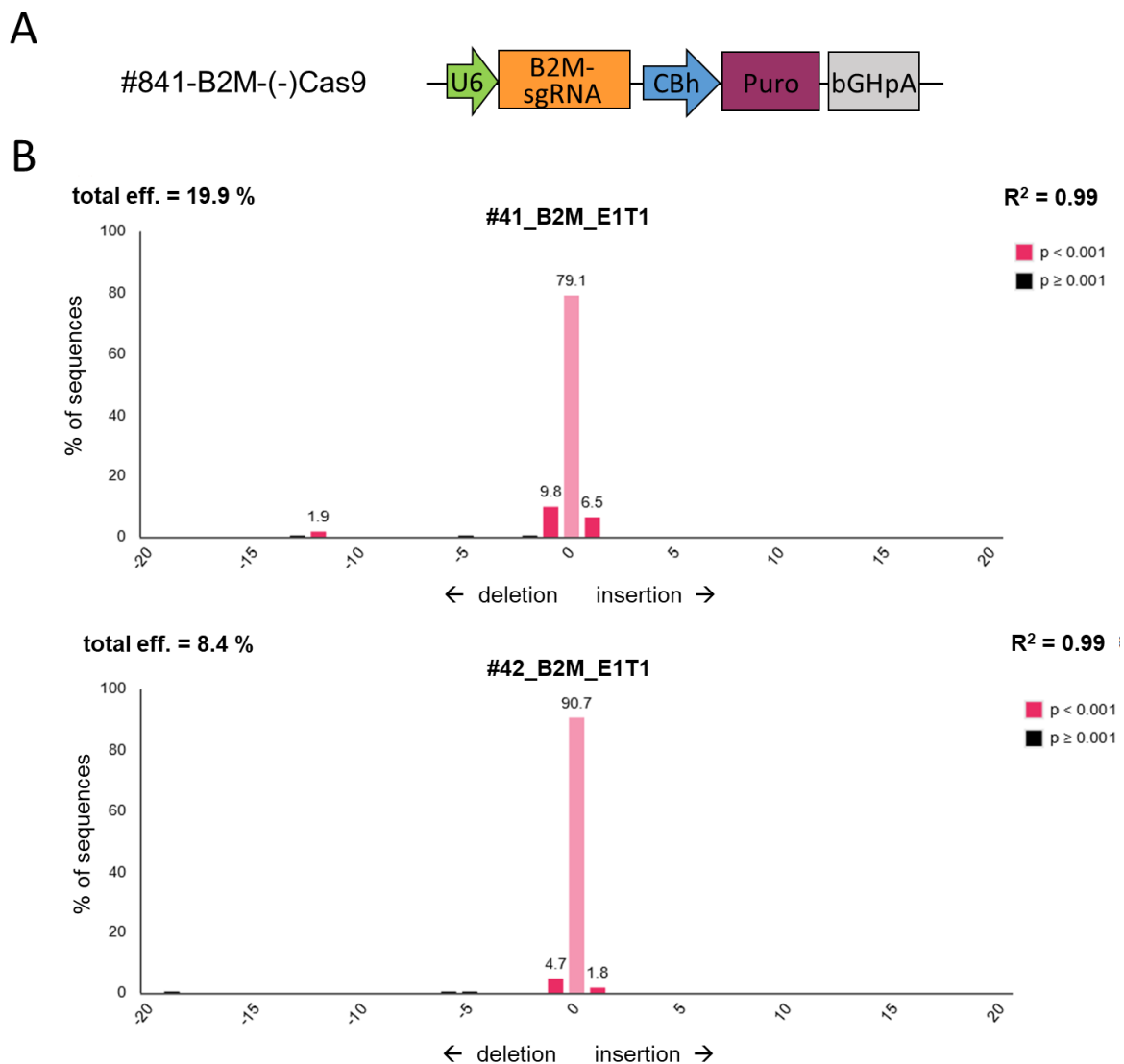


Figure 53: HSpCas9 functionality in PEF cells of ROSA26-hSpCas9 pigs #41 and #42. (A) Structure of the vector #841-B2M(-)Cas9. Figure not to scale (B) Spectrum and frequency of indels at the B2M-gRNA target site mediated by a functional hSpCas9 in ROSA26-hSpCas9 pigs #41 (top) and #42 (bottom).

ROSA26-hSpCas9 pig #41 died at day 56 for unknown reasons, but ROSA26-hSpCas9 pig #42 grew up healthy and served as a founder to establish a hSpCas9 transgenic herd. Pig #42 was bred with a KRAS^{G12D/+} boar and gave birth to twelve piglets. The transgenes and mutant alleles were inherited in Mendelian fashion and five ROSA26-hSpCas9 and three ROSA26-hSpCas9, KRAS^{G12D/+} pigs were obtained (Figure 54A).

ROSA26-hSpCas9, KRAS^{G12D/+} piglet #395 and KRAS^{G12D/+} piglet #393 were sacrificed for detailed analyses. Organ samples were collected and pMSC, PAEC and PEF cells derived for functional analysis. RT-PCR analysis revealed hSpCas9 mRNA expression in all organs examined (Figure 54B).

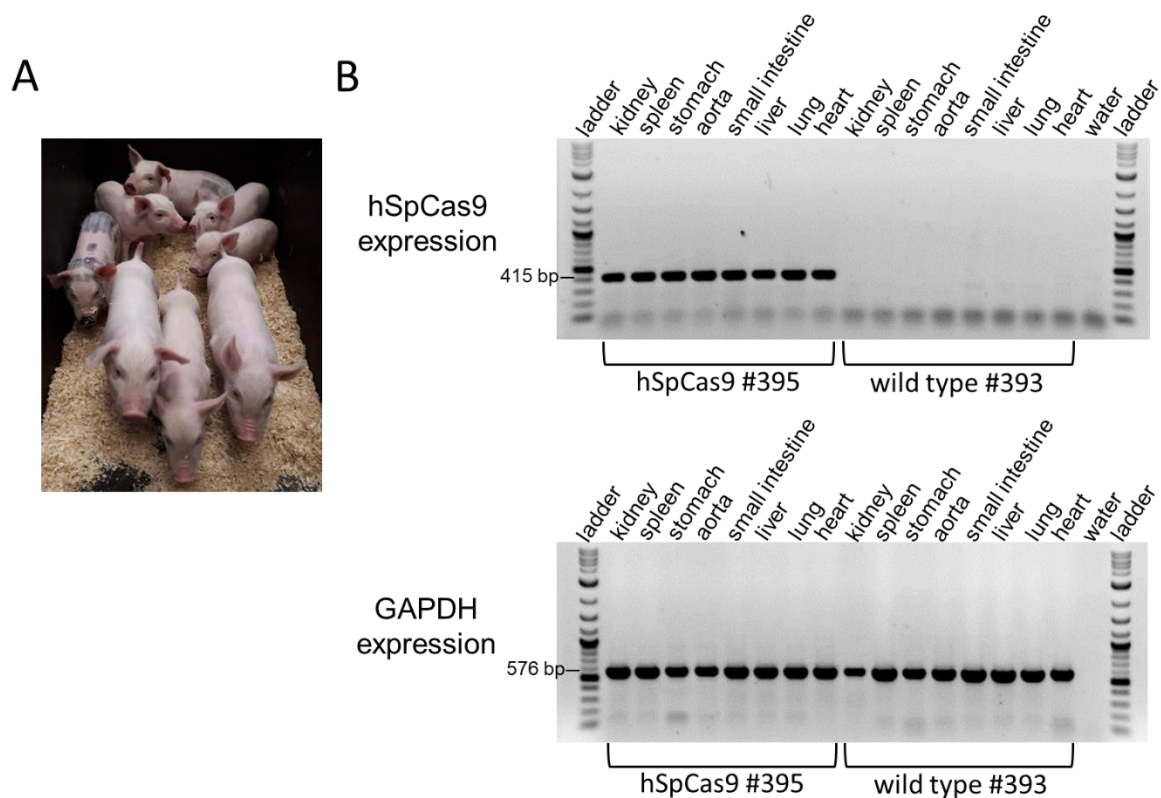


Figure 54: Analysis of hSpCas9-transgenic offspring. (A) hSpCas9-transgenic pig herd at an age of 2 weeks. Five piglets were transgenic for hSpCas9 and three hSpCas9 and *Kras*^{G12D/+}. (B) RT-PCR analyses of various organ samples from ROSA26-hSpCas9, KRAS^{G12D/+} piglet # 395. hSpCas9 expression was shown by a 415 bp fragment and pGAPDH expression by a 576 bp amplicon. CDNA from various organs of KRAS^{G12D/+} piglet #393 served as controls.

To test Cas9 function, the vector #841-GGTA1(-)Cas9 was generated containing a sgRNA directed against a sequence in *GGTA1* and lacking the hSpCas9 coding sequence. (Supplementary figure 7 and Figure 55A). PMSC, PAEC and PEF cells from ROSA26-hSpCas9, KRAS^{G12D/+} piglet # 395 were transiently transfected with this vector, genomic DNA from cell pools prepared, the GGTA1_E7T6-gRNA target site amplified and the sequence of

the fragments determined. The frequency of targeted indels across the GGTA1_E7T6 target site was identified by TIDE analysis, which revealed 14.5 - 25.9% total cleavage efficiency for the different cell types used (Figure 55B). This confirmed that the hSpCas9 construct placed at the porcine *ROSA26* locus is capable of introducing indels in various cell types upon delivery of sgRNAs.

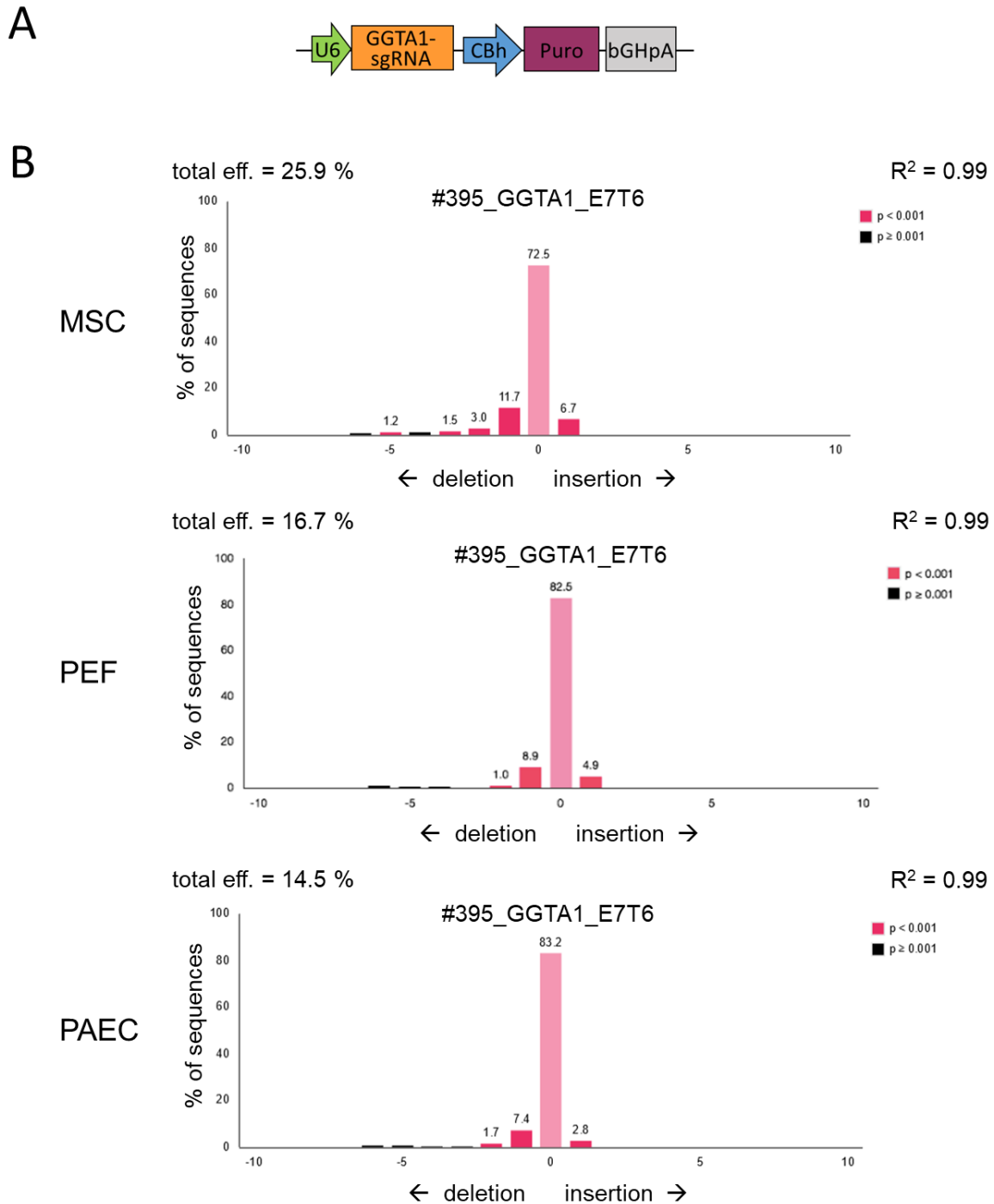


Figure 55: HSpCas9 functionality in pMSC, PEF and PAEC cells of ROSA26-hSpCas9, KRAS^{G12D} piglet #395. (A) Structure of the vector #841-B2M(-)-Cas9 (B) Spectrum and frequency of indels at the GGTA1_E7T6-gRNA target site mediated by a functional hSpCas9 in PEF, pMSC and PAEC cells of ROSA26-hSpCas9, KRAS^{G12D} piglet #395.

4 Discussion

The major aim of this work was to generate pigs for xenotransplantation by means of targeted transgene placement as well as targeted inactivation of endogenous porcine genes. Within this work, two strategies were addressed for controlled placement of multiple independently-expressed transgenes at a predetermined integration site. Section 4.1 discusses a transgene stacking approach at the porcine *ROSA26* locus and section 4.2 a Bxb-1 recombinase-mediated approach for controlled placement of a seven-fold transgene cassette at the CD46 3' flanking region. Besides transgene addition, endogenous porcine genes responsible for xenograft rejection were inactivated by targeted gene editing using the CRISPR/Cas9 system which is discussed in section 4.3. Single-, double- and four-fold knockout pigs were generated, being deficient in at least one of the major xenoantigens α Gal, Neu5Gc and Sda and SLA class I epitopes which are discussed in section 4.4. In addition, hSpCas9-expressing pigs were generated to facilitate *in vivo* gene editing for a variety of biomedical applications. These are discussed in section 4.5.

4.1 Transgene stacking at the *ROSA26* locus

The first strategy for controlled multi-transgene placement was 'transgene stacking' and aimed to assemble multiple independently-expressed xenoprotective transgenes at the porcine *ROSA26* locus by successive targeted transgene placement via homologous recombination. Each stage involves replacement of the previous drug selection marker, enabling new transgenes to be added by promoter trap selection without accumulating multiple antibiotic resistance genes. This allows controlled step-by-step assembly of a multi-transgene array with predetermined characteristics, providing the opportunity to check transgene expression at each stage and the option of discarding and remedying any undesirable addition. In addition, each transgene can be expressed by the most suitable promoter.

As outlined in the introduction, the porcine *ROSA26* locus has characteristics that make the locus very attractive for xenotransplantation. Besides the need for high levels of transgene expression, bringing xenotransplantation into the clinic means implementation of strict safety requirements. These include exact knowledge regarding the transgene integration locus and exclusion of any adverse effects by introducing transgenes within this site. As the *ROSA26* locus is generally regarded as a genomic 'safe harbour' [246], this site might be the integration site of choice. Moreover, the array and its sequence is precisely defined.

At the onset of the work it was unclear whether the *ROSA26* locus allows placement of a second transgene adjacent to a formerly introduced one. So far, sequential targeting of *ROSA26* was neither reported in pig nor in any other species, which raised the question,

whether and to what extent could *ROSA26* be retargeted without losing its permissive nature. In mice, *Rosa26* has mainly been used to place single transgenes [247] with only a few reports of multi-gene constructs, such as the four-fluorescence gene 'Brainbow construct' [235]. In all cases transgenes were introduced into *Rosa26* by a single gene targeting event in ES cells. As no fully functional ES cells are available for pigs, somatic cells were used to retarget the porcine *ROSA26* locus, which is more challenging than in ES cells. To my knowledge, this is the first report of successful transgene stacking at *ROSA26* in any species.

One of the transgenes placed at the *ROSA26* locus was HO-1 which mediates xenoprotective effects via its anti-oxidative, anti-apoptotic and anti-inflammatory properties [103, 104, 248]. The same HO-1 cDNA construct described here has previously been used by others to generate transgenic pig lines. In previous work at the Chair of Livestock Biotechnology, the HO-1 construct was part of a randomly integrated multi-transgene array and was found to be expressed only in some organs from an estimated 3–4 transgene copies [68]. Similar results with this HO-1 construct were obtained by Petersen et al. who demonstrated low HO-1 transgene expression in heart, kidney and liver from an unknown HO-1 copy number integrated at a random position [104]. In contrast, placement of a single HO-1 transgene at *ROSA26* resulted in mRNA expression in all tissues analysed at levels comparable or higher than that detected in human SCP1 cells. These results strongly support the suitability of *ROSA26* for transgene placement.

The second transgene placed at the *ROSA26* locus, was the human complement regulator CD55. This gene has long been a priority for xenotransplantation research and several groups have demonstrated the potential of CD55 to inhibit complement activation and extend graft survival [249, 250]. Multiple CD55 transgenic pigs carrying diverse CD55 cDNA constructs have been generated by means of random integration, but obtaining ubiquitous and high-level CD55 expression has been challenging [184, 251]. Better results were obtained with CD55 minigenes [161, 252]. Using a CD55 minigene-construct that integrated in multiple copies at a random position, Murakami et al. generated a transgenic pig that expressed CD55 at similar or higher levels than the corresponding human tissues [252]. The CD55 construct used for our transgene stacking approach resembles that of Murakami et al., but is driven by a strong CAG promoter. Placement of a single copy of this construct at the previously targeted *ROSA26* locus was associated with high transgene expression levels in all tissues analysed and to my knowledge the highest expression reported so far. It underlies the importance of the integration site and the usefulness of transgene stacking.

Transgene stacking at the porcine *ROSA26* locus offers a controlled approach to generate multi-transgenic pigs for xenotransplantation with all genes highly expressed and integrated at a single locus. The capacity of the *ROSA26* locus to harbour even more transgenes without

losing its key properties remains unknown, but our data are thus far very encouraging revealing high and ubiquitous expression for two transgenes introduced without any reduction in expression of the formerly integrated transgene. However, transgene stacking is a time consuming process as transgene assembly requires consecutive rounds of gene targeting and SCNT. To streamline this approach, transgene combinations whose effects are already well studied could be assembled on a single targeting vector and be added in one step at the *ROSA26* locus. However, it might be that homologous recombination efficiencies are reduced with increasing size of the transgenes to be introduced. Alternatively, transgene stacking might be combined with an integrase-mediated transgene placement approach where transgene stacking mediates placement of a MIN-tag adjacent to a previously introduced transgene battery and an integrase allows subsequent transgene addition at this site. Such an approach will be discussed in the following section, but at a different locus.

4.2 Seven-fold transgene placement at the CD46 3' flanking region

As outlined in more detail in the introduction, our group previously generated a five-fold transgenic pig line with all transgenes integrated at a single site and the transgene array containing only a single copy of human CD46. A 54 kb 3' flanking region in the single-copy CD46 construct could be used to place additional transgenes, thus maintaining the single locus important for breeding multi-transgenic animals. To omit interference with any regulatory elements in the CD46 3' flanking region, a site approximately 31 kb downstream of the CD46 coding region was chosen for precise placement of a battery of seven individually expressed transgenes using a serine recombinase-mediated approach.

4.2.1 Bxb1 integrase-mediated transgene placement

While transgene placement at *ROSA26* is very efficient, this is much more challenging at other loci, especially when aiming for large inserts. To facilitate targeted transgene placement at these sites, a serine recombinase-mediated approach might be a suitable strategy. Serine recombinases, such as PhiC31 and Bxb1, mediate unidirectional recombination between a phage attachment site (attP/MIN) and a bacterial attachment site (attB) [188, 215]. To use this for precise transgene placement in eukaryotic cells, it is first necessary to insert an attP/MIN site at a suitable position in the host-genome. This can then support transgene placement by recombination with an attB site on a transgene vector.

As each serine integrase requires its own specific attP and attB sites to mediate recombination, it had to be considered in advance which system should be used and hence which attP sequence should be integrated into the CD46 3' flanking region. Two serine integrase candidates gained further consideration, namely PhiC31 and Bxb1. Although PhiC31-integrase

has been used several times to generate transgenic animals [253, 254], this system has a big disadvantage: PhiC31 is capable of mediating recombination at endogenous native docking sites, so-called pseudo-attP sites which are present in the genome of many mammalian species, including humans and pigs [255, 256]. As four pseudo-attP sites recognised by phiC31 have been identified in pigs [255], there was a risk of phiC31-mediated-transgene integration at an unintended site. In contrast, Bxb1 recombinase has the highest accuracy and efficiency among 15 serine recombinases [222] and does not recognise any pseudo-attP sites at least in human cells [257]. While Bxb1 recombination efficiencies have so far not been determined in pigs, the results obtained in other species, as outlined in the introduction, are quite promising and it is reasonable to expect similar efficiencies in pigs. Consequently, an attP site specifically recognised by Bxb1 was integrated within the CD46 3' flanking region.

The first step in placing a MIN tag was to integrate an attP/MIN site via homologous recombination within the flanking region about 31 kb downstream of the CD46 transgene at position 6q22. As gene targeting via homologous recombination in primary somatic cells is a very rare event [189, 190], unless carried out at a permissive site such as *ROSA26*, it was unknown at the onset of this work whether targeted placement of an attP/MIN site plus a hygromycin resistance cassette at the CD46 3' flanking region by homologous recombination would be practically possible. As CRISPR/Cas9 was known to increase the frequency of homologous recombination [196], it was decided to use this to aid CD46 3' targeting. The targeting vector was thus cotransfected with a CRISPR/Cas9 plasmid designed to cleave the target region within the CD46 3' flanking sequence. This resulted in a high proportion (11%) of drug-selected clones being correctly targeted. These reasonable targeting efficiencies suggest that this locus is suitable for the addition of further transgenes. However, as with *ROSA26*, the question remains whether the 6q22 locus will allow insertion of a further large (40.6 kb) multi-transgene construct and maintain its support of abundant transgene expression, and importantly not become unstable over subsequent generations.

Primary cells destined for SCNT have a limited lifespan in culture. This was too short to place an attP/MIN site within the CD46 3' flanking region and then directly carry out recombinase-mediated transgene addition. It is thus necessary to generate nuclear transfer fetuses and re-derive primary cells. Beside addition of the seven-fold transgene construct generated within this work, a variety of other constructs could then easily be introduced at the attP/MIN site. Mullholland et al. used a similar strategy and demonstrated that murine ES cells bearing an attP/MIN site could be used to efficiently generate 15 isogenic lines with different constructs integrated at the attP/MIN site. They reported a Bxb1-mediated recombination efficiency ranging from 33 to 67%, with an average of 50% [214]. This demonstrates that the attP/MIN system provides an efficient and simple system for the integration of prefabricated cassettes

in ES cells. Even if its efficiency in porcine somatic cells still needs to be determined, the results obtained in ES- and a variety of mammalian cell lines [188, 221, 222] give cause for optimism.

4.2.2 Composition of the seven-fold transgene array

The transgene array to be added to the MIN site in the CD46 3' flanking region is composed of seven human transgenes, namely THBD, EPCR, HO-1, mutCIITA, PD-L1, hCD47 and HT. Each is driven by an individual promoter to ensure appropriate expression levels. Most of the transgenes are driven by the CAG promoter, a synthetic promoter known to provide abundant ubiquitous transgene expression [258, 259]. In a comparison of nine candidate promoters, each stably integrated at the *Rosa26* locus in murine ES cells, the CAG promoter resulted in the highest reporter gene expression, at approximately 9- to 10-fold the level of the endogenous *Rosa26* promoter [260]. The CAG promoter is also less prone to epigenetic silencing than many others, such as the viral CMV promoter [261, 262]. These characteristics make the CAG promoter a suitable candidate to direct abundant and ubiquitous transgene expression. Moreover, a CAG-driven transgene might open the chromatin structure of the adjacent area and enhance expression of co-localised transgenes. Such an effect was first observed in mice, where co-integration of an efficiently expressed beta-lactoglobulin transgene with a poorly expressed cDNA construct was associated with enhanced expression of the latter [263]. As the seven-fold transgene construct contains five CAG promoters, cumulative effects might arise which enhance expression of the transgenes being part of the array.

The following paragraphs outline the reasoning behind the choice of these particular seven transgenes. Probably the most important ones were those involved in coagulation control, such as THBD and EPCR. Recently, significant progress has been made towards clinical application of cardiac xenografts; specifically 945 days survival of the recipient after heterotopic and, more importantly, 195 days after orthotopic transplantation into immunosuppressed baboons [127, 128]. The donor pigs lacked α Gal and expressed human CD46 and THBD [126]. This *GGTA1* knockout, CD46, THBD line is distributed by the company Revivicor and will, for brevity, be referred to as the 'Revivicor-line'. Comparison of complement activation in our five-fold transgenic, *GGTA1* knockout pig line and the Revivicor line showed significantly less complement activation in the five-fold transgenic, *GGTA1* knockout line upon challenge with human blood *in vitro* (personal communication with Dr. Konrad Fischer). These findings strongly indicate that the five-fold transgenic, *GGTA1* knockout line is superior to the Revivicor line regarding complement control. This might be because the Revivicor line overexpresses a single complement regulator (human CD46), while the five-fold transgenic line overexpresses high levels of three complement regulators (CD46, CD55 and CD59) providing protection at different stages of the complement cascade. However, the five-fold transgenic line lacks

transgenes to properly control coagulation, such as THBD and EPCR. Balanced coagulation controlled by at least one of these genes seems to be very critical for xenograft survival [264]. It has been shown that porcine THBD is a poor cofactor for the activation of protein C, which leads to impaired coagulation control of xenografts [124]. Overexpression of human THBD in pigs is associated with increased protein C production [125] and enhanced clotting time via inhibiting procoagulatory activity of thrombin [126]. The addition of human THBD dramatically improved survival of heterotopic cardiac xenografts in baboon recipients from 236 to 945 days [127, 265]. Human EPCR further enhances the activation of protein C about 20-fold by binding protein C and presenting it to the thrombomodulin/thrombin complex [129]. Iwase et al. showed reduced platelet aggregation *in vitro* and *in vivo* by expressing human EPCR, even in the presence of the porcine THBD [266]. The authors reasoned that overexpression of human EPCR enhanced the effect of porcine THBD and also anticipated that human EPCR would have a greater effect when coexpressed with human THBD, because the human protein serves as a better cofactor than the porcine version. Human THBD and EPCR are thus the most important transgenes to be added to the five-fold transgenic line and constitute the minimal set to be introduced at the CD46-MIN site.

To further increase xenograft protection, additional transgenes are required that address mechanisms distinct from complement- and coagulation control. Of the five further transgenes included in the multi-transgene vector, mutCIITA, PD-L1 and CD47 address cellular rejection mechanisms. MutCIITA and PD-L1 inhibit T cell activation via two distinct mechanisms. MutCIITA downregulates MHC class II molecules on APCs and consequently reduces activating signals [141] and PD-L1 mediates inhibitory signals suppressing T cell proliferation [150]. Human CD47 inhibits macrophage activation by mediating inhibitory signals. The other two transgenes, human HO-1 and HT, are involved in preventing acute humoral xenograft rejection. As already discussed in section 4.2, human HO-1 has beneficial effects in mediating anti-apoptotic and anti-inflammatory properties. A SV40-driven human HO-1 construct is already part of the transgene array at position 6q22, but its expression is weak and restricted to some tissues [68]. The aim is thus to supplement HO-1 expression by adding a further CAG-driven HO-1 construct. The other gene to prevent AHXR is HT. This gene prevents the formation of new xenogeneic antigens as main drivers for antibody-mediated rejection by using free N-acetyllactosamine residues to generate the well tolerated human blood group 0 antigen. Consequently, free N-acetyllactosamine residues are no longer available for other enzymes that may generate new and potentially xenogeneic glycosylation patterns.

Each of the transgenes included in the seven-fold transgene vector has been shown not to cause health problems, at least in single transgenic animals. For example, single transgenic mutCIITA and PD-L1 pigs have a reduced capacity to activate T cell response, but no reported

detrimental effects on health status [141, 154]. It has also been shown that hPD-L1 has no detrimental effect on porcine T cells [152]. Nevertheless, it is possible that combining multiple transgenes could cause some degree of immunocompromise. Thus, it may be necessary to house such pigs under clean conditions and minimise their exposure to infectious particles. Furthermore, it is not yet known, whether all of the seven transgenes are necessarily required to provide sufficient xenograft protection, or if a smaller set of transgenes would be sufficient. However, as generating multi-transgenic animals by stepwise addition of individual transgenes, such as transgene stacking, is quite laborious and time-consuming, it was decided to try a one-step approach that simultaneously addresses the different rejection mechanisms.

4.3 The CRISPR/Cas9 system for gene editing in pigs

The aim of this part of the project was to generate pigs that lacked up to four xenoreactive antigens. At the time the work commenced, the CRISPR/Cas9 system was emerging as a simple and efficient genome editing tool and so was used to generate single- and multiple gene-edited pigs.

4.3.1 Strategies for high gene editing efficiencies

The effectiveness of CRISPR/Cas9 gene editing varies between different genomic loci. The first step was to identify gRNA sequences that provided high frequency on-target cleavage. As expected, gene editing efficiencies varied between the target genes and even between regions of the same gene. For example, a gRNA targeting a sequence in exon 3 of porcine *CMAH* failed to produce any gene editing, whereas a gRNA directed against a sequence in *CMAH* exon 10 resulted in 17% monoallelic and 10% biallelic edited clones. This could be explained by differences in locus accessibility. It has been reported that chromatin state affects CRISPR/Cas9 gene editing, with higher efficiencies observed in euchromatic than in heterochromatic regions [267]. The same study also showed that secondary structure and stability of gRNAs contribute to variation in gene editing efficiencies [267].

To avoid the need to analyse very large numbers of cell clones, it was important to establish efficient means of isolating gene-edited cell clones, especially for multiplexed gene editing such as double- or four-fold knockouts. This involved identifying efficient gRNAs and also developing additional selection strategies to enrich gene-edited cells. The first selection method used provided indirect selection for Cas9-expressing cells by 2A signal-mediated linkage of a puromycin drug resistance gene to the Cas9 expression cassette, so drug-resistant cells co-expressed Cas9. However, this method increases the possibility of unwanted integration of the DNA vector into the host genome and extended expression of the CRISPR/Cas9 components which might lead to increased off-target cleavage. To avoid this,

antibiotic selection was applied for only a short time to select clones with transient rather than stable marker gene expression. As transient expression typically peaks around 72 hours after transfection, time for selection is limited and requires an antibiotic that acts within a short time frame. Puromycin was chosen as most suitable as it acts very rapidly and kills cells within 48 h [268], and has been shown to be effective by others [269].

To obtain high *GGTA1* knockout efficiencies, we additionally used a magnetic-bead selection strategy that enriched α Gal-negative cells. This method relies on the principle that α Gal-positive cells bind to biotin-conjugated isolectin B4 and are retained within a magnetic field via interaction of biotin with streptavidin-coated magnetic beads. *GGTA1* knockout, α Gal-negative cells do not bind isolectin B4 and pass through the magnetic field. In accordance with the reports of others [270], α Gal-negative cells were successfully enriched and the selected cells revealed almost 100% genome editing at the *GGTA1* target site. When *GGTA1* knockout was aimed to be simultaneously introduced with other knockouts, α Gal-negative cells were first selected via this approach and then the presence of indels within the other genes was checked. In addition to almost all magnetic-bead-selected cells being gene-edited at the target site of *GGTA1*, these cells also revealed high proportions of gene editing events for most of the other genes. This might be explained by the fact that cells with Cas9 cleavage activity within the nucleus, the final target compartment of the CRISPR/Cas9 system, were indirectly selected by the magnetic-bead selection. As a multi-knockout vector was used which co-localised Cas9 and multiple sgRNAs directed against various genes of interest, only a single vector had to be taken up to ensure the presence of all individual components within the cell. Consequently, it is likely that besides Cas9 and the α Gal-sgRNA, further sgRNAs were capable of entering the cell nucleus and mediating gene editing events. My results agree with those obtained by Li et al., who used a similar strategy and reported 1.9-fold co-enrichment of Neu5Gc-deficient cells after magnetic bead selection of α Gal-negative cells [9].

4.3.2 Strategies to minimise off-target cleavage

The major concern with CRISPR/Cas9 is the extent of off-target cleavage. In mammalian cells it has been shown that gRNAs with a single base difference from the target sequence can still cleave the target DNA, albeit less efficiently. Mismatches were tolerated at the 5' end of the target sequence, but not at the 3' end within the 11 bp immediately adjacent to the PAM sequence [207]. These results are consistent with previous *in vitro* experiments that identified the 8-12 bp at the 3' end of the target sequence, the so-called "seed sequence", as crucial for target recognition [203, 271]. Moreover, in mammalian cells off-target cleavage can occur at sites with up to 5 bases mismatch from the on-target site [272, 273]. Minimising off-target cleavage is very important for the production of gene-edited pigs, as gene editing at an off-

target site might result in phenotypic consequences unrelated to on-target gene editing effects. However, it is not trivial to identify whether any off-target event had been introduced. As web-based algorithms assume that off-target sequences are closely related to the on-target site, these might miss off-target cleavage sites with less sequence similarity [274]. Due to the limited capability of *in silico* methods to predict mutations that occur *in vivo* [272], it is possible that off-target effects remain undetected until extensive breeding has been carried out.

Various strategies have been investigated to improve the specificity of the CRISPR/Cas9 system. One approach uses a “paired nickase”, in which two gRNAs target adjacent sites on opposite DNA strands and each recruit a Cas9 variant (Cas9-D10A) that nicks the DNA instead of introducing a double-strand break [244, 275, 276]. Paired nickases can efficiently introduce indels within the on-target region and reduce Cas9-induced cleavage at off-target sites that are known to be cleaved by the equivalent gRNA-Cas9 nuclease complex [244, 275]. Nevertheless, this paired nickase strategy was not viewed as appropriate for this project for the following reasons. Using a second gRNA might introduce new off-target mutations as even single monomeric Cas9 nickases are capable of introducing indels at certain genomic loci [208, 244]. The use of paired nickases is also technically challenging, especially for multiplexed gene editing, as appropriately positioned and orientated paired gRNAs are required for each target site.

Another strategy to increase specificity uses modified gRNA architectures. Cho et al. added two guanine nucleotides to the 5' region of a 20 bp gRNA (5'-GGN₂₀-3') and observed reduced cleavage at 6 out of 7 known off-target sites in human epithelial- and lymphoblast cell lines [244]. In contrast, Fu et al. removed up to three bases from the 5' end of the gRNA (5'-N₁₇₋₁₈-3') and reported reduced cleavage at all 13 off-target sites in two different human epithelial cell lines, with some sites showing more than 5000-fold reduction in off-target cleavage compared to standard gRNAs (5'-N₂₀-3')[243]. The authors state that shortening the gRNA sequence seems counterintuitive as a means of increasing specificity, but hypothesise that nucleotides at the 5' end of the gRNA may not be necessary for activity and that these nucleotides might compensate for mismatches at other positions [243]. In my project, a standard 20 bp gRNA was compared with 5' truncated 18 bp- or GG dinucleotide-added gRNA structures regarding on- and off-target cleavage efficiency. The findings obtained in section 3.4.1.2 accord with those of other groups who also observed reduced on-target cleavage efficiency for GGN₂₀ gRNA structures [244] and similar on-target cleavage efficiencies for 5' truncated and standard 20 bp gRNA sequences [243]. However, the results obtained do not allow a conclusion to be made whether modified gRNA structures reduce off-target events, as no off-target cleavage was identified at any of the six most probable off-target sites, with either a standard 20 bp gRNA sequence or modified gRNA structures. The absence of off-target cleavage could be

explained by the fact that the standard 20 bp gRNA sequence was selected on the basis of a high predicted specificity score according to Hsu et al.[273]. Clearly a firm conclusion would require the analysis of a greater number of cell clones. In addition, only the most likely off-target sites were checked, based on bioinformatic prediction. So it remains possible that there are further off-target sites that are not included or largely underestimated in the bioinformatic prediction. To unequivocally identify off-target cleavage at any position within the genome, whole genome sequencing could be carried out in future experiments for the gene-edited pigs discussed in the next section.

4.4 Pigs deficient in the major xenoreactive antigens

Within this work I created a variety of gene-edited pigs for xenotransplantation designed to provide reduced antigenicity for human recipients. The generation of the first *GGTA1* KO pigs in 2002 was an important step towards clinical application of porcine xenografts by overcoming hyperacute rejection processes as a major humoral barrier [65, 66]. However, despite the tremendously reduced antigenicity of *GGTA1* knockout kidneys upon xenotransplantation into baboons, humoral rejection processes directed against non-Gal-antigens remained a problem [72] indicating the need to remove further xenoreactive antigens from xenodonor pigs.

4.4.1 *CMAH* knockout pigs

Several studies have indicated the value of removing Neu5Gc epitopes. Anti-Neu5Gc antibodies capable of binding porcine red blood cells have been detected in a large proportion of healthy human sera [29], and Neu5Gc-bearing cells are rejected by syngeneic *Cmah* knockout mice due to anti-Neu5Gc antibodies [27]. I thus aimed to disrupt the porcine *CMAH* gene responsible for Neu5Gc synthesis. Several previous attempts had been carried out by other members of the Chair of Livestock Biotechnology using a conventional gene targeting vector, TALENS or the CRISPR/Cas9 system alone or in combination, to mimic in pigs the human 92 bp deletion of exon three that leads to inactivation of the catalytic domain [32]. However, their findings suggested that the corresponding region in pigs (exon four) seemed to be refractory to genetic modification. It was thus decided to target exon ten instead, because two other research groups had independently reported successful inactivation of porcine *CMAH* using zinc finger nucleases directed against this region [73, 277]. Use of the CRISPR/Cas9 system achieved successful gene disruption and porcine cells lacking surface Neu5Gc. Similar to findings from *Cmah* knockout mice [278], porcine *CMAH* knockout cells incubated with human serum showed reduced binding of IgG and IgM antibodies compared to wild type.

4.4.2 *GGTA1/CMAH* double-knockout pigs

Besides the *CMAH* knockout pigs, *GGTA1/CMAH* double-knockout pigs based on a five-fold transgenic- or a wild type background were produced to further reduce xenoantigenicity of porcine donor organs. The results described in section 3.4.3 accord with the findings of other groups who reported absence of α Gal- and Neu5Gc epitopes in multiple organs, such as heart, liver, kidney, lung and pancreas, and in PBMCs and erythrocytes of *GGTA1/CMAH* double-knockout pigs [73, 279, 280]. Porcine *GGTA1/CMAH* double-knockout cells revealed further reduction of human antibody binding compared to wild type and single knockout cells, which again has also been observed by other groups [73, 279, 281]. Moreover, preformed anti- α Gal- and anti-Neu5Gc antibodies were detected in the sera of the *GGTA1/CMAH* double-knockout pigs at levels that varied between individual pigs. This resembles the human situation, as levels of both anti- α Gal- and anti-Neu5Gc-antibodies vary between human serum samples, with anti-Neu5Gc antibodies being detectable in 85% of human samples [29, 34, 279].

The generation of *GGTA1/CMAH* knockout pigs has brought clinical xenotransplantation a step closer. However, the ability to test cells, tissue and organs from these animals *in vivo* is limited because non-human primates express Neu5Gc. Wang et al. and Estrada et al. reported that baboon and rhesus macaque sera showed greater reactivity *in vitro* to porcine *GGTA1/CMAH* double-knockout than to *GGTA1* single knockout cells [42, 279]. The authors proposed that modification of the surface sialic acid profile had generated a species-specific glycosylation pattern that made non-human primates more immunoreactive to *GGTA1/CMAH* knockout pigs [279]. However, this effect was attenuated by additional inactivation of *B4GALNT2*. Cells from *GGTA1/CMAH/B4GALNT2* triple-knockout animals incubated with baboon or rhesus macaque serum bound significantly less IgG and IgM than did *GGTA1/CMAH*- or *GGTA1*- knockout cells [42]. In contrast, human sera showed reduced *in vitro* reactivity to porcine *GGTA1/CMAH* double-knockout cells than to *GGTA1* single knockout cells and inactivation of *B4GALNT2* was associated with further reduction of human antibody binding [282]. As overall levels of antibody binding were less than in non-human primates, porcine double- and triple-knockout cells should be associated with better *in vivo* effects in humans than in non-human primates.

4.4.3 *GGTA1/CMAH/B4GALNT2/B2M* four-fold knockout pigs

The identification of further xenoreactive antigens, such as Sda-bearing epitopes produced by the porcine *B4GALNT2* gene [44] and porcine MHC class I (=SLA class I) molecules [45], justified the generation a four-fold knockout pig lacking α Gal, Neu5Gc, Sda and SLA class I epitopes. The three carbohydrate epitopes could be removed straightforwardly, by inactivating of their synthesising genes *GGTA1*, *CMAH* and *B4GALNT2*. Elimination of SLA class I epitopes was however more challenging, as porcine MHC class I proteins are encoded by a

series of highly polymorphic genes with multiple alleles. Assembly, transport and presentation of a functional MHC class I complex requires the formation of a heterotrimeric complex of these SLA class I molecules with B2M and short peptides [75, 283]. Thus, inactivation of the non-polymorphic single *B2M* gene offered a simple and effective strategy to remove surface porcine MHC class I complexes. As described in results section 3.4.4, a four-fold knockout pig was generated that lacked B2M molecules and functional MHC class I complexes. Genotypic analyses of this animal identified three differentially edited alleles for *B2M*, which can be explained by a *B2M* gene duplication event. Minh Le et al. reported a segmental duplication of a ~45.5 kb fragment on chromosome 1 of pigs that contains the entire *B2M* coding sequence and its regulatory elements [284]. The authors suggested that this gene duplication might have occurred to increase the availability of B2M as complex partner for the relatively large number of MHC class I heavy chain genes in pigs [284]. However, I identified only three differently modified *B2M* alleles in the four-fold knockout pig instead of four, which might be explained by the fact that two alleles carry an identical indel pattern and cannot be further distinguished.

Genetic modifications designed to improve the usefulness of animals as xenodonors should not adversely affect those animals. There have been varying reports on the health status of b2m-deficient mice. While some groups describe no abnormalities [285], others report that b2m-deficient mice lose the ability to regulate iron homeostasis and accumulate iron in the gut mucosa and liver [245, 286, 287]. The *GGTA1/CMAH/B4GALNT2/B2M* four-fold knockout pig generated in this project and B2M-deficient pigs generated by others [80], showed no signs of health problems related to an imbalanced iron homeostasis. Also, contrary to previous observations that mice show B2M-independent assembly of MHC class I molecules with peptides that are stably expressed at the cell surface and capable of activating CD8⁺ T cells [288, 289], PMBCs from the *GGTA1/CMAH/B4GALNT2/B2M* four-fold knockout pig had no MHC class I epitopes at the cell surface detectable by FACS analysis. This result accords with findings by Wang et al. who also detected no SLA-1 epitopes on porcine cell surfaces after depletion of B2M [80]. These results illustrate that findings in mice cannot necessarily be extrapolated to pigs.

Unfortunately, the *GGTA1/CMAH/B4GALNT2/B2M* four-fold knockout pig suffered from an infection at six weeks old and had to be sacrificed. As SLA class I complexes are responsible for activation of CD8⁺ T cells, it seems likely that depletion of SLA class I molecules by inactivation of *B2M* reduced the capacity to activate CD8⁺ T cells, leading to immunocompromise and susceptibility to infection. Reyes et al. showed reduced levels of CD8⁺ T cells in SLA class I deficient pigs [81], but unfortunately, this could not be confirmed in this particular animal as the T cell subsets were not available for analysis. This issue is

currently being addressed by keeping and breeding the new generation of SLA class I deficient pigs under improved hygienic conditions.

As previously mentioned, porcine PBMCs devoid of α Gal, Neu5Gc and Sda epitopes showed reduced human antibody binding levels compared to *GGTA1* and *GGTA1/CMAH* knockout cells [42, 45, 282]. These were further attenuated by removal of SLA class I antigens which cross-react with anti-HLA antibodies in HLA-sensitised patients [45]. As shown in results section 3.4.4, human antibody binding to kidney fibroblasts from the *GGTA1/CMAH/B4GALNT2/B2M* four-fold knockout pig revealed strongest reduction of IgM and IgG antibody binding compared to cells from *GGTA1/CMAH* double-, *CMAH* single-knockout and wild type pigs. These findings are very encouraging, especially considering that triple-knockout red blood cells (RBC), which naturally express no MHC molecules, already showed levels of human antibody binding similar to human blood group 0 RBCs and autologous RBCs [282]. This suggests that we are close to overcoming the xenoreactive antibody-mediated humoral barrier to xenotransplantation.

4.5 ROSA26-hSpCas9 pigs for *in vivo* genome editing

As outlined in more detail in the introduction section, early attempts to perform genome editing *in vivo* in whole animals required simultaneous delivery of the sgRNA and hSpCas9. This approach is inefficient and presents potential safety risks where the human and animal target sequences are highly homologous. The generation of a transgenic pig that expresses hSpCas9 was thus conceived as an efficient, safe platform for CRISPR/Cas9-mediated *in vivo* genome editing. This provides the advantage that hSpCas9 is present endogenously in the cell and only the sgRNA needs to be delivered via lentivirus or AAV vectors. In contrast to hSpCas9, the guide RNAs are quite small and can be efficiently packed into viral particles. For efficient multiplexed genome editing, multiple gRNAs can further be combined on a single vector. This approach also eliminates safety concerns, as accidental exposure to sgRNAs alone carries no discernable risk, enabling viral delivery to be carried out under S1 containment conditions.

As shown in section 3.4, a hSpCas9-transgenic pig line was generated by placement of a CBh-driven hSpCas9 construct at the *ROSA26* locus. Similar to mice that ubiquitously express Cas9, the hSpCas9 expressing pig line is healthy and fertile indicating no apparent deleterious effects of the constitutively expressed hSpCas9 nuclease [231]. hSpCas9 is expressed from the porcine *ROSA26* locus by a synthetic CBh promoter, which is a modified version of the CAG promoter [290]. Analysis of various organs from a *ROSA26*-hSpCas9 pig revealed mRNA expression of hSpCas9 in all organs analysed. These findings are strengthened by CBh activity being demonstrated in a huge variety of different cell lines, such as HEK293, HeLa and HepG2

[269]. Furthermore, the same CBh-hSpCas9 construct has been used for CRISPR/Cas9-mediated genome editing worldwide in a huge variety of different cell types from multiple species with no reports, at least to my knowledge, of Cas9 being inactive in a certain cell type. I'm very enthusiastic to assess hSpCas9 functionality in a multitude of cells derived from different organs or directly *in vivo* in organs of interest by administration of sgRNAs.

Besides the Cas9-expressing pig line generated within this work, a second line has meanwhile been generated by Wang et al [291]. This group generated a Cre-dependent hSpCas9-expressing pig directed by the endogenous *ROSA26* promoter [291]. Although they showed successful *in vivo* genome editing [291], this approach seems to be quite inefficient. Two consecutive recombination events are required to bring the Cas9 expression cassette under the control of the *ROSA26* promoter. As only 0.1% of the cells expressed Cas9 cells upon *in vivo* lentiviral-mediated delivery of Cre [291], it is reasonable to anticipate that genome editing will be more efficient in my Cas9-expressing pig line due to the higher proportion of Cas9-expressing cells.

Given the power of *in vivo* gene editing, I am confident that the hSpCas9 expressing pigs will be useful in a variety of biomedical applications. For example, directly relevant to xenotransplantation these pigs will facilitate tissue-specific knockouts of xenoreactive genes that may be problematic to inactivate in the whole body, using gRNAs delivered locally to the tissue of interest.

The modelling and investigation of the genetic basis of different cancers is another area that will benefit from a hSpCas9 expressing pig. At the Chair of Livestock Biotechnology several genetically modified pig lines have been generated to model human cancers, including an *APC*¹³¹¹ mutant line that replicates a human genetic predisposition to colorectal cancer, familial adenomatous polyposis (FAP) [292]. These pigs develop adenomatous polyps in the colon and rectum in a manner closely resembling the human condition. However, the mutated *APC* gene serves only to initiate polyp formation, and other mutations are required for progression to invasive cancer [293]. In humans, these events occur spontaneously over the lifetime of the patient, or in *APC* mutant mice they can be introduced experimentally [294]. The Cas9 pig line provides a powerful means of investigating disease progression in detail. *APC*¹³¹¹ mutant pigs that also carry the hSpCas9 transgene enable mutation or inactivation of tumour-relevant genes directly in individual polyps by *in vivo* electroporation [295] or AAV-mediated delivery [296] of appropriate sgRNAs. Polyps in the distal colon and rectum can be readily accessed by standard colonoscopic techniques. Such somatic gene editing resembles the events that underlie human oncogenesis more accurately than would whole-body gene editing. This can easily include multiplex gene editing [207], with systematic inactivation of sets of genes used for functional study of cancer development and progression. Moreover, the large size and long

life of the pig enable different combinations of mutated genes to be compared even within a single animal by injecting individual polyps with different sgRNA combinations. The Cas9 pigs thus offer to increase the power of cancer modelling in pigs by increasing the number of genes that can be investigated. In addition, a huge range of *in vivo* gene editing experiments can be performed based on this single pig line, which can be modified as required. This greatly reduces the need for new gene-edited pig lines carrying different mutated cancer-related genes. In accordance with the principle of “replacement, reduction, refinement” that always has to be considered when working with experimental animals, the number of pigs needed for such experiments can be drastically reduced.

5 Concluding remarks and outlook

In this project, novel and improved genetic models for xenotransplantation and *in vivo* genome editing have been generated by means of controlled transgene placement and targeted inactivation of endogenous porcine genes. Once the most effective combination of added transgenes and inactivated porcine genes has been determined, the methods developed and applied as part of this project will expedite the generation of the necessary multi-modified genotype.

Transgene stacking at the porcine *ROSA26* locus has shown to be a suitable approach for assembling multiple independently-expressed transgenes at a single site, however this approach is time-consuming and dependent on serial nuclear transfer. An alternative approach, Bxb1-recombinase mediated integration of a multi-transgene vector at a site adjacent to the transgene-array in a five-fold transgenic line has been facilitated within this project by placement of an attP/MIN site at the desired position and by generation of a multi-transgene vector for Bxb1-mediated integration at the attP/MIN site. Once attP/MIN targeted piglets are available, cells from these animals can be used to test Bxb1-mediated transgene placement and, if successful, to introduce the multi-transgene vector. Both transgene placement methods can be combined to generate the next generation xenodonor pig line that carries all transgenes necessary for efficient protection against rejection by the human recipient.

Pigs deficient in the major xenoreactive antigens have also been generated by CRISPR/Cas9-mediated single- and multiplexed gene editing using appropriate enrichment methods. These gene-edited pigs will find application in a range of projects related to xenotransplantation. The *GGTA1/CMAH* double-knockout line has already been bred with the five-fold transgenic line available at our Chair and the resulting five-fold transgenic, double-knockout line will serve as organ donors for kidney- and heart xenotransplantation into baboons to assess their function and rejection-potential. Heart valve matrices of the *GGTA1/CMAH* double-knockout pigs will be used for orthotopic implantation into baboons and assessment of their function and remodelling. The gene-edited pigs are also interesting for projects in other biomedical fields, such as cancer modelling. To refine an existing model of colorectal polyposis, *CMAH* knockout pigs will be bred with the *APC^{1311/+}* pig line available at our Chair to investigate the relationships between the immune response to Neu5Gc, gut inflammation, the gut microbiome and the development of colorectal cancer.

A pig line with ubiquitous hSpCas9 expression from the porcine *ROSA26* has been generated and shown to be functional. This line provides a valuable new tool for *in vivo* CRISPR/Cas9 based genome editing that will have a wide variety of applications, such as cancer- or

cardiovascular disease-modelling. Such work will however require establishing efficient means of delivering sgRNA to introduce gene editing events within the organ(s) of interest, and the difficulty of this will vary considerably on the type of experiment carried out. Nevertheless this offers a new and potentially powerful means of investigating and modelling the genetic bases of human diseases in pigs without the need to generate whole body mutant animals.

6 Abbreviations

A20 /TNFAIP	Tumor necrosis factor- alpha induced protein
AAV	Adeno-associated virus
ACXR	Acute cellular xenograft rejection
ADCC	antibody-dependent cell-mediated cytotoxicity
AHXR	Acute humoral xenograft rejection
APC	Antigen presenting cell
APS	Ammonium persulfate
attB	Bacterial attachment site
attP	Phage attachment site
AVR	Acute vascular rejection
B2M	β -2-microglobulin
B4GALNT2	β 1,4-N-acetylgalactosaminyl transferase
BAC	Bacterial artificial chromosome
BGHpA	Bovine growth hormone polyadenylation site
BS	Blasticidin S resistance cassette
BSA	Bovine serum albumin
CAG	CMV enhancer/chicken β -actin/rabbit β -globin
Cas9	CRISPR-associated protein 9
cDNA	complementary DNA
CIITA	Class II transactivator
CMAH	cytidine monophosphate-N-acetylneuraminic acid hydroxylase
CO	Carbon monoxide
CRISPR	Clustered regulatory interspaced short palindromic repeat
CRP	Complement regulatory protein
crRNA	CRISPR-RNA
CTLA4	Cytotoxic T lymphocyte-associated antigen 4
ddPCR	droplet digital PCR
DMEM	Dulbecco`s modified eagle medium
DMSO	Dimethyl sulfoxide
DNA	Deoxyribonucleic acid
dNTP	Deoxynucleotide
DSB	Double-strand break
DTT	Dithiothreitol
E.coli	Escherichia coli
EDTA	ethylenediaminetetraacetate

EPCR	Endothelial protein C receptor
ES cells	Embryonic stem cells
EtOH	Ethanol
FACS	fluorescence-activated cell sorting
FBS	Fetal bovine serum
GalNAc	N-acetyl-D-galactosamine
GAPDH	Glyceraldehyde 3-phosphate dehydrogenase
GGTA1	α 1,3-galactosyltransferase
gRNA	Guide RNA
HAR	Hyperacute rejection
H-D antigens	Hanganutziu-Deicher antigens
HEK293	Human embryonic kidney cell line 293
HeLa	Human epithelial cervical cancer cell line
HEPG2	Human liver carcinoma cell line
HLA	Human leucocyte antigen
HMGB1	high mobility group box 1 (protein)
HO-1	Heme oxygenase 1
HPRT	hypoxanthine guanine phosphoribosyltransferase
hSpCas9	humanised version of Cas9 from <i>streptococcus pyogenes</i>
HT, H-transferase	α 1,2-fucosyltransferase
IF	Immunofluorescence
IgG, IgM	Immunoglobulin G, immunoglobulin M
IHC	Immunohistochemistry
Indel	Insertion or deletion
IRES	Internal ribosome entry site
LEA29Y	High affinity variant of CTLA4-Ig
LLD	Lectin-like domain
MAC	Membrane attack complex
MHC	Main histocompatibility complex
MIN	Multifunctional integrase
pMSC	porcine mesenchymal stem cell
mutCIITA, CIITA-DN	dominant-negative variant of class II transactivator
Neo	Neomycin resistance cassette
Neu5Ac	N-acetylneuraminic acid
Neu5Gc	N-glycolylneuraminic acid
NHEJ	Non-homologous end joining
NK cell	Natural killer cell

NKG2D	Natural killer group 2D
NLS	Nuclear localisation signal
PAEC	porcine aortic endothelial cells
PAM	Protospacer adjacent motif
PBMC	Peripheral blood mononucleated cells
PCR	Polymerase chain reaction
PD-1	Programmed cell death-1
PD-L1	Programmed cell death- ligand 1
PEF	Porcine ear fibroblast
PFF	Porcine fetal fibroblast
PKF	Porcine kidney fibroblast
q-RT-PCR	quantitative real-time PCR
RNA	Ribonucleic acid
ROSA β geo26	Reverse Orientated Splice Acceptor β geo clone 26
RT-PCR	Reverse transcriptase PCR
SA	Splice acceptor
SCNT	Somatic cell nuclear transfer
SCP1	Human bone-marrow derived mesenchymal stem cell line
SDS	sodium dodecyl sulfat
sgRNA	Single guide RNA
SIRP α	Signal regulatory protein α
SLA	Swine leucocyte antigen
ST cells	Swine testis cells
TAFI	Thrombin-activatable fibrinolysis inhibitor
TALEN	Transcription activator-like effector nuclease
TCR	T cell receptor
THBD	Thrombomodulin
TIDE	Tracking of indels by decomposition
TNF- α	Tumor necrosis factor-alpha
tracrRNA	Trans-activating RNA
ULBP1	UL16 binding protein 1
UTR	Untranslated region
WB	Western blot
X-Gal	5-bromo-4-chloro-3-indolyl- β -D-galactopyranoside
ZFN	Zinc finger nuclease
α Gal	Galactose- α 1,3-galactose

7 List of tables

Table 1: Chemicals.....	32
Table 2: Enzymes and enzyme buffers	34
Table 3: Kits.....	34
Table 4: Bacterial strains.....	35
Table 5: Eukaryotic cells	35
Table 6: Antibodies.....	36
Table 7: Primers and probes.....	37
Table 8: gRNA oligonucleotides.....	39
Table 9: Nucleic acid ladders	40
Table 10: Molecular cloning vectors and DNA constructs.....	40
Table 11: Tissue culture media, supplements and reagents.....	41
Table 12: Bacterial culture media and supplements	42
Table 13: Buffers and solutions	42
Table 14: Laboratory equipment.....	44
Table 15: Consumables	45
Table 16: Software and online tools	46
Table 17: GoTaq G2 polymerase PCR reaction.....	49
Table 18: FastGene Optima HotStart Ready Mix reaction.....	49
Table 19: Q5 high-fidelity DNA polymerase PCR reaction.....	50
Table 20: PCR extender system reaction	50
Table 21: AccuStart Taq DNA polymerase HiFi PCR reaction	51
Table 22: DNA restriction digest	53
Table 23: Ligation reaction.....	53
Table 24: ddPCR reaction composition and cycling conditions	54
Table 25: q-RT-PCR reaction composition and cycling conditions.....	55
Table 26: Separation- and stacking gel composition.....	58
Table 27: Influence of the gRNA sequence length on on- and off-target cleavage efficiency.	80
Table 28: GRNA efficiencies for four xenorelevant genes	81
Table 29: TIDE analyses of a multiple-knockout cell pool.....	92

8 List of figures

Figure 1: Antibody-mediated rejection processes	11
Figure 2: Structure of the major carbohydrate xenoreactive antigens	12
Figure 3: Cellular rejection mechanisms.....	13
Figure 4: The complement cascade and its control.....	16
Figure 5: Biological functions of HO-1	17
Figure 6: Functions of thrombomodulin	19
Figure 7: Strategies to prevent T cell activation	21
Figure 8: Five-fold transgenic pig line generated at the Chair of Livestock Biotechnology	23
Figure 9: Generation of genetically modified animals	24
Figure 10 Double-strand break repair mechanisms in eukaryotic cells	27
Figure 11: The CRISPR/Cas9 system as potent tool for genome editing.....	28
Figure 12: Schematic outline of Bxb1 serine recombinase- mediated transgene placement	29
Figure 13: Cloning of target guide sequence into CRISPR/Cas9 vectors	60
Figure 14: Transgene stacking at the porcine <i>ROSA26</i> locus	67
Figure 15: Structure of the <i>ROSA26</i> - <i>CD55</i> -retargeting vector	68
Figure 16: Targeting PCR and copy number of <i>ROSA26</i> - <i>CD55</i> - <i>HO-1</i> pig #559.....	69
Figure 17: mRNA expression analyses of <i>ROSA26</i> - <i>CD55</i> - <i>HO-1</i> pig #559	69
Figure 18: <i>CD55</i> protein detection in tissues and cells of <i>ROSA26</i> - <i>CD55</i> - <i>HO-1</i> pig #559....	71
Figure 19: Protection of PKF cells from <i>ROSA26</i> - <i>CD55</i> - <i>HO-1</i> pig #559.....	71
Figure 20: Third-round-targeting of the <i>ROSA26</i> - <i>CD55</i> - <i>HO-1</i> locus	72
Figure 21: Structure of the final 7x transgene vector	76
Figure 22: RT-PCR analysis of a 7x transgene vector transfected PKF cell pool	76
Figure 23: Targeting approach to integrate a MIN site within the <i>CD46</i> 3' flanking region....	76
Figure 24: Structure of the <i>CD46</i> -MIN targeting vector.....	77
Figure 25: PCR-analyses of correctly targeted <i>CD46</i> -MIN clones.....	77
Figure 26: Hygromycin copy number of correctly targeted cell clones	78
Figure 27: Picture of the five-fold transgenic, <i>CMAH</i> knockout boar #890.....	83
Figure 28: Genotypic analysis of <i>CMAH</i> knockout pigs	83
Figure 29: Neu5Gc and GAPDH western blot analyses of pig #463 and #890	84
Figure 30: Genotypic analysis of the double-knockout, 5xtg pigs #544 and #545	85
Figure 31: Flow cytometry analyses of PKFs from piglet #544	86
Figure 32: Workflow for the generation of female <i>GGTA1</i> / <i>CMAH</i> double-knockout pigs.....	86
Figure 33: Picture of sow #551 at an age of 20 months.....	87
Figure 34: Structure of the double-knockout plasmid #705- <i>CMAH</i> - <i>GGTA1</i>	87
Figure 35: Pictures of sows #488 and #490 at an age of 25 months.....	88

Figure 36: Genotypic analyses of the double-knockout pigs #488, #490 and #551	88
Figure 37: Absence of double-knockout vector integration	89
Figure 38: Flow cytometry analyses of PBMCs from pigs #488, #490 and #551	89
Figure 39: Neu5Gc and GAPDH western blot analyses of blood from pigs #488 and #490..	90
Figure 40: Preformed anti-aGal antibodies (A) and anti-Neu5Gc antibodies (B)	90
Figure 41: Breeding of <i>GGTA1/CMAH</i> double-knockout pigs # 488 and #490	91
Figure 42: Structure of the four-fold knockout vector #841-4xKO.....	92
Figure 43: Picture of the four-fold knockout piglet #90 at day 24.....	93
Figure 44: Genotypic analysis of the four-fold knockout pig #90	93
Figure 45: Flow cytometry analyses of PEFs from the four-fold knockout pig #90.....	94
Figure 46: Neu5Gc and GAPDH western blot analyses of various organs from pig #90	95
Figure 47: IgG and IgM antibody binding to single-, double- and four-fold knockout cells.....	96
Figure 48: Targeting of porcine <i>ROSA26</i> to introduce hSpCas9	97
Figure 49: Structure of the <i>ROSA26</i> -hSpCas9 targeting vector	98
Figure 50: Picture of the <i>ROSA26</i> -hSpCas9 piglets #41 and #42	98
Figure 51: Targeting PCRs and hSpCas9 expression analysis of pigs #41 and #42.....	99
Figure 52: Copy number of hSpCas9 in <i>ROSA26</i> -hSpCas9 pigs #41 and #42	99
Figure 53: HSpCas9 functionality in PEF cells of <i>ROSA26</i> -hSpCas9 pigs #41 and #42.....	100
Figure 54: Analysis of hSpCas9-transgenic offspring	101
Figure 55: HSpCas9 functionality in pMSC, PEF and PAEC cells of <i>ROSA26</i> -hSpCas9, <i>KRAS</i> ^{G12D} piglet #395.....	102

9 Literature

1. Tonelli, M. and M. Riella, *Chronic kidney disease and the aging population: World Kidney Day 2014*. Transplantation, 2014. **97**(5): p. 490-3.
2. Eurotransplant. *Organ demand and donation*. 2019 [cited 2019 May 27]; Available from: <https://www.eurotransplant.org/cms/>.
3. Novitzky D, W.W., Cooper DK, Rose AG, Fraser R, Barnard CN, *Electrocardiographic, hemodynamic and endocrine changes occurring during experimental brain death in the Chacma baboon*. J Heart Transplant, 1984. **4**: p. 63.
4. Cooper, D.K., *The case for xenotransplantation*. Clin Transplant, 2015. **29**(4): p. 288-93.
5. Allan, J.S., *The risk of using baboons as transplant donors. Exogenous and endogenous viruses*. Ann N Y Acad Sci, 1998. **862**: p. 87-99.
6. Gao, F., et al., *Origin of HIV-1 in the chimpanzee Pan troglodytes troglodytes*. Nature, 1999. **397**(6718): p. 436-41.
7. Cooper, D.K., *A brief history of cross-species organ transplantation*. Proc (Bayl Univ Med Cent), 2012. **25**(1): p. 49-57.
8. Polejaeva, I.A., et al., *Cloned pigs produced by nuclear transfer from adult somatic cells*. Nature, 2000. **407**(6800): p. 86-90.
9. Li, P., et al., *Efficient generation of genetically distinct pigs in a single pregnancy using multiplexed single-guide RNA and carbohydrate selection*. Xenotransplantation, 2015. **22**(1): p. 20-31.
10. Boneva, R.S. and T.M. Folks, *Xenotransplantation and risks of zoonotic infections*. Ann Med, 2004. **36**(7): p. 504-17.
11. Good, A.H., et al., *Identification of carbohydrate structures that bind human anti-porcine antibodies: implications for discordant xenografting in humans*. Transplant Proc, 1992. **24**(2): p. 559-62.
12. Oriol, R., et al., *Carbohydrate antigens of pig tissues reacting with human natural antibodies as potential targets for hyperacute vascular rejection in pig-to-man organ xenotransplantation*. Transplantation, 1993. **56**(6): p. 1433-42.
13. Schuurman, H.J., J. Cheng, and T. Lam, *Pathology of xenograft rejection: a commentary*. Xenotransplantation, 2003. **10**(4): p. 293-9.
14. Galili, U. and K. Swanson, *Gene sequences suggest inactivation of alpha-1,3-galactosyltransferase in catarrhines after the divergence of apes from monkeys*. Proc Natl Acad Sci U S A, 1991. **88**(16): p. 7401-4.
15. Galili, U., et al., *A unique natural human IgG antibody with anti-alpha-galactosyl specificity*. J Exp Med, 1984. **160**(5): p. 1519-31.
16. Galili, U., et al., *Interaction between human natural anti-alpha-galactosyl immunoglobulin G and bacteria of the human flora*. Infect Immun, 1988. **56**(7): p. 1730-7.
17. Platt, J.L., et al., *Immunopathology of hyperacute xenograft rejection in a swine-to-primate model*. Transplantation, 1991. **52**(2): p. 214-20.
18. Rose, A.G. and D.K. Cooper, *Venular thrombosis is the key event in the pathogenesis of antibody-mediated cardiac rejection*. Xenotransplantation, 2000. **7**(1): p. 31-41.
19. Platt, J.L., S.S. Lin, and C.G. McGregor, *Acute vascular rejection*. Xenotransplantation, 1998. **5**(3): p. 169-75.
20. Yang, Y.G. and M. Sykes, *Xenotransplantation: current status and a perspective on the future*. Nat Rev Immunol, 2007. **7**(7): p. 519-31.
21. Pino-Chavez, G., *Differentiating Acute Humoral from Acute Cellular Rejection Histopathologically*. Graft, 2001. **4**(1): p. 60-62.
22. Vega, A., et al., *Immunohistochemical study of experimental acute cellular rejection*. Transplant Proc, 2002. **34**(2): p. 731-2.
23. Higashi, H., et al., *Antigen of "serum sickness" type of heterophile antibodies in human sera: identification as gangliosides with N-glycolylneuraminic acid*. Biochem Biophys Res Commun, 1977. **79**(2): p. 388-95.

24. Merrick, J.M., K. Zadarlik, and F. Milgrom, *Characterization of the Hanganutziu-Deicher (serum-sickness) antigen as gangliosides containing n-glycolylneuraminic acid*. *Int Arch Allergy Appl Immunol*, 1978. **57**(5): p. 477-80.
25. Morozumi, K., et al., *Significance of histochemical expression of Hanganutziu-Deicher antigens in pig, baboon and human tissues*. *Transplant Proc*, 1999. **31**(1-2): p. 942-4.
26. Springer, S.A., S.L. Diaz, and P. Gagneux, *Parallel evolution of a self-signal: humans and new world monkeys independently lost the cell surface sugar Neu5Gc*. *Immunogenetics*, 2014. **66**(11): p. 671-4.
27. Tahara, H., et al., *Immunological property of antibodies against N-glycolylneuraminic acid epitopes in cytidine monophospho-N-acetylneuraminic acid hydroxylase-deficient mice*. *J Immunol*, 2010. **184**(6): p. 3269-75.
28. Miwa, Y., et al., *Are N-glycolylneuraminic acid (Hanganutziu-Deicher) antigens important in pig-to-human xenotransplantation?* *Xenotransplantation*, 2004. **11**(3): p. 247-53.
29. Zhu, A. and R. Hurst, *Anti-N-glycolylneuraminic acid antibodies identified in healthy human serum*. *Xenotransplantation*, 2002. **9**(6): p. 376-81.
30. Muchmore, E.A., S. Diaz, and A. Varki, *A structural difference between the cell surfaces of humans and the great apes*. *Am J Phys Anthropol*, 1998. **107**(2): p. 187-98.
31. Chou, H.H., et al., *Inactivation of CMP-N-acetylneuraminic acid hydroxylase occurred prior to brain expansion during human evolution*. *Proc Natl Acad Sci U S A*, 2002. **99**(18): p. 11736-41.
32. Chou, H.H., *A mutation in human CMP-sialic acid hydroxylase occurred after*. 1998. **95**(20): p. 11751-6.
33. Varki, A., *Loss of N-glycolylneuraminic acid in humans: Mechanisms, consequences, and implications for hominid evolution*. *Am J Phys Anthropol*, 2001. **Suppl 33**: p. 54-69.
34. Tangvoranuntakul, P., et al., *Human uptake and incorporation of an immunogenic nonhuman dietary sialic acid*. *Proc Natl Acad Sci U S A*, 2003. **100**(21): p. 12045-50.
35. Bardor, M., et al., *Mechanism of uptake and incorporation of the non-human sialic acid N-glycolylneuraminic acid into human cells*. *J Biol Chem*, 2005. **280**(6): p. 4228-37.
36. Banda, K., et al., *Metabolism of vertebrate amino sugars with N-glycolyl groups: mechanisms underlying gastrointestinal incorporation of the non-human sialic acid xeno-autoantigen N-glycolylneuraminic acid*. *J Biol Chem*, 2012. **287**(34): p. 28852-64.
37. Padler-Karavani, V., et al., *Diversity in specificity, abundance, and composition of anti-Neu5Gc antibodies in normal humans: Potential implications for disease*. *Glycobiology*, 2008. **18**(10): p. 818-30.
38. Baumann, B.C., et al., *Reactivity of human natural antibodies to endothelial cells from Galalpha(1,3)Gal-deficient pigs*. *Transplantation*, 2007. **83**(2): p. 193-201.
39. Saethre, M., et al., *Characterization of natural human anti-non-gal antibodies and their effect on activation of porcine gal-deficient endothelial cells*. *Transplantation*, 2007. **84**(2): p. 244-50.
40. Byrne, G.W., et al., *Identification of new carbohydrate and membrane protein antigens in cardiac xenotransplantation*. *Transplantation*, 2011. **91**(3): p. 287-92.
41. Zhao, C., et al., *The Sda and Cad glycan antigens and their glycosyltransferase, beta1,4GalNAcT-II, in xenotransplantation*. *Xenotransplantation*, 2018. **25**(2): p. e12386.
42. Estrada, J.L., et al., *Evaluation of human and non-human primate antibody binding to pig cells lacking GGTA1/CMAH/beta4GalNT2 genes*. *Xenotransplantation*, 2015. **22**(3): p. 194-202.
43. Byrne, G., et al., *B4GALNT2 and xenotransplantation: A newly appreciated xenogeneic antigen*. *Xenotransplantation*, 2018: p. e12394.
44. Byrne, G.W., et al., *Cloning and expression of porcine beta1,4 N-acetylgalactosaminyl transferase encoding a new xenoreactive antigen*. *Xenotransplantation*, 2014. **21**(6): p. 543-54.

45. Martens, G.R., et al., *Humoral Reactivity of Renal Transplant-Waitlisted Patients to Cells From GGTA1/CMAH/B4GalNT2, and SLA Class I Knockout Pigs*. Transplantation, 2017. **101**(4): p. e86-e92.
46. Ide, K., et al., *Role for CD47-SIRPalpha signaling in xenograft rejection by macrophages*. Proc Natl Acad Sci U S A, 2007. **104**(12): p. 5062-6.
47. Dorling, A., et al., *Detection of primary direct and indirect human anti-porcine T cell responses using a porcine dendritic cell population*. Eur J Immunol, 1996. **26**(6): p. 1378-87.
48. Brouard, S., et al., *T cell response in xenorecognition and xenografts: a review*. Hum Immunol, 1999. **60**(6): p. 455-68.
49. Gill, R.G. and L. Wolf, *Immunobiology of cellular transplantation*. Cell Transplant, 1995. **4**(4): p. 361-70.
50. Yamada, K., D.H. Sachs, and H. DerSimonian, *Human anti-porcine xenogeneic T cell response. Evidence for allelic specificity of mixed leukocyte reaction and for both direct and indirect pathways of recognition*. J Immunol, 1995. **155**(11): p. 5249-56.
51. Choo, J.K., et al., *Species differences in the expression of major histocompatibility complex class II antigens on coronary artery endothelium: implications for cell-mediated xenoreactivity*. Transplantation, 1997. **64**(9): p. 1315-22.
52. Mirzaie, M., et al., *Expression of porcine major histocompatibility antigens in cardiac tissue*. Apmis, 1998. **106**(10): p. 935-40.
53. Davis, T.A., et al., *Primary porcine endothelial cells express membrane-bound B7-2 (CD86) and a soluble factor that co-stimulate cyclosporin A-resistant and CD28-dependent human T cell proliferation*. Int Immunol, 1996. **8**(7): p. 1099-111.
54. Rogers, N.J., et al., *Cross-species costimulation: relative contributions of CD80, CD86, and CD40*. Transplantation, 2003. **75**(12): p. 2068-76.
55. Aderem, A. and D.M. Underhill, *Mechanisms of phagocytosis in macrophages*. Annu Rev Immunol, 1999. **17**: p. 593-623.
56. Ide, K., et al., *Antibody- and complement-independent phagocytotic and cytolytic activities of human macrophages toward porcine cells*. Xenotransplantation, 2005. **12**(3): p. 181-8.
57. Yi, S., et al., *CD4+ T cells initiate pancreatic islet xenograft rejection via an interferon-gamma-dependent recruitment of macrophages and natural killer cells*. Transplantation, 2002. **73**(3): p. 437-46.
58. Jin, R., et al., *Human monocytes recognize porcine endothelium via the interaction of galectin 3 and alpha-GAL*. J Immunol, 2006. **177**(2): p. 1289-95.
59. Schneider, M.K. and J.D. Seebach, *Current cellular innate immune hurdles in pig-to-primate xenotransplantation*. Curr Opin Organ Transplant, 2008. **13**(2): p. 171-7.
60. Cosman, D., et al., *ULBPs, novel MHC class I-related molecules, bind to CMV glycoprotein UL16 and stimulate NK cytotoxicity through the NKG2D receptor*. Immunity, 2001. **14**(2): p. 123-33.
61. Lilienfeld, B.G., et al., *Porcine UL16-binding protein 1 expressed on the surface of endothelial cells triggers human NK cytotoxicity through NKG2D*. J Immunol, 2006. **177**(4): p. 2146-52.
62. Taniguchi, S., et al., *In vivo immunoadsorption of antipig antibodies in baboons using a specific Gal(alpha)1-3Gal column*. Transplantation, 1996. **62**(10): p. 1379-84.
63. Costa, C., et al., *Expression of the human alpha1,2-fucosyltransferase in transgenic pigs modifies the cell surface carbohydrate phenotype and confers resistance to human serum-mediated cytolysis*. Faseb j, 1999. **13**(13): p. 1762-73.
64. Sharma, A., et al., *Reduction in the level of Gal(alpha1,3)Gal in transgenic mice and pigs by the expression of an alpha(1,2)fucosyltransferase*. Proc Natl Acad Sci U S A, 1996. **93**(14): p. 7190-5.
65. Dai, Y., et al., *Targeted disruption of the alpha1,3-galactosyltransferase gene in cloned pigs*. Nat Biotechnol, 2002. **20**(3): p. 251-5.
66. Lai, L., et al., *Production of alpha-1,3-galactosyltransferase knockout pigs by nuclear transfer cloning*. Science, 2002. **295**(5557): p. 1089-92.

67. Phelps, C.J., et al., *Production of alpha 1,3-galactosyltransferase-deficient pigs*. Science, 2003. **299**(5605): p. 411-4.
68. Fischer, K., et al., *Efficient production of multi-modified pigs for xenotransplantation by 'combineering', gene stacking and gene editing*. Sci Rep, 2016. **6**: p. 29081.
69. Petersen, B., et al., *Efficient production of biallelic GGTA1 knockout pigs by cytoplasmic microinjection of CRISPR/Cas9 into zygotes*. Xenotransplantation, 2016. **23**(5): p. 338-46.
70. Kuwaki, K., et al., *Heart transplantation in baboons using alpha1,3-galactosyltransferase gene-knockout pigs as donors: initial experience*. Nat Med, 2005. **11**(1): p. 29-31.
71. Yamada, K., et al., *Marked prolongation of porcine renal xenograft survival in baboons through the use of alpha1,3-galactosyltransferase gene-knockout donors and the cotransplantation of vascularized thymic tissue*. Nat Med, 2005. **11**(1): p. 32-4.
72. Chen, G., et al., *Acute rejection is associated with antibodies to non-Gal antigens in baboons using Gal-knockout pig kidneys*. Nat Med, 2005. **11**(12): p. 1295-8.
73. Lutz, A.J., et al., *Double knockout pigs deficient in N-glycolylneuraminic acid and galactose alpha-1,3-galactose reduce the humoral barrier to xenotransplantation*. Xenotransplantation, 2013. **20**(1): p. 27-35.
74. Grey, H.M., et al., *THE SMALL SUBUNIT OF HL-A ANTIGENS IS β 2-MICROGLOBULIN*. J Exp Med, 1973. **138**(6): p. 1608-12.
75. Rammensee, H.G., K. Falk, and O. Rotzschke, *Peptides naturally presented by MHC class I molecules*. Annu Rev Immunol, 1993. **11**: p. 213-44.
76. Zhang, Y. and D.B. Williams, *Assembly of MHC class I molecules within the endoplasmic reticulum*. Immunol Res, 2006. **35**(1-2): p. 151-62.
77. Ho, C.S., et al., *Nomenclature for factors of the SLA system, update 2008*. Tissue Antigens, 2009. **73**(4): p. 307-15.
78. Salter, R.D., *Mutant HLA-A201 heavy chains with lowered affinity for β 2m are transported after growth at reduced temperatures*. Human Immunology, 1992. **35**(1): p. 40-49.
79. Zhang, Q., M. Tector, and R.D. Salter, *Calnexin recognizes carbohydrate and protein determinants of class I major histocompatibility complex molecules*. J Biol Chem, 1995. **270**(8): p. 3944-8.
80. Wang, Y., et al., *Efficient generation of B2m-null pigs via injection of zygote with TALENs*. Scientific Reports, 2016. **6**: p. 38854.
81. Reyes, L.M., et al., *Creating class I MHC-null pigs using guide RNA and the Cas9 endonuclease*. J Immunol, 2014. **193**(11): p. 5751-7.
82. Sarma, J.V. and P.A. Ward, *The complement system*. Cell Tissue Res, 2011. **343**(1): p. 227-35.
83. Seya, T., J.R. Turner, and J.P. Atkinson, *Purification and characterization of a membrane protein (gp45-70) that is a cofactor for cleavage of C3b and C4b*. J Exp Med, 1986. **163**(4): p. 837-55.
84. Medof, M.E., T. Kinoshita, and V. Nussenzweig, *Inhibition of complement activation on the surface of cells after incorporation of decay-accelerating factor (DAF) into their membranes*. J Exp Med, 1984. **160**(5): p. 1558-78.
85. Meri, S., et al., *Human protectin (CD59), an 18,000-20,000 MW complement lysis restricting factor, inhibits C5b-8 catalysed insertion of C9 into lipid bilayers*. Immunology, 1990. **71**(1): p. 1-9.
86. Morgan, B.P., C.W. Berg, and C.L. Harris, *"Homologous restriction" in complement lysis: roles of membrane complement regulators*. Xenotransplantation, 2005. **12**(4): p. 258-65.
87. Rollins, S.A. and P.J. Sims, *The complement-inhibitory activity of CD59 resides in its capacity to block incorporation of C9 into membrane C5b-9*. J Immunol, 1990. **144**(9): p. 3478-83.
88. Liu, D., et al., *Relation between human decay-accelerating factor (hDAF) expression in pig cells and inhibition of human serum anti-pig cytotoxicity: value of highly expressed hDAF for xenotransplantation*. Xenotransplantation, 2007. **14**(1): p. 67-73.

89. Diamond, L.E., et al., *A human CD46 transgenic pig model system for the study of discordant xenotransplantation*. *Transplantation*, 2001. **71**(1): p. 132-42.
90. Langford, G.A., et al., *Production of pigs transgenic for human decay accelerating factor*. *Transplant Proc*, 1994. **26**(3): p. 1400-1.
91. Niemann, H., et al., *Cytomegalovirus early promoter induced expression of hCD59 in porcine organs provides protection against hyperacute rejection*. *Transplantation*, 2001. **72**(12): p. 1898-906.
92. Chen, R.H., et al., *Hearts from transgenic pigs constructed with CD59/DAF genomic clones demonstrate improved survival in primates*. *Xenotransplantation*, 1999. **6**(3): p. 194-200.
93. Zhou, C.Y., et al., *Transgenic pigs expressing human CD59, in combination with human membrane cofactor protein and human decay-accelerating factor*. *Xenotransplantation*, 2005. **12**(2): p. 142-8.
94. Bhatti, F.N., et al., *Three-month survival of HDAFF transgenic pig hearts transplanted into primates*. *Transplant Proc*, 1999. **31**(1-2): p. 958.
95. Azimzadeh, A., et al., *EARLY GRAFT FAILURE OF GaITKO PIG ORGANS IN BABOONS IS REDUCED BY EXPRESSION OF A HUMAN COMPLEMENT PATHWAY-REGULATORY PROTEIN*. *Xenotransplantation*, 2015. **22**(4): p. 310-6.
96. Balla, G., et al., *Ferritin: a cytoprotective antioxidant strategem of endothelium*. *J Biol Chem*, 1992. **267**(25): p. 18148-53.
97. Ryter, S.W. and A.M. Choi, *Carbon monoxide: present and future indications for a medical gas*. *Korean J Intern Med*, 2013. **28**(2): p. 123-40.
98. Silva, G., et al., *The antiapoptotic effect of heme oxygenase-1 in endothelial cells involves the degradation of p38 alpha MAPK isoform*. *J Immunol*, 2006. **177**(3): p. 1894-903.
99. Rosenberg, R.B., C.W. Broner, and M.S. O'Dorisio, *Modulation of cyclic guanosine monophosphate production during Escherichia coli septic shock*. *Biochem Med Metab Biol*, 1994. **51**(2): p. 149-55.
100. Brune, B. and V. Ullrich, *Inhibition of platelet aggregation by carbon monoxide is mediated by activation of guanylate cyclase*. *Mol Pharmacol*, 1987. **32**(4): p. 497-504.
101. Kawamura, K., et al., *Bilirubin from heme oxygenase-1 attenuates vascular endothelial activation and dysfunction*. *Arterioscler Thromb Vasc Biol*, 2005. **25**(1): p. 155-60.
102. Keshavan, P., et al., *Unconjugated bilirubin inhibits VCAM-1-mediated transendothelial leukocyte migration*. *J Immunol*, 2005. **174**(6): p. 3709-18.
103. Yeom, H.J., et al., *Generation and characterization of human heme oxygenase-1 transgenic pigs*. *PLoS One*, 2012. **7**(10): p. e46646.
104. Petersen, B., et al., *Transgenic expression of human heme oxygenase-1 in pigs confers resistance against xenograft rejection during ex vivo perfusion of porcine kidneys*. *Xenotransplantation*, 2011. **18**(6): p. 355-68.
105. Babusikova, E., et al., *Exhaled carbon monoxide as a new marker of respiratory diseases in children*. *J Physiol Pharmacol*, 2008. **59 Suppl 6**: p. 9-17.
106. Song, H.Y., M. Rothe, and D.V. Goeddel, *The tumor necrosis factor-inducible zinc finger protein A20 interacts with TRAF1/TRAF2 and inhibits NF-kappaB activation*. *Proc Natl Acad Sci U S A*, 1996. **93**(13): p. 6721-5.
107. Dixit, V. and T.W. Mak, *NF-kappaB signaling. Many roads lead to madrid*. *Cell*, 2002. **111**(5): p. 615-9.
108. Oropeza, M., et al., *Transgenic expression of the human A20 gene in cloned pigs provides protection against apoptotic and inflammatory stimuli*. *Xenotransplantation*, 2009. **16**(6): p. 522-34.
109. Ahrens, H.E., et al., *Kidneys From alpha1,3-Galactosyltransferase Knockout/Human Heme Oxygenase-1/Human A20 Transgenic Pigs Are Protected From Rejection During Ex Vivo Perfusion With Human Blood*. *Transplant Direct*, 2015. **1**(6): p. e23.
110. Cowan, P.J., et al., *Renal xenografts from triple-transgenic pigs are not hyperacutely rejected but cause coagulopathy in non-immunosuppressed baboons*. *Transplantation*, 2000. **69**(12): p. 2504-15.

111. Shimizu, A., et al., *Thrombotic microangiopathy associated with humoral rejection of cardiac xenografts from alpha1,3-galactosyltransferase gene-knockout pigs in baboons*. Am J Pathol, 2008. **172**(6): p. 1471-81.
112. Houser, S.L., et al., *Thrombotic microangiopathy and graft arteriopathy in pig hearts following transplantation into baboons*. Xenotransplantation, 2004. **11**(5): p. 416-25.
113. Shimizu, A., et al., *Thrombotic microangiopathic glomerulopathy in human decay accelerating factor-transgenic swine-to-baboon kidney xenografts*. J Am Soc Nephrol, 2005. **16**(9): p. 2732-45.
114. Maruyama, I., C.E. Bell, and P.W. Majerus, *Thrombomodulin is found on endothelium of arteries, veins, capillaries, and lymphatics, and on syncytiotrophoblast of human placenta*. J Cell Biol, 1985. **101**(2): p. 363-71.
115. Esmon, C.T., N.L. Esmon, and K.W. Harris, *Complex formation between thrombin and thrombomodulin inhibits both thrombin-catalyzed fibrin formation and factor V activation*. J Biol Chem, 1982. **257**(14): p. 7944-7.
116. Esmon, C.T., *The regulation of natural anticoagulant pathways*. Science, 1987. **235**(4794): p. 1348-52.
117. Fulcher, C.A., et al., *Proteolytic inactivation of human factor VIII procoagulant protein by activated human protein C and its analogy with factor V*. Blood, 1984. **63**(2): p. 486-9.
118. Suzuki, K., et al., *Inactivation of human coagulation factor V by activated protein C*. J Biol Chem, 1983. **258**(3): p. 1914-20.
119. Van de Wouwer, M., et al., *The lectin-like domain of thrombomodulin interferes with complement activation and protects against arthritis*. J Thromb Haemost, 2006. **4**(8): p. 1813-24.
120. Conway, E.M., et al., *The lectin-like domain of thrombomodulin confers protection from neutrophil-mediated tissue damage by suppressing adhesion molecule expression via nuclear factor kappaB and mitogen-activated protein kinase pathways*. J Exp Med, 2002. **196**(5): p. 565-77.
121. Ito, T., et al., *Proteolytic cleavage of high mobility group box 1 protein by thrombin-thrombomodulin complexes*. Arterioscler Thromb Vasc Biol, 2008. **28**(10): p. 1825-30.
122. Campbell, W.D., et al., *Inactivation of C3a and C5a octapeptides by carboxypeptidase R and carboxypeptidase N*. Microbiol Immunol, 2002. **46**(2): p. 131-4.
123. Foley, J.H. and E.M. Conway, *Cross Talk Pathways Between Coagulation and Inflammation*. Circ Res, 2016. **118**(9): p. 1392-408.
124. Roussel, J.C., et al., *Pig thrombomodulin binds human thrombin but is a poor cofactor for activation of human protein C and TAFI*. Am J Transplant, 2008. **8**(6): p. 1101-12.
125. Petersen, B., et al., *Pigs transgenic for human thrombomodulin have elevated production of activated protein C*. Xenotransplantation, 2009. **16**(6): p. 486-95.
126. Wuensch, A., et al., *Regulatory sequences of the porcine THBD gene facilitate endothelial-specific expression of bioactive human thrombomodulin in single- and multitransgenic pigs*. Transplantation, 2014. **97**(2): p. 138-47.
127. Mohiuddin, M.M., et al., *Chimeric 2C10R4 anti-CD40 antibody therapy is critical for long-term survival of GTKO.hCD46.hTBM pig-to-primate cardiac xenograft*. Nat Commun, 2016. **7**: p. 11138.
128. Langin, M., et al., *Consistent success in life-supporting porcine cardiac xenotransplantation*. Nature, 2018.
129. Taylor, F.B., Jr., et al., *Endothelial cell protein C receptor plays an important role in protein C activation in vivo*. Blood, 2001. **97**(6): p. 1685-8.
130. Stearns-Kurosawa, D.J., et al., *The endothelial cell protein C receptor augments protein C activation by the thrombin-thrombomodulin complex*. Proc Natl Acad Sci U S A, 1996. **93**(19): p. 10212-6.
131. Fukudome, K. and C.T. Esmon, *Identification, cloning, and regulation of a novel endothelial cell protein C/activated protein C receptor*. J Biol Chem, 1994. **269**(42): p. 26486-91.
132. Riewald, M., et al., *Activation of endothelial cell protease activated receptor 1 by the protein C pathway*. Science, 2002. **296**(5574): p. 1880-2.

133. Cheng, T., et al., *Activated protein C blocks p53-mediated apoptosis in ischemic human brain endothelium and is neuroprotective*. Nat Med, 2003. **9**(3): p. 338-42.
134. Kondreddy, V., et al., *Factor VIIa induces anti-inflammatory signaling via EPCR and PAR1*. Blood, 2018. **131**(21): p. 2379-2392.
135. Laszik, Z., et al., *Human protein C receptor is present primarily on endothelium of large blood vessels: implications for the control of the protein C pathway*. Circulation, 1997. **96**(10): p. 3633-40.
136. Li, W., et al., *Overexpressing endothelial cell protein C receptor alters the hemostatic balance and protects mice from endotoxin*. J Thromb Haemost, 2005. **3**(7): p. 1351-9.
137. Lee, K.F., et al., *Protective effects of transgenic human endothelial protein C receptor expression in murine models of transplantation*. Am J Transplant, 2012. **12**(9): p. 2363-72.
138. L. Burdorf, E.R., 1 T. Zhang,1 A. Riner,1 G. Braileanu,1 X. Cheng,1 C. Phelps,2 D. Ayares,2 A.M. Azimzadeh,1 R.N. Pierson III, *Human EPCR expression in GalTKO.hCD46 lungs extends survival time and lowers PVR in a xenogenic lung model*. J Heart Lung Transplant, 2013. **32**: p. S137.
139. Reith, W., S. LeibundGut-Landmann, and J.M. Waldburger, *Regulation of MHC class II gene expression by the class II transactivator*. Nat Rev Immunol, 2005. **5**(10): p. 793-806.
140. Reith, W. and B. Mach, *The bare lymphocyte syndrome and the regulation of MHC expression*. Annu Rev Immunol, 2001. **19**: p. 331-73.
141. Hara, H., et al., *Human dominant-negative class II transactivator transgenic pigs - effect on the human anti-pig T-cell immune response and immune status*. Immunology, 2013. **140**(1): p. 39-46.
142. Linsley, P.S., et al., *CTLA-4 is a second receptor for the B cell activation antigen B7*. J Exp Med, 1991. **174**(3): p. 561-9.
143. Linsley, P.S., et al., *Human B7-1 (CD80) and B7-2 (CD86) bind with similar avidities but distinct kinetics to CD28 and CTLA-4 receptors*. Immunity, 1994. **1**(9): p. 793-801.
144. Lenschow, D.J., et al., *Long-term survival of xenogeneic pancreatic islet grafts induced by CTLA4Ig*. Science, 1992. **257**(5071): p. 789-92.
145. Phelps, C.J., et al., *Production and characterization of transgenic pigs expressing porcine CTLA4-Ig*. Xenotransplantation, 2009. **16**(6): p. 477-85.
146. Larsen, C.P., et al., *Rational development of LEA29Y (belatacept), a high-affinity variant of CTLA4-Ig with potent immunosuppressive properties*. Am J Transplant, 2005. **5**(3): p. 443-53.
147. Klymiuk, N., et al., *Xenografted islet cell clusters from INSLEA29Y transgenic pigs rescue diabetes and prevent immune rejection in humanized mice*. Diabetes, 2012. **61**(6): p. 1527-32.
148. Keir, M.E., et al., *Tissue expression of PD-L1 mediates peripheral T cell tolerance*. J Exp Med, 2006. **203**(4): p. 883-95.
149. Latchman, Y.E., et al., *PD-L1-deficient mice show that PD-L1 on T cells, antigen-presenting cells, and host tissues negatively regulates T cells*. Proc Natl Acad Sci U S A, 2004. **101**(29): p. 10691-6.
150. Sharpe, A.H., et al., *The function of programmed cell death 1 and its ligands in regulating autoimmunity and infection*. Nat Immunol, 2007. **8**(3): p. 239-45.
151. Ma, D., et al., *PD-L1 Deficiency within Islets Reduces Allograft Survival in Mice*. PLoS One, 2016. **11**(3).
152. Plege, A., et al., *Suppression of human T-cell activation and expansion of regulatory T cells by pig cells overexpressing PD-ligands*. Transplantation, 2009. **87**(7): p. 975-82.
153. Buermann, A., et al., *Inhibition of B-cell activation and antibody production by triggering inhibitory signals via the PD-1/PD-ligand pathway*. Xenotransplantation, 2016. **23**(5): p. 347-56.
154. Buermann, A., et al., *Pigs expressing the human inhibitory ligand PD-L1 (CD 274) provide a new source of xenogeneic cells and tissues with low immunogenic properties*. Xenotransplantation, 2018.

155. Seiffert, M., et al., *Human signal-regulatory protein is expressed on normal, but not on subsets of leukemic myeloid cells and mediates cellular adhesion involving its counterreceptor CD47*. Blood, 1999. **94**(11): p. 3633-43.
156. Vernon-Wilson, E.F., et al., *CD47 is a ligand for rat macrophage membrane signal regulatory protein SIRP (OX41) and human SIRPalpha 1*. Eur J Immunol, 2000. **30**(8): p. 2130-7.
157. Oldenborg, P.A., et al., *Role of CD47 as a marker of self on red blood cells*. Science, 2000. **288**(5473): p. 2051-4.
158. Raulet, D.H., R.E. Vance, and C.W. McMahon, *Regulation of the natural killer cell receptor repertoire*. Annu Rev Immunol, 2001. **19**: p. 291-330.
159. Sullivan, J.A., et al., *Analysis of polymorphism in porcine MHC class I genes: alterations in signals recognized by human cytotoxic lymphocytes*. J Immunol, 1997. **159**(5): p. 2318-26.
160. Lilienfeld, B.G., et al., *Transgenic expression of HLA-E single chain trimer protects porcine endothelial cells against human natural killer cell-mediated cytotoxicity*. Xenotransplantation, 2007. **14**(2): p. 126-34.
161. Cozzi, E., et al., *Characterization of pigs transgenic for human decay-accelerating factor*. Transplantation, 1997. **64**(10): p. 1383-92.
162. Lin, S.S., et al., *The role of anti-Galalpha1-3Gal antibodies in acute vascular rejection and accommodation of xenografts*. Transplantation, 2000. **70**(12): p. 1667-74.
163. Gordon, J.W., et al., *Genetic transformation of mouse embryos by microinjection of purified DNA*. Proc Natl Acad Sci U S A, 1980. **77**(12): p. 7380-4.
164. Hammer, R.E., et al., *Production of transgenic rabbits, sheep and pigs by microinjection*. Nature, 1985. **315**(6021): p. 680-3.
165. Uchida, M., et al., *Production of transgenic miniature pigs by pronuclear microinjection*. Transgenic Res, 2001. **10**(6): p. 577-82.
166. Wall, R.J., *Transgenic livestock: Progress and prospects for the future*. Theriogenology, 1996. **45**(1): p. 57-68.
167. Kikuchi, K., et al., *Morphological features of lipid droplet transition during porcine oocyte fertilisation and early embryonic development to blastocyst in vivo and in vitro*. Zygote, 2002. **10**(4): p. 355-66.
168. Schwartzberg, P.L., S.P. Goff, and E.J. Robertson, *Germ-line transmission of a c-abl mutation produced by targeted gene disruption in ES cells*. Science, 1989. **246**(4931): p. 799-803.
169. Willadsen, S.M., *Nuclear transplantation in sheep embryos*. Nature, 1986. **320**(6057): p. 63-5.
170. Campbell, K.H., et al., *Sheep cloned by nuclear transfer from a cultured cell line*. Nature, 1996. **380**(6569): p. 64-6.
171. Wilmut, I., et al., *Viable offspring derived from fetal and adult mammalian cells*. Nature, 1997. **385**(6619): p. 810-3.
172. Schnieke, A.E., et al., *Human factor IX transgenic sheep produced by transfer of nuclei from transfected fetal fibroblasts*. Science, 1997. **278**(5346): p. 2130-3.
173. McCreath, K.J., et al., *Production of gene-targeted sheep by nuclear transfer from cultured somatic cells*. Nature, 2000. **405**(6790): p. 1066-9.
174. Onishi, A., et al., *Pig cloning by microinjection of fetal fibroblast nuclei*. Science, 2000. **289**(5482): p. 1188-90.
175. Betthausen, J., et al., *Production of cloned pigs from in vitro systems*. Nat Biotechnol, 2000. **18**(10): p. 1055-9.
176. Wolf, E., et al., *Transgenic technology in farm animals--progress and perspectives*. Exp Physiol, 2000. **85**(6): p. 615-25.
177. Kurome, M., et al., *Factors influencing the efficiency of generating genetically engineered pigs by nuclear transfer: multi-factorial analysis of a large data set*. BMC Biotechnology, 2013. **13**(1): p. 43.
178. Solter, D., *Mammalian cloning: advances and limitations*. Nature Reviews Genetics, 2000. **1**: p. 199.

179. Wilson, C., H.J. Bellen, and W.J. Gehring, *Position effects on eukaryotic gene expression*. *Annu Rev Cell Biol*, 1990. **6**: p. 679-714.
180. Clark, A.J., et al., *Chromosomal position effects and the modulation of transgene expression*. *Reprod Fertil Dev*, 1994. **6**(5): p. 589-98.
181. Deng, W., et al., *Use of the 2A peptide for generation of multi-transgenic pigs through a single round of nuclear transfer*. *PLoS One*, 2011. **6**(5): p. e19986.
182. Park, S.J., et al., *Production and characterization of soluble human TNFRI-Fc and human HO-1(HMOX1) transgenic pigs by using the F2A peptide*. *Transgenic Res*, 2014. **23**(3): p. 407-19.
183. Fisicaro, N., et al., *Versatile co-expression of graft-protective proteins using 2A-linked cassettes*. *Xenotransplantation*, 2011. **18**(2): p. 121-30.
184. Kwon, D.J., et al., *Generation of alpha-1,3-galactosyltransferase knocked-out transgenic cloned pigs with knocked-in five human genes*. *Transgenic Res*, 2017. **26**(1): p. 153-163.
185. Jeong, Y.H., et al., *Production of multiple transgenic Yucatan miniature pigs expressing human complement regulatory factors, human CD55, CD59, and H-transferase genes*. *PLoS One*, 2013. **8**(5): p. e63241.
186. Mizuguchi, H., et al., *IRES-dependent second gene expression is significantly lower than cap-dependent first gene expression in a bicistronic vector*. *Mol Ther*, 2000. **1**(4): p. 376-82.
187. Hurh, S., et al., *Expression analysis of combinatorial genes using a bi-cistronic T2A expression system in porcine fibroblasts*. *PLoS One*, 2013. **8**(7): p. e70486.
188. Russell, J.P., et al., *Phage Bxb1 integrase mediates highly efficient site-specific recombination in mammalian cells*. *Biotechniques*, 2006. **40**(4): p. 460, 462, 464.
189. Denning, C., et al., *Gene targeting in primary fetal fibroblasts from sheep and pig*. *Cloning Stem Cells*, 2001. **3**(4): p. 221-31.
190. Jin, D.I., et al., *Targeting efficiency of a-1,3-galactosyl transferase gene in pig fetal fibroblast cells*. *Exp Mol Med*, 2003. **35**(6): p. 572-7.
191. Lin, F.L., K. Sperle, and N. Sternberg, *Model for homologous recombination during transfer of DNA into mouse L cells: role for DNA ends in the recombination process*. *Mol Cell Biol*, 1984. **4**(6): p. 1020-34.
192. Thomas, K.R. and M.R. Capecchi, *Site-directed mutagenesis by gene targeting in mouse embryo-derived stem cells*. *Cell*, 1987. **51**(3): p. 503-12.
193. Sedivy, J.M. and P.A. Sharp, *Positive genetic selection for gene disruption in mammalian cells by homologous recombination*. *Proc Natl Acad Sci U S A*, 1989. **86**(1): p. 227-31.
194. Friedel, R.H., et al., *Gene targeting using a promoterless gene trap vector ("targeted trapping") is an efficient method to mutate a large fraction of genes*. *Proc Natl Acad Sci U S A*, 2005. **102**(37): p. 13188-93.
195. Bibikova, M., et al., *Enhancing gene targeting with designed zinc finger nucleases*. *Science*, 2003. **300**(5620): p. 764.
196. Ruan, J., et al., *Highly efficient CRISPR/Cas9-mediated transgene knockin at the H11 locus in pigs*. *Sci Rep*, 2015. **5**: p. 14253.
197. Zaboikin, M., et al., *Non-Homologous End Joining and Homology Directed DNA Repair Frequency of Double-Stranded Breaks Introduced by Genome Editing Reagents*. *PLoS One*, 2017. **12**(1): p. e0169931.
198. Sander, J.D. and J.K. Joung, *CRISPR-Cas systems for editing, regulating and targeting genomes*. *Nature Biotechnology*, 2014. **32**: p. 347.
199. Carroll, D., *Genome Engineering With Zinc-Finger Nucleases*. *Genetics*, 2011. **188**(4): p. 773-82.
200. Miller, J.C., et al., *A TALE nuclease architecture for efficient genome editing*. *Nature Biotechnology*, 2010. **29**: p. 143.
201. Wiedenheft, B., S.H. Sternberg, and J.A. Doudna, *RNA-guided genetic silencing systems in bacteria and archaea*. *Nature*, 2012. **482**: p. 331.

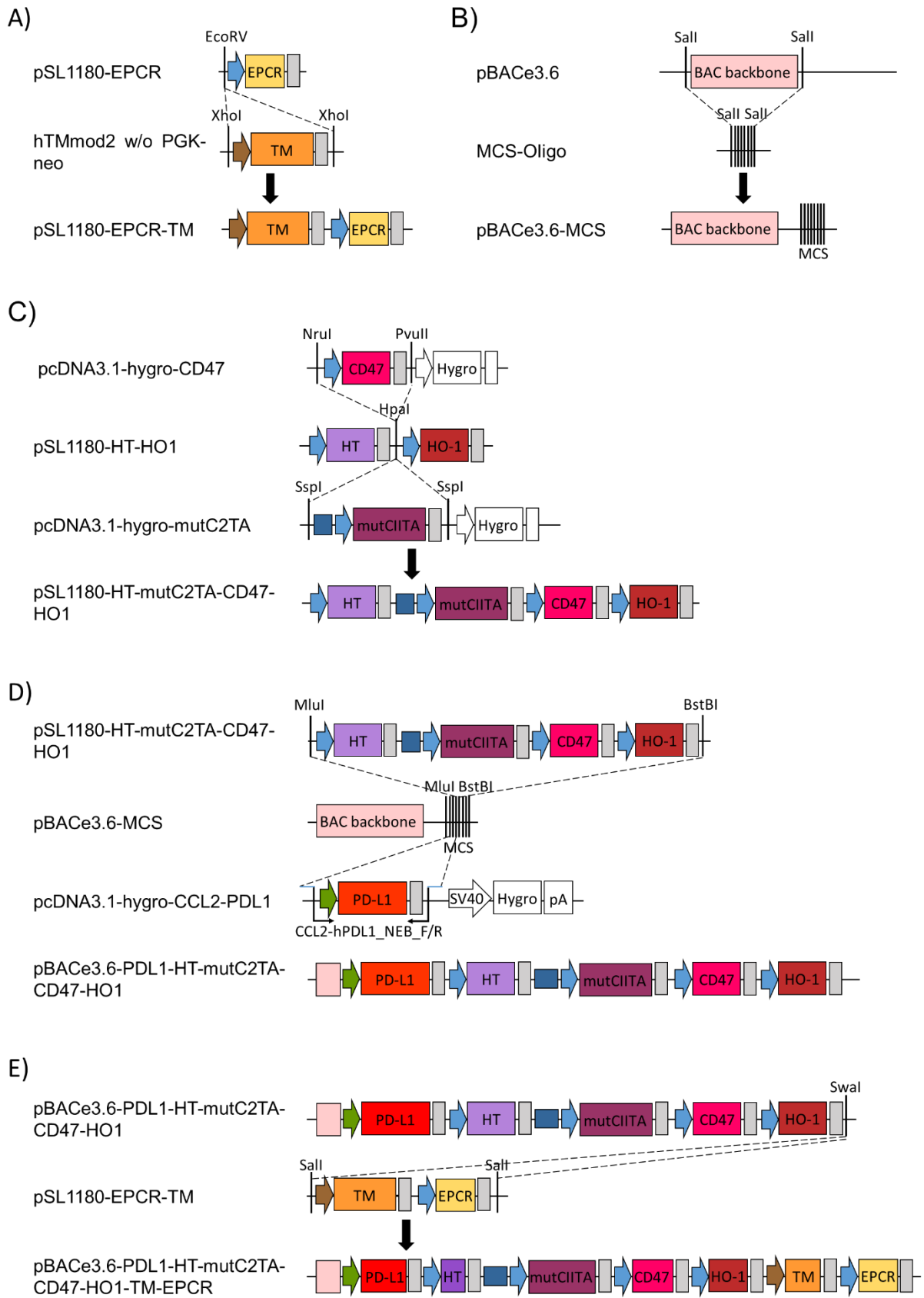
202. Bhaya, D., M. Davison, and R. Barrangou, *CRISPR-Cas systems in bacteria and archaea: versatile small RNAs for adaptive defense and regulation*. *Annu Rev Genet*, 2011. **45**: p. 273-97.
203. Jinek, M., et al., *A programmable dual-RNA-guided DNA endonuclease in adaptive bacterial immunity*. *Science*, 2012. **337**(6096): p. 816-21.
204. DiCarlo, J.E., et al., *Genome engineering in *Saccharomyces cerevisiae* using CRISPR-Cas systems*. *Nucleic Acids Res*, 2013. **41**(7): p. 4336-43.
205. Yu, Z., et al., *Highly efficient genome modifications mediated by CRISPR/Cas9 in *Drosophila**. *Genetics*, 2013. **195**(1): p. 289-91.
206. Hwang, W.Y., et al., *Efficient genome editing in zebrafish using a CRISPR-Cas system*. *Nat Biotechnol*, 2013. **31**(3): p. 227-9.
207. Cong, L., et al., *Multiplex genome engineering using CRISPR/Cas systems*. *Science*, 2013. **339**(6121): p. 819-23.
208. Mali, P., et al., *RNA-guided human genome engineering via Cas9*. *Science*, 2013. **339**(6121): p. 823-6.
209. Redman, M., et al., *What is CRISPR/Cas9?* *Archives of disease in childhood - Education & practice edition*, 2016. **101**(4): p. 213.
210. Grindley, N.D.F., K.L. Whiteson, and P.A. Rice, *Mechanisms of Site-Specific Recombination*. *Annual Review of Biochemistry*, 2006. **75**(1): p. 567-605.
211. Grainge, I. and M. Jayaram, *The integrase family of recombinase: organization and function of the active site*. *Mol Microbiol*, 1999. **33**(3): p. 449-56.
212. Smith, M.C. and H.M. Thorpe, *Diversity in the serine recombinases*. *Mol Microbiol*, 2002. **44**(2): p. 299-307.
213. Sauer, B., *Site-specific recombination: developments and applications*. *Curr Opin Biotechnol*, 1994. **5**(5): p. 521-7.
214. Mulholland, C.B., et al., *A modular open platform for systematic functional studies under physiological conditions*. *Nucleic Acids Res*, 2015. **43**(17): p. e112.
215. Thorpe, H.M. and M.C. Smith, *In vitro site-specific integration of bacteriophage DNA catalyzed by a recombinase of the resolvase/invertase family*. *Proc Natl Acad Sci U S A*, 1998. **95**(10): p. 5505-10.
216. Kim, A.I., et al., *Mycobacteriophage Bxb1 integrates into the *Mycobacterium smegmatis* groEL1 gene*. *Mol Microbiol*, 2003. **50**(2): p. 463-73.
217. Groth, A.C., et al., *A phage integrase directs efficient site-specific integration in human cells*. *Proc Natl Acad Sci U S A*, 2000. **97**(11): p. 5995-6000.
218. Thyagarajan, B., et al., *Site-Specific Genomic Integration in Mammalian Cells Mediated by Phage ϕ C31 Integrase*. *Mol Cell Biol*, 2001. **21**(12): p. 3926-34.
219. Thorpe, H.M., S.E. Wilson, and M.C. Smith, *Control of directionality in the site-specific recombination system of the *Streptomyces* phage ϕ C31*. *Mol Microbiol*, 2000. **38**(2): p. 232-41.
220. Smith, M.C.A., R. Till, and K. Brady, *Synapsis and DNA cleavage in ϕ C31 integrase-mediated site-specific recombination*. 2004. **32**(8): p. 2607-17.
221. Inniss, M.C., et al., *A novel Bxb1 integrase RMCE system for high fidelity site-specific integration of mAb expression cassette in CHO Cells*. *Biotechnol Bioeng*, 2017. **114**(8): p. 1837-1846.
222. Xu, Z., et al., *Accuracy and efficiency define Bxb1 integrase as the best of fifteen candidate serine recombinases for the integration of DNA into the human genome*. *BMC Biotechnol*, 2013. **13**: p. 87.
223. Fish, M.P., et al., *Creating transgenic *Drosophila* by microinjecting the site-specific ϕ C31 integrase mRNA and a transgene-containing donor plasmid*. *Nat Protoc*, 2007. **2**(10): p. 2325-31.
224. Callesen, H., et al., *Increasing efficiency in production of cloned piglets*. *Cell Reprogram*, 2014. **16**(6): p. 407-10.
225. Sanchez-Rivera, F.J., et al., *Rapid modelling of cooperating genetic events in cancer through somatic genome editing*. *Nature*, 2014. **516**(7531): p. 428-31.
226. Cheng, R., et al., *Efficient gene editing in adult mouse livers via adenoviral delivery of CRISPR/Cas9*. *FEBS Lett*, 2014. **588**(21): p. 3954-8.

227. Xie, C., et al., *Genome editing with CRISPR/Cas9 in postnatal mice corrects PRKAG2 cardiac syndrome*. *Cell Res*, 2016. **26**(10): p. 1099-1111.
228. Wu, Z., H. Yang, and P. Colosi, *Effect of genome size on AAV vector packaging*. *Mol Ther*, 2010. **18**(1): p. 80-6.
229. Kumar, M., et al., *Systematic determination of the packaging limit of lentiviral vectors*. *Hum Gene Ther*, 2001. **12**(15): p. 1893-905.
230. Truong, D.J., et al., *Development of an intein-mediated split-Cas9 system for gene therapy*. *Nucleic Acids Res*, 2015. **43**(13): p. 6450-8.
231. Platt, R.J., et al., *CRISPR-Cas9 knockin mice for genome editing and cancer modeling*. *Cell*, 2014. **159**(2): p. 440-55.
232. Friedrich, G. and P. Soriano, *Promoter traps in embryonic stem cells: a genetic screen to identify and mutate developmental genes in mice*. *Genes Dev*, 1991. **5**(9): p. 1513-23.
233. Zambrowicz, B.P., et al., *Disruption of overlapping transcripts in the ROSA beta geo 26 gene trap strain leads to widespread expression of beta-galactosidase in mouse embryos and hematopoietic cells*. *Proc Natl Acad Sci U S A*, 1997. **94**(8): p. 3789-94.
234. Soriano, P., *Generalized lacZ expression with the ROSA26 Cre reporter strain*. *Nat Genet*, 1999. **21**(1): p. 70-1.
235. Snippert, H.J., et al., *Intestinal crypt homeostasis results from neutral competition between symmetrically dividing Lgr5 stem cells*. *Cell*, 2010. **143**(1): p. 134-44.
236. Irion, S., et al., *Identification and targeting of the ROSA26 locus in human embryonic stem cells*. *Nat Biotechnol*, 2007. **25**(12): p. 1477-82.
237. Kobayashi, T., et al., *Identification of Rat Rosa26 Locus Enables Generation of Knock-In Rat Lines Ubiquitously Expressing tdTomato*. *Stem Cells Dev*, 2012. **21**(16): p. 2981-6.
238. Li, S., et al., *Dual fluorescent reporter pig for Cre recombination: transgene placement at the ROSA26 locus*. *PLoS One*, 2014. **9**(7): p. e102455.
239. Addgene.
240. Brinkman, E.K., et al., *Easy quantitative assessment of genome editing by sequence trace decomposition*. *Nucleic Acids Res*, 2014. **42**(22): p. e168.
241. Fischer, K.J., *Multi-transgenic pigs for xenotransplantation*. 2016, Technische Universität München: München.
242. Rieblinger, B., et al., *Strong xenoprotective function by single-copy transgenes placed sequentially at a permissive locus*. *Xenotransplantation*, 2018. **25**(2): p. e12382.
243. Fu, Y., et al., *Improving CRISPR-Cas nuclease specificity using truncated guide RNAs*. *Nat Biotechnol*, 2014. **32**(3): p. 279-284.
244. Cho, S.W., et al., *Analysis of off-target effects of CRISPR/Cas-derived RNA-guided endonucleases and nickases*. *Genome Res*, 2014. **24**(1): p. 132-41.
245. de Sousa, M., et al., *Iron overload in beta 2-microglobulin-deficient mice*. *Immunol Lett*, 1994. **39**(2): p. 105-11.
246. Sadelain, M., E.P. Papapetrou, and F.D. Bushman, *Safe harbours for the integration of new DNA in the human genome*. *Nature Reviews Cancer*, 2011. **12**: p. 51.
247. Madisen, L., et al., *A robust and high-throughput Cre reporting and characterization system for the whole mouse brain*. *Nat Neurosci*, 2010. **13**(1): p. 133-40.
248. Zhen-Wei, X., et al., *Heme oxygenase-1 improves the survival of discordant cardiac xenograft through its anti-inflammatory and anti-apoptotic effects*. *Pediatr Transplant*, 2007. **11**(8): p. 850-9.
249. Cozzi, E., et al., *Long-term survival of nonhuman primates receiving life-supporting transgenic porcine kidney xenografts*. *Transplantation*, 2000. **70**(1): p. 15-21.
250. Vial, C.M., et al., *Life supporting function for over one month of a transgenic porcine heart in a baboon*. *J Heart Lung Transplant*, 2000. **19**(2): p. 224-9.
251. Byrne, G.W., et al., *Transgenic pigs expressing human CD59 and decay-accelerating factor produce an intrinsic barrier to complement-mediated damage*. *Transplantation*, 1997. **63**(1): p. 149-55.
252. Murakami, H., et al., *Transgenic pigs expressing human decay-accelerating factor regulated by porcine MCP gene promoter*. *Mol Reprod Dev*, 2002. **61**(3): p. 302-11.

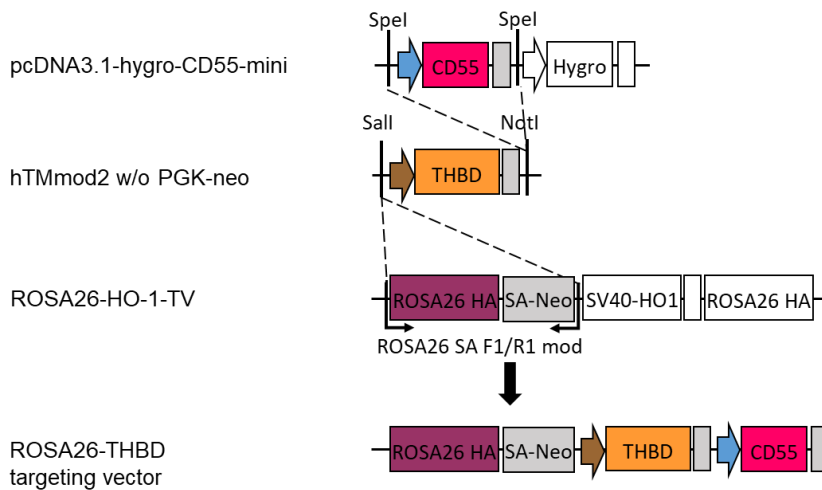
253. Olivares, E.C., et al., *Site-specific genomic integration produces therapeutic Factor IX levels in mice*. Nat Biotechnol, 2002. **20**(11): p. 1124-8.
254. Chalberg, T.W., et al., *phiC31 integrase confers genomic integration and long-term transgene expression in rat retina*. Invest Ophthalmol Vis Sci, 2005. **46**(6): p. 2140-6.
255. Bi, Y., et al., *Pseudo attP sites in favor of transgene integration and expression in cultured porcine cells identified by Streptomyces phage phiC31 integrase*. BMC Mol Biol, 2013. **14**: p. 20.
256. Ma, Q.W., et al., *Identification of pseudo attP sites for phage phiC31 integrase in bovine genome*. Biochem Biophys Res Commun, 2006. **345**(3): p. 984-8.
257. Keravala, A., et al., *A diversity of serine phage integrases mediate site-specific recombination in mammalian cells*. Mol Genet Genomics, 2006. **276**(2): p. 135-46.
258. Niwa, H., K. Yamamura, and J. Miyazaki, *Efficient selection for high-expression transfectants with a novel eukaryotic vector*. Gene, 1991. **108**(2): p. 193-9.
259. Okabe, M., et al., *'Green mice' as a source of ubiquitous green cells*. FEBS Lett, 1997. **407**(3): p. 313-9.
260. Chen, C.M., et al., *A comparison of exogenous promoter activity at the ROSA26 locus using a PhiC31 integrase mediated cassette exchange approach in mouse ES cells*. PLoS One, 2011. **6**(8): p. e23376.
261. Alexopoulou, A.N., J.R. Couchman, and J.R. Whiteford, *The CMV early enhancer/chicken beta actin (CAG) promoter can be used to drive transgene expression during the differentiation of murine embryonic stem cells into vascular progenitors*. BMC Cell Biol, 2008. **9**: p. 2.
262. Hsu, C.C., et al., *Targeted methylation of CMV and E1A viral promoters*. Biochem Biophys Res Commun, 2010. **402**(2): p. 228-34.
263. Yull, F., et al., *Transgene rescue in the mammary gland is associated with transcription but does not require translation of BLG transgenes*. Transgenic Res, 1997. **6**(1): p. 11-7.
264. Singh, A.K., et al., *Cardiac xenografts show reduced survival in the absence of transgenic human thrombomodulin expression in donor pigs*. Xenotransplantation, 2019. **26**(2): p. e12465.
265. Mohiuddin, M.M., et al., *B-cell depletion extends the survival of GTKO.hCD46Tg pig heart xenografts in baboons for up to 8 months*. Am J Transplant, 2012. **12**(3): p. 763-71.
266. Iwase, H., et al., *Regulation of human platelet aggregation by genetically modified pig endothelial cells and thrombin inhibition*. Xenotransplantation, 2014. **21**(1): p. 72-83.
267. Jensen, K.T., et al., *Chromatin accessibility and guide sequence secondary structure affect CRISPR-Cas9 gene editing efficiency*. FEBS Lett, 2017. **591**(13): p. 1892-1901.
268. Liesche, C., et al., *Death receptor-based enrichment of Cas9-expressing cells*. BMC Biotechnol, 2016. **16**: p. 17.
269. Ran, F.A., et al., *Genome engineering using the CRISPR-Cas9 system*. Nat Protoc, 2013. **8**(11): p. 2281-2308.
270. Hauschild, J., et al., *Efficient generation of a biallelic knockout in pigs using zinc-finger nucleases*. Proc Natl Acad Sci U S A, 2011. **108**(29): p. 12013-7.
271. Jiang, W., et al., *RNA-guided editing of bacterial genomes using CRISPR-Cas systems*. Nat Biotechnol, 2013. **31**(3): p. 233-9.
272. Fu, Y., et al., *High-frequency off-target mutagenesis induced by CRISPR-Cas nucleases in human cells*. Nat Biotechnol, 2013. **31**(9): p. 822-6.
273. Hsu, P.D., et al., *DNA targeting specificity of RNA-guided Cas9 nucleases*. Nat Biotechnol, 2013. **31**(9): p. 827-32.
274. Zhang, X.-H., et al., *Off-target Effects in CRISPR/Cas9-mediated Genome Engineering*. Molecular Therapy - Nucleic Acids, 2015. **4**: p. e264.
275. Ran, F.A., et al., *Double nicking by RNA-guided CRISPR Cas9 for enhanced genome editing specificity*. Cell, 2013. **154**(6): p. 1380-9.
276. Mali, P., et al., *CAS9 transcriptional activators for target specificity screening and paired nickases for cooperative genome engineering*. Nat Biotechnol, 2013. **31**(9): p. 833-8.

277. Kwon, D.-N., et al., *Production of biallelic CMP-Neu5Ac hydroxylase knock-out pigs*. Scientific Reports, 2013. **3**: p. 1981.
278. Basnet, N.B., et al., *Deficiency of N-glycolylneuraminic acid and Galalpha1-3Galbeta1-4GlcNAc epitopes in xenogeneic cells attenuates cytotoxicity of human natural antibodies*. Xenotransplantation, 2010. **17**(6): p. 440-8.
279. Wang, Z.Y., et al., *Erythrocytes from GGTA1/CMAH knockout pigs: implications for xenotransfusion and testing in non-human primates*. Xenotransplantation, 2014. **21**(4): p. 376-84.
280. Miyagawa, S., et al., *Generation of α 1,3-galactosyltransferase and cytidine monophospho-N-acetylneuraminic acid hydroxylase gene double-knockout pigs*. J Reprod Dev, 2015. **61**(5): p. 449-57.
281. Burlak, C., et al., *Reduced binding of human antibodies to cells from GGTA1/CMAH KO pigs*. Am J Transplant, 2014. **14**(8): p. 1895-900.
282. Wang, Z.Y., et al., *Eliminating Xenoantigen Expression on Swine RBC*. Transplantation, 2017. **101**(3): p. 517-523.
283. Bjorkman, P.J. and P. Parham, *Structure, function, and diversity of class I major histocompatibility complex molecules*. Annu Rev Biochem, 1990. **59**: p. 253-88.
284. Le, T.M., et al., *beta2-microglobulin gene duplication in cetartiodactyla remains intact only in pigs and possibly confers selective advantage to the species*. PLoS One, 2017. **12**(8): p. e0182322.
285. Zijlstra, M., et al., *β 2-Microglobulin deficient mice lack CD4-8+ cytolytic T cells*. Nature, 1990. **344**(6268): p. 742-746.
286. Santos, M., et al., *Defective iron homeostasis in beta 2-microglobulin knockout mice recapitulates hereditary hemochromatosis in man*. J Exp Med, 1996. **184**(5): p. 1975-85.
287. Rothenberg, B.E. and J.R. Volland, *beta2 knockout mice develop parenchymal iron overload: A putative role for class I genes of the major histocompatibility complex in iron metabolism*. Proc Natl Acad Sci U S A, 1996. **93**(4): p. 1529-34.
288. Schell, T.D., et al., *The assembly of functional beta(2)-microglobulin-free MHC class I molecules that interact with peptides and CD8(+) T lymphocytes*. Int Immunol, 2002. **14**(7): p. 775-82.
289. Bix, M. and D. Raulet, *Functionally conformed free class I heavy chains exist on the surface of beta 2 microglobulin negative cells*. J Exp Med, 1992. **176**(3): p. 829-34.
290. Gray, S.J., et al., *Optimizing promoters for recombinant adeno-associated virus-mediated gene expression in the peripheral and central nervous system using self-complementary vectors*. Hum Gene Ther, 2011. **22**(9): p. 1143-53.
291. Wang, K., et al., *Cre-dependent Cas9-expressing pigs enable efficient in vivo genome editing*. Genome Res, 2017. **27**(12): p. 2061-2071.
292. Flisikowska, T., et al., *A porcine model of familial adenomatous polyposis*. Gastroenterology, 2012. **143**(5): p. 1173-1175.e7.
293. Fearon, E.R. and B. Vogelstein, *A genetic model for colorectal tumorigenesis*. Cell, 1990. **61**(5): p. 759-67.
294. Janssen, K.P., et al., *APC and oncogenic KRAS are synergistic in enhancing Wnt signaling in intestinal tumor formation and progression*. Gastroenterology, 2006. **131**(4): p. 1096-109.
295. Veron, N., et al., *CRISPR mediated somatic cell genome engineering in the chicken*. Dev Biol, 2015. **407**(1): p. 68-74.
296. Polyak, S., et al., *Identification of adeno-associated viral vectors suitable for intestinal gene delivery and modulation of experimental colitis*. Am J Physiol Gastrointest Liver Physiol, 2012. **302**(3): p. G296-308.

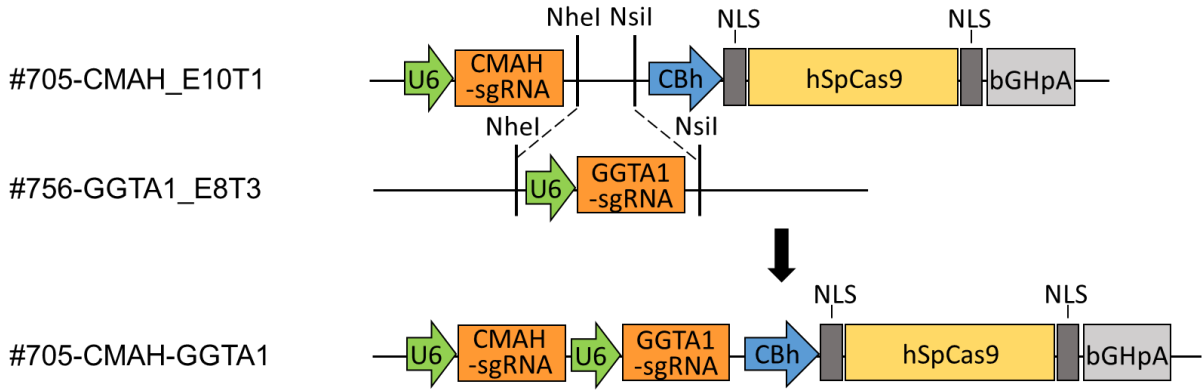
10 Supplementary



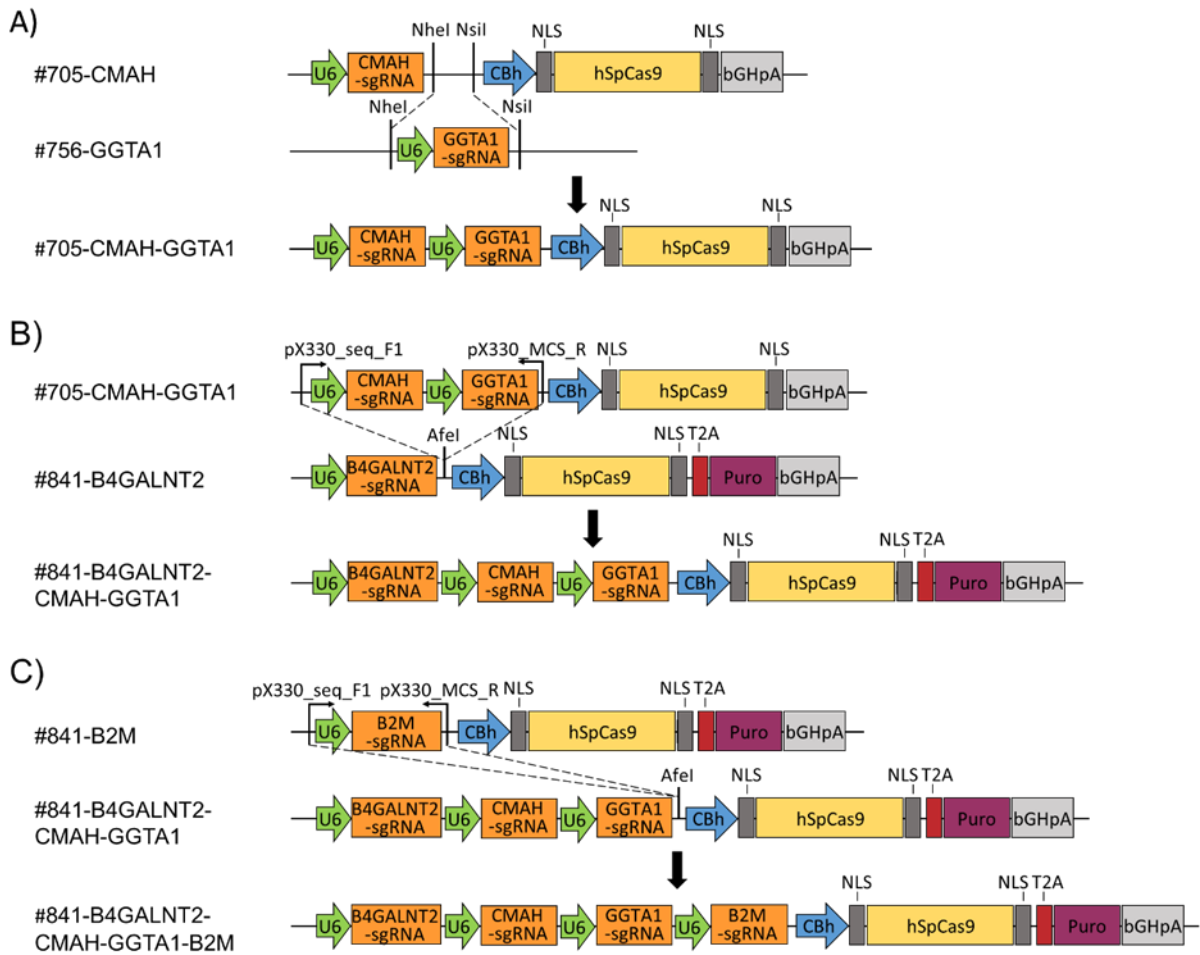
Supplementary figure 1: Schematic diagram for the generation of a seven-transgene vector. A) Cloning of THBD into pSL1180-EPCR. The plasmid hTMmod2 w/o PGK-neo was XhoI-digested and the cassette consisting of porcine THBD promoter and human THBD gene cloned into the EcoRV-digested plasmid pSL1180-EPCR. B) Introduction of a multiple cloning site (MCS) into pBACe3.6. The vector pBACe3.6 was Sall-digested and the fragment containing the BAC-backbone was ligated with Sall-overhangs of an oligonucleotide (pBACe3.6 MCS F/R) containing a MCS. C) Cloning of mutCIITA and CD47 into pSL1180-HT-HO1. The plasmid pcDNA3.1-hygro-CD47 was NruI-, PvuII-digested and the CAG-CD47 cDNA construct cloned into the HpaI-digested plasmid pSL1180-HT-HO1. Subsequently, the plasmid pcDNA3.1-hygro-mutCIITA was SspI-digested and the cassette consisting of Tie2 enhancer, CAG promoter and mutCIITA minigene cloned into the HpaI restriction site of the previously generated vector. D) Cloning of HT, mutCIITA, CD47, HO1 and PD-L1 into pBACe3.6-MCS. The plasmid pSL1180-HT-mutCIITA-CD47-HO1 was MluI-, BstBI-digested and the fragment containing the four human genes cloned into the MluI-, BstBI-digested vector pBACe3.6-MCS. Subsequently, the CCL2-PD-L1 construct was amplified using the primer CCL2-hPD-L1 NEB F/R and the generated amplicon introduced into the previously generated, MluI-digested vector via NEB Builder. E) Cloning of THBD and EPCR into pBACe3.6-PD-L1-HT-mutCIITA-CD47-HO1. The plasmid pSL1180-EPCR-THBD was Sall digested and the fragment consisting of the THBD cassette and CAG-EPCR-cDNA construct was cloned into the SwaI-digested BAC-vector pBACe3.6-PD-L1-HT-mutCIITA-CD47-HO1. The final seven-transgene vector was termed pBACe3.6-PD-L1-HT-mutCIITA-CD47-HO1-THBD-EPCR and had a size of 40.6 kb. Blue coloured arrows represent the CAG promoter, brown coloured arrows the porcine THBD promoter and green coloured arrows the CCL2 promoter. Grey coloured boxes represent the BGHpA and pink boxes the pBACe3.6 backbone. Black lines represent restriction sites.



Supplementary figure 2: Schematic diagram for the generation of ROSA26-THBD targeting vector. To generate this vector a pcDNA3.1-hygro(+)-CAG-CD55-mini vector was SpeI digested and the 3.8 kb CAG-CD55-minigene fragment, serving as new long homology arm, cloned into the NotI-linearised hTMmod2-w/o-PGK-neo plasmid. The vector ROSA26-HO-1 TV was used as template DNA to amplify a 3.8 kb fragment containing the ROSA26-short homology arm and a splice acceptor-kozak-neomycin cassette using the primers ROSA26 SA F1 mod/R1 mod. The amplified fragment was cloned into the Sall-digested "hTMmod2-w/o-PGK-neo vector resulting in the final ROSA26-THBD re-retargeting vector.

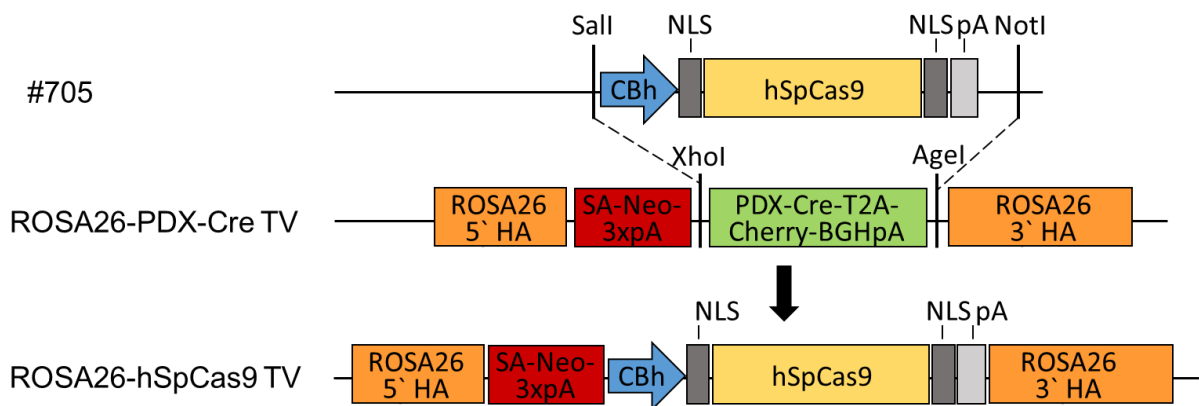


Supplementary figure 3: Schematic diagram for the generation of the double-knockout vector #705-CMAH-GGTA1. Excision of the U6-Promoter and GGTA1_E8T3 sgRNA sequence out of the plasmid #756-GGTA1_E8T3 using NheI/NsiI and sticky end insertion into the NheI, NsiI digested vector #705-CMAH_E10T1 results in the vector #705-CMAH-GGTA1. #705 refers to the plasmid “pX330-U6-Chimeric_BB-CBh-hSpCas9 + MCS” and #756 refers to the vector “pSL1180 rev-U6-trac”.

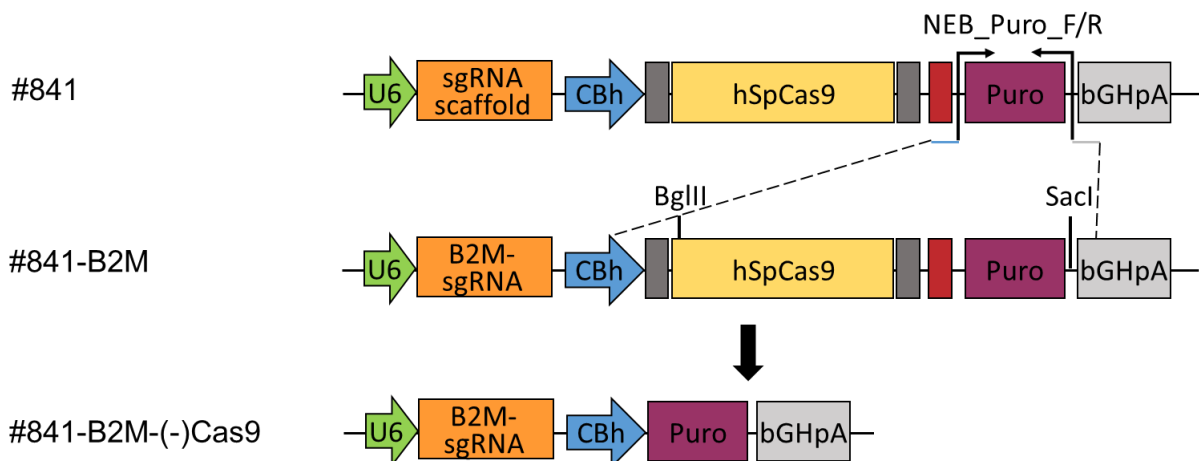


Supplementary figure 4: Schematic diagram for the generation of the #841-4xKO plasmid. A) Generation of the double-knockout plasmid #705-CMAH-GGTA1. Excision of the U6-Promoter and GGTA1 E7T6 sgRNA sequence

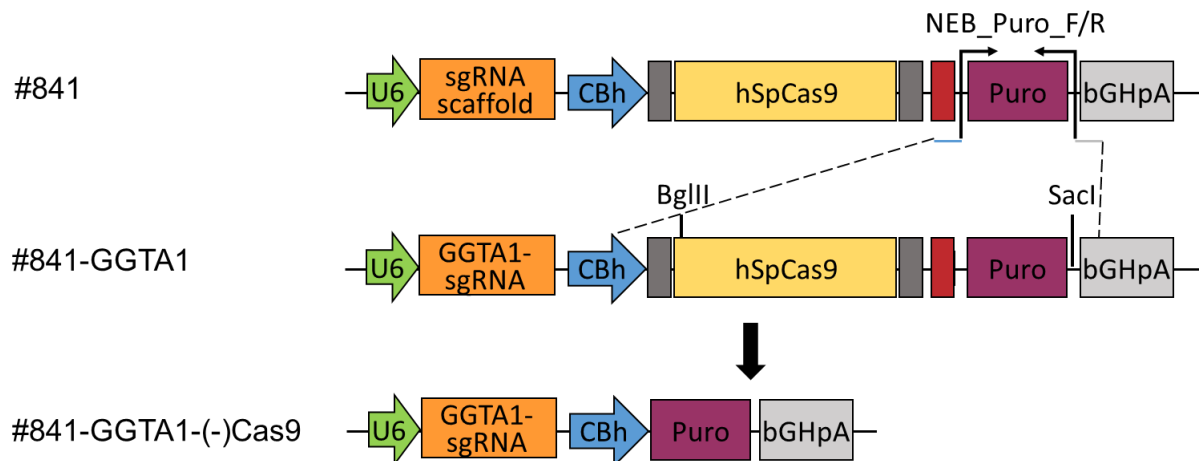
out of the plasmid #756-GGTA1 using NheI/NsiI and sticky end insertion into the NheI, NsiI digested vector 705-CMAH results in the plasmid #705-CMAH-GGTA1. B) Generation of the triple-knockout plasmid #841-B4GALNT2-CMAH-GGTA1. PCR amplification using the primer pX330 seq F1 and pX330 MCS R and the plasmid #705-CMAH-GGTA1 as template generated a fragment carrying the CMAH E10T1- and GGTA1 E7T6-sgRNA sequences each under the control of an U6 promoter. This fragment was cloned into the AfeI-digested plasmid #841-B4GALNT2 via blunt-end insertion resulting in the plasmid #841-B4GALNT2-CMAH-GGTA1. C) Generation of the four-fold knockout plasmid #841-B4GALNT2-CHAM-GGTA1-B2M. PCR amplification using the primer pX330 seq F1 and pX330 MCS R and the plasmid #841-B2M as template generated a fragment carrying the B2M- E1T1 sgRNA sequences under the control of an U6 promoter. This fragment was cloned into the AfeI-digested plasmid #841-B4GALNT2-CMAH-GGTA1 via blunt-end insertion resulting in the final plasmid #841-B4GALNT2-CMAH-GGTA1-B2M. #705 refers to the plasmid “pX330-U6-Chimeric_BB-CBh-hSpCas9 + MCS”, #756 refers to the plasmid “pSL1180 rev-U6-trac” and #841 refers to the plasmid “pX330-U6-Chimeric_BB-CBh-hSpCas9-T2A-puro+MCS”.



Supplementary figure 5: Schematic diagram for the generation of the ROSA26-hSpCas9 Targeting vector. Excision of CBh-promoter driven hSpCas9 out of the plasmid #705 using Sall/NotI and blunt end insertion into the XhoI-, AgeI-digested vector ROSA26-PDX-Cre TV results in the plasmid ROSA26-hSpCas9 TV. #705 refers to the plasmid “pX330-U6-Chimeric_BB-CBh-hSpCas9 + MCS”.



Supplementary figure 6: Generation of the plasmid #841-B2M(-)Cas9. Puromycin resistance was amplified using the primers NEB Puro F/R and inserted into the BglII/SacI digested vector #841 -B2M via NEB Builder. Grey boxes represent NLS and red boxes T2A-signal sequence. #841 refers to the plasmid “pX330-U6-Chimeric_BB-CBh-hSpCas9-T2A-puro + MCS”.



Supplementary figure 7: Generation of the plasmid #841-GGTA1(-)Cas9. Puromycin resistance was amplified using the primers NEB Puro F/R and inserted into the BglII/SacI digested vector #841 -GGTA1 via NEB Builder. Grey boxes represent NLS and red boxes T2A-signal sequence. #841 refers to the plasmid “pX330-U6-Chimeric_BB-CBh-hSpCas9-T2A-puro + MCS”.

Supplementary table 1: Analysis of multiple-knockout cell clones. Compound heterozygous means, that both alleles are modified, but differed in the indels introduced at each allele.

Clone	<i>GGTA1</i>	<i>CMAH</i>	<i>B4GALNT2</i>	<i>B2M</i>
#2	compound heterozygous	heterozygous	wild type	homozygous
#3	compound heterozygous	heterozygous	wild type	homozygous
#4	homozygous	homozygous	homozygous	homozygous
#5	homozygous	compound heterozygous	heterozygous	compound heterozygous
#6	compound heterozygous	homozygous	heterozygous	compound heterozygous
#7	compound heterozygous	heterozygous	compound heterozygous	homozygous
#8	compound heterozygous	compound heterozygous	homozygous	homozygous
#10	compound heterozygous	compound heterozygous	homozygous	homozygous
#11	compound heterozygous	homozygous	compound heterozygous	homozygous
#12	homozygous	homozygous	compound heterozygous	homozygous

#16	compound heterozygous	compound heterozygous	compound heterozygous	homozygous
#18	homozygous	compound heterozygous	compound heterozygous	compound heterozygous
#19	compound heterozygous	homozygous	compound heterozygous	compound heterozygous
#22	heterozygous	heterozygous	heterozygous	homozygous

Supplementary table 2: Supplementary primer

Name	Sequence
pX330 MCS R	5`-accaagcttacgtcgactgt-3`
CCL2-hPD-L1 NEB F	5`-aacgtacgaaagggttaaactcgatttccccatagccc-3`
CCL2-hPD-L1 NEB R	5`-ccgcctgcagctggcgccatgggtccgcaagctctagtcg-3`
ROSA26 SA F1 mod	5`-tggtaccgggcccccggttaaacttaggccccctcactgcat-3`
ROSA26 SA R1 mod	5`-agccacctggtgggttttcaggccatggtgctg-3`
pX330 seq F1	5`-gggagaaaggcggacaggta-3`
NEB Puro F	5`-gttgaccggtgccaccatgaccgagtacaagcccacg-3`
NEB Puro R	5`-ctggcaactagaaggcacagcagtggtgacgcatgcatg-3`
pBACe3.6 MCS F	5`-tcgacggccgcatcgctcaacgtacgaaagggttaaactcaaacgcggtcggcggtttcgaataggatttaaatggcccgtagctcaagcgatcgccatg-3`
pBACe3.6 MCS R	5`-tcgaccatggcgatcgcttgacgtacggccatttaaacctattcgaaaacgccgaacgcggttgagttaaaccttcgtacgttgacgcatcgggccg-3`

11 Acknowledgement

Zuerst möchte ich mich bei meiner Betreuerin Frau Prof. Angelika Schnieke bedanken, dass sie mir die Möglichkeit gegeben hat meine Promotion am Lehrstuhl durchzuführen und an einem solch interessanten Projekt mitzuwirken. Danke für das entgegengebrachte Vertrauen und die Freiheit, die wir genießen dürfen. Vielen Dank auch für die schnelle Korrektur meiner Arbeit und dass ich an so vielen Konferenzen und Workshops teilzunehmen durfte, um dort unsere Forschungsarbeit zu präsentieren und mich selbst weiterzuentwickeln.

I would like to thank Dr. Alex Kind for his participation in writing publications and for the correction of my thesis. Thank you so much for the helpful advises, the great ideas, and the time and ambition in improving my English and writing skills.

Ich bedanke mich bei allen Kooperationspartnern für die angenehme Zusammenarbeit. Prof. Reinhard Schwinzer und Dr. Björn Petersen danke ich auch für die Ermöglichung eines Forschungsaufenthaltes in ihren Arbeitsgruppen. Vielen Dank an Wiebke Baars für die intensive Laborbetreuung und an alle Mitglieder beider Arbeitsgruppen für die freundliche Aufnahme.

Ein großer Dank geht an Steffen und Viola Löbnitz für die zuverlässige Zusammenarbeit, die großartige Pflege der Tiere und das Beschaffen von Probenmaterial. Vielen lieben Dank auch für die vielen Fotos meiner Schweinchen sowie die regelmäßigen Updates bei Geburten.

Ein weiterer Dank gebührt Nina Simm für die ihre Hilfsbereitschaft die Unterstützung im Labor. Danke für die äußerst angenehme Zusammenarbeit und das Engagement im Cas9-Projekt und darüber hinaus. Des Weiteren danke ich Sulith Christan für ihre Hilfsbereitschaft, ihre positive Einstellung und Ausstrahlung und ihre unendliche Geduld, egal wie oft man zu ihr läuft, weil man etwas sucht oder bestellt braucht. Vielen Dank auch an Alexander Carrapeiro und Peggy Müller-Fliedner für die oftmals spontane Übernahme von Arbeit und deren zuverlässige Ausführung. Weiter möchte ich Kristina Mosandl, Lea Radomsky, Marlene Stummbaum, Johanna Tebbing, Toni Kuhnt, Robert Grötschl und Kilian Skowranek für die angenehme Zusammenarbeit danken.

Bei Barbara Bauer möchte ich mich für die Hilfe bei sämtlichen verwaltungstechnischen Angelegenheiten bedanken. Ebenso möchte ich Bärbel sowie Peggy, Alex, Nina und Sulith einen großen Dank aussprechen für die Organisation von Geschenken, Feiern und Betriebsausflügen. Vielen Dank für euren Einsatz und dass ihr den Laden zusammenhaltet.

Auch danke ich meinen Studenten Annika Schneider, Eva Stork, Benedikt Saller, Julia Zuber, Marvin Schwarz und Nicola Berner für die lehrreiche Zusammenarbeit und ihren Beitrag an

meiner Forschung. Ich hoffe, dass ihr möglichst viel mitnehmen konntet und wünsche euch alles Gute für die Zukunft.

Ein großes Dankeschön geht an meine ehemaligen und jetzigen Mitstreiter, besonders an Erica Schulze, Daniela Huber, Carolin Perleberg, Andrea Schäffler, Bernhard Klinger, Alessandro Grodziecki, Melanie Manyet, und Daniela Kalla. Ich danke euch für die schöne gemeinsame Zeit am Lehrstuhl und darüber hinaus, sowie für das Teilen von Freude, Erfolg, Sorgen und Problemen.

Weiter danke ich Simone Kraner-Scheiber, Daniela Huber und Melanie Manyet für die schöne und harmonische Zeit gemeinsam im Büro. Danke Simone für dein offenes Ohr, deine Ratschläge und deine äußerst angenehme Art. Danke Dani für die oft amüsanten Geschichten aus deinem Leben sowie die zahlreichen After-Work Unternehmungen. Ich wünsche euch Beiden alles Gute für euren weiteren Weg und werde euch sehr vermissen!

Ein Dankeschön gebührt auch der Xeno-Gruppe, insbesondere Konrad Fischer und Andrea Schäffler. Vielen Dank, dass ich Teil dieses Teams sein durfte, danke für die Gesellschaft bei der nachmittäglichen Kaffeepause und danke für die gemeinsamen Aktivitäten, wie Schlittschuhlaufen und das Verzieren von Torten bis tief in die Nacht. Andrea, dir wünsche ich noch ganz viel Erfolg für den letzten Abschnitt deiner Promotion.

Krzysztof Flisikowski und Tatiana Flisikowska möchte ich für die gute Zusammenarbeit, die stetige Gastfreundschaft und die schönen Partys in Polen und Thalhausen danken. Danke Krzysztof für das Vertrauen in mich von Beginn an und die entgegengebrachte Wertschätzung.

Des Weiteren danke ich Erica Schulze, Kilian Skowranek und Konrad Fischer für die wahnsinnig schöne und lustige gemeinsame Zeit am Lehrstuhl. Danke, dass ihr mich so lieb aufgenommen habt, danke für die zahlreichen privaten Unternehmungen, wie Grillen am See, Kochen bei Frau Schulze usw. Ganz besonders danke ich euch, dass aus Arbeitskollegen Freunde geworden sind, die ich keinesfalls missen möchte.

Ein ganz besonders großer Dank geht an meinen Mentor und Freund Konrad Fischer. Danke Konrad für deine hervorragende Betreuung, die aktive und engagierte Teilnahme an meiner Arbeit, deine guten Ratschläge, deine positive Einstellung und die tolle Zusammenarbeit. Du hast einen großen Teil zum Erfolg meiner Arbeit beigetragen, dafür danke ich dir von ganzen Herzen. Ich danke dir auch für die für die leckere Verköstigung, egal ob brasilianisch, Steckerlfisch oder Spanferkel, für deine Bereitschaft so manchen Blödsinn (z.B. Weiberfasching) mitzumachen und dafür, dass du wann immer nötig mit Rat und Tat zur Stelle warst.

Von ganzen Herzen möchte ich auch meiner Familie danken. Danke Mama und Papa, dass ihr es mir ermöglicht habt diesen Weg zu gehen. Danke, dass ihr mich immer unterstützt habt und ich mich jederzeit auf euch verlassen konnte. Vielen Dank, dass ihr mir vorgelebt habt, dass man mit einer Portion Fleiß und Engagement so Einiges erreichen kann. Danke Gela, für die Übernahme von etlichen „Marktschichten“ und dass du immer zur Stelle bist, wenn man dich braucht. Michael, vielen Dank für deine Unterstützung, deine Geduld und deine unendlich große Rücksichtnahme insbesondere in den letzten Monaten. Danke, dass ich in dir meinen Weggefährten durchs Leben gefunden habe, auf den ich mich zu 100% verlassen kann, mit dem ich jeden schönen Moment teilen kann und der mir auch in schwierigen Zeiten niemals von der Seite weicht.

12 Curriculum vitae

Persönliche Daten

Name: Beate Rieblinger
 Geburtsdatum: 28.09.1988
 Geburtsort: Schrobenhausen, Deutschland

Ausbildung

01/2014-07/2019 Promotion am Lehrstuhl Biotechnologie der Nutztiere, Technische Universität München
 Thema der Doktorarbeit: Genetic porcine models for *in vivo* genome editing and for xenotransplantation

10/2011-10/2013 Master of Science, Molekulare Biotechnologie, Technische Universität München
 Abschlussnote: 1,2
 Thema der Masterarbeit: Modifikation verschiedener Xenogen-Konstrukte und deren Analyse in Zellen und Geweben des Schweins

10/2008-08/2011 Bachelor of Science, Molekulare Biotechnologie, Technische Universität München
 Abschlussnote: 1,5
 Thema der Bachelorarbeit: Zusammenhang zwischen der PEG3 Methylierung und pränataler Letalität beim Rind

09/1999-06/2008 Gymnasium Schrobenhausen
 Allgemeine Hochschulreife
 Abschlussnote: 2,0

Veröffentlichungen und Präsentationen

Peer-reviewed Originalmanuskripte

Fischer K*, **Rieblinger B*** (Co-first author), Hein R, Sfriso R, Zuber J, Schäffler A, Klinger B, Wei L, Flisikowski K, Kurome M, Zakhartchenko V, Kessler B, Wolf E, Rieben R, Schwinzer R, Kind A, Schnieke A. Viable pigs after simultaneous inactivation of porcine MHC class I and three xenoreactive antigen genes GGTA1, CMAH and B4GALNT2. Xenotransplantation, 2019. (30/05/2019: Angenommen mit kleineren Änderungen).

Rieblinger B, Fischer K, Kind A, Saller BS, Baars W, Schuster M, Wolf-van Buerck L, Schäffler A, Flisikowska T, Kurome M, Zakhartchenko V, Kessler B, Flisikowski K, Wolf E, Seissler J, Schwinzer R, Schnieke A. Strong xenoprotective function by single-copy transgenes placed sequentially at a permissive locus. Xenotransplantation, 2018. 25(2): e12382.

Xu H, Pausch H, Venhoranta H, Rutkowska K, Wurmser C, **Rieblinger B**, Flisikowska T, Frishman D, Zwierzchowski L, Fries R, Andersson M, Kind A, Schnieke A, Flisikowski K. Maternal placenta modulates a deleterious fetal mutation. Biol Reprod, 2017. 97(2):249-257.

Fischer K, Kraner-Scheiber S, Petersen B, **Rieblinger B**, Buermann A, Flisikowska T, Flisikowski K, Christan S, Edlinger M, Baars W, Kurome M, Zakhartchenko V, Kessler B, Plotzki E, Szczerbal I, Switonski M, Denner J, Wolf E, Schwinzer R, Niemann H, Kind A, Schnieke A. Efficient production of multi-modified pigs for xenotransplantation by 'combineering', gene stacking and gene editing. *Sci Rep*, 2016. 6: 29081.

Weitere Publikationen

Rieblinger B, Fischer K, Schäffler A, Schwinzer R, Wolf E, Kind A, Schnieke A. Transgene stacking to generate multi-transgenic pigs for xenotransplantation. Abstracts of the 14th congress of the International Xenotransplantation Association, Baltimore, USA, September 20 – 23, 2017. *Xenotransplantation*, 2017.24(5):e12328.

Fischer K, **Rieblinger B**, Schäffler A, Petersen B, Schwinzer R, Niemann H, Wolf E, Kind A, Schnieke A. Multi-modified donor pigs for xenotransplantation. Abstracts of the 14th congress of the International Xenotransplantation Association, Baltimore, USA, September 20 – 23, 2017. *Xenotransplantation*, 2017.24(5):e12328.

Schäffler A, Fischer K, **Rieblinger B**, Knolle P, Kind A, Schnieke A. Cytokine-inducible promoters for dynamic transgene expression. Abstracts of the 14th congress of the International Xenotransplantation Association, Baltimore, USA, September 20 – 23, 2017. *Xenotransplantation*, 2017.24(5):e12328.

Fischer K, Kraner-Scheiber S, **Rieblinger B**, Flisikowska T, Petersen B, Buermann A, Schwinzer R, Niemann H, Kind A, Schnieke A. Modifying pigs to overcome barriers to xenotransplantation. *Xenotransplantation*, 2015. 22 (S1): S185-S201.

Vorträge

- 04/2018 Präsentation der Fortschritte von Projekt B2- Genetically modified pigs to modulate vascular and cellular rejection. Meeting des SFB TRR 127 der Deutschen Forschungsgemeinschaft (DFG). Mariensee, Deutschland, 18.-19.04.2018.
- 10/2017 Präsentation der Fortschritte von Projekt B2- Genetically modified pigs to modulate vascular and cellular rejection. Meeting des SFB TRR 127 der Deutschen Forschungsgemeinschaft (DFG). San Servolo, Italien, 11.-13.10.2017.
- 09/2017 Transgene stacking to generate multi-transgenic pigs for xenotransplantation. 14. Kongress der "International Xenotransplantation Association (IXA)", Baltimore, USA, 20.-23.10.2017.
- 09/2017 Multi-modified donor pigs for xenotransplantation. 14. Kongress der "International Xenotransplantation Association (IXA)", Baltimore, USA, 20.-23.09.2017.
- 05/2017 Präsentation der Fortschritte von Projekt B2- Genetically modified pigs to modulate vascular and cellular rejection. Meeting des SFB TRR 127 der Deutschen Forschungsgemeinschaft (DFG). Göttingen, Deutschland, 03.-04.05.2017.

- 05/2016 Generation of multi-transgenic pigs for xenotransplantation by gene stacking. 11. Frühjahrsmeeting der Arbeitsgruppe "Transplantationsimmunologie" der deutschen Gesellschaft für Immunologie (DGfI). Hannover, Deutschland, 27.-28.05.2016.
- 09/2015 Präsentation der Fortschritte von Projekt B2- Pigs deficient in the major xenoreactive non-Gal antigen Neu5Gc. Meeting des SFB TRR 127 der Deutschen Forschungsgemeinschaft (DFG). Freising, Deutschland, 28.-30.09.2015.

Posterpräsentationen

- 04/2017 Gene stacking at the porcine ROSA26 locus. 3rd HEZagrar PhD Symposium. Weihenstephan, Deutschland, 25.04.2017.
- 11/2016 Gene stacking at the porcine ROSA26 locus. Meeting des SFB TRR 127 der Deutschen Forschungsgemeinschaft (DFG). München, Deutschland, 24.-25.11.2016.
- 11/2015 Modifying pigs to overcome barriers to xenotransplantation. Joint IPITA-IXA-CTS Congress. Melbourne, Australien, 15.-19.11.2015.
- 10/2014 Further improvement of transgenic pigs – A second round of genetic modification. Meeting des SFB TRR 127 der Deutschen Forschungsgemeinschaft (DFG). München, Deutschland, 23.-24.10.2014.

Auszeichnungen und Stipendien

- 10/2017 TTS-IXA 2017 Congress Scientific Award. Verliehen von der International Xenotransplantation Association (IXA) und der Transplantation Society (TTS) beim „International Xenotransplantation Association (IXA) Congress“, Baltimore, USA, 22.09.2017.
- 08/2017 Reisestipendium für Kongressreise zum „14th International Xenotransplantation Association (IXA) Congress“ in Baltimore, USA. Gefördert vom Deutschen Akademischen Austauschdienst (DAAD). Bonn, Deutschland, 4.8.2016.
- 11/2016 Posterpreis für das Poster "Gene stacking at the porcine ROSA26 locus". Meeting des SFB TRR 127 der Deutschen Forschungsgemeinschaft (DFG). München, Deutschland, 24.-25.11.2016.
- 05/2015 Stipendium zur Teilnahme an der SALAAM COST Action BM1308 Training School "Large animal genome engineering" in Gödöllo, Ungarn. Gefördert von COST Action BM1308. 10.-13.05.2015
- 10/2014 Posterpreis für das Poster "Further improvement of transgenic pigs – A second round of genetic modification". Meeting des SFB TRR 127 der Deutschen Forschungsgemeinschaft (DFG). München, Deutschland, 23.-24.10.2014.